ANTIBODY TARGETS IN AUTOIMMUNE ENCEPHALITIS

Dr Sarosh R Irani
Somerville College
Oxford University

THESIS SUBMITTED FOR DEGREE OF DOCTOR OF PHILOSOPHY. TRINITY TERM 2010

DEPARTMENT OF CLINICAL NEUROLOGY,
MEDICAL SCIENCES DIVISION, UNIVERSITY OF OXFORD

OSS ID: 273439

ACKNOWLEDGEMENTS

I would like to thank a number of people sincerely for their help, advice and commitment throughout the DPhil. In particular, my two supervisors: Professor Angela Vincent and Dr Bethan Lang. Angela, as the primary supervisor, thank you for your ongoing drive, interest and time and for hosting me in your laboratory. It was a real pleasure and education to watch you work through data to generate figures and spark further thoughts. Special thanks for your, often pivotal, ideas during the projects. Beth, you have been a real pillar of support both technically, by the bench-side, and as a friend and colleague in the laboratory. Thank you for your enthusiasm and hard work.

Dr Patrick Waters has contributed significantly by performing the molecular biology associated with the project: thank you Paddy. In addition, it was great to have Dr Luigi Zuliani in the laboratory. It was a pleasure to discuss the clinical implications of the laboratory data with someone as interested in the literature as I am. Luigi, thanks for your ideas and input. I am also grateful to the many other people, particularly Mrs Susan Maxwell, Ms Kasia Bera, Ms Philippa Pettingill, Dr Leslie Jacobsen and Mrs Linda Clover, who have been key in their help with a number of experiments. Thank you also to Mr James Hafseth who very helpfully proof-read the thesis (J Hafseth, unpublished observations).

I would also like to thank the National Institute of Health Research (NIHR), Department of Health, UK for awarding me a fellowship.

Finally, I would like to thank Anushka, my wife, who has heard every twist in the project as it developed. In particular during the early period where it appeared that experiments were consistently giving the 'wrong' answers. At this stage, the hypotheses were being modified and, as an impatient medic with little wet science background, I was rather frustrated. Also when circumstances did not appear fair, Anushka helped resolve the issues in my mind. Her support, love and understanding have been invaluable. Thank you.

CONTENTS

ACKNOWLEDGEMENTS 2
ABSTRACT 7
CHAPTER ONE: INTRODUCTION 8
Koch's postulates 8
The paradigms of myasthenia gravis and Lambert-Eaton myasthenic syndrome 11
Neuromyotonia: clinical features 12
Neuromyotonia: electrophysiological features 13
Is neuromyotonia also an autoimmune disease? 13
Voltage-gated potassium channel antibody (VGKC-Ab) assay 14
VGKC-ANTIBODY ASSOCIATED CLINICAL SYNDROMES 15
The spectrum of peripheral nervous system hyperexcitability 15
MORVAN'S SYNDROME 16
The aetiology of Morvan's syndrome 18
Demographics of Morvan's syndrome 20
Tumours and autoimmune conditions in MoS 20
Clinical features of Morvan's syndrome 21
Dysautonomia 21
Dyssomnia 23
Pain 23
Neuropsychiatric features 24
Brain imaging 24
Seizures, movement disorders and other features 25
Seropositivity and blood results 25
Outcomes 26
From MoS to limbic encephalitis 26
PARANEOPLASTIC SYNDROMES WITH PARTICULAR REFERENCE TO LIMBIC ENCEPHALITIS 27
LIMBIC ENCEPHALITIS – PARANEOPLASTIC ORIGINS 32
LIMBIC ENCEPHALITIS WITH VGKC-ABS: A PREDOMINANTLY NON-PARANEOPLASTIC, IMMUNOTHERAPY-RESPONSIVE DISEASE 36
Initial observations 36
Clinical and paraclinical observations in VGKC-Ab associated LE 38
Seizures in VGKC-Ab associated LE 39
Dysomnia in VGKC-Ab associated LE 40
An expanded clinical spectrum: VGKC-Ab associated CNS features 41
Creutzfeldt-Jakob Disease (CJD) and VGKC-Ab associated LE 44
Summary: VGKC-Ab associated diseases 44
LE WITH OTHER AUTOANTIBODIES 45
N-methyl D-aspartate receptor antibodies (NMDAR-Abs) 46
Potential for pathogenicity 48
A European NMDAR-antibody study 48
A model for NMDAR-antibody pathogenicity in humans 49
NMDAR-Ab positive children and Encephalitis Lethargica 50
AMPA receptor (AMPAR) antibodies 51

GABAB receptor antibodies 52
Other autoantibodies in central nervous system diseases 52
Kv1: VOLTAGE-GATED POTASSIUM CHANNEL SHAKER FAMILY 53
Kv1 structure 54
Non-neural Kv1 expression 54
Kv1 heteromerisation and glycosylation 55
Cellular and subcellular Kv1 distribution: relations to function 56
Beta subunits and membrane-associated guanylate kinases (MAGUKs) 58
Kv1 MUTATIONS IN ANIMAL AND HUMANS 60
Animals 60
Humans 61
Kv1S AS ANTIGENIC TARGETS MODULATED BY PATIENT IGG 62
EVIDENCE FOR VGKC-AB PATHOGENICITY 65
THE BLOOD-BRAIN BARRIER 66
HOW MAY MULTIPLE PHENOTYPES BE EXPLAINED BY VGKC-ABS? 68
Clinical aspects 68
Molecular aspects 69
SUMMARY 72
CHAPTER 2: METHODS 74
Clinical material 74
Antibodies used 77
VGKC-antibody determination 77
Plasmid constructs: molecular biology performed by Dr Patrick Waters (Neurosciences Group, Oxford) 78
Transfection and human embryonic kidney cell culture 79
Cell-based assay (CBA) 80
Subclasses and complement fixation 81
Protein extraction and labelling 81
^{125}I-αDTX surface binding assay. 82
Other antibody assays 83
Immunohistochemistry and immunofluorescence on brain sections 83
Antibodies binding to primary hippocampal cultures 84
Western blotting 84
Statistical analysis 85
CHAPTER 3: VGKC-ANTIBODY ASSOCIATED SYNDROMES 86
Introduction 86
Limbic Encephalitis, Morvan's Syndrome and Neuromyotonia: clinical features 86
Demographics 88
Cognitive features 88
Sleep, pain and autonomic features 90
EMG data 91
Tumours 91
Infectious prodrome 93
Investigations 93
Immunotherapies 94
DYSTONIC EPILEPSY ASSOCIATED WITH VGKC-ABS 97

Faciobrachial seizures as a prodrome to limbic encephalitis 102
Investigations 103
Treatment issues 108
Summary and conclusions 113
CHAPTER 4: Kv1 POTASSIUM CHANNELS AS ANTIGENIC TARGETS 117
Introduction 117
Specificity of commercial antibodies 117
Absent binding of patient sera to the extracellular domain of Kv1s expressed in a mammalian cell line 119
Optimisation of Kv1 surface expression 120
Number of surface Kv1 channels per cell 125
Varied Kv1-subunit quantities in brain tissue 125
A comparison of Kv1 and patient binding patterns in cerebellar tissue, ependymal cells and hippocampal neuronal cultures 128
^{125}I-αDTX-labelled, Kv1-transfected HEK cell extracts are not precipitated by patient sera 133
Summary 140
CHAPTER 5: LGI1, CASPR2 AND CONTACTIN-2 AS ANTIGENIC TARGETS ... 142
Distinction between Kv1 channels and antigenic targets of patient sera: 'Stripping' experiments 142
Which proteins, other than Kv1s, exist within ^{125}I-αDTX-bound Kv1-complexes? .. 144
CASPR2 is an antigenic target 149
Contactin 2 / TAG-1 is an antigenic target 160
Lgi1 (leucine-rich glioma-inactivated 1) is an antigenic target 162
Retrospective blinded observations 171
Summary and limitations 173
CHAPTER 6: CLINICO-SEROLOGICAL CORRELATIONS 176
Introduction 176
Clinico-serological correlations 176
Overall clinical-serological correlations 178
Clinical features of CASPR2-Ab positive cases 180
Serological value over clinical segregations 182
Clinical features of Lgi1-antibody positive cases 185
Clinical features of Contactin-2 antibody positive cases 186
Clinical features of Kv1.2 antibody positive cases 186
Clinical features of cases with no confirmed antigenic target 187
Neuromyotonia cohort with low positive VGKC-Ab titres 187
Summary and limitations 189
CHAPTER 7: DISCUSSION 192
Introduction 192
Kv1-associating molecules around the node of Ranvier: an overview 193
PDZ-domain containing molecules 196
CASPR2 (CONTACTIN-ASSOCIATED PROTEIN 2) 196
Molecular characteristics 196
CASPR2-Kv1 interactions 197
CASPR2 mutations in animals 199

CASPR2 mutations in humans 200
CASPR and contactin 201
CASPR3, 4 and 5 201
CONTACTIN-2/TAG-1 201
Molecular characteristics 201
Contactin-2/TAG-1 mutations in animals 202
Contactin-2/TAG1 polymorphisms and antibodies in humans 203
LGI1 (LEUCINE-RICH GLIOMA INACTIVATED 1) 204
Molecular characteristics 204
Lgi1 mutations in humans 206
Lgi1 mutations in animals 207
VGKC-COMPLEX ANTIBODY ASSOCIATED CLINICAL SYNDROMES 208
CASPR2-antibodies 208
Lgi1-antibodies 210
No antibody group 210
PATHOPHYSIOLOGY OF CASPR2, LGI1 AND CONTACTIN-2 ANTIBODY ASSOCIATED DISEASES 213
A 'systems' perspective 214
A molecular perspective 218
Novel phenotypes generated by novel pathological mechanisms 219
FUTURE DIRECTIONS 220
Basic biology 221
Clinico-scientific questions 222
REFERENCES 224
APPENDIX 1: N-METHYL-D-ASPARTATE ANTIBODY ENCEPHALITIS: TEMPORAL PROGRESSION OF CLINICAL AND PARACLINICAL OBSERVATIONS IN A PREDOMINANTLY NON-PARANEOPLASTIC DISORDER OF BOTH SEXES 244
APPENDIX 2: N-METHYL-D-ASPARTATE RECEPTOR ANTIBODIES IN PEDIATRIC DYSKINETIC ENCEPHALITIS LETHARGICA 262

ABSTRACT

DPHIL THESIS: ANTIBODY TARGETS IN AUTOIMMUNE ENCEPHALITIS
By SAROSH R IRANI, SOMERVILLE COLLEGE, TRINITY TERM 2010

Voltage-gated potassium channel antibodies (VGKC-Abs) have been described in a spectrum of immunotherapy-responsive neurological diseases. These include neuromyotonia (NMT), a peripheral nervous system disease, limbic encephalitis (LE) a central nervous system disease, and Morvan's syndrome which affects both the peripheral and central nervous systems. Occasionally, these diseases can be associated with tumours. VGKC-Abs are defined by their ability to precipitate VGKCs from 2% digitonin-solubilised rabbit brain membranes labelled with ^{125}I-α-dendrotoxin. α-dendrotoxin is known to bind Kv1.1, 1.2 and 1.6. We asked whether the clinical heterogeneity could be explained by the specificity of the patient antibodies for the different Kv1 channels.

We received clinical data regarding 113 VGKC-antibody positive cases: 78 had LE/Epilepsy, 17 had NMT, 13 had MoS and five had other syndromes. In addition, we collected clinical data about 26 patients with a unique form of dystonic epilepsy in association with VGKC-Abs.

Surprisingly, a series of biochemical and immunohistochemical experiments in both brain tissue and in Kv1-transfected cells showed that potassium channels were the target of only 3% of the 113 'VGKC'-Ab positive sera. We proposed that the 'VGKC'-antibodies were not directed against Kv1s but against other proteins in the ^{125}I-α-dendrotoxin labelled rabbit brain complexes.

Lgi1 (leucine-rich glioma inactivated 1), CASPR2 (contactin-associated protein 2) and contactin-2 were found within these complexes and, when individually expressed in a heterologous mammalian cell line, were found to be the direct target of the 'VGKC'-Abs. Lgi1-antibodies were found in 58% of the cases with LE/Epilepsy, 71% of the dystonic epilepsy patients and 15% of the MoS cases. By contrast, CASPR2 antibodies were found in 85% of the MoS, 61% of the NMT and 12% of the LE/Epilepsy cases. CASPR2 antibodies had a 99% negative predictive value for the presence of an underlying tumour. Contactin-2 antibodies were found uniquely in 2 of 113 cases.

These findings describe novel antigenic targets which help to explain the clinical heterogeneity seen in 'VGKC-complex'-antibody associated diseases. In addition, they offer a method to predict the cases with underlying tumours. These findings have important implications for understanding the biology of these diseases.

CHAPTER ONE: INTRODUCTION

Although many diseases are known to be associated with autoreactive antibodies, only the minority of such antibodies are thought to be directly pathogenic. Since the 1970s, it was known that peripheral nervous system diseases, such as myasthenia gravis (MG) and Lambert-Eaton myasthenic syndrome (LEMS) have clear associations with pathogenic antibodies, at least in a significant number of cases. MG and LEMS patients often improved dramatically with immunotherapies. Within the central nervous system, a number of conditions such as multiple sclerosis, some cerebellar ataxias and stiff-person syndrome were known to respond to various immunomodulatory therapies. However, none of these have clearly defined pathogenic antibodies. Hence, the area of central nervous system (CNS) antibody-mediated, immunotherapy-responsive syndromes is a newly evolving field. Very recently, a number of potentially pathogenic antibodies have been proposed.

Koch's postulates

Microbiological pathogenicity has long been defined by Koch's postulates. The translation of Koch's postulates to autoimmune diseases resulted in Witebsky's criteria in 1957 (modified by Rose and Bona, 1993). These are listed and discussed below with reference to autoantibody pathogenicity.

1. An autoimmune response should be recognised in the form of an autoantibody (or cell-mediated immunity).

2. The corresponding antigen should be defined.
3. An analogous autoimmune response should be induced in an experimental animal.
4. The immunised animal should also develop a similar disease.

Koch's original criteria required an all-or-nothing response, for example transfer of the organism *must* always produce a disease. The relative lenience seen in Witebsky's criteria reflects an appreciation of the other factors which may modulate disease susceptibility such as genetic background of an individual. Indeed, there are clear examples of HLA-dependent susceptibilities to autoimmune diseases, as seen in multiple sclerosis and MG. Even in diseases where antibody-mediated pathology is undoubted, such as MG, there is no correlation between individual antibody titres and relative severity of disease: other factors and thresholds must play a role.

Although criterion 1 is irrefutable, it may be supplemented by the observation that complement deficiencies (notably C1q) are seen in patients with systemic lupus erythematosus (SLE), suggesting that other immunological components may also determine autoimmune susceptibility. The second criterion is clearly of great interest. The native distribution of the antigen may determine the likely anatomical sites of the pathology and may inform potential mechanisms of disease. Furthermore, knowledge of the precise antigenic target is needed to measure specific antibody levels. However, this does not seem necessary to determine antibody pathogenicity as even without this knowledge an IgG-fraction could surely be shown to cause disease. Of greater

importance to this question of pathogenicity is the extracellular nature of the antigenic epitope as an absolute necessity for the antibody to directly modulate the target antigen.

The final two criteria require an animal model of the disease. The concepts of passive and active immunisation have been used to study a variety of diseases, not least MG and LEMS. Passive immunisation involves immunoglobulin transfer to an experimental animal, whereas active immunisation transfers the putative antigen. Successful evidence for passive transfer may be augmented by transplacental immunoglobulin transfer and subsequent development of neonatal disease. If physiological concentrations of antibody were generated, both these concepts would lend strong weight to the potential pathogenicity of the antibody. The active immunisation model also allows a role for cell-mediated mechanisms. Maintenance of the active immunogen in its native conformation may be important for successful development of a disease. Despite the utility of Witebsky's criteria, two other types of study seem equally informative.

Human studies performed to examine antibody levels during clinical therapies have informed our understanding of these illnesses. The correlation over time between antibody levels and clinical state in an individual are very useful both to the clinician and to understand the relevance of the autoantibody response. Maybe the most marked effect is seen after plasma exchange (PEx) or even after absorption of specific antibodies against their immobilised antigenic target. Particularly with CNS diseases, given differences in assessment of cognitive function and quality of life between humans and mice, detailed studies in individual cases with sequential cerebrospinal fluid (CSF) -

serum antibody titres and T/B cell studies may highlight a further potential criterion. Finally, the *in vitro* assessment of antibody pathogenicity may offer a complementary technique to the in vivo approach.

The paradigms of myasthenia gravis and Lambert-Eaton myasthenic syndrome

An accumulation of clinical and scientific evidence have showed that MG and LEMS are antibody-mediated autoimmune illnesses of the peripheral nervous system. These diseases of the neuromuscular junction produce a subacute onset of weakness, good responses to immunotherapies (notably PEx), commonly associate with underlying distant malignancies (thymoma and small cell lung carcinoma, respectively) and other autoimmune diseases and often associate with specific HLA-haplotypes (reviewed by A Vincent, in Antel et al, Clinical Neuroimmunology, 2nd edition). Radioimmunoassays have allowed quantitative detection of serum autoantibodies against the skeletal muscle acetylcholine receptor (AChR) and nerve terminal voltage-gated calcium channel (VGCC; P/Q-type), respectively. These were excellent candidate antigens due to their relatively unique localisation at the regions of pathology and their functional importance in determining muscle excitability. Passive transfer animal models have shown these autoantibodies can reproduce the principal electrophysiological changes seen in the patients and can induce structural pathological effects at the neuromuscular junction. The main mechanisms were antibody-mediated protein downregulation and complement fixation by the bound antibody (in MG). In MG, immunisation with AChRs has been shown to reproduce these electrophysiological and morphological abnormalities. Hence, these two diseases fulfil Witebsky's criteria.

Neuromyotonia: clinical features

Neuromyotonia (NMT, Isaac's syndrome) is an immunotherapy-responsive peripheral nerve hyperexcitability (PNH) syndrome due to spontaneous and continuous muscle fibre contractions (Newsom-Davis and Mills 1993; Maddison 2006). Patients complain of muscle twitching and stiffness (90%), cramping (70%) and more rarely weakness. The disease has a chronic onset and symptoms are variable, often over a period of months. Occasionally, muscle hypertrophy can occur and is thought to be secondary to continuous muscle activity. Successful treatment with antiepileptics or prednisolone have been reported to reverse the hypertrophy (Zisfein et al 1983). Other features may include pseudomyotonia (delayed relaxation; 30%), sensory features (particularly paraesthesiae), increased sweating and some central nervous system features such as delusions and hallucinations. The hyperhidrosis may be due to generalised increased muscle activity or sudomotor nerve dysfunction, although the latter has never been specifically examined. Limbs are sites of disease in all patients, with lower limbs more commonly affected than upper limbs (Hart et al 2002). Not uncommonly the facial and bulbar musculature may also be involved. More rarely, trunk and laryngeal muscles are affected. The clinical predilection for distal muscles, in addition to electrophysiological data which showed most neuromyotonic discharges were found in the distal lower limbs muscles, suggested the disease originated within the peripheral arborisations of the motor nerves (reviewed by Maddison 2006). Consistently, sleep, general anaesthesia and local anaesthesia to the proximal brachial nerves did not affect the neuromyotonia whereas curare abolished the phenomenon. Only a few reports have suggested a more proximal localisation. Hence, it

seems likely that in the majority of cases neuromyotonic discharges are generated at the motor nerve terminals.

Neuromyotonia: electrophysiological features

The electromyographic observations included spontaneous continuous irregular motor unit discharges occurring in high-frequency runs known as doublets or multiplets (>2). These discharges characteristically have a high interburst frequency (30-300 Hz) and occur at irregular intervals (0.1 to 30 seconds). These discharges may be induced with electrical nerve stimulation or with voluntary contraction. Characteristic discharges may be detected without visible twitching (Newsom-Davis and Mills 1993). Such electrical appearances are also seen with motor neuron disease, spinal muscular atrophy, Guillian-Barré syndrome, certain drugs (such as gold and oxaliplatin) and toxins (such as alcohol and insecticides; Hart et al 2002).

Is neuromyotonia also an autoimmune disease?

Akin to MG, NMT has a clear association with autoimmune diseases (including rheumatoid arthritis, lupus, systemic sclerosis, Guillian-Barré syndrome, hyper/hypothyroidism, vitiligo) and malignancies (thymomas and lung carcinomas, in particular). As with MG, D-penicillamine can induce NMT with subsequent drug withdrawal coinciding with disease amelioration (Reeback et al 1979). These observations suggested NMT had an autoimmune basis and prompted PEx in an attempt to clear potentially pathogenic antibodies, where antiepileptics were unsuccessful. Three studies reported cases in which PEx clearly reduced the spontaneous discharge rate and

left six patients symptom free for a few weeks (Sinha et al 1991; Newsom-Davis and Mills 1993; Shillito et al 1995). These initial observations prompted passive transfer of NMT-patient serum and purified IgG to mice. Although no spontaneous activity was noted, the mice administered test IgG showed a nerve-diaphragm preparation with resistance to the blocking action of D-tubocurarine (Sinha et al 1991; Shillito et al 1995).This observation considerably strengthened the hypothesis of a humoral-autoimmune basis for the NMT.

Voltage-gated potassium channel antibody (VGKC-Ab) assay

Mutations in Kv1.1 were known to cause episodic ataxia with myokymia (Browne et al 1994, see below for more details). This genetic observation, the concept of nerve terminal hyperexcitability secondary to reduced repolarisation capacity generated by Kv1 blockade and the blood-nerve barrier-deficient Kv1-rich distal nerve terminal arborisations cumulatively led to the hypothesis that antibodies targeted the Kv1 channels. Hence, iodinated alpha-dendrotoxin was used to establish a radioimmunoassay to detect voltage-gated potassium channel antibodies.

Alpha dendrotoxin (αDTX, also known as DTXi) is a small molecule (7kDa, 59 amino acids) derived from the venom of the Green mamba (dendroaspis angusticeps), which binds the pore region of three Kv1s: Kv1.1, 1.2 and 1.6 (see below for more detailed molecular descriptions). αDTX has highest affinity for Kv1.2>1.1>1.6. A 1:1 ratio of αDTX binding to a Kv1 heterotetramer is well-established after mutagenesis experiments showed that all four Kv1 alpha-subunits are required for creation of the high-affinity

αDTX-binding site (Tytgat at al 1995). These Kv1 proteins are also 3-4 diaminopyridine (3,4-DAP) sensitive. DTXk is a Kv1.1 selective blocker and margatoxin is a selective blocker of Kv1.2 and 1.3.

Based on the evidence above suggesting Kv1s were the targets of NMT IgG, a specific radioimmunoprecipitation assay was established which utilised αDTX (Shillito et al 1995; Hart et al 1997). Using human cerebral cortex membranes extracted in 1% digitonin as a source of Kv1s, three of six NMT patients were found to have raised levels (Shillito et al 1995). Remarkably, this assay has not been significantly modified since its original description. Detergents which were more 'harsh' than digitonin (Privé 2007) did not allow efficient αDTX precipitation (A Vincent, unpublished observations). 5µl of patient serum was used as a screening test where 5µl saturates precipitation. Titres were subsequently determined using 1µl of serum, on the linear part of the titration curve (see Chapters 2, 3 and 4 for details). Later it was established that around 2 - 5% of elderly subjects have VGKC-Ab titres of 100 – 400 pM (Vincent et al 2004).

VGKC-ANTIBODY ASSOCIATED CLINICAL SYNDROMES

The spectrum of peripheral nervous system hyperexcitability

The quantitative determination of serum VGKC-Abs and the autoimmune / neoplastic associations of neuromyotonia were studied with respect to the apparent expansion in the clinical spectrum of 'NMT-like' syndromes. Terms such as cramp-fasciculation syndrome (CFS), peripheral nerve hyperexcitability (PNH), Isaac's syndrome and generalised myokymia were used alongside neuromyotonia. However, the patients with

CFS were anecdotally considered to be those with less severe and more localised features. In a study designed to address whether this spectrum of disorders shared a common pathogenesis, Hart et al (2002) compared clinical and electromyographic features in 60 patients: 42 with and 18 without the presence of neuromyotonic electrical discharges. They concluded that despite EMG distinctions, both groups shared features characteristic of autoimmune diseases, including underlying neoplasms and associated autoimmune disorders, with similar frequencies. However, these features were non-significantly, but rather consistently, commoner in the 42 cases with electrically proven neuromyotonic discharges. Nevertheless, this study suggested a common immunopathogenesis to the PNH-spectrum of diseases. Of future relevance, around 25% of the 60 patients with neuromyotonia had cognitive/psychiatric features and the two with the most severe features had the highest VGKC-Ab titres. However, the question of whether detection of VGKC-antibodies predicted a better response to immunotherapy was never answered.

MORVAN'S SYNDROME

Morvan's syndrome (MoS) was named after an early description, in a male patient, of peripheral nerve hyperexcitability (cramping, weakness and irregular muscular contractions) associated with dysautonomia, insomnia and fluctuating delirium. A French physician, Augustin Marie Morvan, named the syndrome 'la chorée fibrillaire' (Morvan 1890). The index case died five weeks into a very severe disease. Since, some cases of contemporary Morvan's may have been overlooked. For example, cases of NMT with additional features such as dysautonomia and insomnia may not have been termed

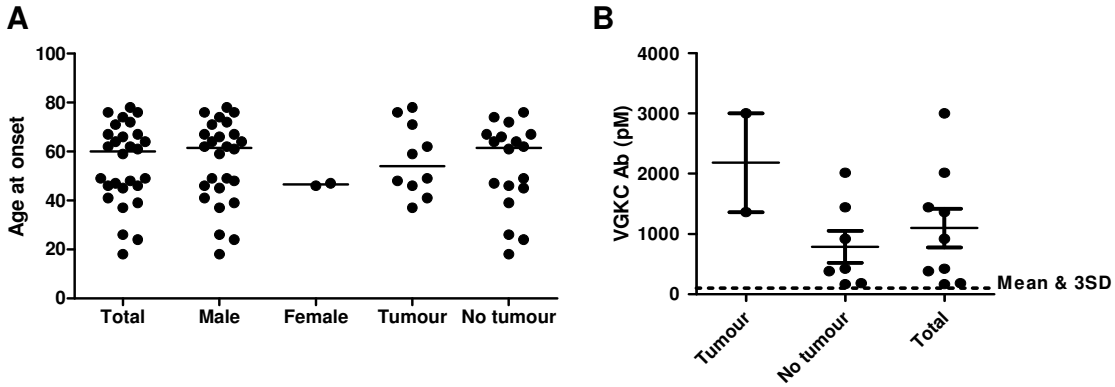


Figure 1.1 A and B. Morvan's cases published in the English literature. Age (A) and VGKC-antibody titre (B, pM) divided by sex (A) and presence of tumour (A and B). Dotted line at 100 pM represents the mean plus three standard deviations from healthy controls (Vincent et al 2004).

Morvan's. Hart et al (2002), as described above, noted some cases with psychosis, hallucinations and other cognitive features but did not use the term Morvan's. In addition, Heidenreich and Vincent (1998) described a case in which a malignant thymoma was associated with myasthenia gravis, neuromyotonia, hallucinations and disorientation with only one reference to 'Morvan's' within this article. Similarly, cases with limbic encephalitis (LE) have been described with autonomic disturbances or sleep difficulties (see detailed account below). It is this spectrum of diseases and their association with VGKC-Abs which this thesis has explored.

A Pubmed search for "Morvan's", limited by available full text and English language, generated 36 hits: nine were reviews, without novel clinical data, and nine were irrelevant articles (which described limbic encephalitis (Takahashi et al 2008, Sekiguchi et al 2008), alcohol related insomnia (Plazzi et al 2002), an environmental study in Morvan's National Park (Azimi et al 2003), syringomyelia (Fletcher 1910, Pernet 1917, Yealland 1925, Holley 1947) and which detailed no clinical features (Kleopas et al 2006)). In

addition, a search of 'Morvan syndrome' (using the same constraints) generated 46 hits, of which only five were reports of cases with MoS without replication of the above papers. The reference lists from these papers generated one other relevant paper (Halbach et al 1987). Overall, the 24 relevant papers, discussing 28 cases of MoS, are reviewed below and summarised in Table 1.1 and Figure 1.1A and B (Vernay et al 1986; Halbach et al 1987 (n=2); Haug et al 1989; Madrid et al 1996 (n=2); Schott et al 1996; Agius et al 1998; Lee et al 1998; Maselli et al 1998; Barber et al 2000; Liguori et al 2001; Cottrell et al 2004; Josephs et al 2004 (n=2); Loscher et al 2004; Deymeer et al 2005; Vetrugno et al 2005; Bajaj and Shrestha 2007; Diaz-Manera et al 2007; Hudson et al 2007; Winger et al 2007; Goldberg 2008; Spinazzi et al 2008; Toosy et al 2008; Donadio et al 2009 (n=2); Rinaldi et al 2009).

The aetiology of Morvan's syndrome

In much of the early literature, MoS was attributed to heavy metal intoxications such as mercury, manganese and gold (Vernay et al 1986; Haug et al 1989). Given similarities between the acrodynia of mercury poisoning and the painful peripheral symptoms in MoS, this hypothesis may require further investigation. However, very few reports show raised cerebral heavy metal levels. For example, Haug et al (1989) report manganese poisoning with a serum manganese level of 10.8ng/ml (where the normal range is <5), but cerebral manganese concentrations were normal.

By contrast, Madrid et al (1996) were the first to report the successful use of PEx in MoS. The second case in this article was only treated with PEx, with great success. This observation, and the association with NMT and thymomas (see Table 1.1), suggested a

	FREQUENCY (%)
Male	**26 (93%)**
Age (median and range)	**60 (18-78)**
Tumours	**10 (36%)**
Thymoma	6 (21%)*
Medullary thyroid	1 (4%)
Non small-cell lung	1 (4%)
Prostate adenoma and sigmoid polyp	1 (4%)
Dysautonomia	**27 (96%)**
Hyperhidrosis	26 (93%)
Anhidrosis	1 (4%)
Tachycardia	14 (50%)
Hypertension	8 (29%)
Constipation	6 (21%)
Diarrhoea	3 (11%)
Urinary urgency/incontinence	6 (21%)
Urinary retention	2 (7%)
Hypersalivation	3 (11%)
Hyperlacrimation	1 (4%)
Fever	3 (11%)
Hypothermia	1 (4%)

	FREQUENCY (%)
Dysomnia	**27 (96%)**
Insomnia	26 (93%)
Hypersomnia	3 (11%)
Dream reenactment	5 (18%)
REM sleep behaviour disorder	1 (4%)
Peripheral nerve features	**22 (79%)**
Painful / burning legs	12 (43%)
Back pain (severe)	1 (4%)
Peripheral neuropathy	18 (64%)
Cognitive features	**27 (96%)**
Hallucinations	16 (57%)
Confusion / delirium	14 (50%)
Delusions	8 (29%)
Amnesia	6 (21%)
Anxiety	5 (18%)
Executive dysfunction	5 (18%)
Seizures	**4 (14%)**

Table 1.1. Summary of clinical details of the 28 cases of Morvan's syndrome from English literature. * one unspecified mediastinal tumour has been classified as a thymoma

more probable aetiology was autoimmune. Subsequently, Lee et al (1998) were the first to report raised VGKC-Ab levels in the serum of MoS patients although neither a description of the assay nor quantitative data were shown. Below, the clinical features associated with MoS from all the cases in the English literature are reviewed.

Demographics of Morvan's syndrome

Of the 28 identified cases in the English literature since 1986, remarkably 26 (93%) were male. Median age of onset was 60 years overall: 61.5 in males and 46.5 in the two females. Ages were not different between cases with and without tumours (Figure 1.1A). Cases were reported from ten different countries: Austria (n=1), France (n=2), Germany (n=3), Italy (n=6), Nepal (n=1), New Zealand (n=1), Spain (n=3), Turkey (n=1), United Kingdom (n=2) and United States of America (n=8). These regional differences may represent a genetic or environmental contribution to the aetiology of MoS or simply reflect reporting biases. However, in only three cases were ethnic backgrounds of cases stated: Italian, Bangladeshi and Nepalese.

Tumours and autoimmune conditions in MoS

Tumours were found in ten cases (36%) and included six thymomas, one with an unspecified mediastinal tumour (Donadio et al 2009), medullary thyroid carcinoma, non-small cell lung cancer and one patient with both a prostate adenoma and sigmoid polyp. In five of the remaining 18 cases, body imaging was not specifically mentioned. Thymomas (and the mediastinal tumour) were present only in the reported cases that

were less than 63 years of age. In the older cases, the non-thymomatous tumours were detected. The two females had no tumour detected.

Autoimmune disease associations were seen in 12 (43%) and included MG (n=5), diabetes (n=2), psoriasis, hypothyroidism, rheumatoid arthritis, pulmonary fibrosis and polyarthrosis and pulmonary hyalinising granulomae. Twenty-six patients had neuromyotonic discharges demonstrated on EMG, one only had fasciculations and EMG results were not provided in one case. The most unique features of MoS have been attributed to sympathetic overactivity and have been termed agrypnia excitata (insomnia; motor and autonomic hyperactivity; Donadio et al 2009): these will be addressed first.

Clinical features of Morvan's syndrome

Dysautonomia

Hyperhidrosis was the single commonest autonomic feature, reported in 26 of 28 (93%) cases including the ten cases with tumours. One case also showed areas of anhidrosis. Fourteen cases (50%) had cardiac abnormalities: these always included tachycardia, three had arrhythmias (decreased R-R interval and supraventricular extrasystoles reported) and two had angina/chest pain. Eleven cases had blood pressure abnormalities which included hypertension (n=8), postural hypotension (n=3), syncope (n=3) and labile blood pressure (n=2). Two cases had hypertension and syncope while one had hypertension and a postural drop. Only two cases with blood pressure abnormalities did not have a tachycardia. Constipation was reported in six cases, diarrhoea in three (one of whom also had constipation: Lee et al 1998). Bladder symptoms were recognised in eight cases: two

with retention and six others with incontinence/urgency/frequency. One case had both retention and frequency/urgency (Lee et al 1998). Four cases described impotence. Three cases showed hypersalivation whereas only one case showed hyperlacrimation. Three cases had a fever and one had a low body core temperature. One case was said to have died from thermoregulatory failure. Eleven had weight loss and six had a reduced appetite. Five of the 11 (45%) had a tumour detected. Ten cases described fatigue as a prominent feature. Eleven cases with skin lesions are included within the dysautonomic features as a vasoactive mechanism and/or skin follicle damage secondary to the hyperhidrosis is their probable aetiology. Indeed, miliaria – the consequence of the latter mechanism – was histologically diagnosed in one case studied in great detail (Liguori et al 2001). Eight cases suffered from pruritis/itching, three showed erythema, two with scaly skin and one had a swollen hand. One patient had a vescicular rash on their leg and arms.

The two cases without hyperhidrosis were atypical. Both cases had no/limited autonomic features (one had some constipation) and positive VGKC-Abs (380 pM and quantification not stated). One had EMG-evidence of diffuse fasciculations (not neuromyotonic discharges), confusion, constipation as their only autonomic feature, ataxia and 475/mm^3 lymphocytes in their CSF (Hudson et al 2007). The other case had EMG-proven NMT with psychosis and seizures (Goldberg 2008). Many of these observations are unusual in MoS (see below). Limiting the definition of MoS to cases with hyperhidrosis may therefore miss some seropositive cases with consistent cognitive features.

Dyssomnia

Sleep disturbances were noted in all but one case (Winger et al 2007). Twenty-six of 28 (93%) cases suffered from insomnia: the two outstanding cases were different from the two without hyperhidrosis. Daytime hypersomnolence was a rare feature seen in only three cases, all of whom also had insomnia and was therefore, at least in part, likely to be compensatory. Eight cases had complex sleep behaviours most commonly including dream reinactment (n=5). One case had REM-sleep behaviour disorder. The case from Vetrugno et al (2005) was described in limited detail because the article reporting this case focused on detailed sleep structure/pattern analysis in five patients with NMT (two with KCNA1 mutations and two with raised VGKC-Abs) and one with MoS (and raised VGKC-Abs) (Vetrugno et al 2005). They used detailed polysomnography to show very few sleep abnormalities in the NMT cases with florid disruption of sleep structure in the case of MoS. By contrast, the EMG discharges were not especially different between the six patients, suggesting that the muscle hyperactivity alone was not sufficient to severely disrupt sleep, as seen in MoS.

Pain

Pain was reported commonly, 12 cases described painful (often burning) sensation in the legs or joint pains (n=2) or severe back pain (n=1). Eighteen patients (64%) had clinical or electrophysiological evidence of a peripheral neuropathy. This is significantly more common than in cases with NMT (Hart et al 2002), maybe suggesting that the damage to distal nerves is more severe in MoS than in NMT.

Neuropsychiatric features

Only one case was reported without clear higher cognitive features, and this case was reported only briefly but did have insomnia and raised VGKC-Abs (Vetrugno et al 2005). Higher cognitive features included confusion / delirium / disorientation (n=14), agitation (n=10), delusions (n=8), amnesia (n=6), anxiety (n=5), executive dysfunction (n=5), personality changes (n=2), cognitive impairment (n=2) and increased aggression (n=1). Clearly, many of these features were present in any one individual. In all, 16 (57%) cases suffered with hallucinations: four visual and auditory, nine visual only and three unspecified.

Brain imaging

Despite the high frequency of clear, often multiple, CNS features only two MR/CT brain images were clearly abnormal, showing medial temporal lobe changes. These two cases were two of only four cases with seizures. The presence of medial temporal lobe high signal, may have prompted one of the authors to include in the title of their paper "Morvan's-Like Syndrome", not Morvan's per se (Deymeer et al 2005). Six cases had age related changes (n=3), small vessel disease (n=2) or generalised cerebral atrophy (n=1).

PET imaging did disclose abnormalities in three patients without abnormalities on more conventional imaging. Basal ganglia hypermetabolism, biorbitofrontal and left medial temporal hypometabolism, in addition to hypometabolism of the left inferofrontal /

temporal and bilateral anterior temporal regions, were observed (Josephs et al 2004; Spinazzi et al 2008, Toosy et al 2008).

Seizures, movement disorders and other features

All four cases with seizures were found within the five cases with abnormal MR or PET imaging. By contrast, none of the cases with normal imaging had seizures (Fisher's t test, p=0.0002). Furthermore, tumours were not found in the cases with seizures (Fisher's t test, p=0.13). These observations suggest an epileptic subgroup, possibly with a different causative mechanism. EEG data were reported in 17 cases: nine showed slow waves, two showed epileptic features and seven were normal.

Four cases reported myoclonus or focal spasms: one was phenytoin-responsive and one provoked by startle. These may well represent the dystonic seizures we have recognised in VGKC-Ab positive patients (Irani et al 2008, Chapter 3). Other features included respiratory failure / hyperventilation/dyspnoea (n=7), dysarthria (n=5), gait abnormalities (n=4), tremor (n=1), piloerection (n=1) and hyperphagia (n=1).

Seropositivity and blood results

VGKC-Abs were positive in 14 of the 18 patients tested, suggesting a seronegative Morvan's rate of around 22%. Of those five cases with MRI/PET abnormalities, four had raised VGKC-Ab levels and the fifth only had antibodies tested after treatment. This may represent an 'overlap' with limbic encephalitis, as LE cases often have the highest VGKC-Ab levels. VGKC-Ab levels were higher in the cases with tumours although only two such cases were available (Figure 1.1B).

MoS cases often show some peripheral inflammatory response with a raised ESR (n=7), raised CK (n=7), raised CRP (n=2) and thrombocytosis (n=1) reported. Maybe this represents a cytokine storm or tumour response in the often very ill Morvan's cases.

Outcomes

Although outcomes were very difficult to generalise from case reports, a few observations emerged. Three of the five cases not given immunotherapy showed some often complete, albeit prolonged, recovery (Vernay et al 1996; Barber et al 2000; Josephs et al 2004 (case 2)), whereas the two other cases that did not receive immunotherapies died (Halbach et al 1987 (Case 2); Haug et al 1989). However, sudden deaths were also described in two more recently described patients who did receive immunotherapies (Liguori et al 2001; Hudson et al 2007). PEx seemed to be the most effective therapy and prednisolone was considered to be of real value too. Responses to intravenous immunoglobulins (IvIg) were relatively disappointing. In two cases treatments were not detailed.

From MoS to limbic encephalitis

Soon after the association of VGKC-Abs with MoS, it became clear that a number of patients with a purely central nervous system syndrome – limbic encephalitis (LE) – also had high VGKC-Ab levels (Buckley et al 2001; Schott et al 2003; Vincent et al 2004; Thieben et al 2004; Tan et al 2008). The origins of LE are discussed below.

PARANEOPLASTIC SYNDROMES WITH PARTICULAR REFERENCE TO LIMBIC ENCEPHALITIS

The concept of paraneoplastic disease first arose in the 1950s with reference to patients with multiple, mainly sensory, neuropathies and suspected malignancies without detectable metastatic deposits. The term is still used to describe diseases dependent on the presence of a tumour but whose manifestations are distant to any detectable tumour and therefore without metastases in areas of pathology. Tumours frequently associated with these diseases express neuroendocrine cells (small-cell lung cancer, neuroblastoma, testicular germ-cell), contain neural tissue (teratomas) or affect organs with immunological actions (thymomas, lymphomas). Around 3-5% of patients with small-cell lung cancer (SCLC) and 15-20% with thymomas have associated neurological syndromes. As reviewed in detail by both Darnell and Posner (2003) and by Dalmau and Rosenfeld (2008), paraneoplastic syndromes are usually thought to be mediated by a predominantly T cell mechanism, where the antibodies are useful diagnostic markers but are raised against intracellular, and hence inaccessible, epitopes. More rarely, antibodies may target membrane bound cell-surface antigens. The target antigens of either the antibodies or T cells are commonly expressed within the tumours, suggesting this loss of tolerance initiates the immunological response. On this basis, MG and LEMS are two syndromes that can have a paraneoplastic aetiology. The characteristics of the paraneoplastic antibodies, their associated clinical features and syndromes are presented in Tables 1.2 and 1.3. In brief, these antibodies are all against intracellular antigens, very commonly associated with underlying tumours and their titres correlate poorly with the rare clinical improvements. Passive transfer experiments have never demonstrated pathogenicity of these antibodies in animals. These antibodies are therefore considered to

be functional ‘bystanders’ but may be useful diagnostic markers. Recommended clinical diagnostic criteria for paraneoplastic syndromes were published by the PNSEURONET consortium (www.pnseuronet.com; Graus et al 2004).

Antibody	Associated clinical syndrome	Commonly associated tumours	Immunohistochemistry	Western blot band size
Anti-Hu * (ANNA-1)	Limbic encephalomyelitis, sensory neuronopathy, cerebellar degeneration, dysautonomia	SCLC; neuroblastoma; prostate	All neuronal nuclei and weak cytoplasmic staining. Spares nucleolus.	35-40kDa
Anti-Ma2* (Anti-Ta)	Limbic – brainstem encephalitis in young men	Testicular (germ cell); non-SCLC	Subnuclear and cytoplasmic neuronal staining.	41.5kDa
Anti-CV2/CRMP5*	Limbic encephalomyelitis; cerebellar degeneration; sensory neuronopathy; chorea; optic neuritis	SCLC; thymoma	Oligodendrocyte and neuronal cytoplasm staining	66kDa
Anti-Ma*	Limbic – brainstem encephalitis in men and women	SCLC, breast, others (>variety than Ma2)	Subnuclear and cytoplasmic staining of neurons	40kDa
Anti-GAD 65*	Limbic encephalitis; cerebellar ataxia; stiff-person syndrome	Thymoma, breast, SCLC	Cytoplasmic staining of interneurons	65kDa
Anti-amphiphysin*	Encephalomyelitis; stiff-person syndrome	Breast; SCLC	CNS presynaptic terminals	128kDa
Anti-Tr	Cerebellar degeneration	Hodgkin's	Purkinje cell cytoplasm and dendrites	Unknown
Anti-Ri (ANNA-2)	Ataxia +/- opsoclonus-myoclonus; brainstem encephalitis	Breast; SCLC; bladder; gynaecological	All CNS neuronal nuclei and weaker cytoplasmic staining. Spares nucleolus	55 and 80kDa
Anti-Yo (PCA-1)	Cerebellar degeneration	Breast; ovarian; uterine; SCLC	Purkinje cell cytoplasm staining	62kDa

Table 1.2. Well-characterised paraneoplastic antibodies associated with central nervous system neurology: clinical, tumour and molecular characteristics. * = antibodies associated with encephalitis. SCLC = small cell lung cancer. GAD = glutamic acid decarboxylase.

Definite PND

1. Classic syndrome with cancer diagnosed within five years of neurological symptom development
2. Non-classic syndrome that resolves or significantly improves after cancer treatment without concomitant immunotherapy, provided that the syndrome is not susceptible to spontaneous remission
3. Non-classic syndrome with cancer diagnosed within five years of neurological symptom development and positive neuronal antibodies
4. Neurological syndrome (classic or not) without cancer and with well characterised antineuronal antibodies (Hu, Yo, CV2/CRMP5, Ri, Ma2 or amphiphysin)

Possible PND

1. Classic syndrome with high risk of cancer, without antineuronal antibodies
2. Neurological syndrome (classic or not) without cancer and with partly characterised antineuronal antibodies
3. Non-classic syndrome with cancer diagnosed within two years of neurological symptom development, without neuronal antibodies

These criteria were generated in 2004 when neurological antibody-associated syndromes – often regarded as classical, such as limbic encephalitis – were very commonly associated with underlying neoplasms. However, two simultaneously published VGKC-Ab limbic encephalitis papers showed that these neuronal antibodies are commonly

associated with no underlying tumour (Vincent et al 2004; Thieben et al 2004). These patients have a similar presentation to the paraneoplastic LE patients and, when examined, their limbic system shows a chronic lymphocytic encephalitis (Bien et al 2000). Therefore, definite criterion '4' should be extended to include VGKC-Abs: however, this will not commonly define a *paraneoplastic* neurological disease. The criteria of Bien and Elger (2007), albeit specific to limbic encephalitis, suggest updated definitions in light of these non-paraneoplastic observations. Bien and Elger show greater flexibility in their proposals of:

1. Recent onset (<5 years) clinical "limbic" syndrome with one of:
    a) Disturbance of memory
    b) Temporal lobe seizures
    c) Affective disturbance, typically loss of inhibition and lability of mood

2. Plus one of the following four:
    a) Tumour (within five years of onset)
    b) One well-characterised autoantibody (Hu, Ma/Ta, CV2, amphiphysin, VGKC, novel cell membrane antigens)
    c) Otherwise unexplained temporomedial T2/FLAIR signal increase
    d) Temporomedial chronic lymphocytic-micronodular encephalitis

These criteria now allow a diagnosis of limbic encephalitis in a larger number of patients within this spectrum of clinical features. Examples may include cases with isolated TLE

and VGKC-Abs, pure amnesia with VGKC-Abs, or labile mood with a subsequent tumour. These clearly raise questions about the frequency of LE-like syndromes and also about the value and validity of offering empirical immunotherapies to some of these cases.

LIMBIC ENCEPHALITIS – PARANEOPLASTIC ORIGINS

Limbic encephalitis (LE) was originally described by Brierley et al (1960), although Corsellis et al (1968) were the first to coin the term. In the first of these reports, the autopsy material showed prominent involvement of hippocampus, cingulate gyri, amygdala and uncus in all three cases, although more subtle involvement of the striatum, lateral temporal cortex and hypothalamus/thalamus were also recognised. These cases had a spectrum of well-characterised features including amnesia, temporal lobe seizures, psychosis, ataxia and headaches. The clinical and histological localisation of predominant pathology to the temporal regions was the most remarkable feature noted by the authors. Two patients had evidence of lung malignancies and it was stated that 'it seems unlikely that this finding is in any way related to the encephalitis but its occurrence should be noted.' The relevance of the carcinoma was recognised in a subsequent article that described three further cases by Corsellis et al (1968), probably at least in part due to the pioneering work of Lord Brain et al (1965). These publications set the trend for LE to be associated with malignancies, as emphasised in a major contemporary review of limbic encephalitis (Gultekin et al 2000). Of 50 patients fulfilling the definition of paraneoplastic limbic encephalitis, common neoplasms included those of the lung (50%), testis (20%), breast (8%), Hodgkin's lymphoma (4%), ovarian teratoma (4%) and

thymoma (2%). Other tumours included one adenocarcinoma of the colon and ovary, one chronic myeloid leukaemia and a plasma cell dyscrasia. The type of tumour correlated well with data from a simultaneously presented review of the English literature. Neurological features preceded the cancer diagnosis in 60% (by a median of 3.5 months). 57% of cases had limbic system signal change, particularly in the medial temporal regions. Over 80% of cases had abnormal CSF examinations including pleocytosis (around half of these), raised protein or oligoclonal bands. None of the patients had malignant cells in their CSF. Paraneoplastic antibodies were identified in 30 patients (60%): 18 with Hu and 10 with Ma2 antibodies. These patients had tumours associated with the respective antibodies as described in Tables 1.3 and 1.4. This review and the original papers described above meant that the LE-literature was dominated by paraneoplastic cases.

More recently, limbic encephalitis associated with VGKC-Abs and N-methyl D-aspartate receptor antibodies (NMDAR-Abs) have been described. The published cases would suggest that these two antibodies have approximately 20% and 56% rates of neoplasms, respectively. They will be summarised below with particular emphasis on the VGKC-Abs, as NMDAR-Abs are summarised in the published articles (Appendix 1 and 2).

	Classical paraneoplastic antibodies (Hu, CV2, Ma, Ma2, GAD, Amphiphysin)	VGKC antibodies	NMDA antibodies	Antibodies to novel cell membrane antigens
Intracellular or extracellular epitope	Intracellular	Extracellular	Extracellular	Extracellular
CSF pleocytosis	Common	Rare	Common	Common
Serum : CSF antibody titres	High	High (>50)	High (mean = 12 – see Appendix 2)	Unknown
Intrathecal antibody synthesis	Yes	No	Yes	Yes
Serum hyponatraemia	Uncommon (<5%)	Common (~50%)	No	No
Characteristic clinical features	Varying according to the antibody – see Table 1.2	REM-sleep behaviour disorder, dystonic seizures, neuromyotonia	Psychiatric onset, hyper/hypo-kinetic movement disorder	Typical limbic encephalitis
MRI findings*	MTL and more extensive cerebral hyperintensity	Bilateral, unilateral MTL signal hyperintensity. Can be normal.	Often normal but cortical/cerebellar/MTL hyperintensity described	Typical bilateral MTL hyperintensity
Paraneoplastic rate (%)	>80%	<20%	>50%	>50%
Commonly associated tumours	As described in Table 2	Thymoma and lung cancers	Ovarian teratomas	Various including SCLC, thymoma and pancreas
Response to tumour removal/immunotherapy	Poor except for around 35% of Ma2 patients	Good – excellent	Good – excellent	Good – excellent
Titre of antibodies after immunotherapy	Little fall / no change	Often dramatic fall	Often slower decrease	Fall
In vitro/vivo evidence for pathogenicity	Evidence suggests that these antibodies are not pathogenic	Little direct evidence in the central nervous system forms of the disease	Downregulation of surface NMDARs by antibodies	Downregulation of surface receptors by antibodies **

Table 1.3. Categorisation of antibodies in limbic encephalitis. * FLAIR/T2 imaging findings. MTL = medial temporal lobe. ** seen for AMPA subtype of the antibodies. SCLC = small cell lung cancer.

	Method used to detect VGKC antibody	Cell type used; mammalian?	Did the study directly examine Kvs? Which Kv1 was proposed as the target?	Was antibody binding to the cell surface visualised? ***	Were extracellular epitopes specifically examined?	Was denatured antigen assayed?	#NMT cases	Magnitude of effect
Shillito et al 1995*	Quantal content, end plate potential and spontaneous discharge measurements	Dissected peripheral nerve and dorsal root ganglion cultures; yes	No, but effects in intact nerve mimicked by 3,4 DAP. 3,4 DAP-sensitive Kvs.	No	Yes, assuming truly intact nerve preparation	No	6	2mV increase EPP amplitude above baseline of 21mV. Doubled duration of Aαβ current (1.5 to 2.9msec in tests). Repetitive firing in 9/13 (test) and 1/13 (control) recordings from DRG cultures.
Hart et al 1997	Immunocytochemistry and αDTX-labelled immunoprecipitations	Xenopus oocytes; no	Yes. Kv1.6.	No, intracellular epitopes overwhelm in sectioned oocytes	No, but could have been precipitated	No	12	Eight times above HC for KCNA6 and four times for KCNA2
Sonoda et al 1996*	Net K+ current	PC-12; yes	Yes, but little channel characterisation. Not stated.	No	Yes, intact cell electrophysiology	No	2	3-4 fold reduction in steady-state and peak currents after six hours incubation
Arimura et al 1997*	Denaturing Western blot	PC-12; yes	No, only show αDTX binding to denatured Kv-band; Not stated.	No, but show serum binds to the surface of PC12s	No, western blotting used	Yes	1	No band in one HC
Nagado et al 1999*	Patch-clamp	NB-1 and human Kv1.1/1.6 transfected CHO cells; yes	No, only IV plot to characterise channel. Not stated	No	Yes, intact cell electrophysiology	No	4	30-50% reduction in steady state and peak K+ current in NB-1 cells and Kv1.1/1.6 transfected CHO cells
Tomimitsu et al 2004*	Patch-clamp	NB-1 cells; yes	No characterisation of Kv current. Not stated	No	Yes, intact cell electrophysiology	No	4	Peak K+ current density reduced from mean of 27 to 17 mV
Kleopas et al 2006	Immunohistology and immunocytochemistry	HeLa cells and fixed mouse brain sections; yes	Yes, Kv1-transfected HeLa cells Kv1.2.	Yes, but most data shown from permeabilised cells	Yes, Kv1-transfected cells but most data shown from permeabilised cells	No. Infact no VGKC-Ab binding to denatured antigen	10**	Number of Kv1.1-expressing cells binding LE sera was 20-30 times above background. Number of Kv1.2-expressing cells binding NMT sera was often indistinguishable from the LE sera.

Table 1.4. In vitro and vivo VGKC-antibody studies. Important studies that have examined the characteristics of VGKC antibodies, only one study (Kleopas et al 2006) examined this outside the context of neuromyotonia alone. * = study not asking which Kv1 may be bound by patient sera. ** = only five of ten cases examined using brain sections. ***= immunocytochemistry or FACS. # = number of. HC = healthy control.

LIMBIC ENCEPHALITIS WITH VGKC-ABS: A PREDOMINANTLY NON-PARANEOPLASTIC, IMMUNOTHERAPY-RESPONSIVE DISEASE

Initial observations

The first report of two cases of VGKC-Ab associated LE was published in 2001 (Buckley et al 2001). One patient had a long history of MG and a recurrent metastatic thymoma, and the other had no significant past medical history. The patient with MG was treated using plasma exchange with substantial cognitive recovery. The second patient showed an almost complete spontaneous recovery of mental function with reduction in VGKC-Abs and did not have a detectable tumour. A second article showed that four of 15 patients with limbic encephalitis had VGKC-Abs (Pozo-Rosich 2003). Two had high VGKC-Ab levels (810 and 992 pM) without evidence of tumours. The other two had lower titres (170 and 300 pM) associated with a small-cell lung cancer and possible mediastinal lesion (defined on PET imaging). Three of these four patients showed a good response to immunotherapies while the other had a surprisingly long survival and therefore probably no tumour. The authors concluded that while VGKC-Abs could be associated with tumours, they may nevertheless predict a good immunotherapy response and outcome. However, these patients were collected from a centre with paraneoplastic expertise. Although these reports suggested associated autoimmune conditions and tumours were not uncommonly detected in VGKC-Ab LE, this has not been borne out in larger subsequent studies.

The two most informative larger studies, from groups in Oxford and at the Mayo clinic, were simultaneously published in 2004 and defined patients with a subacute onset of

amnesia, seizures and confusion as predominant clinical features. These patients tended towards very high VGKC-Ab titres (>400 pM). Vincent et al (2004) described ten patients with non-paraneoplastic LE with an immunotherapy-responsive serological response in the half of cases that received early steroids. This was less pronounced in those receiving late steroids or other immunotherapies (IvIg and/or PEx). Overall, six of ten cases were judged to have attained definite clinical improvement, only one showed no improvement: this clinical response broadly correlated with the serological findings. Although follow-up was too short to formally exclude underlying neoplasms, none of these patients have subsequently developed a tumour (Vincent A, unpublished observations). The simultaneous publication from the Mayo group highlighted many of the same features in seven patients (Thieben et al 2004) but two had histories of cancer: one with active prostate adenocarcinoma (aged 69) and one with a remote history of tongue carcinoma. These two malignancies are not commonly associated with paraneoplastic neurological conditions and the prostate carcinoma is not surprising in a 69 year old male. This study also recognised the potential for an excellent immunotherapy-response which correlated with a fall in serum VGKC-Ab levels and was especially successful in those receiving early immunotherapies (<2 months). Although more rarely than in Morvan's syndrome, some cases were noted to show autonomic dysfunction including hypersalivation and hyperhidrosis. This has been noted in subsequent reports (for example Tan et al 2008, Sekiguchi et al 2008). Similarly, insomnia has been infrequently observed in LE. Some cases were also reported to have more psychiatric symptoms such as anxiety, depression and hallucinations (Vincent et al 2004). These findings are very important in defining a predominantly non-paraneoplastic

syndrome with acute/subacute onset of confusion, amnesia and seizures and an often very good immunotherapy-response.

Clinical and paraclinical observations in VGKC-Ab associated LE

In both studies there was a clear male predominance (male to female ratios 9:1 and 5:2 in Oxford and Mayo, respectively), age range from the 40s to 70s (ranges 44-79 and 44-69 years, respectively), high incidence of MRI abnormalities demonstrating medial temporal lobe high signal bilaterally or unilaterally (which often exquisitely demarcated the hippocampus), high rates of plasma hyponatraemia (8/10 and 4/7 respectively; where assessed these were consistent with a pattern of inappropriate ADH secretion (SIADH)), no concomitant paraneoplastic antibodies detected and higher VGKC-Abs in serum than CSF. The latter highlights an important pathophysiological observation.

Thieben et al (2004) estimated cerebrospinal fluid levels of VGKC-Abs to be around 2% those of serum levels, although CSF VGKC-Abs were not detected in the patients with the lower serum VGKC-Ab levels. Vincent et al (2004) showed the same value to lie between 1 and 10%. Unmatched CSF oligoclonal bands were only detected in one patient in each study. The Mayo study showed normal CSF IgG index and IgG synthesis. These observations strongly suggested that the primary immune response is peripherally generated. The antibodies may subsequently diffuse into the CSF or be synthesised locally by B cells which have transmigrated the blood-brain barrier (BBB). Hence, these data may counter the traditional dogma of BBB impermeability to large molecules such as immunoglobulins (del Zoppo and Milner 2006).

The amnesia, predominant temporal lobe seizures, medial temporal lobe high signal and psychotic flavour of many cases of VGKC-Ab associated LE strongly suggested that the disease is centred upon the medial temporal lobe, and particularly the hippocampus. Hence, to further potential for antibody pathogenicity, the antibodies should bind to the hippocampus. This has been shown in many studies with absent hippocampal binding in post-convalescence serum samples (e.g. Buckley et al 2001; Ances et al 2005; Graus et al 2008).

While the 'core' phenotype of VGKC-Ab associated LE was now established, a number of small reports described cases within an extended spectrum of clinical features. Below, the less frequent observations will be briefly mentioned and the more substantial papers discussed in greater detail.

Seizures in VGKC-Ab associated LE

Seizures are clearly a prominent feature in VGKC-Ab associated LE and other autoimmune encephalopathies (reviewed in Vincent, Irani and Lang (2010)). One study examined a number of cases with various forms of epilepsies, including cases where an autoimmune basis was suspected. VGKC-Abs were detected in 16 of the 139 cases (11%, McKnight et al 2005). Ten of 16 had a good response to immunotherapies (five of these cases had limbic encephalitis and the highest VGKC-Ab titres) and the other cases did not undergo a trial of immunotherapies. Two cases were from a cohort of 67 with drug-resistant epilepsy and had a median age of onset of 14 years. This was particularly

interesting as very few children with VGKC-Abs have been identified. Subsequently, data from a separate cohort showed 6% of drug-resistant epileptics had low levels of VGKC-Abs (Majoie et al 2006). These observations have extended the VGKC-Ab spectrum to include cases with pure epilepsy, albeit often with low antibody titres.

Finally, a characteristic seizure semiology was identified in three patients with VGKC-Abs (Irani et al 2008; larger cohort described in more detail within Chapter 3). These patients had very brief, frequent dystonic form of antiepileptic-refractory epilepsy often with involvement of face and arm and an onset in late life. Immunotherapy produced a dramatic fall in VGKC-Ab levels with a simultaneous reduction in seizure frequency. Marked similarities exist between these cases and features described in cases from a number of VGKC-Ab publications from a number of different authors (for example Park et al 2007, Toosy et al 2008, Geschwind et al 2008, Barajas et al 2009).

Dysomnia in VGKC-Ab associated LE

One interesting study described five of six VGKC-Ab associated LE cases with rapid eye movement sleep behaviour disorder (REMSBD, Iranzo et al 2006). This remarkably high proportion may be due to the sleep interest of the centre which identified the patients. REMSBD resolution paralleled the fall in VGKC-Abs in three patients. Many of the features associated with VGKC-Ab LE in the previously described studies were again observed and included hyponatraemia, an immunotherapy-response, temporal lobe MRI changes and an absence of neoplasms. One interesting unanswered question is how the pathophysiology of these sleep alterations relates to those seen in the Morvan's cases and

whether this may be a discrete avenue to study whether antibody specificities define the development of Morvan's in 'preference' to LE or NMT.

An expanded clinical spectrum: VGKC-Ab associated CNS features

Another small series of four patients described severe hypothermia (<35˚C) in the context of VGKC-Ab associated LE (Jacob et al 2008). One case also had severe neuropathic pain, reminiscent of that seen in some cases of Morvan's syndrome. Again, features including normal CSF parameters, hyponatraemia, dysautonomia and absence of tumours were reported in three of four cases and the clinical response was mirrored by the fall in VGKC-Ab titres. One of these patients was previously published as a case of non-paraneoplastic, non-herpetic limbic encephalitis with severe hypothermia (Fukushima et al 2005), suggesting an under-recognition of VGKC-Abs even in the peer-reviewed literature (Irani et al 2007). One 46 year-old female did have a thymoma. Since this report, very few cases in the literature have also had thymomas detected (e.g. Ohshita et al 2006).

Subsequently, one paper reported VGKC-Abs in a 58 year-old male with frontal lobe seizures and/or panic attacks, delusions and hallucinations that were initially confused with psychogenic non-epileptic seizures. This clinical syndrome was clearly immunotherapy-responsive and successful therapy produced a concomitant reduction in VGKC-Abs and normalisation of sodium levels (Parthasarathi et al 2006).

One paper showed a patient without features of LE or NMT who developed spontaneous or auditory / somatosensory stimuli-elicited massive muscle jerks with raised VGKC-Abs (562 pM). This startle syndrome was responsive to plasma exchange plus oral cyclophosphamide but not to prednisolone or antiepileptic agents (Antozzi et al 2007).

The only substantial published case-series of patients with VGKC-Abs presented some rather surprising data, possibly accounted for by the multiple methodological discrepancies (Tan et al 2008). The Mayo group identified 80 samples whose IgG bound to rodent cerebellar cortex in a pattern consistent with VGKC immunoreactivity from 130,000 referred samples from Mayo and non-Mayo clinicians. They showed these 80 samples were also 'positive' in their ^{125}I-αDTX precipitation assay. Immunofluorescence in our laboratory's experience is a rather insensitive and clearly non-specific method to detect VGKC-Abs. Correspondingly, we have found that only some of the high-positive VGKC-Ab patients showed detectable immunofluorescence staining and that cases without VGKC-Abs by immunoprecipitation may also show a very similar pattern of reactivity with brain tissue. By inference, one would suspect that Tan et al were only collecting high-positive values. However, their VGKC-Ab precipitation assay cut-off is set at 20 pM (ours is 100 pM) suggesting a relative lack of specificity, especially given that 2 to 5% of elderly patients have VGKC-Abs from 100 to 400 pM (Vincent et al 2004). Finally, they described clinical features which were significantly different when Mayo and non-Mayo cases are compared and acknowledged this ascertainment bias was due to the availability of more complete Mayo medical records. Despite these worrying limitations, their findings are described below. In eight cases, there were insufficient

clinical data and so data were presented from 72 cases. Fifty-one percent of their cohort was female with median age at diagnosis of 66 years (11-84). Around one-third of cases presented with a history of disease of more than six months in duration. Cognitive impairment and seizures were common findings (75 and 71%, respectively). Other common features included hyponatraemia (36%), dysautonomia (33%), myoclonus (29%), dysomnia (26%), peripheral nerve involvement (25%) and cranial nerve / brainstem features (19%). The latter are particularly novel in the VGKC-Ab positive population and indeed this was one of the features found to be statistically more significant in the Mayo cohort. Twenty-four (33%) patients had histological confirmation of a tumour which included small-cell lung carcinoma (n=5), prostate adenocarcinoma (n=4), thymic carcinoma (n=3), haematological (n=3 – two with lymphoma, one chronic myeloid leukaemia), squamous cell carcinoma (n=3), breast adenocarcinoma (n=2) and one colonic adenocarcinoma. Benign neoplasms included five adenomas, one thymoma, one renal oncocytoma and one gastric leiomyoma. They suggested, based on whole-body imaging findings that up to 47% of their cohort had an underlying tumour. This high rate of malignancies is clearly at odds with the rest of the VGKC-Ab literature and is probably a reflection of the described multiple ascertainment biases. However, their point that clinician referrals will bias towards patients with NMT/MoS/LE-like features is fair and VGKC-Ab determination in other cohorts will be of value in the future (Pittock and Tan 2009, reply to Vincent et al 2009). One recent article has attempted to collate the clinical data from 40 published cases of VGKC-Ab associated LE with antibody titres >400 pM (Reid et al 2009). They concluded that treatment before five months of

symptom onset was the only factor predictive of a significant recovery. This paper did not include the studies of Tan et al (2008) or Irani et al (2008).

Creutzfeldt-Jakob Disease (CJD) and VGKC-Ab associated LE

In light of this expanded spectrum with a maintained predominance towards LE-like features, one study examined 15 cases with suspected CJD, of whom sixty percent fulfilled WHO criteria for the diagnosis of CJD, and all had VGKC-Abs (Geschwind et al 2008). Despite entertainment of this terminal diagnosis, 92% showed a response to immunotherapy. The authors suggested features to differentiate LE from CJD. Electroencephalography never showed periodic sharp wave complexes, hyponatraemia was seen in 60%, there was a 33% rate of confirmed neoplasms, high rate of seizures (80%) and dysautonomia (33%); all would be unusual albeit not impossible in CJD. Interestingly, some MRI changes were considered compatible with CJD.

Summary: VGKC-Ab associated diseases

The VGKC-Ab assay was originally defined in patients with neuromyotonia. This seropositive-spectrum grew to include cases with Morvan's syndrome, limbic encephalitis and, more recently, epilepsy. While patients in all these clinically-defined categories show a number of overlapping features, including dysautonomia, sleep dysfunction and hallucinations, the frequency of these features varies hugely between these subgroups. For example, when dysautonomia and insomnia are florid in any one patient, it seems likely that this patient also has neuromyotonia and hallucinations often without seizures. By contrast, a patient with seizures would be likely to have amnesia

without neuromyotonia. Hence, although a continuum of clinical features are apparent between the individual syndromic classifications, there are some clear emphases within any one syndrome.

Does this mean that no single antibody specificity will account for one 'syndrome'? Should the syndromes be redefined with respect to the individual clinical features as opposed to the presence of central and peripheral nervous system features? Hypotheses regarding this question are experimentally addressed within this thesis.

LE WITH OTHER AUTOANTIBODIES

Instead of continuing to diversify the phenotypes associated with the VGKC-Abs, some authors have begun from a clinical viewpoint. Not all cases of LE are associated with the 'classical' paraneoplastic antibodies or VGKC-Abs. A few papers have reported LE patients with serum / CSF antineuronal antibodies and / or immunotherapy responses (Ances et al 2005, Samarasekera et al 2007, Graus et al 2008; Modoni et al 2009). These have strongly suggested that antibodies against other neuronal antigens are present in the cases without currently defined antigens.

One study explored the serological specificities in some detail using various neural tissue preparations (Ances et al 2005). Antibodies to the neuropil of the hippocampus were reported in seven patients (five paraneoplastic) who developed subacute LE. These were detected on brain sections which were fixed for 10 days in paraformaldehyde and by visualized binding to the surface of live hippocampal neurons. Only one of the seven sera was found to contain VGKC antibodies. While specific antigens were not characterized,

this offered the potential for an assay to detect cases of antibody-associated LE and to further explore the antigenic specificities.

These neuropil antibodies were subsequently examined in 39 patients with LE, 17 from a single institution (Bataller et al 2007). This study found 19 patients (49%) had antibodies to known antigens including Hu (n=7), Ma2 (n=6) and VGKCs (n=5). Seventeen of 39 (44%) cases had 'neuropil' positivity, now termed novel cell-membrane antigens (nCMAg). Interestingly, although rather intuitively, patients with cell surface reactivity had a much better response to treatment. Other reports highlighting cases with seronegative limbic encephalitis now need to be retrospectively tested (e.g. Samarasekera et al 2007). It is clear that some patients entered into this thesis, the Ances et al study and a few case reports (e.g. Shimazaki et al 2007) eventually had proven NMDAR-Abs. The NMDAR-Abs were very likely to have been responsible for the neuropil staining and hippocampal surface binding.

N-methyl D-aspartate receptor antibodies (NMDAR-Abs)

NMDAR-Abs were first described by Dalmau et al (2007). They reported 12 young females (14-44 years) who developed a severe encephalopathy with some characteristic features that included psychiatric symptoms, amnesia, seizures, autonomic dysfunction, reduction in conscious level and a movement disorder. Sera from these patients labelled the neuropil of the hippocampus and bound to HEK 293 cells that expressed NR1/2B subunits. Eleven of the 12 patients had ovarian teratomas and one had a mature mediastinal teratoma. The tumours strongly expressed the NR2B subunit which was

considered the major epitope of the patient sera. Patients commonly had medial temporal lobe and cortical imaging abnormalities with a CSF pleocytosis. Many patients showed some improvement with tumour resection plus immunotherapies. This interesting report opened up a number of questions. As the assay of Dalmau et al used permeabilised transfected cells (with serum dilution of 1:200 and CSF at 1:10), was this really an extracellular epitope and hence did the antibodies show pathogenic potential? Were in vitro or vivo assays able to prove pathogenicity? Did all patients require the presence of a tumour to develop this syndrome? Would males develop this disease? How common was this syndrome?

These questions were partially addressed in their second major description of this syndrome (Dalmau et al 2008). In this article, the authors had accrued 100 patients with NMDAR-antibodies: a rather rapid feat of case ascertainment. Median age was 23 years (range 5-76), 91 of their cases were women and 59% had ovarian teratomas. All patients presented with psychiatric symptoms or memory problems. Other features included decreased consciousness (88), dyskinesias (86), autonomic instability (69), seizures (66) and hypoventilation (66). Intensive care unit admissions were common. MRI often showed medial temporal lobe, cortical or meningeal abnormalities and 91% of the CSF showed pleocytosis. EEGs were abnormal in 92% of cases. These observations suggested that NMDAR-antibodies do not associate with a purely 'limbic' encephalitis and maybe the term panencephalitis is more accurate for this serologically-defined subtype of encephalitis.

Potential for pathogenicity

In their 2008 publication, the authors now claimed that the extracellular N-terminal domain of the NR1 subunit was the epitope, which as the ubiquitous NMDAR-subunit is more consistent with the multifocal brain disease seen in the patients. NR1-antibody titres were higher in the paraneoplastic cases and did not change or rose in three of the four cases with no clinical improvement. The authors normalized CSF and serum NR1 titres to the total amount of IgG and showed that CSF contained more normalized antibody. Confusingly, however, the y-axis on their figure reads NR1-antibody 'titre', not normalized level. Earlier tumour removal (often combined with immunotherapy) produced a better outcome and these clinical improvements were associated with a reduction in serum antibody titres. The patients without tumours had the poorest prognosis. Using primary hippocampal cultures, these authors showed downregulation of surface NR1-clusters and reduced total surface NR1-levels after 7-14 days incubation with patient CSF IgG. These effects were reversed with removal of patient IgG.

A European NMDAR-antibody study

Simultaneously, our laboratory conducted a clinical and serological study of 44 patients with NMDAR-Abs (Irani et al 2010). The main differences between our study and those of the Dalmau group are briefly discussed below: the full paper is attached in Appendix 1. Our HEK cell-based assay (CBA) did not use permeabilised cells, employed a 3:1 ratio of NR1:NR2B cDNA in the transfection mix and used a 1:20 serum dilution. Clinical data from the NMDAR-Ab positive cases described a much higher proportion of males (30% of the cohort Vs 9% in Dalmau et al 2008, Fisher's test p=0.004) and many fewer cases with tumours detected (20%, Vs 59% in Dalmau et al 2008, Fisher's test,

p<0.0001). Eighty-nine percent of these tumours were in young females (15-35 years old) with ovarian teratomas and one male had a lymphoma (Zandi et al 2009). We also detected patients with isolated epilepsy as part of our NMDAR-Ab positive cohort. We showed that serum titres of NMDAR-Abs – with the NR1 as their major epitope – are significantly higher than CSF titres. This is of great pathophysiological importance in understanding the mechanisms involved in generating the peripheral antibody. We found many fewer MRI abnormalities – often conspicuously normal in such a severe disease. In individual cases and across the cohort, we showed good correlations between clinical outcomes (modified Rankin Score) and serum antibody levels. As our cohort is predominantly non-paraneoplastic, it seemed important to understand immunotherapy outcomes. Our data showed that outcomes were poor in cases not administered immunotherapy or those administered late immunotherapies (> 40 days). The patients given immunotherapy early had the best outcomes and those given more than one immunotherapy gained the most benefit.

A model for NMDAR-antibody pathogenicity in humans

Finally, our clinical and paraclinical data fit a hypothetical model in which a cortical-to-subcortical disease transition may be proposed. Time at onset of likely cortical features (higher cognitive dysfunction, psychiatric symptoms and seizures) preceded the subcortical features (movement disorder, dysautonomia and reduction in consciousness) by 10 to 15 days. The paraclinical data supported this hypothesis and offered pathophysiological explanations for the clinical observations. MRI cortical abnormalities preceded subcortical abnormalities and EEG-determined cortically-generated

epileptiform discharges preceded diffuse slow waves, more characteristic of diffuse subcortical pathology. Interestingly, the CSF pleocytosis occurred early in the disease and oligoclonal bands were commonly seen later in the disease. These observations suggested a model by which cortical features are generated by the NMDAR-Abs and subcortical features by the intrathecal expansion of the immunological repertoire. However, this is just one hypothesis. Many alternative explanations exist and these can be formally investigated in the future with analysis of serial CSF-serum samples, larger cohorts and with animal models of NMDAR-Ab encephalitis. Our data also concur with many of the reported findings in the literature: there was clear intrathecal synthesis of NMDAR-Abs, the antibodies were predominantly of the IgG1 subclass (as reported in Tuzun et al 2009), NMDAR-Abs were highest in the patients with tumours and those with the poorest outcomes and early tumour removal was critical in achieving optimal outcomes.

NMDAR-Ab positive children and Encephalitis Lethargica

In marked contrast to VGKC-Abs, NMDAR-Abs have been commonly found in children with encephalitides, often with a lower rate of tumours (Dale, Irani et al 2009 (Appendix 2), Florance et al 2009). We observed that the described clinical phenotypes of patients with encephalitis lethargica (EL) – first described by Von Economo in the 1910s – were remarkably similar to that described in NMDAR-Ab positive patients. Hence, we requested EL sera from Dr R Dale (Sydney, Australia) and found that 10 of 20 sera had NMDAR-Abs with higher levels in serum than in CSF. The 10 NMDAR-Ab positive cases were more often associated with seizures, agitation, insomnia and early dyskinesias

when compared to the 10 NMDAR-Ab negative cases (Dale, Irani et al 2009, Appendix 2).

Finally, although antibodies to NMDARs have been described in neuropsychiatric lupus (DeGiorgio et al 2001; Kowal et al 2004; Lapteva et al 2006) and epilepsy syndromes including Rasmussen's encephalitis (termed GluRepsilon2 antibodies: Takahashi et al 2003, Takahashi et al 2005), these antibodies have never been proven to bind to the extracellular domain of intact NMDARs and are likely to indicate an aetiological immune basis but not one with NMDAR-specificity or pathogenic potential.

AMPA receptor (AMPAR) antibodies

The antigenic targets of the neuropil antibodies continued to be specifically characterised. Excitingly, AMPAR antibodies were discovered by mass spectrometry after immunoprecipitation from live hippocampal cultures using patient sera / CSF. A confirmatory diagnostic CBA was subsequently employed using GluR1/2 transfected HEK cells. AMPAR-Abs were described in ten patients with a form of limbic encephalitis without particular clinical features other than frequent relapses (Lai et al 2009). This may be an artefact as the lack of a clear diagnosis meant minimal immunotherapy was offered at initial presentation. Median age was 60 years (38-87) and nine of ten cases were female. Seven patients had tumours of the lung, thymus or breast and all expressed GluR1/2. Nine patients offered immunotherapy and oncologic treatment showed some improvement. As with the NMDAR-Ab literature from this group, there was likely to be a strong bias towards paraneoplastic cases. In a similar

manner to their NMDAR-Ab article, patient CSF significantly decreased the number of GluR2-containing AMPAR clusters at synapses: this effect was reversed with antibody removal.

GABAB receptor antibodies

One more recent paper from the same group (Lancaster et al 2009) has further expanded the antigenic targets associated with LE to include GABAB receptors, as detected using a proteomic approach. From 410 cases with LE, 357 had serum/CSF in which anti-neuropil antibodies could be recognised: 275 had NMDAR-Abs, 27 VGKC-Abs, 19 GAD65-Abs, 15 AMPARs, 11 Ma2 antibodies, eight Hu-Abs and two CRMP5-Abs. This clearly represented a significant referral bias from clinicians who recognised the features associated with NMDAR-Abs (and by contrast, a prior survey of LE patients (Graus et al 2009) showed VGKC-Abs were the single commonest known antigenic specificity). Of the 15 identified LE cases with GABAB receptor antibodies, eight were male and median age was 62 years (24-75). Seizures were a prominent and early part of the LE. Ten patients had medial temporal lobe high signal and CSF pleocytosis was seen in 80% of cases. Six clear malignancies were detected: small-cell lung cancer and a neuroendocrine lung tumour. Again, immunotherapies and tumour treatments produced good outcomes in around half the cases.

Other autoantibodies in central nervous system diseases

Many other human autoantibodies have been associated with a number of putative immune-mediated diseases. We published a review that described clinical syndromes

associated with many of these antigenic targets (Irani and Lang 2008) which include aquaporin-4, glutamic acid decarboxylase (GAD), anti-'basal ganglia' (ABGA) and anti-thyroid antibodies (the latter found in Hashimoto's encephalopathy). ABGA and GAD antigenic targets have reactivity for intracellular targets and are therefore highly unlikely to have pathogenic capabilities. However, one recent report implicated GAD antibodies in younger patients with a more treatment-refractory form of LE, when compared to VGKC-Abs (Malter et al 2010). Anti-thyroid antibodies in Hashimoto's encephalopathy (HE) do not correlate with the disease process - titres do not fall with successful treatments (Castillo et al 2004). Furthermore, the definition of the disease entity has not been clearly defined and features overlap with cases of LE and vasculitis, producing studies with heterogenous disease populations.

Kv1: VOLTAGE-GATED POTASSIUM CHANNEL SHAKER FAMILY

The voltage-gated potassium channel family include Kv1 subunits numbered through to Kv12. Kv1s (*Shaker* family) are possibly the best studied of these, have a clear neural tissue predominance and were discovered early on to be bound by the epileptogenic snake-venom derived toxin, α-dendrotoxin (αDTX). As αDTX binds Kv1.1, 1.2 and 1.6, and forms the basis for the definition of VGKC-Abs, these molecules will be focussed upon below. The majority of the Kv1 family are delayed rectifiers, which open to allow K+ efflux in response to membrane depolarisation secondary to sodium influx. Hence, Kv1s are responsible for action potential repolarisation in neural tissue. Below we discuss structures, likely functions and mutation analyses with respect to the Kv1 channels.

Kv1 structure

Kv1 channels are composed of alpha and beta subunits. Based on the molecular weight of the αDTX-purified complex, $\alpha_4\beta_4$ stoichiometry was originally proposed (Parcej et al 1992) and is still believed to represent the neural predominant composition. Extensive reviews have described the structure of these channels (for example, Dolly and Parcej 1996; Li et al 2006). There are 12 known Kv1 alpha subunits (Kv1.1-1.12) and three beta subunits (Kvβ1-3). Each α subunit contains six transmembrane domains (S1-6) and has intracellular N- and C-termini. The S4 region is thought to act as a charge sensor and the four α-subunit S5-6 regions form the pore-containing domain. The channel has four small extracellular loops: taking Kv1.1 as an example, the largest two loops are 72 and 44 amino acids in length. Human and mouse Kv1.1, 1.2, 1.4 and 1.6 channels show >93% identity. The predicted molecular weight of Kv1.1 and Kv1.2 is 56kDa, Kv1.6 is 59kDa and Kv1.4 is 80kDa (www.hprd.org). There is >50% identity between all these channels in humans, with Kv1.1 and Kv1.2 exhibiting 80% identity.

Non-neural Kv1 expression

The Kv1 α-subunits are predominantly, but not uniquely, expressed in neurons. Many articles have recognised potassium channels within glia, in relation to their K+ buffering function. However, from the Kv1-family, only Kv1.5 has been reported in glia (Horio 2001). Other studies showed cardiac expression of Kv1.1 and 1.5 (London et al 1998), lymphocytic and dendritic cell expression of Kv1.3 and 1.5 (e.g. Mullen et al 2006), cerebral endothelial expression of Kv1.2, 1.3 and 1.6 (Cheong et al 2001) and expression of Kv1.1 and 1.3 in the choroid plexus (Speake et al 2004). Selective Kv1 blockade may modulate vascular tone in the cerebral endothelium and alter lymphocyte surface

expression profiles. Therefore, evidence exists to suggest these channels are functional in non-neural sites.

Kv1 heteromerisation and glycosylation

The neural distributions of Kv1s have been most intensively studied. Essentially, these studies looked at either the heteromeric combinations of Kv1s or the anatomical localisation of Kv1s within the CNS. The former studies used dendrotoxins (αDTX and $_{K}$DTX) and sequential immunoprecipitations with specific anti-Kv1 antibodies and concluded that only a small subset of the theoretical Kv1 combinations were detected in brain tissue (Scott et al 1994; Shamotienko et al 1997; Coleman et al 1999; Wang et al 1999a and 1999b; Sokolov et al 2007). Kv1.2 was found to be present in almost all Kv1 heteromers (83 +/- 6%) with Kv1.1 in around half (47 +/- 4%), Kv1.6 in 16% (+/- 4%) and Kv1.4 in 8% (+/-2%). A number of common heteromeric and homomeric combinations were elucidated. These included the Kv1.2 homotetramer, Kv1.2-heteromers (1.1/1.2; 1.1/1.2/1.6; 1.1/1.2/1.4/1.6; 1.2/1.6) and also the much less frequent combinations without Kv1.2 (1.1/1.4; 1.1/1.4/1.6; 1.4 homotetramer). All combinations were found to contain Kvβ2. When the cerebral distribution of these combinations was examined it was found that there was a uniform distribution of Kv1.2/1.6 heteromers in grey and white matter but a more varied distribution of Kv1.1/1.4. However, this was only examined briefly. In a study more tailored to answer this question, varied Kv1 distributions were seen across hippocampal subfields suggesting regional specialisations (Monaghan et al 2001). Although these channels almost all contained Kv1.2, this is not a necessity for surface expression: Kv1.1, 1.2, 1.4 and 1.6 were shown to be capable of

independent surface expression when transfected into heterologous cell lines, although efficiency of surface expression varied (see below, Shi et al 1996; Tiffany et al 2000).

Kv1.1/1.2 and 1.4 have a single consensus N-glycosylation site within their first extracellular domain (Kv1.6 is not glycosylated). Differences in glycosylation seen between Kv1s in rat brain tissue and transfected HEK cells were most marked for Kv1.1 and 1.2, where reduced glycosylation was seen in HEK cells (Shi and Trimmer 1999). This may be one reason to account for the slightly differing interstudy molecular weights determined for Kv1s.

Cellular and subcellular Kv1 distribution: relations to function

The cellular and subcellular distribution of these channels were studied using specific anti-Kv1 antibody incubations and in situ-hybridisation with brain sections, pre and post-lesions, and with hippocampal cultures (Rhodes et al 1996; Grosse et al 2000; Monaghan et al 2001). The most detailed study examined these questions in adult rat hippocampal sections (Monaghan et al 2001). This is a particularly convenient model for lesion studies given its well-characterised neuronal pathways/interconnections. They detected the majority of Kv1s in nerve terminals and axons while somatodendritic expression was less frequent. The exceptions to this were the intense staining for Kvβ2 in the apical dendrites of CA subfields (Monaghan et al 2001; although this study did not specifically examine Kv1.6 distributions) and Kv1.4 being sorted to either somatodendritic compartments or axons (Grosse et al 2001). Nevertheless, neurotoxic lesions to the entorhinal cortex (the input to the hippocampal dentate gyrus), to the mossy fibres and to the Schaffer's

collaterals produced a marked reduction in Kv1 expression profiles in areas to which these neurons project, suggesting a prominent presynaptic localisation of Kv1 channels (Monaghan et al 2001). Within hippocampal cultures, Kv1.1 expression is seen at postnatal day 10 and all Kv1s were detected by day 18 (Grosse et al 2001).

The CNS region with highest expression of Kv1s (especially Kv1.1 and 1.2) are the basket cells of the cerebellum (Koch et al 1997; Chung et al 2001 and 2005). These cells provide inputs to the Purkinje cells and hence influence the overall cerebellar output. Only Kv1.5 was actually detected on the Purkinje cells themselves. By contrast, there was expression of Kv1.2/1.2/1.3 and 1.6 within the cerebellar molecular layer.

The detection of Kv1s within axons is consistent with the concept of the juxtaparanode (JXTPN) as a domain of clustered Kv1 expression (Figure 1.2). This area will be reviewed later and has gained much recent attention (starting with Poliak et al 1999). In this region the Kv1s are thought to be responsible for the maintenance of a resting potential and to stabilise conduction. In the presynaptic regions, the Kv1 channels are thought to regulate neurotransmitter release. This is supported by studies showing that intracerebral administration of DTX produced limbic seizures and epileptiform bursts which are preceded by increased release of multiple neurotransmitters that are blocked by administration of NMDAR-antagonists (Dorandeu et al 1997). The action potential which is back-propagated from the axon initial segment is also thought to be regulated by potassium channels: the (somato)dendritic Kv1s may have a role here.

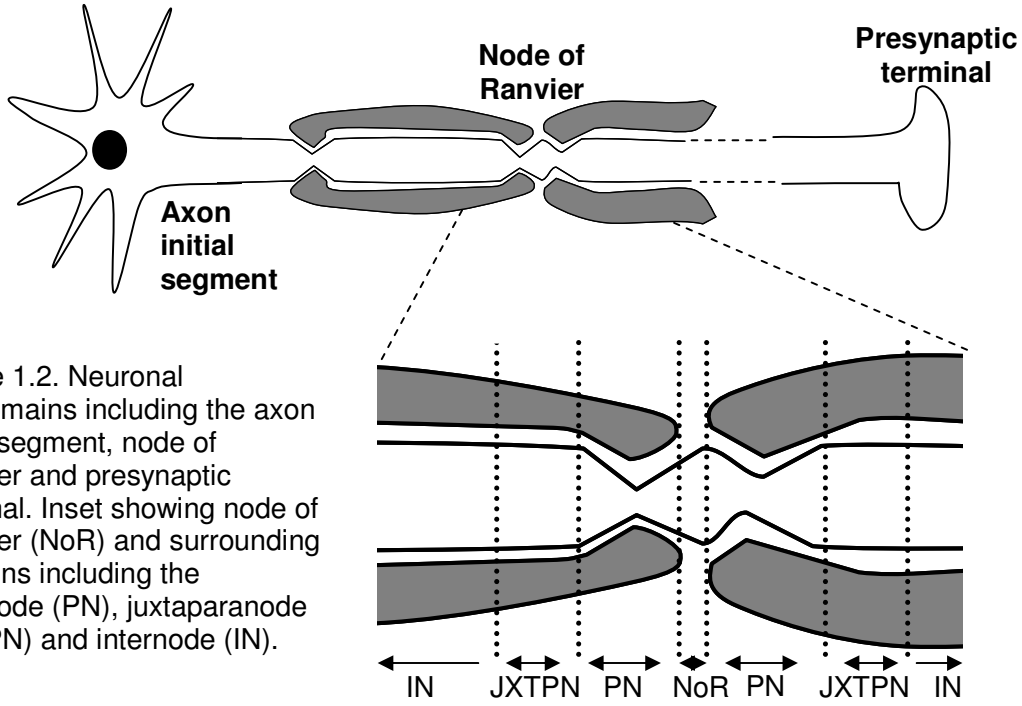


Figure 1.2. Neuronal subdomains including the axon initial segment, node of Ranvier and presynaptic terminal. Inset showing node of Ranvier (NoR) and surrounding domains including the paranode (PN), juxtaparanode (JXTPN) and internode (IN).

Beta subunits and membrane-associated guanylate kinases (MAGUKs)

The β-subunits are entirely intracellular and contain a C-terminal 'inactivation ball' which interacts with the α-subunit. Kvβ1 and 3 accelerate the inactivation of most Kv1s. By contrast, the Kvβ2 subunit has no inactivation effect and is by far the most abundant in brain tissue, detected in almost all Kv1 complexes (Shi et al 1996; Rhodes et al 1996). The Kvβ2 subunit produced an increase in surface expression of Kv1s, most markedly a three-fold increase in Kv1.2 when co-transfected in heterologous cells (Shi et al 1996). This was of particular interest as surface expression of Kv1.1 and 1.2 was only 2% and 23% of the total Kv1-protein expression, respectively (Tiffany et al 2000). Similarly, Kv1.4 increased surface expression of Kv1.1 (and less so Kv1.2) in heterologous cell lines (Manganas and Trimmer 2000).

Most Kv1s have a C-terminal consensus sequence known as the PDZ-binding domain which may bind intracellular membrane-associated guanylate kinases (MAGUKs). This basic observation triggered a number of studies to examine the role of MAGUKs in Kv1 function. In vitro studies showed that co-transfection of Kv1s plus PSD95 and SAP97 produced surface and intracellular clustering respectively, without alterations in levels of surface expression (Kim and Sheng 1996; Tiffany et al 2000). The clusters were seen in 80% of cells transfected with Kv1.4 but only around 10% with Kv1.1/1.2. However, a PSD95 knockout mouse showed no disruption of juxtaparanodal clustered Kv1s, suggesting this may be a redundant mechanism in vivo (Rasband et al 2002). It is the three αDTX-binding Kv1s (Kv1.1, 1.2 and 1.6) which showed poorest enhancement of surface expression, whereas Kv1.3, 1.4 and 1.5 surface expressed well. Interestingly, the surface expression of Kv1.1 and 1.2 were enhanced by the co-expression of αDTX in COS cells. This was explained by the ER retention signals of Kv1.1/1.2 being within the DTX-binding site (Vacher et al 2007).

In addition to these molecules, there are a multitude of specific molecular interactions which define nodal, paranodal and juxtaparanodal regions (Figure 1.3A and B). Implicated molecules such as CASPR, CASPR2, Lgi1 and contactin-2 have been studied in vitro and in vivo, and proven to modulate Kv1 structure and function.

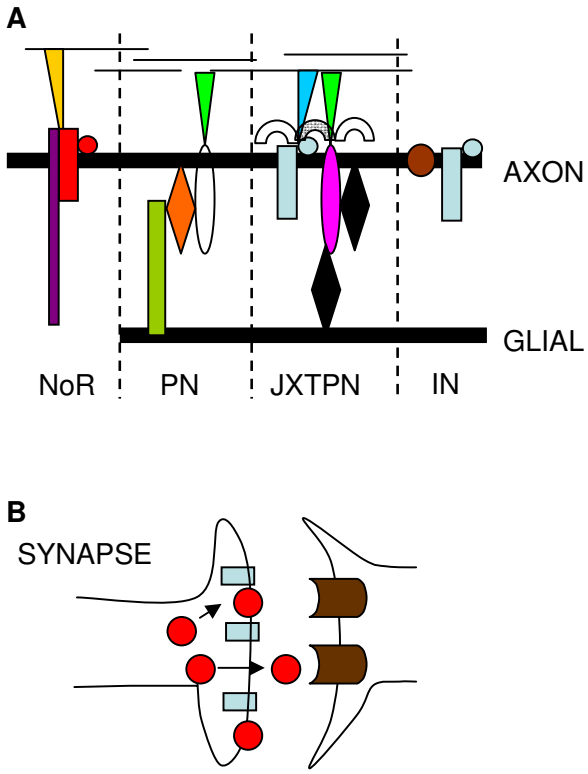


Figure 1.3 A and B. A. Nodal, paranodal and juxtaparanodal molecular organisation with respect to Kv1s. Molecules illustrated are located at the:

- Node of Ranvier (NoR): sodium channels (red, alpha subunit = rectangle, beta subunit = circle), neurofascin 186 (purple), ankyrin G / βIV spectrin (yellow)
- Paranode (PN): neurofascin 155 (green rectangle), CASPR (empty oval), contactin (orange diamond), ankyrin B/ βII spectrin / protein 4.1B/αII spectrin (green triangle).
- Juxtaparanode (JXTPN): Kv1 channels (blue, alpha subunit = rectangle, beta subunit = circle), CASPR2 (pink oval), contactin-2 (black diamond), MAGUKS (semicircles), protein 4.1B/spectrins/ankyrins (green/blue triangles)
- Internode (IN): Kv1 channels (blue, alpha subunit = rectangle, beta subunit = circle), Na-K ATPase (brown circle). Cytoskeleton shown by thin horizontal black lines.

B. Synaptic Kv1 organisation. Kv1s (blue), Lgi1 (red) and ADAM22 (brown) at central nervous system synapses.

Kv1 MUTATIONS IN ANIMAL AND HUMANS

Animals

Kv1.1 is the only Kv1 to have its function examined in such studies. Initially, it was found that Kv1.1 null mice developed frequent spontaneous seizures in the third week of life and there was more rapid induction of seizures in the heterozygotes when compared to wild types (Smart et al 1998). These animals had an auditory startle response and many of them died by the fifth week of life, assumed to be related to the epileptic activity. Electrophysiology in brain slices of null mice revealed a hyperexcitable CA3 neuronal network with multiple discharges seen upon mossy fibre stimulation: these effects were more subtle than the effect of αDTX. In the peripheral nervous system,

electrophysiological analyses suggested slowed repolarisation although a peripheral nerve phenotype was not reported (Smart et al 1998). Petersson et al (2003) made the observation that the previously discovered megencephalic mouse had a heterozygous Kv1.1 truncation mutation, expressing the N-terminal half of Kv1.1. This mouse also suffered from recurrent seizures and an auditory startle response. Interestingly, this mouse showed increased lacrimation. Neurons were hypertrophic, producing the megencephalic appearance. Surprisingly, this group identified the wild-type Kv1.1 protein as an 80kDa band. In postnatal days 14-21, before the onset of seizures, Kv1.1 null mice show a marked temperature-sensitivity of neuromuscular transmission (Zhou et al 1998).

Humans

Episodic ataxia type 1 (EA1; MIM 160120) is a rare autosomal dominant disorder associated with point mutations in the gene encoding Kv1.1 (KCNA1) (Browne et al 1994). The condition is characterized by brief episodes of ataxia and continuous interattack myokymia. The especially high density of Kv1.1 in cerebellar basket cells may generate the ataxia. The myokymia may only be detected with electromyography. Although this correlates well with the immunological-parallel of neuromyotonia, there is little to support the amnesia or epilepsy seen in patients with limbic encephalitis and ataxia is rare in patients with VGKC-Abs. However, the report of Zuberi et al (1999) suggested the occurrence of partial epilepsy in some of these cases both in the family they report and in a review of the EA1 literature. This link has recently been estimated to be 10 times that of the general population (Rajakulendran et al 2007). Functional studies

suggested that Kv1.1 mutant subunits, expressed in Xenopus oocytes, produced a significant decrease in the voltage-activated current. Acetazolamide and antiepileptics may be useful treatments. Cases with severe isolated neuromyotonia and EA1 without myokymia have recently been reported (Rajakulendran et al 2007).

Kv1S AS ANTIGENIC TARGETS MODULATED BY PATIENT IGG

The studies discussed below are summarised in Table 1.4. Having already demonstrated the increased resistance to D-tubocurarine in mice administered NMT IgG (Sinha et al 1991), further passive transfer experiments and some in vitro approaches were undertaken (Shillito et al 1995). Serum and purified IgG from six NMT patients (including three with detectable VGKC-Abs), were passively transferred to mice. These mice showed no visible NMT and no spontaneous muscle discharges. However, increased end-plate potentials and quantal contents were noted in intact dissected nerves from NMT-IgG injected mice. These effects were mimicked by 4-aminopyridine application. Finally, in this study it was shown that NMT IgG could induce repetitive firing of rat dorsal root ganglion cells in culture. This was particularly interesting as it suggested the VGKC-Abs could generate electrical hyperactivity despite an intact myelin sheath. Throughout this study, results were compared to healthy control serum/IgG. This study did not attempt to explain whether specific Kv1 subunits were targeted by the IgG. A study which directly addressed this question unfortunately used Xenopus oocytes (Hart et al 1997). It found that NMT IgG precipitated eight or four times more from αDTX-labelled 1% digitonin-solubilised, Kv1.6 or 1.2-cDNA injected oocytes than healthy control IgG. It also showed sectioned Kv1.6, Kv1.2 and Kv1.1 cDNA-injected oocytes

were labelled by patient sera. It concluded that 11/12 NMT sera bound Kv1.6, 10/12 bound Kv1.2 and 5/12 bound Kv1.1. Six healthy control sera did not bind any of the oocytes and none of the NMT sera bound water-injected oocytes. Significant limitations of these methods included the observation of binding to intracellular epitopes, lack of Kv1-coexpression studies and the use of amphibian cells.

A study using a single NMT subject showed serum IgM binding to denatured PC12 cell extracts (Arimura et al 1997). They also showed that the 50kDa band identified by patient IgM was bound by αDTX. Finally, the IgM fraction bound the surface of fixed PC12 cells. This study, therefore, claimed to show binding of one NMT serum to VGKCs. However, they used denatured (albeit mammalian) tissue, looked for IgM antibodies in a patient with a probable five-year history of NMT and surprisingly showed αDTX could bind denatured VGKCs. This study should not be considered as a useful demonstration of an antigenic target. However, one study did replicate these confusing western blot data but more convincingly showed that application of patient serum (but not purified IgM fractions) produced suppression of potassium currents in the PC12 cell line (Tanosaki et al 1999). These electrophysiological data had previously been shown by Sonoda et al (1996) where currents were suppressed after three to six days incubation with patient sera but not control sera. By contrast to previous studies from this group, there was no comment regarding IgM. However, a later study did show a similar effect of patient IgM in one of three NMT cases (Kurono et al 2006). A more detailed patch-clamp study showed NB-1 cell potassium, but not sodium, currents were reduced after three days' exposure to four NMT patient sera (Nagado et al 1999). Shorter exposures produced little

effect. The channel kinetics were not altered. This effect was also seen with sera from two Guillian-Barré and two idiopathic generalised myokymia patients and was reproduced in CHO cells transfected with human Kv1.1 or Kv1.6. However, this paper did not pharmacologically characterise the potassium currents, did not show surface immunoglobulin binding to either the NB-1 or transfected CHO cells and did not measure VGKC-antibody levels in any patients. Furthermore, the replication of current suppression in patients very unlikely to have VGKC-antibodies (with Guillian-Barré syndrome) suggests that the VGKC-antibodies as defined in NMT were not responsible for the current suppression. Another major criticism of this paper is that they show their NB-1 cells did not express Kv1.6. More recently, in NB-1 cell exposure to NMT IgG reduced K+ peak current density after three days in culture (Tomimitsu et al 2004). This effect was closely mimicked by the IgG $F(ab')_2$ fragment but no effect was seen with the Fab or Fc fragment.

A more definitive study examined the binding of NMT sera to peripheral nervous system and central nervous system tissue in addition to Kv1-transfected HeLa cells (Kleopa et al 2006). After initial examination of Kv1.1, 1.2 and 1.6 tissue expression profiles, there seemed to be some concordance with NMT sera binding in tissue and Kv1-transfected HeLa cells. Kv1.1 and 1.2 rich regions were most clearly bound by NMT sera (e.g. JXTPN of sciatic nerve and cerebellar pinceau) and cells transfected with Kv1.2 were the only ones to consistently bind NMT sera. However, the cerebellar Purkinje cells, with exclusive Kv1.6 expression, were also bound by NMT sera. Much of the immunocytochemistry data was shown on permeabilised cells, unpermeabilised cell data

were not shown. However, this was a rather pleasing result given the literature suggested that Kv1.6 was expressed at very low levels within peripheral nerve JXTPNs and the only previous study addressing specificities suggested Kv1.6 was the likeliest target (Hart et al 1997).

EVIDENCE FOR VGKC-AB PATHOGENICITY

A broad spectrum of diseases as described above are known to be associated with VGKC-Abs. Many cases show a fall in VGKC-Ab titres with successful immunotherapies (Buckley et al 2001; Vincent et al 2004; Irani et al 2008) and LE / NMT IgG binds to brain regions that are likely to be responsible for many of the neurological features. The one autopsy study performed during the acute phase of LE (Khan et al 2009) has shown some neuronal loss in the hippocampal CA4 pyramidal layers, with some perivascular lymphocytic infiltration (also seen by Park et al 2007 and Dunstan and Winer 2006), predominantly B cells and only a few T cells. There was no clear excess or specific immunoglobulin deposition. These appearances were less pronounced in the amygdala and even less so in the more lateral temporal cortex. In MoS, the dysautonomia and insomnia are likely to arise from hypothalamic and thalamic dysfunction. Indeed, thalamic regions in mouse brain sections were shown to bind MoS IgG and MoS post-mortem tissue was shown to have significant thalamic IgG deposition (Liguori et al 2001). Hence, multiple pieces of evidence exist to suggest direct antibody pathogenicity with relevance to tissue distribution of putative antigen, although these do not meet Witebsky's criteria.

As the predominant antibody response is peripherally generated, it is reasonably straightforward to understand how antibodies may access the peripheral nerve. This may not be so simple at the myelin-shielded VGKCs at the JXTPN but once arborisations of the motor nerve become unmyelinated and the blood-nerve barrier is weakened distally, this becomes more plausible. However, antibodies would need to access the CNS in order to generate a LE / complete MoS phenotype, this would go against the dogma of blood-brain barrier impermeability to antibodies.

THE BLOOD-BRAIN BARRIER

It is possible that the serum titre of VGKC-antibody required to generate a CNS disease needs to be particularly high to access the brain. This possibility is strengthened by the observation that the patients with the highest VGKC-Ab levels, from a study of NMT cases (Hart et al 2002), had the most florid psychiatric features. In addition, the LE cases have consistently higher VGKC-Ab levels, in comparison to the NMT patients (Vincent et al 2004). The BBB-deficient circumventricular organs – including the hypothalamus – may be easily accessed by VGKC-Abs and account for many of the CNS features of MoS and the MoS-like phenotypes in LE cases. If so, maybe MoS-like features would be expected more commonly within the LE cohorts than is observed. The access of antibodies to the CNS, via the BBB, is beyond the scope of this introduction but has been a contentious subject for some years. Dogma would suggest the BBB is impermeable to antibodies. Although many groups have detected intrathecal antibodies in CNS diseases (against VGKCs, NMDARs and aquaporin-4), these have consistently been found at

higher levels in the serum than the CSF (see detailed data for NMDAR-Abs; Appendix 1). In fact, in the case of VGKC-Abs, CSF antibodies are commonly not detectable.

It may be that IgG does not need to itself cross the BBB, and that B cells / plasma cells may transmigrate into the CNS to generate specific intrathecal IgG. This phenomenon has recently been exploited for therapeutics in the field of multiple sclerosis. Leucocyte chemoattraction, rolling, tethering and adhesion are well-studied endothelial-leucocyte interactions which allow parenchymal infiltration of leucocytes from the circulation. One of the important molecules in the adhesion process is the lymphocyte alpha4 integrin. A monoclonal antibody which directly targets this integrin (nataluzimab) has been shown to reduce brain lymphocyte infiltration and relapse frequency in multiple sclerosis (Polman et al 2006). The remarkable results seen with this drug in the more acute, inflammatory phases of multiple sclerosis may provide a paradigm for antibody-mediated neurological illnesses. Indeed, this concept is supported by the finding of intrathecal aquaporin-4-antibody secreting plasma cells in cases with neuromyelitis optica (Bennett et al 2009).

The lack of CSF-IgG, particularly in the VGKC-Ab associated diseases, may depend upon a number of factors. It is not implausible that the VGKC-Ab which does (possibly constitutively) cross the BBB is bound rapidly and with high affinity to its target antigen. This may mean unbound CSF IgG is undetectable. It may also mean a steady stream of serum to CSF VGKC-Ab migration does not occur. Alternatively, the VGKC-antigen specific serum B / plasma cells which transmigrate only proliferate and secrete IgG near

or at their target antigen. This regional synthesis of antibody may not be detected in *lumbar* punctures.

Maybe these constitutive mechanisms of serum-to-CSF IgG transfer are not operating in the context of the VGKC-Abs. Groups have suggested a number of BBB-modulators could allow access of previously impermeable substances – including IgG (Kovak et al 2004). The main modulator is likely to be lipopolysaccharide (LPS). Humans may be exposed to LPS in the form of a preceding infection prior to the onset of LE. Hence, in summary, it seems very likely that mechanisms exist to allow IgG access to the CNS.

HOW MAY MULTIPLE PHENOTYPES BE EXPLAINED BY VGKC-ABS?

Clinical aspects

Complete explanations for the above pathophysiological mechanisms also necessitate an understanding of why the same serological assay can be associated with very different clinical syndromes. The simplest explanation is based upon the fact that αDTX binds three Kv1 channels (Kv1.1, 1.2 and 1.6), and the three major syndromes may be accounted for by these varying specificities. This would require a differential CNS and PNS expression of these channels; however all three have been shown to have CNS expression profiles and Kv1.1 and 1.2 are well-described in the PNS. The hypothesis that different Kv1 channels account for the differing syndromes means that an infectious 'hit' to the BBB –symptomatically noted in only a few cases – may not be necessary. The lack of clinical involvement in organs which clearly express Kv1s – such as the blood vessels, heart and kidney – is surprising in a disease with high levels of serum antibodies. Only

one report has described involvement of the vasculature: cerebral microbleeds occurring with disease progression (Kapina et al 2009) and whilst sudden (presumably cardiac) death has been reported (e.g. Liguori et al 2001, Khan et al 2009), this is most likely to be associated with a central dysautonomia.

Nevertheless, a molecule with pure neural expression may be the optimal candidate antigen for the LE cases: no such Kv1 subunits are known. Post-mortem studies do not aid our understanding as these have never explored the issue of Kv1 expression. One observation which directly supports the role of Kv1s in the generation of LE is a case report which showed that 4-AP (a known Kv1 blocker) induced LE (Badruddin et al 2009). This patient had profound amnesia without seizures, bilateral medial temporal lobe high signal, an inflammatory myopathy (possibly due to Kv1.5 involvement) and a transient cardiomyopathy. 4-AP toxicity causing seizures and psychosis has been previously reported (Johnson and Morgan 2006). However, as with much of the electrophysiological data presented earlier – summarised in Table 1.4 – such functional outcomes do not necessarily identify the structural antigenic target.

Molecular aspects

Given radioimmunoassay-defined antibodies in MG and LEMS, it seemed no coincidence that NMT sera immunoprecipitated above background quantities of αDTX-labelled brain extracts. However, the well-established heteromerisation of Kv1s may suggest that specificities for individual alpha-subunits are insufficient to describe three distinctive syndromes. Furthermore, the observation of isolated epilepsy, psychotic and

extrapyramidal presentations may suggest further subunits are required to explain all the phenotypes with this hypothesis. And this could be the case as Kv1.3, 1.4 and 1.5 may exist in αDTX-bound heteromers. The very small extracellular domains of the Kv1 proteins make these unlikely a priori targets for pathogenic antibodies. Correspondingly, very few studies since the initial assay development have convincingly shown Kv1s to be the direct target of these antibodies. These studies have been summarised in Table 1.4 but below some of the more convincing data which examine whether the various syndromes can be explained by serological specificities are summarised.

Hart et al (1997) showed NMT sera had preferences for Kv1.2 and Kv1.6 expressed in oocytes. Most of the NMT studies showed effects in neural cells lines consistent with Kv1 dysfunction (Sinha et al 1991, Shilitto et al 1995, Arimura et al 1997, Tomimitsu et al 2004). Nagado et al (1999) did show modulation of Kv currents in CHO cells transfected with Kv1.1 and 1.6. However, they also showed this effect in patients without detectable Kv1 antibodies. Interestingly, an abstract from one of these Japanese groups suggested that while NB-1 Kv1 currents were suppressed by NMT sera, they were unable to reproduce this effect using LE sera (Watanabe et al 2006). Finally, one study showed that in two cases with LE there was partial co-localisation of Kv1.2 and patient sera (Buckley et al 2001). This co-localisation was more exact than co-localisation of patient IgG with Kv1.1. However, immunohistochemistry and current suppression are not the ideal methods to ask which antigens are directly bound by the patient sera. Immunohistochemistry does not exclude direct IgG binding to co-localised molecules and suppression of currents may be produced by modulation of interacting proteins. Despite

the above reports, only one study has appropriately asked the question of which subunits the LE/MoS sera bind in a mammalian cell line over-expressing Kv1s (Kleopa et al 2006).

Kleopa et al (2006) used NMT (n=10), MoS (n=2) and LE (n=5) sera and initially examined co-localisation with commercial antibodies to Kv1.1, 1.2 and 1.6 on mouse cerebellar / hippocampal sections and in teased sciatic fibres (TSF). Three of the 17 sera did not have detectable VGKC-Abs using the diagnostic assay, while three others had levels between 100 and 200 pM. They were able to define individual Kv1 distributions in the CNS and PNS tissue. Half of the NMT cases (as mentioned above) bound to the juxtaparanodal regions of TSF – these sera did not necessarily have the higher VGKC-Ab titres. Six of seven LE/MoS cases also bound the JXTPNs. Within the cerebellum, the Purkinje cells (which only express Kv1.6) were only bound by three sera. By contrast, the pinceau (basket cell terminals with strong Kv1.1 and 1.2 expression profiles) and granule cells were bound by all LE/MoS sera and by two NMT sera. Surprisingly, one of these NMT cases had undetectable VGKC-Abs. Only the LE and MoS sera bound to the hippocampal sections. This was difficult to understand as Kv1.1, 1.2, 1.4 and 1.6 were clearly expressed within the hippocampus. Subsequently, this study examined Kv1-transfected HeLa cells and found some mixed results. All five LE sera, one MoS serum and no NMT sera showed appreciable quantified binding to permeabilised Kv1.1-transfected cells. By contrast, almost all the sera tested showed Kv1.2 binding and very few showed Kv1.6 binding. The two sera showing most clear Kv1.2 binding were from patients with MoS and NMT. The authors concluded that LE sera had a preference for

Kv1.1 and NMT sera bound more strongly to Kv1.2. However, as alluded to above there were some clear discrepancies in the data. In particular, the binding of NMT sera to PNS, not hippocampal, tissue (relevant Kv1s are expressed in both) and the LE sera binding to both tissue types. These data may have suggested the possibility that the NMT sera were not binding Kv1s but to a neurally-restricted protein which is co-localised with Kv1s.

SUMMARY

Autoimmune limbic encephalitis is a rapidly expanding field now being increasingly recognized by neurologists. The clinical diagnosis has allowed for the concomitant expansion of serological specificities, some of which help define unique clinical characteristics. The clinical diagnosis allows for timely and appropriate immunotherapies and/or tumour treatments to be commenced. The origins of autoimmune, non-paraneoplastic limbic encephalitis lie in the discovery of an association between VGKC-Abs and autoimmune neuromyotonia / Morvan's syndrome.

The assay used to detect VGKC-Abs utilises αDTX which binds Kv1.1, 1.2 and 1.6 in mammalian brain homogenates. However, as these channels do not show exclusive CNS / PNS expression profiles, it seems implausible that antibody specificities for each channel would explain the three clinical syndromes seen in association with potentially pathogenic antibodies. No study has clearly and convincingly answered this question using mammalian tissue. Furthermore, the one study to systematically compare the staining patterns of LE/NMT IgG showed that LE IgG bind to both CNS and PNS tissue whereas NMT IgG do not show reactivity with CNS tissue which has dense Kv1

expression. This may suggest that Kv1 channels are not themselves the direct target of some sera. However, these observations are offset by the remarkably similar phenotypes seen in humans and mice with Kv1.1 gene mutations and by the clear and high expression of Kv1s at the peripheral nerve terminals and within the hippocampus.

This thesis directly addresses the question of how multiple syndromes can be explained by the VGKC-Abs.

CHAPTER 2: METHODS

Clinical material

The Neurosciences Group in Oxford receives all national and many international requests for voltage-gated potassium channel antibody (VGKC-Ab) testing and this allowed us to identify patients with positive VGKC-Abs. Ethical approval for the study was first obtained from the Oxfordshire Research Ethics Committee A(07/Q160X/28). The accepted application permitted us to approach clinicians and request them to consent their patients, to share information regarding clinical features, symptoms, investigation results and treatment outcomes, and for follow-up sera to be sent to Oxford.

One hundred and thirty-five unselected VGKC-Ab positive patients with titres over 400pM and contact details available on request cards were identified. Questionnaires and consent forms were distributed to their clinicians. Sufficient data (comprehensive questionnaires or clinic letters) were received from 104 cases (see Figure 2.1 for details). Another 13 patients with possible MoS, and VGKC-Ab titres greater than 100 pM, were added to overcome under-representation of this group (Figure 2.1). Four sera were subsequently found to bind untransfected HEK cells and, therefore, prevented antigen determination by cell based assays (see Chapters 4 and 5).

The resulting 113 patients were divided into those only with central nervous system features and those with NMT. Cases with only CNS features were defined as LE by published criteria (Bien and Elger 2007). Four of these 78 cases had isolated epilepsy and so while fulfilling criteria for

LE, were designated as isolated epilepsy. Cases with NMT were further sub-classified by the referring neurologists into those with MoS or those with pure NMT.

Modified Rankin scores (from Graus et al 2001) were requested at serial time points, chosen by the attending physician, to describe the level of functional disability and ranged from zero to six (0=asymptomatic patient; 1=Symptoms do not interfere with lifestyle; 2=Symptoms lead to some restriction of lifestyle but do not prevent totally independent existence; 3=Symptoms significantly interfere with lifestyle or prevent totally independent existence; 4=Symptoms prevent independent existence, but patient does not need constant attention day & night; 5=Severe disability, with patient totally dependent and requiring constant attention day and night; 6=Death due to the encephalopathy).

Patients that were found to have 'dystonic epilepsy associated with VGKC-Abs' classification (see Chapter 3) were contacted individually to ascertain further clinical details, where unavailable in casenotes or questionnaires. All sera were aliquoted and stored at -20 ^{o}C until required.

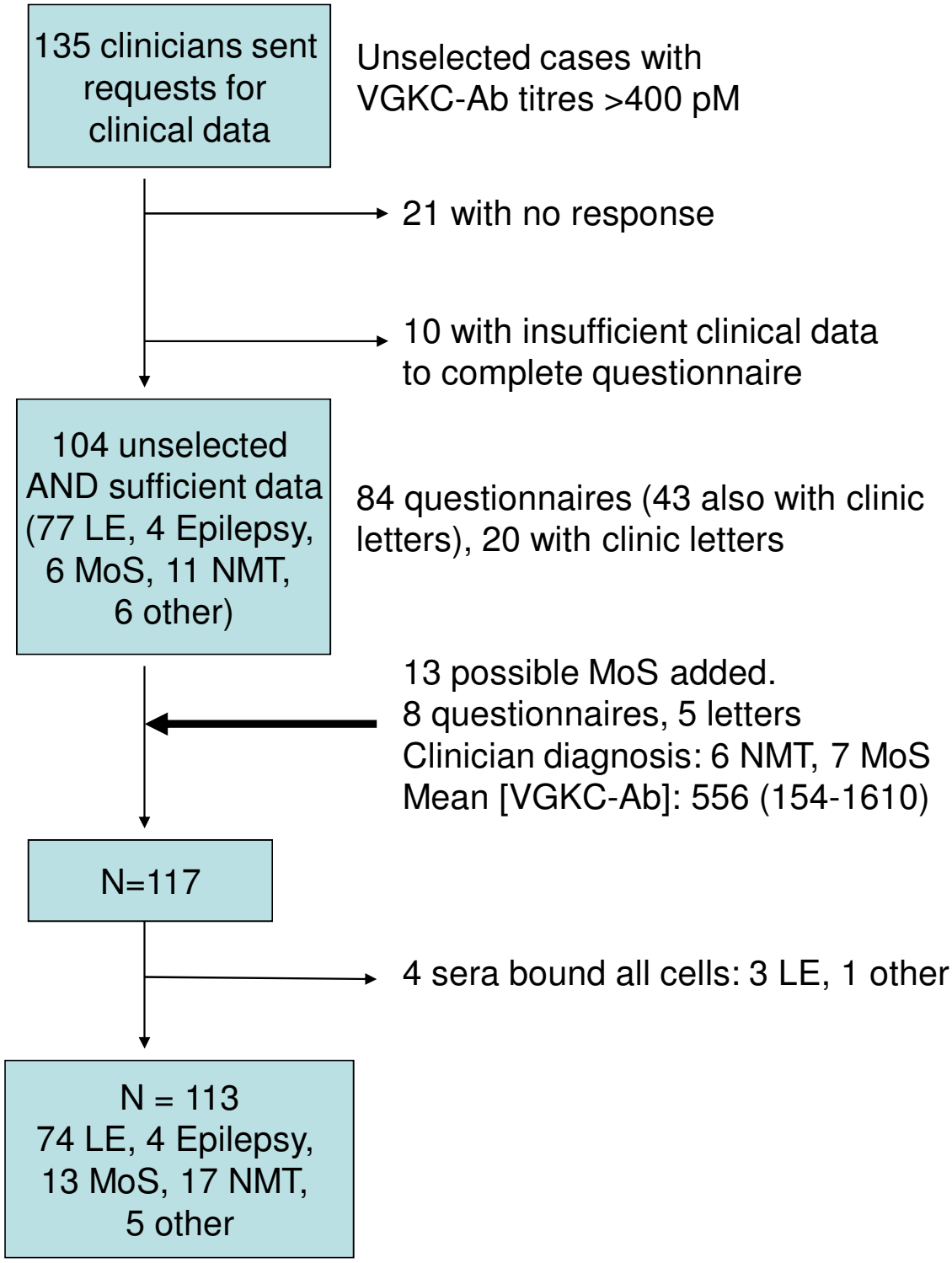


Figure 2.1. Patient selection flowchart.

Antibodies used

A large number of antibodies were used during this work and are named below. All antibodies are directed against the intracellular domain of the intended protein, unless stated otherwise. Neuromab, USA produced mouse monoclonal antibodies against: Kv1.1 (extracellular and cytoplasmic), 1.2, 1.3, 1.4, 1.5, 1.6, β2, CASPR2 (extracellular), CASPR, contactin (extracellular), GIT-1, Nav1.6, pan-MAGUK, SAP-102, SAP-97, PSD-95, PSD-93/Chapsyn-110, ADAM-22 (extracellular and cytoplasmic), ankyrin G, CASK, pan-neurofascin, MMP8, KCNQ1 and KCNQ2. Sigma-Aldrich, UK: rabbit anti-GFAP, mouse anti-MAP2, synaptophysin and Na-K ATPase. Alamone (USA) produced rabbit polyclonal antibodies against Kv1.1, 1.2, 1.4 and 1.6. Novus Biologicals, Inc (USA) produced chicken polyclonal anti-CNPase. Developmental Studies Hybridoma Bank (DHSB) produced mouse monoclonal anti-contactin-2 and Santa Cruz Biotechnology produced goat anti-Lgi1 (N-18 (N-terminal signal peptide directed), H-56 (C-terminal directed) and C-19 (more distal C-terminal directed). Rabbit anti-CASPR2 and protein 4.1B antibodies, were gifts from Dr E. Peles (Weizmann Institute, Israel)

VGKC-antibody determination

This was performed as previously described (Vincent et al 2004) and is termed the 'diagnostic assay' throughout this thesis. VGKC complexes were extracted from rabbit whole brain membranes solubilised using 2% digitonin (Calbiochem, USA) in DTX-buffer (100mM NaCl, 20mM Tris, 5mM KCl adjusted to pH 7.12) at 37^{o}C for 20 minutes and then centrifuged at 15,000g for 15 minutes at room temperature (RT). The supernatant was harvested and diluted 1:2 with PTX (0.02M phosphate buffer and 0.1% Triton X100, pH 7.2) and incubated with ^{125}I-αDTX (specific activity 2000 Ci/mmole,

Perkin Elmer, USA). This extract was further diluted with DTX-buffer to give 1 million counts per minute (cpm) per ml (an approximate concentration of 250 fmoles of ^{125}I-αDTX / ml). 50µl of ^{125}I-αDTX-labelled extract was incubated with serum or commercial antibodies (made up to a constant volume of 50µl with PTX) overnight at 4^{o}C. Secondary antibodies (anti-human IgG, RSR Ltd, UK or anti-goat IgG, Jackson Immunoresearch Laboratories Inc, USA) were added. The addition of normal human or goat carrier serum (1-2µl) was added for precipitation with commercial antibodies. After 90 minutes at RT, 0.5ml of PTX was added and the precipitates were spun at 15,000g for 5 minutes and resulting pellets washed twice in PTX and read on a gamma counter (Cobra 2, Perkin Elmer). When expressed as specific cpm, results have the non-specific binding, determined by precipitation in the presence of healthy control serum, subtracted. For dissociation/'stripping' experiments, different concentrations of sodium dodecyl sulfate (SDS) were added to the ^{125}I-αDTX labelled extract for two hours at RT before incubation with primary antibodies.

Plasmid constructs: molecular biology performed by Dr Patrick Waters (Neurosciences Group, Oxford)

cDNAs encoding full-length human Kv1.1, 1.2, 1.4, 1.6 and β2 were cloned into pcDNA3.1-hygro (Invitrogen Ltd, CA, USA).

The full-length human MuSK-EGFP construct has been described previously (Leite et al 2008).

The vector pCR4-TOPO that contained the cDNA for CASPR2 (IMAGE: 7939625 from Geneservice Ltd, Cambridge, England) was digested with EcoRI. The fragment was subcloned into pcDNA3.1 (+) (Invitrogen, UK) to give an untagged CASPR2 that expressed in mammalian cells. In order to tag CASPR2 with eGFP, the pcDNA3.1 (+)-CASPR2 plasmid was digested with XhoI and XmaI. The fragment was subcloned into pEGFP-N1 (Clontech Laboratories, CA, USA).

For human Lgi-1, the cDNA was bought from Geneservice Ltd. and amplified by PCR with the following primers:

FPlgiIpcdna: GATCGCTAGCCCACCATGGAATCAGAAAGAAGCAAAAGG NheI

RPlgiIpcdna: GATCCTCGAGTCATGCGCTTAAGTCAACTATGACATG XhoI

The purified product was subcloned into pGEM-Teasy. This clone and the plasmid pcDNA3.1(+) (Clontech) were digested with NheI and XhoI. The fragments were ligated together; the construct was purified and verified by sequencing.

FPlgiIpcdna: GATCGCTAGCCCACCATGGAATCAGAAAGAAGCAAAAGG NheI

RPlgiIpcdna: GATCCTCGAGTCATGCGCTTAAGTCAACTATGACATG XhoI

TAG1 cDNA was a gift from Dr D Karagenos, Cyprus and Dr P Waters confirmed the full-length human sequence.

Transfection and human embryonic kidney cell culture

HEK293 cells were maintained in Dulbecco's modified Eagle's Medium (DMEM), supplemented with 10% foetal calf serum (FCS, TCS Cellworks Ltd, Buckingham, UK)

and 1% penicillin-streptomycin-amphotericin (PSA, Invitrogen, CA, USA). For transfection HEK293 cells (at a concentration of approximately 400,000 cells/well) were plated on poly-L lysine (PLL) coated glass coverslips (for subsequent microscopy) or without coverslips (for toxin binding and immunoabsorption experiments) in six-well plates at 37^0C in a 5% CO_2 atmosphere. Cells were grown to approximately 40% confluence and then transfected using a total of 3µg cDNA (diluted to a concentration of 0.8µg/µl with nuclease free water) in the presence of 1.25µl of polyethylimine and 1.5µl of 20% sterile glucose solution per well, unless stated otherwise. After 15 hours, the transfection mix was removed and fresh media added. Coverslips were transferred to a 24-well plate at 48 hours post-transfection for the cell-based assay.

Cell-based assay (CBA)

Live cells were incubated for 45 minutes at RT with 1:20 - 1:100 patient sera or commercial antibodies diluted in wash buffer (DMEM supplemented with 4-(2-hydroxyethyl)-1-piperazineethanesulfonic acid (HEPES) and 1% bovine serum albumin, BSA). Cells were washed, fixed in 3% formaldehyde for 15 minutes, washed again and an appropriate Alexa Fluor secondary antibody was applied (1:750) for 30 minutes at RT. 4',6-diamidino-2-phenylindole (DAPI) was used as a nuclear counterstain (1:1000).

For cell permeabilisation, cells were incubated for five minutes in 0.2% Triton X100/5% BSA post-fixation and subsequently treated as above but all solutions subsequently contained 0.2% TritonX100. Patient sera were used at 1:500-1:1000 and commercial antibodies at 1:100-1:750.

Mounted coverslips were visualised using a fluorescence microscope (Leica DM1000) or a confocal microscope (BioRad MRC1024-UV with LaserSharp imaging software).

Subclasses and complement fixation

For subclass determination, after serum incubation and fixation, specific mouse anti-human IgG1/2/3/4/IgM antibodies (1:50, The Binding Site, UK) were applied for 45 minutes, and anti-mouse Alexa Fluor 568 antibody was used to visualise the binding.

For detection of deposited complement on transfected cells, live cells were incubated with heat-inactivated patient sera and fresh human plasma, as a source of complement (as in Waters et al., 2008). After 30 minutes at 37˚C the cells were put on ice, fixed with 3% formaldehyde and incubated with rabbit antibodies against C3b (DAKO Group, Denmark) or membrane attack complex (MAC, kind gift from Prof BP Morgan, Cardiff), both at 1:250, and Alexa Fluor 568 anti-rabbit IgG (1:750).

Protein extraction and labelling

HEK cells (seeded at around 5 million /flask) were grown in 175cm^2 flasks until 40% confluent, and transfected with a total of 60µg of cDNA, 30µl of PEI and 25µl of 20% glucose. At 15 hours post-transfection, media was changed. At 48 hours post-transfection, the media was removed, flasks were washed with PBS (phosphate buffered saline) and lysed in 3mls of 2% digitonin in DTX-buffer, with 1:100 protease inhibitor cocktail. Lysates were gently rotated for one hour at 4^{o}C, spun (13,000rpm for 5 minutes)

at 4°C and labelled with ^{125}I-αDTX as above. Both these and EGFP-tagged extracts (100fU/assay) were subject to immunoprecipitation usually with human sera (usually 1-5µl) or commercial antibody (usually 1-5µl).

For the fluorescent immunoprecipitation assay (FIPA), the fluorescently tagged proteins were precipitated as before and then the pellets re-suspended in PTX (180ul), transferred to a 96 well plate and analysed using a fluorescent plate reader (Gemini XS, Molecular Probes and Victor3, 1420 Multilabel counter, Perkin-Elmer).

Lgi1 transfected cells from flasks were incubated with 1% sodium carbonate for five minutes at 4˚C to elute non-membrane integral proteins (see Schulte et al 2006).

^{125}I-αDTX surface binding assay.

Cells were plated (as described above) and transfected in duplicate directly on six well plates, as described above. Forty hours post-transfection, when the cells were approximately 80% confluent, the cells were washed in phosphate buffered saline (PBS) and incubated with DTX-buffer (400µl) with or without 40µl of 1x10^{-6}M αDTX ('unlabelled DTX') for 20 minutes. After PBS washing, 100,000cpm of ^{125}I-αDTX (25 fmoles) was added to each well for 40 minutes. After through washing, cells were lysed in 2% Triton X100 (0.5mls) transferred to an Eppendorf tube and radioactivity determined using a gamma counter. Specific binding was determined by subtracting the non-specific binding in the presence of an excess of unlabelled DTX from the total binding.

Other antibody assays

All CASPR2-Ab positive patients were tested by Dr Bethan Lang for autoantibodies to onconeural antigens HuD, Yo, Ri, Ma2 and amphiphysin using a RAVO kit (Raven Ltd) as per the manufacturers instructions. Other assays were performed as previously described (VGCC and GAD: McKnight et al 2005). NMDAR-Ab, MuSK and glycine antibody assays were performed as previously described (Irani et al 2010 (Appendix 1 and 2); Leite et al 2008; Hutchinson et al 2008).

Immunohistochemistry and immunofluorescence on brain sections

Adult rats (older than 10 weeks) were killed by terminal anaesthesia and the brains were snap-frozen mounted in tissue tek and cryostat sectioned (10µm thickness). Sections were fixed in 4% paraformaldehyde (PFA) for three minutes, washed in PBS and sequentially exposed to primary antibody (1:200-1:1000, diluted in 10% goat serum), further PBS washes and secondary antibody (1:200-1:500; Alexa Fluor or HRP-conjugated). After final PBS washes, sections were counterstained with DAPI or incubated with a DAB-solution (Thermo Scientific) and counterstained with haemalun. 0.2% TritonX100 was used in solutions where membrane permeabilisation was attempted. Slides were viewed under a light microscope (Nikon Eclipse E400), fluorescent microscope (Leica DM1000 with a MacProbe v4.3 digital imaging system) or a confocal microscope (BioRad MRC1024-UV with LaserSharp imaging software).

Antibodies binding to primary hippocampal cultures

Primary hippocampal neuronal cultures were prepared from decapitated P0/P1 rats (Dr B Lang). Briefly, hippocampi were dissected and collected in chilled EBSS (Earle's Balanced Salt Solution) with PSA, and incubated in 0.05% trypsin-EDTA solution at 37°C for 30 minutes. Hippocampi were gently triturated in complete MEM (Minimal Essential Medium) with 10% horse serum, 0.25% glucose, 1% glutamine and 1% PSA. After low speed centrifugation (1000 rpm at 5 minutes, RT), the cells were resuspended in complete MEM and plated on poly-L-lysine-coated glass coverslips at around 100,000 viable cells per coverslip. Separately, mechanical dissociation was attempted, using forceps and a scalpel. Cultures were grown at 37°C in a humidified 5% CO_2 atmosphere. Twice-weekly, half of the medium was replaced with neurobasal culture medium (Invitrogen, UK), supplemented with glutamine, PSA and B27 supplement (as per manufaturers instructions, Invitrogen, UK).

After 10 – 20 days *in vitro* the cells were fixed in 3% PFA and were incubated with patients' sera (diluted 1:100 – 1:1000 in neurobasal medium with 20% goat serum) / mouse monoclonal anti-MAP2 (1:500) for one hour at RT, followed by washing and incubation with appropriate Alexa Fluor anti-species IgG-488/568 (Invitrogen-Molecular Probes, Paisley, UK) for 40 minutes. Subsequently, cells were washed, mounted and visualized as for the cell based assay (see above).

Western blotting

Transfected cell extracts were boiled for 15 minutes with SDS-based loading buffer and reducing agent, as per manufacturer's instructions (Invitrogen, CA, USA). 4-12%

NuPAGE BisTris SDS polyacrylamide gel lanes (Invitrogen, UK) were each loaded with 10-20µl of solubilised extracts harvested from confluent 175cm^2 flasks and run for 60-90 minutes at 200mV. Gels were transferred to nitrocellulose paper over 90 minutes at 30mV. Individual strips were blocked with a PBS-0.1% tween, 5% milk protein (Marvel) solution. Subsequently, membranes were incubated for 1 hour with primary antibodies (1:200 - 1:1000) diluted in 2% Marvel solution, PBS-0.1% tween for 3 washes and 30 minutes in HRP-conjugated anti-species IgG secondary antibodies (1:500, DakoCytomation, UK) diluted in 2% Marvel blocking solution. Blots were developed with diaminobenzidine (DAB) kits (Thermo Scientific).

Statistical analysis

All statistics were performed using GraphPad Prism version 5 for Windows (San Diego, USA). The statistical analysis performed in each experiment is described in the appropriate section.

CHAPTER 3: VGKC-ANTIBODY ASSOCIATED SYNDROMES

Introduction

The literature surrounding clinical syndromes associated with VGKC-Abs have traditionally categorised cases into three main syndromes: LE, MoS and NMT. Analysis of clinical data here aimed to phenotype these cases in detail, determine optimal treatment responses and describe novel phenotypes associated with VGKC-Abs. Most importantly, the ascertainment of well-characterised clinical cohorts was intended to inform the scientific aspects of antigen detection and antibody functionality. Specifically, could the clinical data allow us to explain why an individual with VGKC-Abs will develop LE, MoS or NMT?

Limbic Encephalitis, Morvan's Syndrome and Neuromyotonia: clinical features

After the addition of the under-represented MoS and NMT cases (see Figure 2.1), detailed clinical data in 113 cases were available for analysis. Median patient follow-up was four years (2-19 years). Underlying malignancy was only excluded after at least one whole body imaging modality (CT, MRI or PET) in 110 patients. Three patients without whole body imaging had LE (n=2) and neuromyotonia (n=1).

While 108 of 113 cases segregated into the four established VGKC-Ab-associated syndromes (Isolated epilepsy, LE (by criteria of Bien and Elger 2007), MoS or NMT), with clinical features summarised in Table 3.1, five cases did not fit these patterns. These

	Epilepsy	Limbic encephalitis	Morvan's	Neuromyotonia
Total	4	74	13	17
VGKC-Ab (mean and range, pM)	3215 (639-5410)	2248 (411-8840)	1087 (154-3670)	759 (201-1745)
Age (median, range)	65 (51-70)	61 (17-83)	60 (30-76)	54 (37-74)
Male	3	54	12	11
Tumour	0	0*	8	7*
Neuromyotonia	0	0	13	17
Infectious precipitant	0	11	0	0
Any neuropsychiatric features	0	74	13	1
Amnesia	0	71	8	0
Confusion	0	63	11	0
Disorientation	0	56	9	0
Hallucinations	0	15	9	0
Depressive	0	13	3	1
Anxiety	0	8	1	1
Psychosis	0	13	3	0
Any seizures	4	63	5	0
Simple partial seizures	1	20	1	0
Complex partial seizures	3	44	2	0
Generalised tonic-clonic seizures	0	43	5	0
Ataxia	1	9	1	1
Hypersomnia	0	9	0	0
Insomnia	0	6	13	2
REM-SBD	0	5	1	0
Sleep cycle reversal	0	3	0	0
Hyperhidrosis	0	6	9	6
Any autonomic features	0	7	12	8
Movement disorder	0	2	0	1
Pain	0	3	12	7
Weight loss	0	2	8	4
Peripheral neuropathy	0	1	6	0
EMG-proven neuromyotonia	0 of 2	0 of 38	13	14
History of myasthenia gravis	0	1	6	2
MRI: medial temporal lobe changes	0	42	0	0
MRI: normal	4	32	11 of 11	5 of 5
Serum hyponatraemia	0	42	3	0
Normal CSF	4	48 of 69	7 of 10	2 of 2
Fall in mRS (mean and range)	3 (2 to 5)	3.04 (-1 to 5)	-1 (-4 to 4)	-0.86 (-4 to 3)
Death	0	0	8	4

Table 3.1. Clinical features, treatments and outcome of 108 of 113 patients with VGKC-Abs and epilepsy, limbic encephalitis, Morvan's or neuromyotonia. Five other cases which did not fit into this classification are described in the text. Denominators noted only when data not available from whole cohort. REM-SBD = rapid eye movement sleep behaviour disorder; EMG = electromyography; MRI = magnetic resonance imaging; CSF = cerebrospinal fluid; mRS = modified Rankin Score (as Graus et al 2001); * = no body imaging in two LE cases and 1 NMT case.

cases were diagnosed with a fixed dystonia with auditory startle (VGKC-Abs = 646 pM), a pure startle syndrome (VGKC-Abs = 801 pM; Antozzi et al 2007), depression and headache (VGKC-Abs = 1184 pM), meningoencephalitis (VGKC-Abs = 1342 pM) and a diffuse pain syndrome (VGKC-Abs = 643 pM). In addition, one of four cases whose sera bound all cells had Guillian-Barré syndrome (VGKC-Abs = 4044 pM).

Demographics

The main features from Table 3.1 highlight some clinical aspects of the groups. Of the incident cohort, before 13 cases of possible MoS were added (finally classified by clinicians as seven with MoS and six with NMT), 77/104 (74%) of the total cohort had LE, 11 NMT (11%), six MoS (6%) and six had other syndromes (6%; as described above). From the final cohort of 113 cases, a 'hierarchy' of VGKC-Ab titres was apparent with highest titres in the LE/Epilepsy cases and lowest in the NMT cases (Figure 3.1, Kruskal-Wallis test $p<0.0001$). These data also showed that males were more commonly affected than females (80:33). The MoS cases had the highest percentage of males (92%). The ages of onset were non-significantly lower in the group with 'other' syndromes (Figure 3.2, Kruskal-Wallis test $p=0.051$). Strikingly, active tumours were restricted to the MoS/NMT groups (15/30 Vs 0/83, $p < 0.0001$, Fisher's t test) and are discussed in greater detail below.

Cognitive features

Patients in the LE cohort commonly had amnesia (96%), confusion (85%), disorientation (76%) and more rarely were found to have psychosis (18%), depression (18%), anxiety

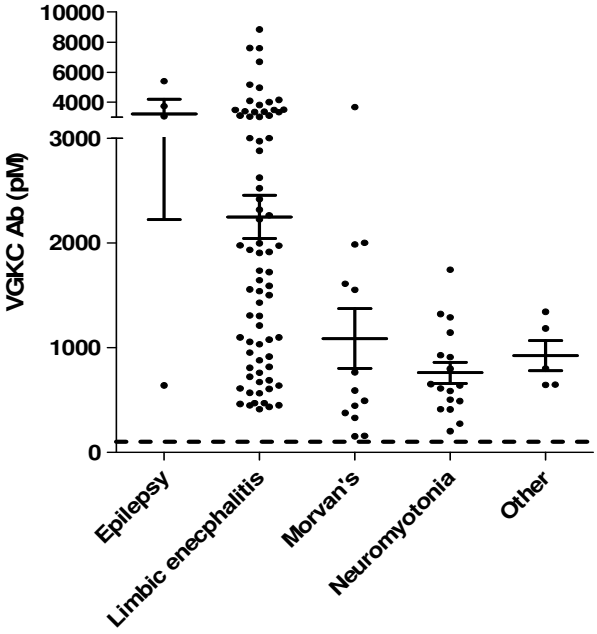


Figure 3.1. VGKC-Ab titres amongst 113 cases distributed by syndromic classification. Dotted line denotes 100 pM titre (mean plus 3 standard deviations derived from healthy controls). Table 1 summarises the clinical features. Kruskal-Wallis test $p<0.0001$.

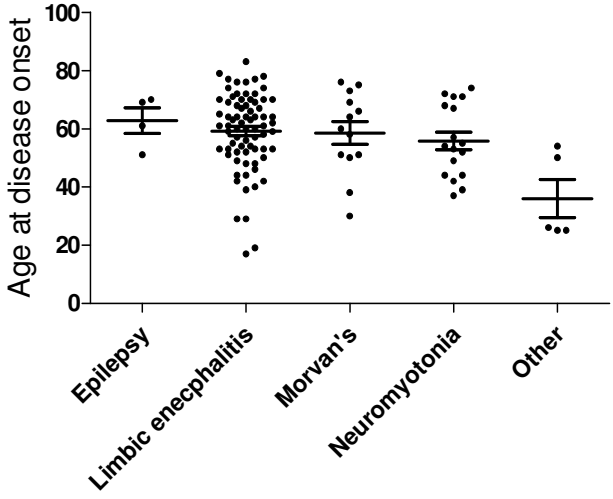


Figure 3.2. Age at onset of cases with VGKC-Ab associated syndromes. Kruskal-Wallis test $p=0.051$.

(11%) or hallucinations (21%). The 4% without amnesia showed confusion. Seizures were found in 63 of the 74 with LE (85%) and were significantly more common in LE than MoS (63/74 Vs 5/13, p=0.0008 (Fisher's t-test)). By definition, no cases from the pure-epilepsy cohort had neuropsychiatric features, however one of the NMT cases had (probably secondary) mild depressive/anxiety features. By contrast, 9/13 (69%) MoS cases had hallucinations and 3/13 had psychosis (23%).

Sleep, pain and autonomic features

Hypersomnia was only noted within the LE group (12%). By contrast, insomnia was seen in all the MoS cases and only in 8% of the LE cohort ($p<0.0001$, Fisher's t-test, see Table 3.1). Insomnia was reported in two of the NMT cases.

Pain was a prominent feature in 23 (20%) cases. Pain was present in lower limbs, especially feet (n=19), back (n=3), hand joints (n=2) and upper limbs (n=1). The pain was described as burning (n=10), sharp (n=4), dysaesthetic (n=1) or cramping (n=1) in nature, with no description available in eight cases. Pain was described in cases with MoS (92%) more frequently than in those NMT (41%) or LE (4%).

Hyperhidrosis was reported in 21 cases. Eleven of these had other autonomic features such as hypersalivation (n=2), tachycardia (n=4), arrhythmias (n=2), postural hypotension (n=3), urinary retention/incontinence (n=3), constipation (n=4), impotence (n=1) and pyrexia (n=1). Six other cases had no hyperhidrosis but did develop hypersalivation (n=1), tachycardia (n=2), arrhythmia (n=1), postural hypotension (n=1),

urinary retention (n=1), constipation (n=3), impotence (n=1) and pyrexia (n=1). As with pain, these dysautonomic features were more frequently seen in MoS (92%) when compared to NMT (47%) or LE (9%).

EMG data

Four of the 17 cases with NMT did not have electrophysiological evidence of neuromyotonic discharges, although two had fasciculations detected. All the MoS cases had EMG-proven neuromyotonic discharges. Of the 78 cases with LE/Epilepsy, EMG was normal in the 43 tested.

The features with particular relevance to the potential disease pathophysiology are elaborated on below. In particular, potential aetiological factors included tumours and the presence of possible infectious precipitants.

Tumours

110/113 (97%) cases underwent body imaging: CT chest/body (n=96), PET body (n=28), MRI body (n=2). In addition, three cases went to post-mortem. Three cases did not have body imaging.

Tumours have been previously reported at around 10-30% rates in VGKC-Ab associated LE from centres with a paraneoplastic interest (Pozo-Rosich et al 2003, Graus et al 2008). However, in this cohort no active tumours were found in 78 patients with LE/Epilepsy. In comparison, active tumours were found in 15/30 (50%) of the patients with MoS/NMT

($p<0.0001$, Fisher's exact t-test). The frequency of active tumours were not significantly different between MoS and NMT cases (Table 3.1; $p=0.26$, Fisher's exact t test). Thirteen of the tumours were thymomas (nine metastatic and four non-metastatic), one was a non-small cell lung cancer and one was a metastatic endometrial adenocarcinoma. Of these 15 tumours, three were not detected on CT body imaging (and PET in one case) at times when VGKC-Abs were present: one was detected on PET imaging two years later (thymoma) and two only detected at post-mortem (thymoma and non-small cell lung cancer). The tumour (or its recurrence) was detected prior to the MoS/NMT features in three of 15 cases. Eight of 13 patients with thymomas had a previous diagnosis of MG. In these eight patients, thymomas were originally detected at the time of MG diagnosis (median four years earlier, range five months to 16 years earlier). Ten of the thymomas were previously thought to have been removed (eight in patients with MG) and recurred as metastases (n=8) or local thymic tumours (n=2). During the MoS/NMT episode, seven patients underwent thymectomy. In two cases the onset of the MoS/NMT syndrome was noted a few days after thymectomy (one had a residual thymoma).

Other tumours were noted in the past medical history of patients but were highly unlikely to be pathologically relevant to the VGKC-Ab associated disease: NSCLC (epidermoid tumour) in remission since 10/2003 without recurrence on CT/PET in 2009, monoclonal gammopathy of uncertain significance (MGUS) diagnosed in 05/2004 with stable clonal-IgG level in 2005, left inguinal angiolipoma removed in 2005 with subsequent normal CT body, pleural plaques noted in 2006 with subsequent body PET showing nostril high uptake and a normal nasal biopsy (patient well in 08/2009), benign basal cell carcinoma removed from shoulder with subsequent normal whole body PET and post-mortem, long

standing prostate carcinoma in two cases (six and 19 years) with normal CT/PET body imaging and a breast cancer diagnosed in 2003 without recurrence detected in 2007 or 2009 after CT body imaging.

Infectious prodrome

Another potential aetiological distinction between LE/Epilepsy and MoS/NMT cases manifest as the high number of prodromal infectious events in the LE/Epilepsy group (11/78 Vs 0/30, p=0.03, Fisher's exact t test). Precipitating events occurring prior to the onset of the limbic encephalitis included fever/sweats (in four cases at 7, 10, 14 and 21 days prior to onset of neurological syndrome), upper respiratory infections (in three cases at 10, 21 and 45 days prior to onset of neurological syndrome), eye infections (probably conjunctivitis, in two cases 21 and 60 days prior to onset of neurological syndrome), diarrhoea and vomiting (in one case at 14 days prior to onset of neurological syndrome) and salmonella sepsis (in one case, concurrent with neurological onset). As the LE group had no active tumours detected, none of these 11 cases were found in patients with tumours.

Investigations

The hyponatraemia was present in 45 cases ranging from 110 to 134 mmol/L (mean 126 mmol/L) and was more common in LE (57%) than MoS (23%) and was reported in none of the NMT/Epilepsy cases.

CSF was normal in 62 and abnormalities were found in 26 cases. Eight raised protein levels were noted (0.68 – 1.36 g/L, mean = 0.90), 12 raised white counts (6 – 125 cells/mm^3, mean = 23), with 11 lymphocyte-predominant and one neutrophilia. The only CSF abnormalities in the MoS group were unmatched oligoclonal bands (n=2) and raised protein (0.79 g/L, n=1)).

MRI changes, in 42 cases LE, affected the hippocampus unilaterally in five (three right and two left), including one case with amygdala involvement. Thirty-five cases had bilateral hippocampal involvement and seven had additional amygdala involvement. Cerebral atrophy occurred in nine individuals, seven of whom had high medial temporal high signal initially.

Immunotherapies

Therapeutic manoeuvres in the MoS/NMT cohort were highly variable, reflecting the complexity of the disease and the presence of tumours in 50%. Overall, it was clear that the epilepsy and LE cohorts made a better improvement than the MoS or NMT cases. This has been shown as the absolute mRS at presentation (black) and last follow-up (red) and as the change in mRS (Figure 3.3A and B, respectively). Figure 3.4 and 3.5 aimed to determine whether specific immunotherapies were responsible for these outcomes. As the LE/epilepsy cohort is more homogeneous and much larger, interpretation of therapeutic intervention is probably more meaningful within this cohort. Patients were divided into the type of immunotherapy received: steroids, IvIg and/or plasma exchange. These data suggested that immunotherapies are important, with steroids the most important single

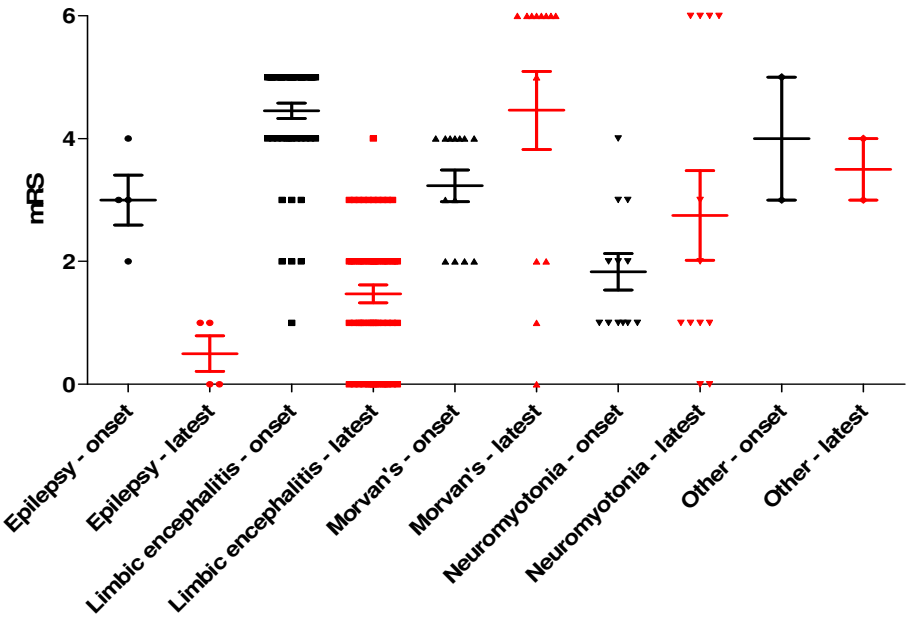


Figure 3.3A. mRS (modified Rankin Score) at disease onset (onset - black) and at latest follow-up (latest - red) divided according to clinical syndrome. Downward deflection implies clinical improvement.

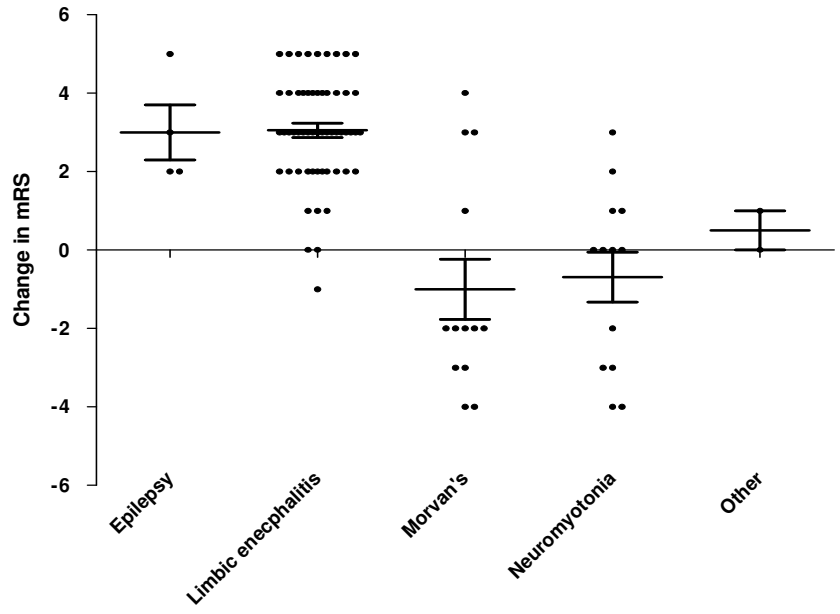
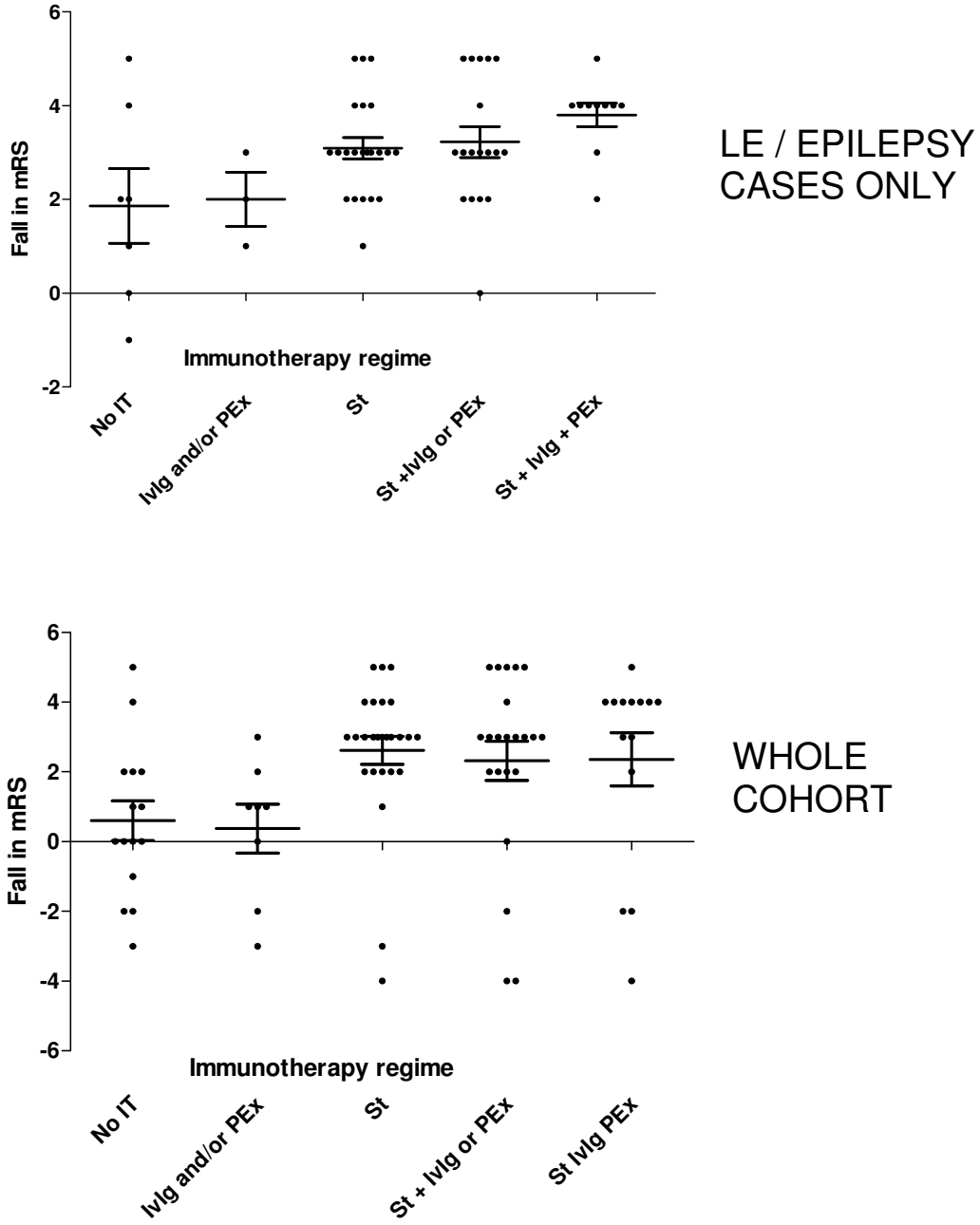


Figure 3.3B. Change in mRS (modified Rankin Score) divided according to clinical syndrome. Positive deflection implies clinical improvement. Kruskal-Wallis test $p<0.0001$ (Dunn's multiple comparison showed LE Vs MoS and LE Vs NMT, $p<0.0001$).



Figures 3.4 and 3.5. Fall in mRS (positive deflection) and its relationship to type of immunotherapy administered for patients with epilepsy/LE only (Figure 3.4) and for the whole cohort (Figure 3.5). IT = immunotherapy, IvIg = intravenous immunoglobulins, PEx = plasma exchange and St = steroids. Data available from 60 of 78 and 85 of 113 patients (Figure 3.4 and 3.5, respectively).

therapy for this disease. There was a non-significant trend towards using multiple immunotherapies (Figure 3.4, p=0.053, Kruskal-Wallis test). When immunotherapy regimes were compared across all patients with VGKC-Abs (including the MoS/NMT cases; Figure 3.5), the same pattern of relative efficacy remains but the ANOVA shows significant differences across the groups (p=0.0034, Kruskal-Wallis test; Dunn's multiple comparison showed a significant difference between those receiving no immunotherapy and those receiving steroids alone).

Probably related to the presence of an active (often aggressive) tumour, death from the VGKC-Ab associated disease was only noted in the MoS/NMT cohorts (12/30 Vs 0/83, p<0.0001, Fisher's t test). This is consistent with the overall poor outcomes of the MoS and NMT cohorts (Figure 3.3A and B).

DYSTONIC EPILEPSY ASSOCIATED WITH VGKC-ABS

Whilst gathering the above data, we identified a characteristic seizure semiology in three 69-year old patients (two females and one male) in collaboration with Dr Shelagh Smith (Consultant Neurophysiologist, London). All three cases had raised VGKC-Abs titres (5409 pM, 3355 pM and 238 pM; the latter sample was obtained three weeks after immunotherapy had been commenced). The phenotype was that of frequent, unprovoked, limb dystonia and/or facial grimacing which was very brief (<3 seconds usually), highly stereotyped, occurred up to 70 times per day and began in later life. Examples of dystonic seizure 'snapshots' are shown in Figure 3.6. Seizures were responsive to immunotherapy, and often refractory to antiepileptic drugs. Fall in seizure frequency correlated well with



Figure 3.6. Five video snapshots show the characteristic short-lived faciobrachial seizure. Patients have kindly provided written consent for non-anonymised photos to be shown for research/educational purposes.

reduction in VGKC-Ab levels. The attending neurologists / epileptologists could not recall other similar cases, making this a distinctive semiology (Irani et al 2008).

Subsequently, from responses to our questionnaires and examination of casenotes/clinic letters in the UK (Dr Sarosh Irani, n=13), with clinical observations from London (Dr Shelagh Smith (n=5) and Dr Mike Johnson (n=2)) and from Sydney (Professor Ernie Somerville/Dr Andrew Michell (n=6)), we became aware of 26 similar cases in total. Twenty-one of these cases underwent telephone-based interviews and casenote/questionnaire review and for five only casenotes were available. Videos of events were available in 19 cases (73%). Table 3.2 summarises the principle clinical features of the 26 cases.

The 26 patients identified showed an age range of 36 to 73 years old (median = 64.5) with males affected more commonly than females in around a 2:1 ratio (17:9; Figure 3.7). These seizures were very brief (usually < three seconds) and occurred at a median of 49 / day at their peak (range 6 to 200 / day). They always involved the arm and commonly involved face (73%), leg (35%) and trunk (31%) (Figure 3.8). Hence, these have been termed faciobrachial seizures (FBSz). The hand involvement caused many patients to regularly break crockery or drop items within their grasp. Seventy-three percent of cases showed bilateral seizures which most commonly occurred independently, and spread contralaterally over a few seconds. Twenty-seven percent of patients also showed vocalizations at the start of their seizure. Loss of awareness was noted in 62% of cases,

Age	36 – 73, median = 64.5 years
Sex (M:F)	17:9
VGKC-Abs (pM) (median and range)	2143 (238-6129)
Dystonic seizures	
Seizure frequency	Median = 49/day (Range 6-200/day)
Alteration in consciousness	16 (62%)
Additional seizure semiologies	19 (73%; GTCSz = 13, CpxPTLS = 10, SPS = 1)
Startle response	7 (27%)
Drop attacks / falls	15 (58%)
Vocalisations	7 (27%)
Other clinical features	
Amnesia	23 (88%)
Confusion	18 (69%)
Depressive	3 (12%)
Hallucinations	9 (35%)
Sleep disturbance	8 (31%)
Dystonia	1 (4%)
Cerebellar features	2 (8%)
Dysautonomia	4 (15%)
Pain	4 (15%)

Table 3.2. Clinical features of 26 patients with faciobrachial dystonic seizure semiology. GTCSz = generalised tonic-clonic seizure; CpxPTLS = complex partial temporal lobe seizure, SPS = simple partial seizure.

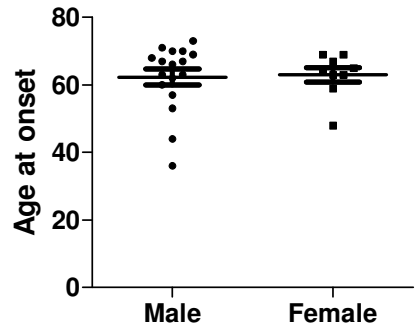


Figure 3.7. Gender distribution and age at onset from 26 cases with dystonic seizures.

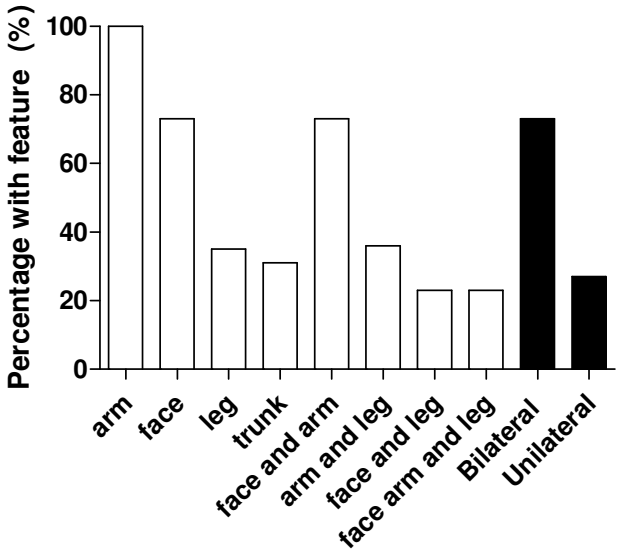


Figure 3.8. Percentage of cases with dystonic seizures that showed involvement of face, arm, trunk and leg and uni- or bi-laterality of seizures

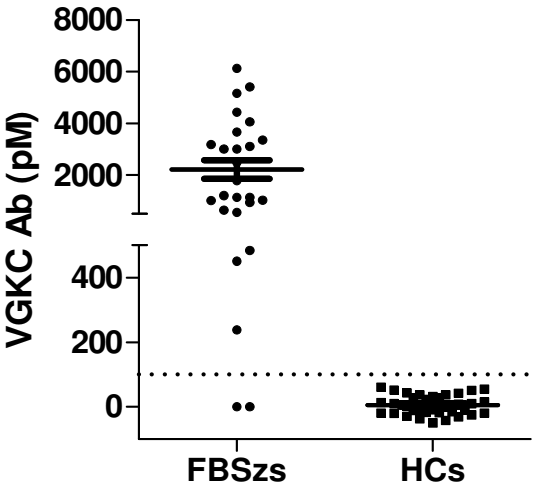


Figure 3.9. VGKC-Antibody levels in 26 cases with dystonic seizures, also stratified by antigenic target. FBSz = faciobrachial seizures. HCs = 35 healthy controls – mean plus 3 standard deviations from this cohort defines the 100 pM cut-off (dotted line). Two VGKC-Ab negative cases with FBSzs had serum tested 4 years after onset of their disease.

albeit not during all seizures. 27% of cases had seizures which could be triggered by auditory stimuli and high emotion. Unexplained drop attacks, often with backward falls, were reported in 58% without clear lower limb involvement. Nineteen of 26 (73%) cases also developed other seizure phenotypes that included generalised tonic-clonic seizures (n=13), complex partial temporal lobe seizures (n=10) and one with simple partial seizures. Possible precipitants were only found in three cases: nausea and vomiting (two days prior to onset), nasal polypectomy (eight days prior to onset) and conjunctivitis (21 days prior to onset). As shown in Figure 3.9, 24 of 26 patients had high levels of VGKC-Abs with median 2143 pM (range 238-6129 pM). The one patient with levels < 400 pM had their sample taken three weeks after immunotherapy had been commenced, and the two VGKCAb-negative cases only had VGKC-Ab testing four years after their initial presentation, and VGKC-Abs may have fallen spontaneously (see introduction).

Faciobrachial seizures as a prodrome to limbic encephalitis

Seventeen out of twenty-three (74%) patients developed FBSz before the onset of constant amnesia and confusion while six cases developed amnesia with subsequent onset of FBSz. Three cases only ever had seizures without amnesia, disorientation or confusion. For the cases where FBSz were the initial feature, the interval from onset of FBSzs to onset of confusion or amnesia was between two and 850 days (median 42 days; Figure 3.10A). Seizures would typically begin at a relatively low frequency and increase in frequency until they reached a crescendo at around the time of confusion or amnesia onset (Figure 3.10B-D). There were no clear clinical triggers for this marked transition from frequent seizures to constant amnesia. During the period of isolated seizures, most

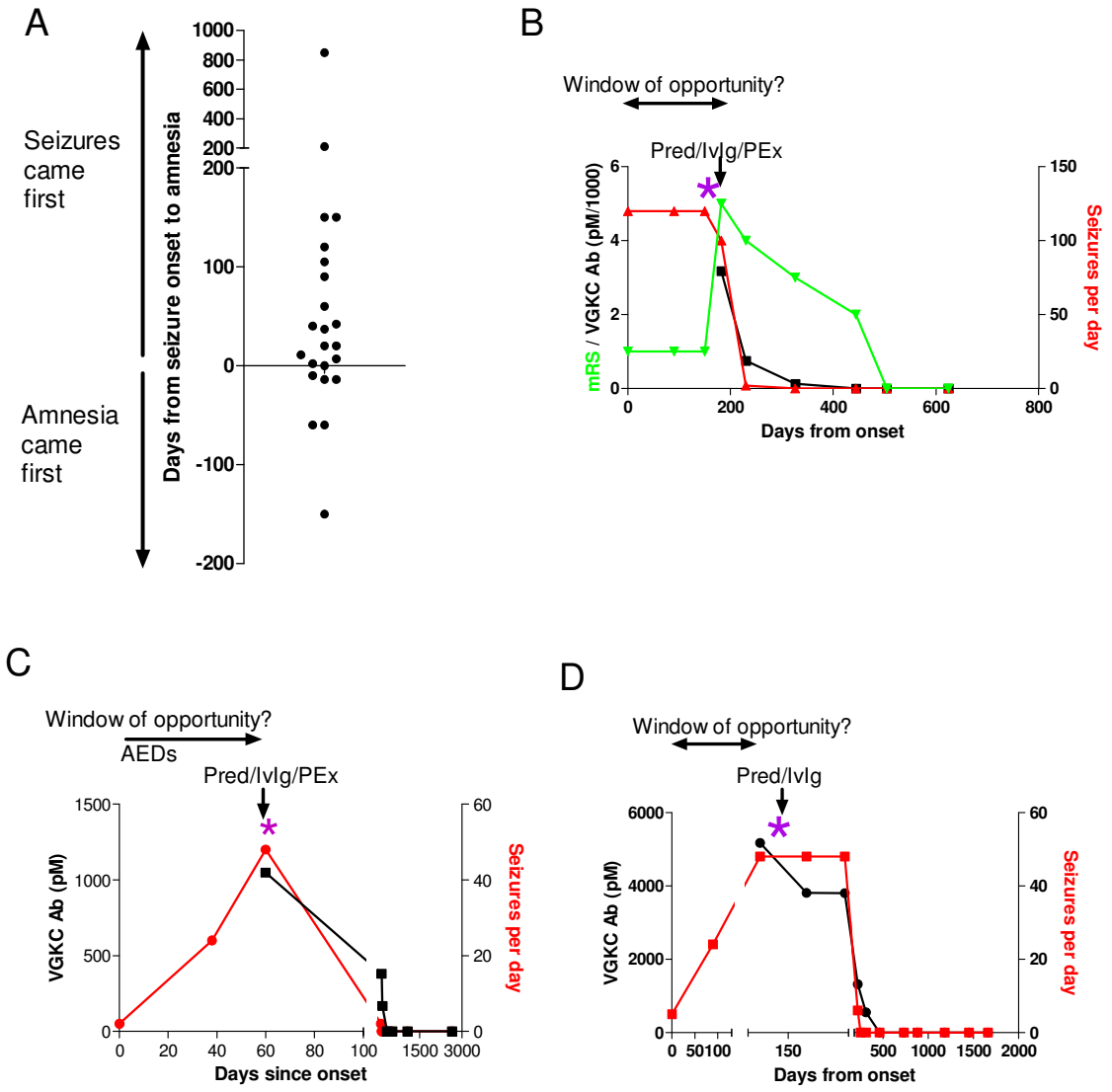
patients were able to perform daily activities independently, although many noted crockery was frequently broken and carpet stains were common. However, at the onset of memory impairment or confusion, clear functional disability was acquired (see modified Rankin Scale (mRS), Figure 3.10B). The prodrome of seizures without amnesia may represent a therapeutic 'window of opportunity' to prevent the amnesia (see discussion).

Once manifest, the limbic encephalitis (as shown in table 3.2) had features that included amnesia (88%), confusion (69%), psychiatric features (up to 35%), sleep disturbance (including REM-sleep behavior disorder, hypersomnolence and insomnia in equal proportions; 31%) and, more rarely, cerebellar ataxia (8%), dysautonomia (including hyperhidrosis and erectile dysfunction; 15%) and neuropathic pain (15%). One case had ongoing foot dystonia.

Investigations

Investigations were most commonly performed while patients had a florid cognitive disturbance. However, as the prodromal phase was occasionally prolonged and troublesome, some data are available from this period.

Serum hyponatraemia was seen in 22/26 cases, always during the period of LE (mean = 123 mmol/L, range 112-132 mmol/L; Figure 3.11). By contrast, the three cases with isolated epilepsy (who did not progress to amnesia or confusion) had normal serum sodium levels. Furthermore, in the five cases with measurements obtained during their period of isolated seizures, prior to the onset of amnesia, sodium levels were normal.



Figures 3.10 A-D. A. Number of days from seizure onset to development of amnesia. This figure excludes the three cases who never developed amnesia. B, C, D. Correlations between number of seizures per day (red), VGKC-Ab titre (black) and modified Rankin Score (mRS, green in 3.10B) in three cases. Purple stars indicate point of amnesia onset. Hypothetical window of opportunity for therapy prior to onset of amnesia. Treatments shown: Pred (prednisolone); IvIg (intravenous immunoglobulins); PEX (plasma exchange); AEDs = antiepileptic drugs. In Figure 3.10B, the VGKC-Ab titres have been expressed in nM (pM/1000), to fit on the left y-axis. Window of opportunity explained within text.

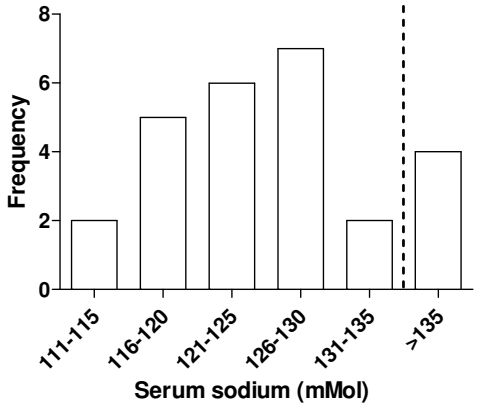


Figure 3.11. Lowest serum sodium levels detected during disease (normal ≥135mMol = dashed line).

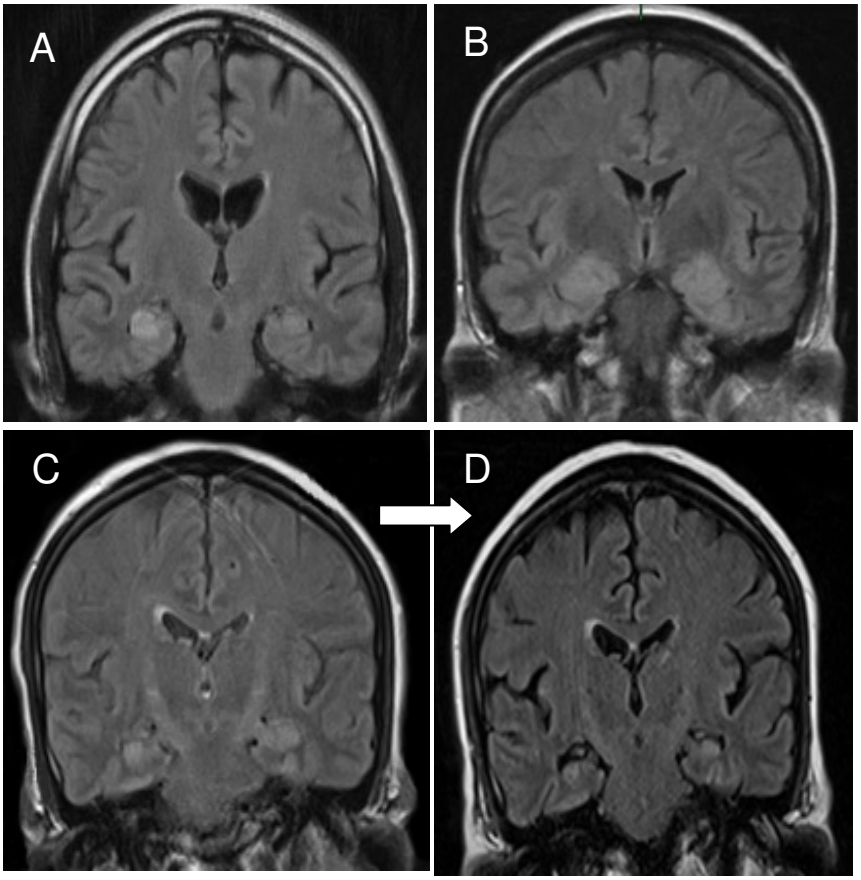


Figure 3.12. A-D. Three magnetic resonance images showing bilateral high hippocampal signal (A-C). Patient in C progressed to hippocampal and diffuse brain atrophy at six months (D).

MRI revealed 15 normal initial scans: four of these progressed to medial temporal lobe T2-weighted high intensity. Of the other 11 cases, ten showed unilateral (n=2) or bilateral (n=8) MTL high signal (Figure 3.12A-D) and one showed caudate high signal. Four cases, all with initial MTL bilateral signal hyperintensity, showed subsequent hippocampal atrophy (at median follow-up for eight months, range six to ten; example in Figure 3.12D) and the case with caudate high signal resolved to leave caudate atrophy at three months. Strikingly, all eight MRIs taken at times of pure-seizures were normal and three of these cases progressed to bilateral high signal in their medial temporal lobes.

Twenty-five out of twenty-six cases had cerebrospinal fluid (CSF) sampled. Analysis for white cells, protein, glucose and CSF-predominant unmatched oligoclonal bands were entirely normal in 20 of these cases (80%). Overall, five patients had abnormal results: two showed isolated lymphocytosis (eight and 10 cells/mm3), one showed isolated high protein (0.96g/L) and two showed elevated protein (0.75 and 0.8 g/L) plus lymphocytosis (11 and six, respectively).

Two cases underwent SPECT (example in Figure 3.13) and six cases underwent PET. The SPECT images showed hyper- and hypo-perfusion in the medial temporal lobe (hypoperfusion shown in Figure 3.14). Five of six cases undergoing PET showed medial temporal lobe hypermetabolism (n=3, example in Figure 3.14A) or hypometabolism (n=2, example in Figure 3.14C). Surprisingly, four showed abnormalities of the basal ganglia: three showed hypermetabolism (two bilateral and one right sided, Figure 3.14 B

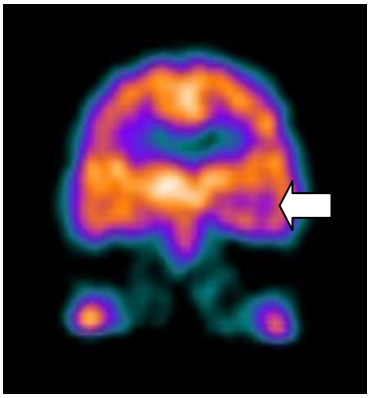


Figure 3.13. SPECT image showing left temporal hypoperfusion (arrow).

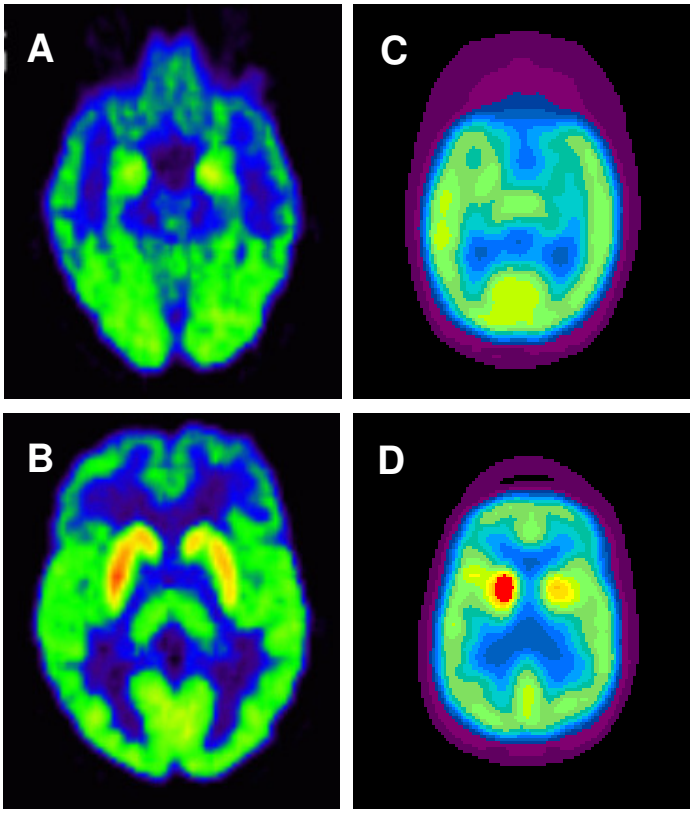


Figure 3.14 A-D. FDG PET images showing bilateral hypermetabolism in the mesial temporal lobes (A) and basal ganglia (B) in one patient, and hypometabolism in the region of the right hippocampus (C) with hypermetabolism of the right sided basal ganglia (D) in a second patient. Note that these images were acquired when the patients were having many brief seizures per hour, so could not be timed precisely to be ictal or postictal.

and D) and one showed right hypometabolism. Three of the PET/SPECTs were abnormal while the MRI was normal.

Electroencephalography (EEG) demonstrated ictal abnormalities in seven cases including frontotemporal (n=2, see Figure 3.15 for example), frontal (n=2) and temporal (n=2) epileptic activity or diffuse slowing (n=2). Interictal EEG abnormalities included diffuse slowing (n=9), frontotemporal slowing (n=6) and temporal sharp waves (n=2). In nine cases, no EEG abnormalities were detected.

Whole body imaging was normal in all 25 cases when performed. CT body/chest was performed in all the cases and whole body PET in 11. The one patient not undergoing body imaging is alive and no tumour has manifest at six-year follow-up. Follow-up of the cohort has been for a median of 2.75 years (range 1 to 8) without tumour detection. All patients were found to be negative for 'conventional' paraneoplastic antibodies (Hu, Yo, Ri, Ma, Ma2, CV2: RAVO kit). Three patients had raised thyroid antibodies – microsomal 110, 171 (<34); thyroglobulin 40 (<1).

Treatment issues

Both across the cohort and within individual cases, seizure response to multiple antiepileptic drugs (AEDs) was usually poor and produced a large number of side-effects (Figure 3.10 B-D and Figure 3.16), although five cases showed a good (20-50%) or excellent (>50%) AED-induced reduction in seizure frequency within one month (Figure 3.16). From all 26 cases, a total of 68 AEDs were administered (range 1-6 per case,

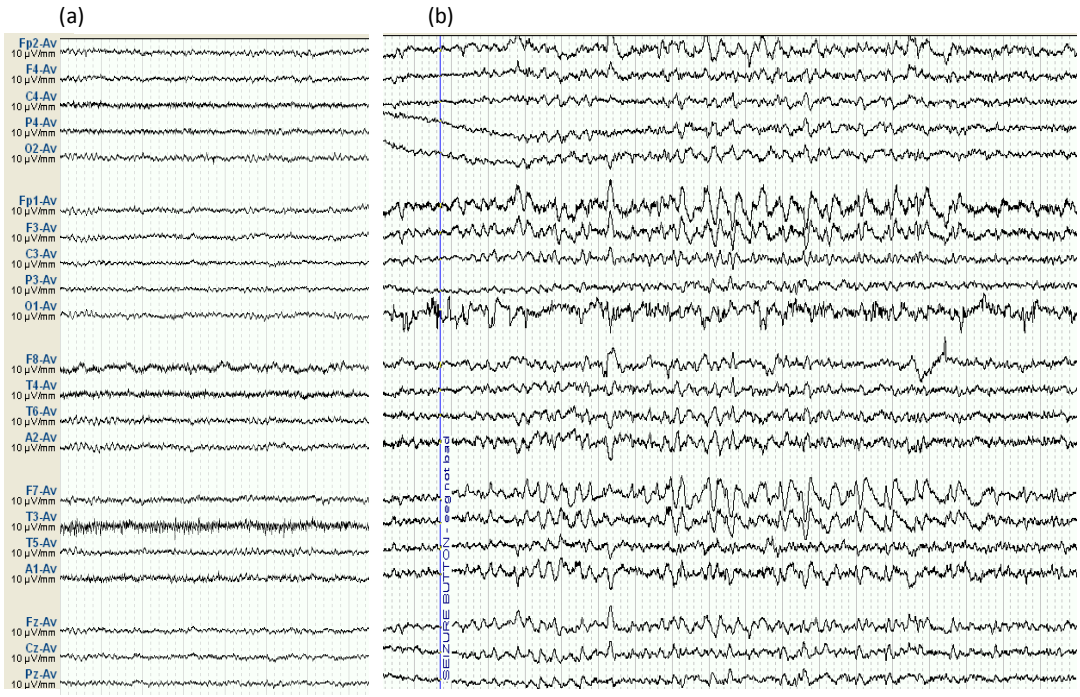


Figure 3.15. Electroencephalography with ictal frontotemporal spikes. Interictal (a) and ictal (b) EEG recorded during one of the brief characteristic seizures. On this occasion ictal 2-4 Hz spike-wave activity is noted of maximal amplitude over the left frontotemporal region. The interictal EEG is normal.

median = 2). Importantly, not only was AED therapy broadly ineffective but a remarkably high rate of adverse effects were noted. Twelve patients (46%) showed adverse reactions to AEDs (Figure 3.16, left blue bar) with rash in 10 (carbamazepine in four, phenytoin in three, lamotrigine in two and levitiracetam in one) including two cases with erythroderma. In addition, one case developed Stevens-Johnson syndrome secondary to carbamazepine and one case developed near-fatal multi-organ hypersensitivity to carbamazepine requiring intensive care admission.

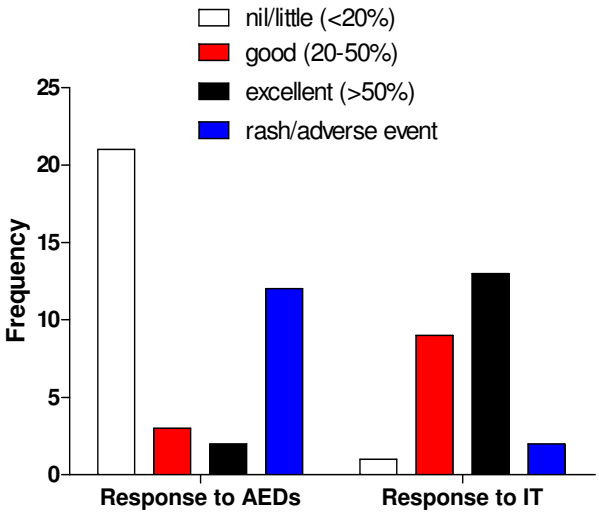


Figure 3.16. Seizure response and adverse effects with AED and IT. Seizure response to antiepileptic drugs (AEDs) and immunotherapy (IT) graded as<20% (white bars), 20-50% (red bars) and >50% (black bars). Blue bars indicate the number of cases with adverse effects to AEDs or IT.

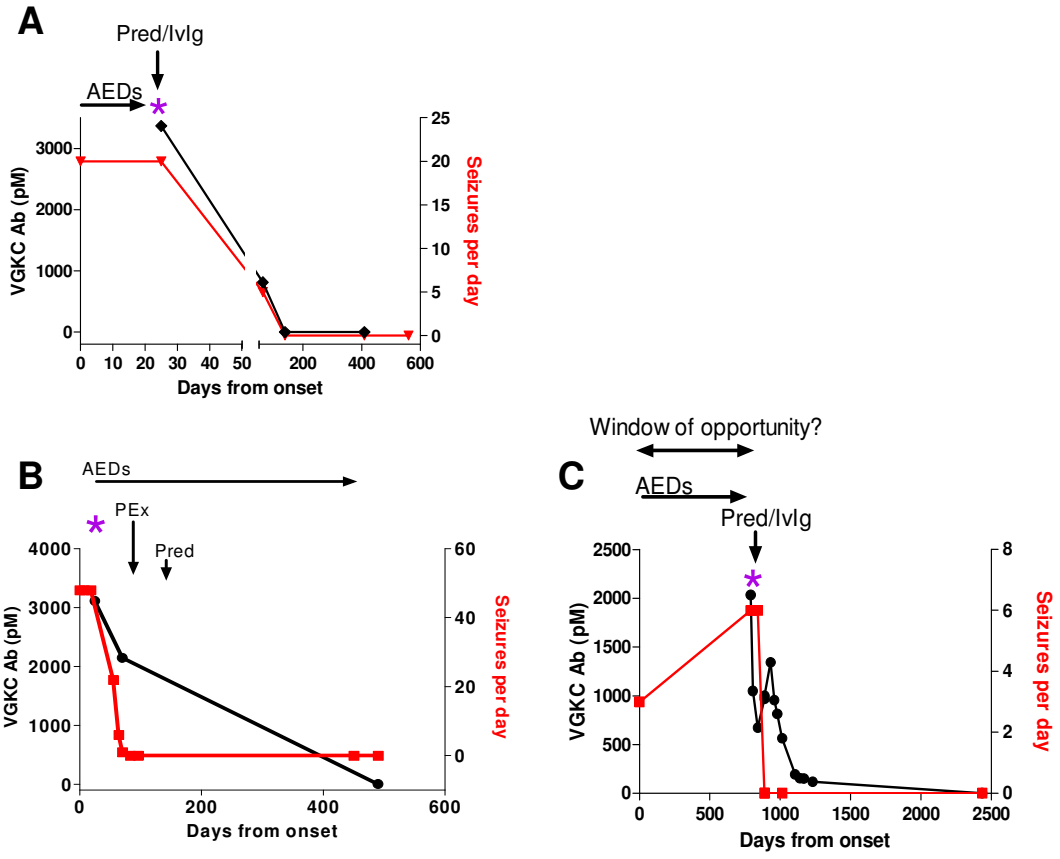


Figure 3.17 A-C. Three cases showing lack of response to AEDs (antiepileptic drugs), hypothesised window of opportunity and the response of seizure frequency (red) and VGKC-Ab levels (black) to various therapies (Pred = prednisolone; IvIg = intravenous immunoglobulins; PEx = plasma exchange).

By contrast, the seizure response to immunotherapy was excellent (Figures 3.10 B-D, 3.16 and 3.17). Immunotherapy was prednisolone or intravenous methylprednisolone in all except two cases. In addition, 16 patients were administered intravenous immunoglobulins, ten plasma exchange and one rituximab. Nine cases showed a >50% reduction in seizure frequency, eight showed a 20-50% reduction and only one case had <20% reduction over the first month of administration (Figure 3.16). Most commonly, there was an excellent correlation between seizure reduction and fall in VGKC-Abs, often after unsuccessful AED therapy (Figures 3.10B-D and 3.17A-C). Again by contrast to AEDs, adverse events to immunotherapies were rare but a fatal infection and a steroid-induced psychosis were noted in two cases (Figure 3.16). There was no clear effect of early immunotherapy or the type of immunotherapy on seizure frequency (data not shown). However, intravenous immunoglobulin was considered to have been entirely ineffective in four cases.

This cohort contained two cases with the described typical seizures, progression from seizures-only to amnesia and concomitant development of hyponatraemia, who were diagnosed before widespread knowledge of VGKC-Abs in CNS syndromes. These two cases made immunotherapy-independent limited recovery at four year follow-up with one case still suffering from daily dystonic seizures.

CNS-relapses have never been reported in VGKC-Ab associated LE, however three of our cases developed recrudescence of seizures after rapid weaning of immunotherapy. In all cases, the seizures were exquisitely responsive to reinstitution of prednisolone (Figure

3.18A-C). Case A relapsed when prednisolone was reduced from 60mg daily to 45mg daily over two months. Case B had prednisolone reduced from 50mg daily to 25mg daily

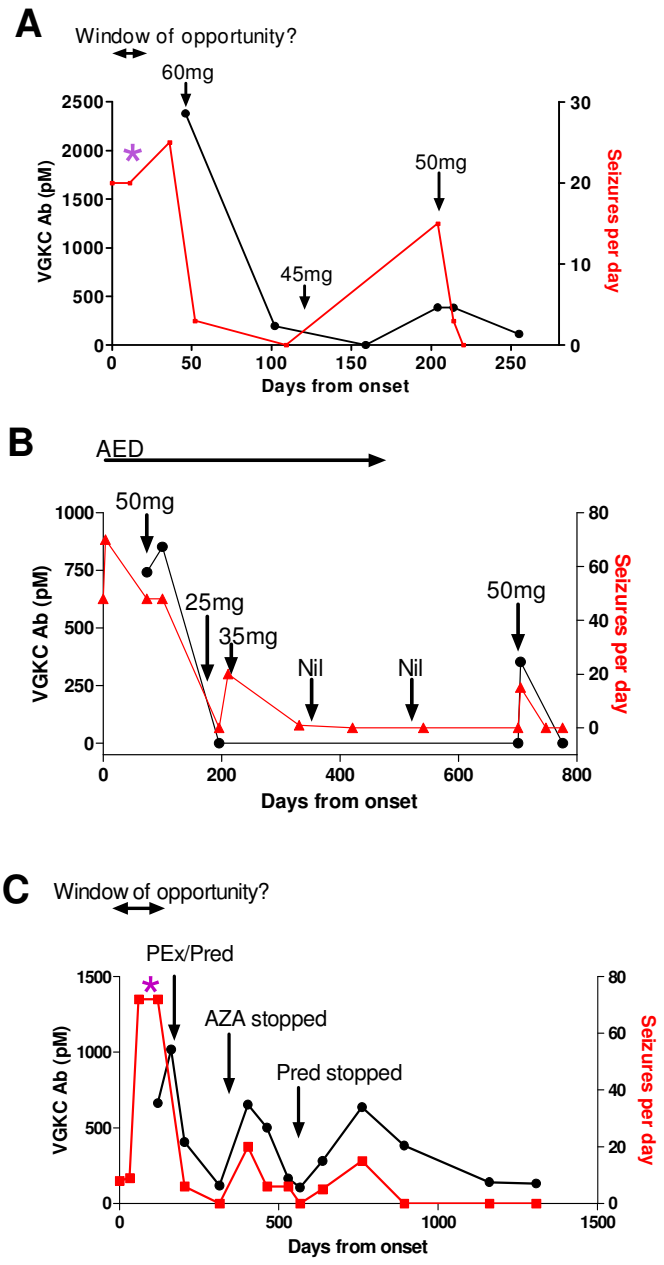


Figure 3.18 A-C. Three cases with relapses showing lack of response to AEDs, hypothesised window of opportunity, the response of seizure frequency (red) and VGKC-Ab levels (black) to various therapies. Pred = prednisolone; IvIg = intravenous immunoglobulins; PEX = plasma exchange; AZA = azathioprine.

in three months, which precipitated the first relapse. Subsequently, the second relapse occurred after prednisolone was reduced from 35mg to nil over five months although only after 18 months of no immunotherapy. The final relapsing case (C) had prednisolone reduced from 50mg to nil over three months, prior to the first relapse, azathioprine was stopped before the second relapse and prednisolone was reduced from 25mg to 15mg over five months before the third relapse.

Sixteen of the 26 cases were incidentally included in our unselected cohort of 78 cases with VGKC-Ab-positive LE, suggesting this seizure phenotype is present in around 20% of VGKC-Ab-positive LE cases. Since collecting data for this study, we have prospectively clinically identified five further cases with this seizure phenotype who have subsequently been proven to have high VGKC-Ab levels.

Summary and conclusions

This chapter described the clinical features from the largest reported cohort of VGKC-Ab positive patients. Our centre uses the most specific (and probably most sensitive) first-line assay, by marked contrast to brain immunofluorescence used in other diagnostic centres (e.g. Ances et al 2005; Tan et al 2008; Lancaster et al 2010). This, and the study restriction to cases with high VGKC-Abs levels, may have accounted for the clear categorisation of 108/113 (96%) cases into the three conventional syndromes of LE/epilepsy, MoS and NMT (in striking comparison to Tan et al (2008)). Within the LE group, amnesia was present in 71 of 74 cases (96%) and all had neuropsychiatric features (100%). Seizures were a feature in 63 of 74 (85%); however data were not gathered with

regards to seizure semiology and possible localisation. This has some potential implications for the strict and definitive diagnosis of LE (Bien and Elger 2007) but conversations with referring clinicians and casenote reviews suggested the vast majority of localisation-related seizures were temporal in semiology.

The LE group were by far the most frequently identified, although this may reflect the predominance of high titre patients within our cohort (60% had VGKC-Abs >1000 pM). Given VGKC-Ab LE has only been well-established for about five years, its frequency and recognition are still likely to be rising and it is likely to prove to be much more common than the other two relatively well-established conditions. This is especially pertinent given that questionnaires and letters were only received from neurologists. Further biases from questionnaires arise from the 100% response rate from the 13 possible MoS cases (this high response rate may reflect the helpfulness of clinicians referring these difficult cases, whose complexity is likely to aid to information retention) and the deferral of NMT or MoS syndrome classification to the referring clinicians. For example, there were two NMT cases with insomnia, it could be argued that these cases have CNS features plus NMT which should be classified as MoS. The inherent reliance on the clinician's classification is carried through this thesis, however this obviated the need for authors to interpret the data, often without having met the patient.

The consequent spectrum of disorders from NMT to MoS to LE clearly show a significant number of shared, otherwise uncommon, neurological features. However, a number of these features such as pain, dysautonomia, hypersomnia, insomnia and

seizures should strongly suggest the diagnosis of one syndrome over another. It is of particular interest that the MoS cohort may show some specific cognitive patterns particularly in their high rate of hallucinations (69%) and low frequency of seizures (38%), when compared to the LE group (20% and 85%, respectively; both p=0.0008, Fishers t test). These varying frequencies, taken together with the significantly differing VGKC-Abs titres in the LE, MoS and NMT groups, strongly suggest differing pathophysiological mechanisms between the NMT, MoS and LE cohorts. Further insights into potential aetiologies arose from the observation of high tumour frequencies within the MoS/NMT cohorts and higher prodromal infectious features in the LE cohort. As infectious prodromes were not seen in the MoS or NMT cohorts, it is unlikely that these reflect a background rate of infection. The high rate of thymomas in the MoS/NMT cohorts may reflect serum referrals to a centre famous for work in myasthenia gravis. This may be akin to the remarkably high rate of paraneoplastic VGKC-Ab positive LE seen by groups with a paraneoplastic interest (e.g. Graus et al 2008, Tan et al 2008).

A major limitation of the immunotherapy data analyses is that we do not have consistent data to assess the importance of the timing of immunotherapy or the doses of immunotherapy – both could have a major influence on the outcome. In addition, the natural history of the disease is usually monophasic and we do not have data to understand the effect of immunotherapy above this baseline spontaneous remission in a significant number of cases (see introduction). A future analysis with respect to the cases treated without immunotherapies may be useful.

Finally, the observation that a distinctive epilepsy semiology may be present in the VGKC-Ab positive individuals is akin to the presence of a characteristic movement disorder in the NMDAR-Ab positive cohorts (see introduction and Appendix 1). This gives weight to the theory that novel modulatory mechanisms to specific pathways may generate novel phenotypes. Although 30% of cases lacked video evidence of their episodes, the marked stereotypy of clinician-descriptions across patients strongly suggested we are reporting a homogeneous cohort identified by interested clinicians. The seizure focus may be in the frontal lobes. Therefore, these observations should prompt study to explain the mechanism by which the burden of this disease spreads from the frontal to temporal lobes. In addition, this observation may provide a specific avenue to predict the onset of VGKC-Ab associated LE.

In the following chapters, the scientific aspects of the thesis are developed and finally correlated to the clinical findings presented in this chapter.

CHAPTER 4: Kv1 POTASSIUM CHANNELS AS ANTIGENIC TARGETS

Introduction

The work in this chapter aimed to ask which Kv1-channels are major targets of autoantibodies in limbic encephalitis, Morvan's syndrome and neuromyotonia. Specifically, it was hypothesised that IgG from patients with the three major VGKC-Ab associated syndromes (LE, MoS and NMT) showed differential binding to the three DTX-sensitive Kv1 channels (Kv1.1, 1.2 or 1.6). As the scientific experiments below began before the clinical data described in Chapter 3 were gathered and available, a few VGKC-Ab positive sera with known clinical features were chosen to examine the possible Kv1-specificities within the three clinical groups. Once the clinical data became available, some of the more definitive experiments were repeated using all the 113 sera.

As shown in Chapter 3 (Figure 3.1), the patients examined all precipitated appreciable amounts of VGKCs from digitonin-solubilised rabbit brain extract. Hence, the initial question asked whether these sera could bind Kv1 channels when specifically expressed in human embryonic kidney (HEK) cells.

Specificity of commercial antibodies

Initially, the only available commercial antibodies were raised against the intracellular domains of Kv1 channels. Hence, permeabilised cell immunofluorescence and western blots were used to confirm the Kv1-subtype specificity of the commercial antibodies.

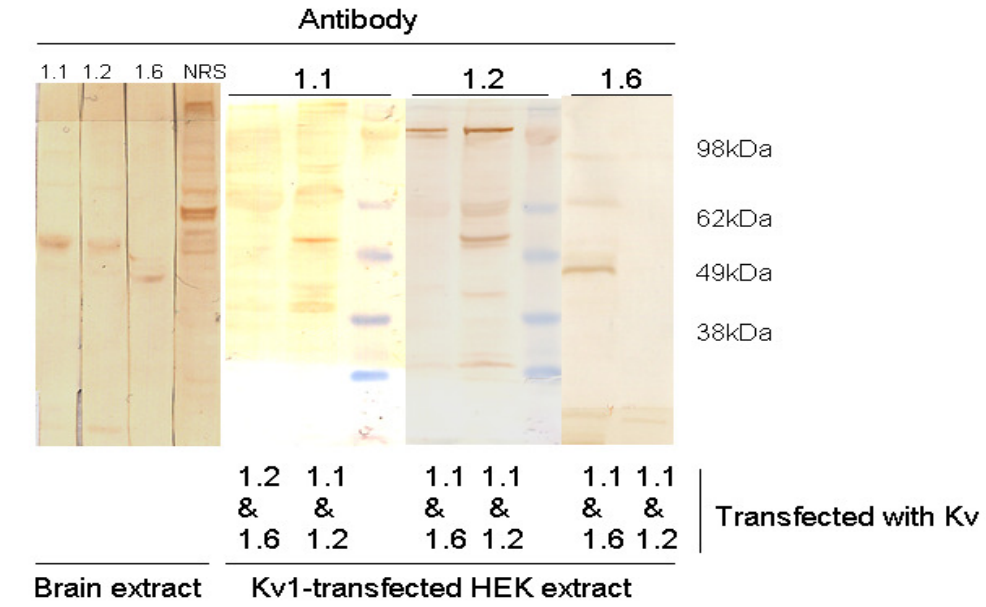


Figure 4.1. Western blots using rabbit anti-Kv1.1, 1.2 and 1.6 commercial antibodies (1:500-1:1000) and normal rabbit serum (NRS) to probe lanes containing solubilised rabbit brain membranes (brain extract) or Kv1-transfected HEK cell extract. Cells were each transfected with two Kv1 cDNAs (combinations of Kv1.1, 1.2 and 1.6).

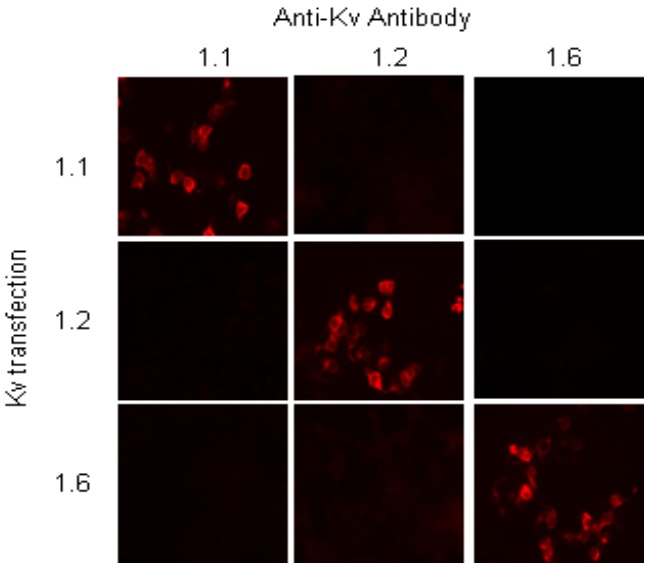


Figure 4.2. Permeabilised Kv1.1/1.2/1.6-transfected HEK cells stained with rabbit anti-Kv1.1/1.2/1.6 commercials antibodies (1:750-1:1000). Magnification x 200.

Anti-Kv1.1, anti-Kv1.2 and anti-Kv1.6 antibodies bound specifically to bands at around 55kDa, 55kDa and 45kDa, respectively, in rabbit brain extract (Figure 4.1). Furthermore, from Kv1.1, Kv1.2 and Kv1.6-containing HEK cell extracts, these antibodies were able to recognise similarly sized bands (Figure 4.1). All three Kv1 antibodies used were able to bind to the intracellular domains of their intended Kv1 channels when expressed in HEK cells (Figure 4.2).

Absent binding of patient sera to the extracellular domain of Kv1s expressed in a mammalian cell line

Antibodies with pathogenic potential should bind the extracellular domain of their candidate antigen. Hence, unpermeabilised Kv1-transfected HEK cells were incubated with patient sera, in the knowledge that they expressed the Kv1 proteins of interest (from Figure 4.1) towards their cell surface (from Figure 4.2). Surprisingly, however, LE (n=10), MoS (n=3) and NMT (n=6) sera (at 1:10-1:100 dilutions (2.5–25µl serum per coverslip)) did not bind to Kv1.1, 1.2 or 1.6-transfected HEK cells, despite good transfection efficiencies (often >50%) as determined by EGFP co-expression (Figure 4.3). This was in direct contradiction to previously published work using Xenopus oocytes and HeLa cells (Hart et al 1997, Kleopa et al 2006). It was possible that levels of Kv1-surface expression may be insufficient to detect bound IgG. Hence, a series of immunocytochemistry and surface dendrotoxin-binding experiments were undertaken to optimise Kv1 surface expression.

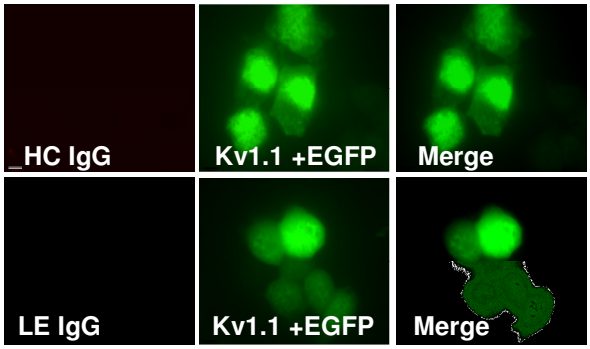


Figure 4.3. Sera did not bind Kv1 at the cell surface. Unpermeabilised Kv1.1/1.2/1.6–EGFP co-transfected HEK cells labelled patient sera (LE/MoS/NMT all produced identical results: magnification x1000; LE IgG shown) or healthy control IgG (HC)

Optimisation of Kv1 surface expression

The time course of Kv1-surface expression was determined in transfected HEK cells with a 'hot-cold' αDTX assay. This assay subtracted non-specific surface-bound ^{125}I-αDTX from total surface-bound ^{125}I-αDTX to estimate specific surface-bound ^{125}I-αDTX, a measure of Kv1-heteromer surface expression. Although absolute expression levels were rather low in comparison to data presented later (compare Figure 4.4A to Figure 4.5B), surface expression was maximal at around 48 hours post Kv1.1, 1.2 and 1.6-transfection (Figure 4.4A). To further enhance Kv1-surface expression, increased amounts of individual Kv1 cDNAs were used for transfection. Results, measured at 48 hours post-transfection, showed maximal surface expression capacity from around 3µg of cDNA per well of a 6-well-plate (Figure 4.4B, green, red and blue). However, this did not account for the potential additive effect of Kv1.1/1.2/1.6 multimerisation. Therefore, HEK cells were transfected with Kv1.1, Kv1.2 and Kv1.6 in a 1:1:1 ratio, up to a total of 6µg cDNA per well which enhanced expression to almost 40,000 cpm (Figure 4.4B, pink). 1.5µl of PEI was used for transfection of around 6µg of cDNA. More PEI, and therefore the potential for more cDNA, caused unacceptable cell loss (visual estimate of cells remaining adherent) and cell lysis (as determined by a commercial LDH-assay, performed by Ms Kasia Bera,

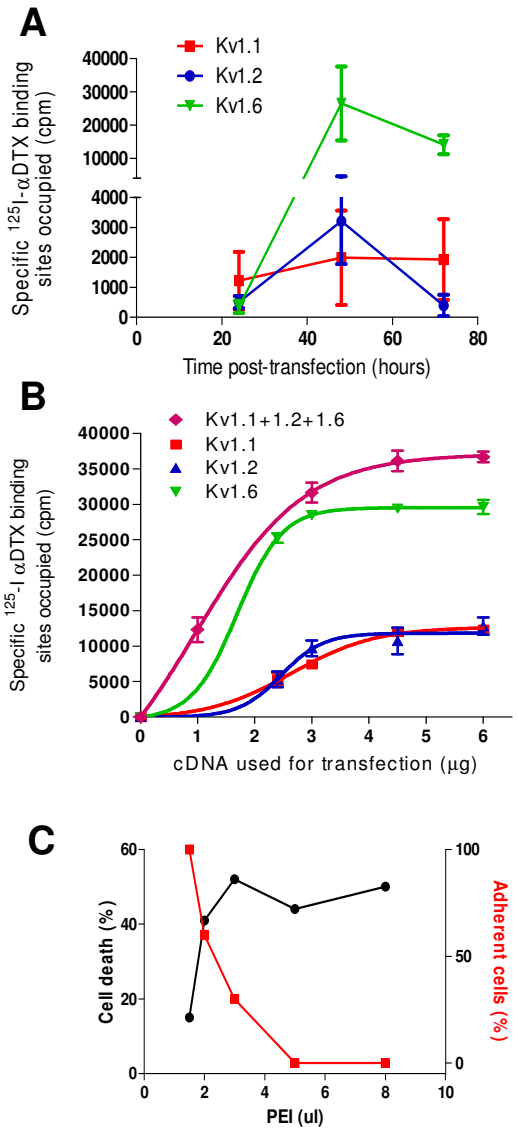


Figure 4.4. Dendrotoxin cell surface quantification: 'Hot-cold' ^{125}I-α-dendrotoxin binding assays.
A. ^{125}I-α-dendrotoxin added (100,000cpm per well) to Kv1-transfected HEK cells assessed at 24, 48 and 72 hours post-transfection (n=3).
B. Increased amounts of Kv1-cDNA were used to maximise ^{125}I-α-dendrotoxin binding (n=3).
C. Cell viability (in one well of a six-well plate) with increased amounts of PEI (death was normalised to Tx100-treated cells = 100%; LDH assay performed by Ms K Bera) and percentage of adherent cells were visually estimated.

Figure 4.4C). Despite a combination of these optimised conditions, surface-bound patient IgG was not seen on Kv1-transfected cells (for example, Figure 4.3).

At this stage, Dr J Trimmer (California, USA) kindly provided us with a mouse antibody generated against the extracellular domain of Kv1.1 (Kv1.1e). This antibody clearly and specifically labelled the surface of Kv1.1-transfected cells (Figure 4.5, top panels). It did not bind Kv1.2 (Figure 4.5, middle panels) or Kv1.6 (data not shown) transfected cells.

The Kv1.1e antibody also detected surface Kv1.1 expression when Kv1.1, 1.2 and 1.6 were co-transfected (i.e. with a reduced total amount of Kv1.1 cDNA), although this binding was consistently fainter than when Kv1.1 alone was expressed (Figure 4.5, third horizontal panel). Despite immunocytochemical evidence of detectable Kv1 surface expression, the LE (n=10), MoS (n=3) and NMT (n=6) sera (at a 1:20 dilution) did not bind the cell surface (Figure 4.3, example from LE patient).

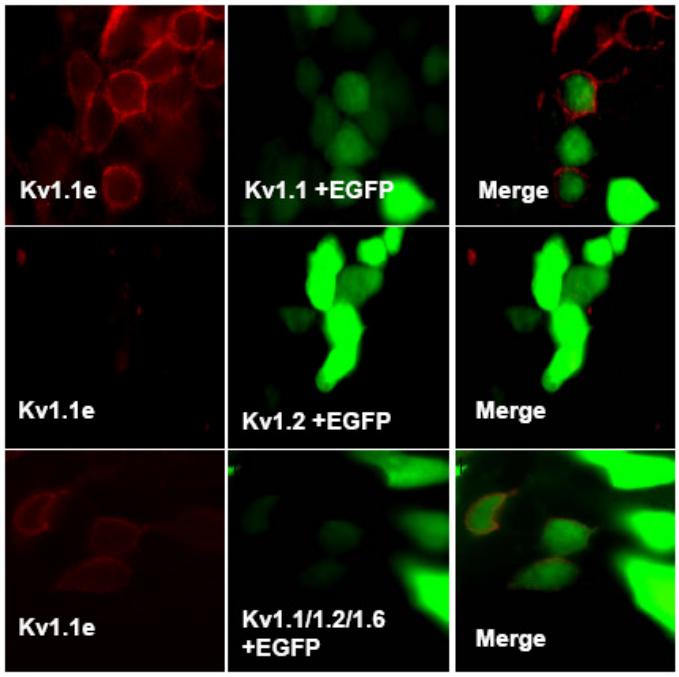


Figure 4.5. Kv1-transfected cells. Combinations of unpermeabilised Kv1.1/1.2/1.6 singly or co-transfected HEK cells were labelled with mouse anti-Kv1.1 extracellular domain (Kv1.1e) antibody. EGFP co-transfection performed throughout. Magnification x 1000.

Although disappointing, a number of possibilities remained including the Kv1.1e antibody was of a particularly high concentration/affinity/avidity in comparison to patient IgG, or the patient sera bound heteromeric combinations of Kv1 channels which are near the limit of detection when using immunofluorescence, or the patient IgG required higher Kv1 surface densities or Kv1-clustering proteins which may only be available in neural tissue. Hence, further surface expression optimisation experiments were necessary. For

various reasons, explained later in the thesis, we became aware of the importance of Kv1-associated proteins. As outlined in the introduction, these included the Kv beta subunits (especially Kvβ2), some post-synaptic density proteins (PSD-95 and 93, in particular), contactin-associated protein 2 (CASPR2) and leucine-rich glioma inactivated-1 (Lgi1). Mammalian expression vectors for these proteins were subcloned by Dr Patrick Waters, within our laboratory.

The effects of co-transfection with these molecules on Kv1 surface expression were examined (Figure 4.6A and B). The β2 subunit (the most prevalent of the three Kv-beta subunits within the brain) produced an almost four-fold increase in the Kv1.2 subunit surface expression but had no effect on Kv1.1 or Kv1.6. By contrast, the Kv1.4 subunit had no effect on levels of Kv1.1, Kv1.2 or Kv1.6 surface expression (Figure 4.6A). In a separate series of experiments, performed with a different batch of HEK cells, absolute levels of surface expression were markedly higher than presented in Figure 4.6A. Using these cells, 1.5µg of Kvβ2, Kv1.4, PSD93, PSD95, Lgi1 or CASPR2 cDNA were co-transfected with 3µg of Kv1.1, 1.2 and 1.6 cDNA (1µg of each Kv1 in a 1:1:1 ratio). The results, shown in Figure 4.6B, demonstrated significantly increased levels of Kv1-surface expression with addition of all these molecules other than Kv1.4 and PSD93. There was no additive effect of PSD93 or PSD95 to the effect of Kvβ2.

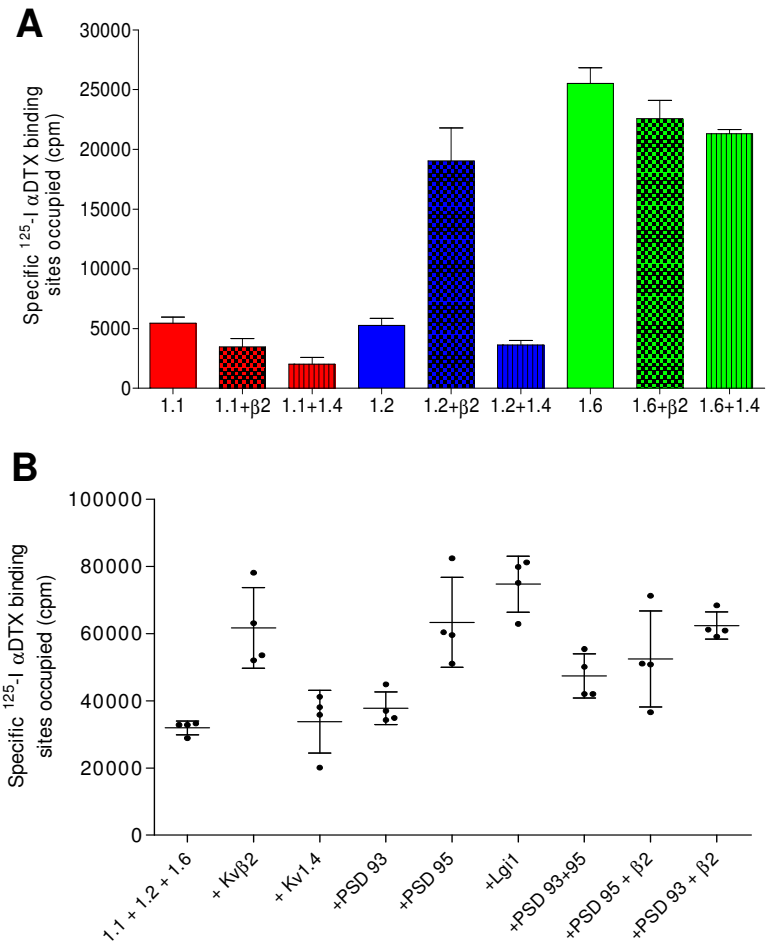


Figure 4.6.Kv1 surface expression. A. ^{125}I-α-dendrotoxin binding assays for individual Kv1 subunits (n=3, plain bars), plus Kvβ2 (n=3, checked bars) or Kv1.4 (n=2, vertical stripes). B. Kv1.1, 1.2 and 1.6 co-transfection shown individually (furthest left) and with multiple or single accessory subunit co-transfection (n=4). Specific ^{125}I-α-dendrotoxin binding determined with 'hot-cold' assay

Number of surface Kv1 channels per cell

It was possible that the absolute optimised Kv1-surface expression was insufficient to allow detection of bound patient sera. Using radioiodinated bungarotoxin, it has been estimated that there are around 20,000 AChRs per cell which are detected by patient sera in a similar cell-based assay (Leite and Vincent, unpublished). Below, the number of Kv1-channels per Kv1-transfected cell are estimated:

1Ci equals 2.2 x 10^{12} cpm. With a maximum of 80,000cpm in a single well of a six well plate containing 2 million cells.

80,000 cpm / 2.2 x 10^{12} cpm = 4 x 10^{-8} Ci.

Based on the ^{125}I-αDTX specific activity, 2000Ci=1mmoles of DTX binding sites and, so 1Ci = 5 x 10^{-4} mmoles

Therefore, 80,000cpm = 5 x 10^{-4} x 4 x 10^{-8} mmoles = 2 x 10^{-14} mmoles.

Given 1 mole = 6 x 10^{23} molecules (Avagadro's number), 2 x 10^{-14} moles = 1.2 x 10^{10} molecules within one well, which equals 6000 molecules per cell. Which is equivalent to 6000 dendrotoxin binding sites or, assuming Kv1-channel:DTX = 1:1, 6000 surface expressed Kv1 channels per cell. When adjusted for the 80% efficiency of the counter, this equals 7500 Kv1 channels per cell.

Varied Kv1-subunit quantities in brain tissue

The above experiments showed that HEK cells surface-expressed approximately sufficient quantities of Kv1 to allow detection by immunofluorescence with a commercial antibody. However, despite a number of optimisation steps, sera from patients which

precipitated Kv1s from mammalian brain tissue did not bind these Kv1-expressing HEK cells.

In parallel with the above experiments, we used the ^{125}I-αDTX-labelled rabbit brain tissue (from the diagnostic VGKC-Ab assay) to understand the Kv1 subunit compositions within ^{125}I-αDTX-labelled Kv1s and to compare the maximal number of ^{125}I-αDTX-binding sites precipitated by patient sera and commercial antibodies from brain tissue. As a preliminary experiment, varied amounts of precipitating secondary antibody (goat anti-human IgG) were titrated against a fixed amount of a high positive MoS patient's serum (Figure 4.7A). This allowed use of optimal amounts of secondary antibody to precipitate patient sera. This secondary antibody was particularly useful as it showed reactivity against rabbit, mouse and human IgG, allowing direct comparisons to be made between patient and commercial antibodies. In fact, this antibody showed far better maximal precipitation and lower assay backgrounds when compared to anti-rabbit and anti-mouse secondaries, respectively (data not shown). Precipitations used increasing amounts of specific commercial antibodies showed that Kv1.2 was the most abundant subunit followed by Kvβ2 > Kv1.1 > Kv1.6 > Kv1.4 > Kv1.3 (Figure 4.7B). Using this approach, appreciable amounts of Kv1.5 were not detected. Next, combinations of anti-Kv1 commercial antibodies allowed estimation of the relative quantities of each subunit within ^{125}I-αDTX-labelled Kv1 complexes in mammalian brain membranes. Kv1.2 maximally precipitated around 40,000cpm and was therefore likely to be present in most (if not all) ^{125}I-αDTX-labelled complexes. As shown in Figure 4.7C, addition of anti-Kv1.6 antibodies to a non-maximally precipitated amount of Kv1.1 (using 2.5µl of the anti-Kv1.1 antibody), produced a small increase (by around 4000

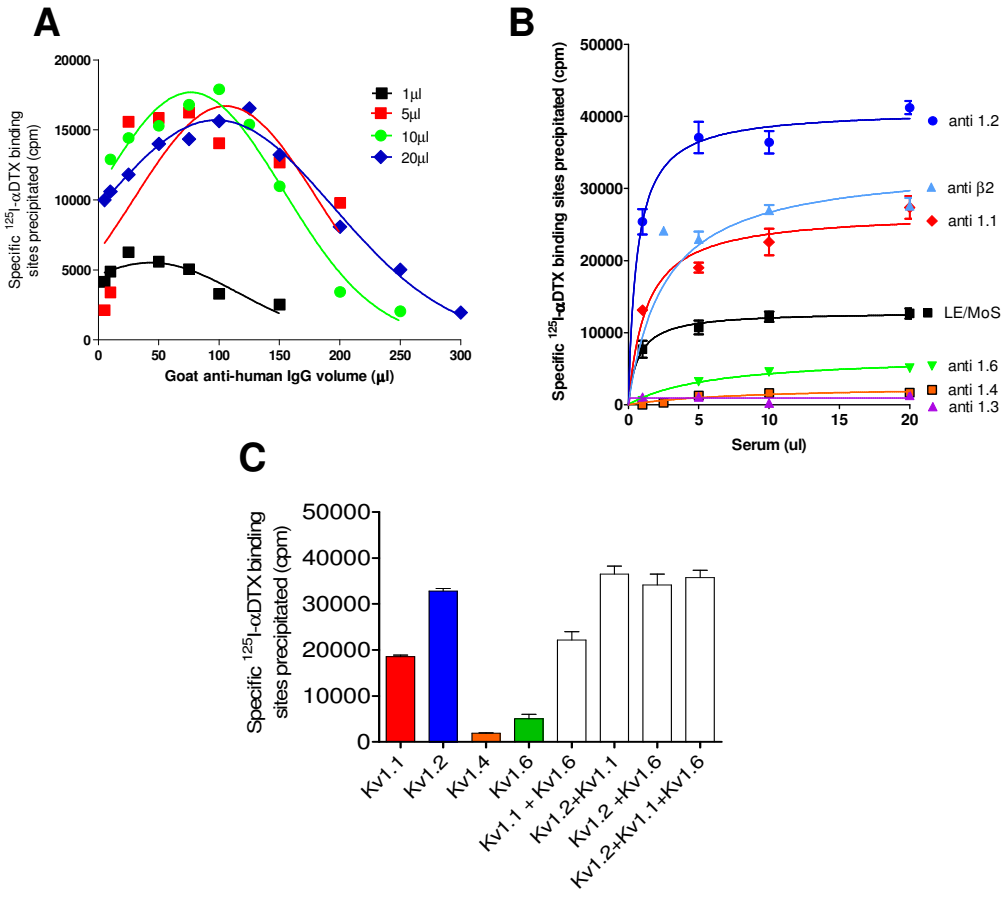


Figure 4.7. Diagnostic assay data: immunoprecipitations from ^{125}I-αDTX-labelled rabbit brain membranes. A. Goat anti-human IgG precipitation capacity with varying amounts of primary antibody (serum, 1-20µl, n=1). B. Saturation of precipitation using a variety of commercial anti-Kv antibodies (n=3) and LE/MoS sera (black, n=8). C. Precipitation used 2.5µl of each antibody from 'B' individually or in combinations (n=3; Kruskal-Wallis test, p=0.0035 with Dunn's correction only showing p<0.05 for Kv1.1+1.2 Vs Kv1.4).

cpm) in the mean number of ^{125}I-αDTX binding sites precipitated. This was also true of Kv1.1 and Kv1.6 addition to Kv1.2, although the magnitude was even smaller. Collectively, these data suggested that Kv1.2 was present in essentially all ^{125}I-αDTX-labelled Kv1 complexes and was homomeric in around 30% of these complexes. From the remaining heteromers, most Kv1.2 was associated with Kv1.1. Kv1.6 without Kv1.2 represented the vast minority of complexes (Figure 4.7C). When LE/MoS sera were

tested with the same assay, these did not precipitate at a level equivalent to any individual Kv1 (Figure 4.7B).

A comparison of Kv1 and patient binding patterns in cerebellar tissue, ependymal cells and hippocampal neuronal cultures

Taken together, these data suggested that the patient antibodies may bind the intracellular domain of Kv1s or possibly to Kv1s which were expressed in a conformation within neural tissue that was unavailable at the surface of HEK cells.

Some studies from the LE/MoS literature showed similarities between patient and Kv1 distributions in mammalian brain sections with a particular focus on the hippocampus (Buckley et al 2001; Ances et al 2005, Kleopa et al 2006). However, the cerebellum – specifically, the basket cell layer – had previously been reported to show the highest Kv1 density in the CNS (Koch et al 1997; Chung et al 2001 and 2005). Therefore, this region was explored in further detail.

The basket cells are Kv1-rich neurons with dendritic terminals that project to Purkinje cell bodies (white arrow, Figure 4.8A). Kv1.1 and Kv1.2 antibodies showed specific and intense binding to the basket cells. It was possible to differentiate these from the Purkinje cells themselves both structurally (Figure 4.8B) and with anti-Yo antibody positive sera (red, Figure 4.8A). LE patient sera usually bound to the cerebellar molecular layer, and relatively spared the granule cell layer with complete exclusion from the Purkinje layer (Figure 4.8B and 4.9A and B). Using immunohistochemistry and immunofluorescent co-

localisation, LE patient sera showed only very faint or no staining of the Kv1.1/1.2-expressing basket cells (Figures 4.9B, left and right panels, respectively).

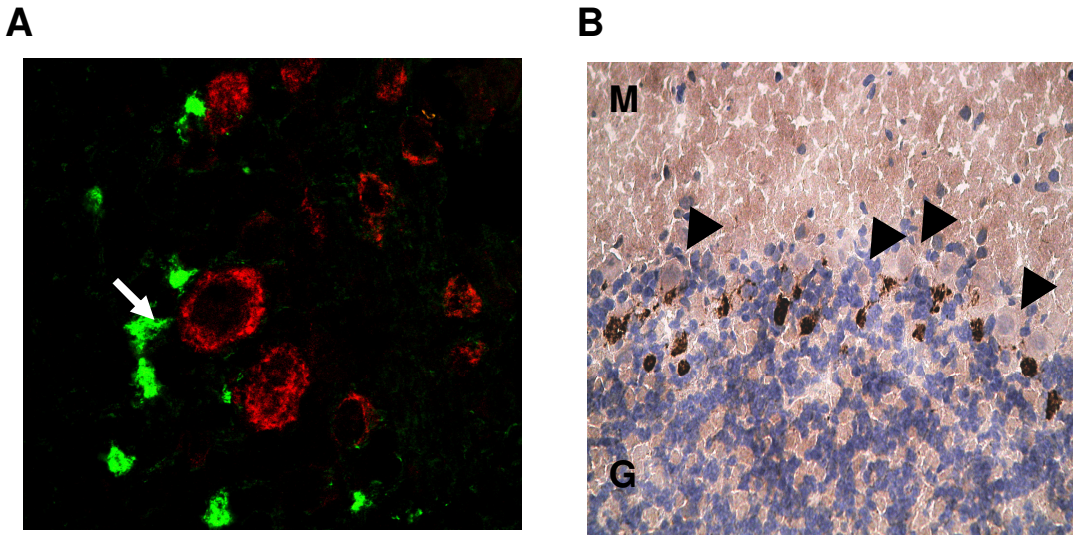


Figure 4.8. A. Cerebellar immunofluorescence. Purkinje cells delineated with human anti-Yo serum (red) and basket cells with rabbit anti-Kv1.1 antibodies (green). White arrow showing likely basket cell dendritic extension onto Purkinje soma (magnification x 500). B. Cerebellar immunohistochemistry. Rabbit anti-Kv1.2 antibodies developed with DAB (brown). Arrowheads = Purkinje cells. M = molecular layer. G = granule cell layer (magnification x 100). Haemalun nuclear counterstain (blue).

Binding to the ventricular ependyma was noted with the anti-Kv1.6 antibody (Figure 4.10, left panel). This intense staining was seen neither with Kv1.1/Kv1.2 antibodies nor with LE sera and did not colocalise with the choroid plexus apical cell surface marker Na-K ATPase (Figure 4.10, red, right-hand panel). These cells may have represented the few non-Kv1.2 containing heteromers detected in brain extracts. Similarly, a subset of brainstem neurons – sectioned at the level of the cerebellum – were bound by Kv1.1 and Kv1.2 commercials but were not bound by patient sera (Figure 4.11).

Standard immunohistochemistry techniques require sections to be fixed before primary serum incubation and patients' antibodies may be selectively reactive against non-denatured, native epitopes. In addition, sections allow visualisation of intracellular and

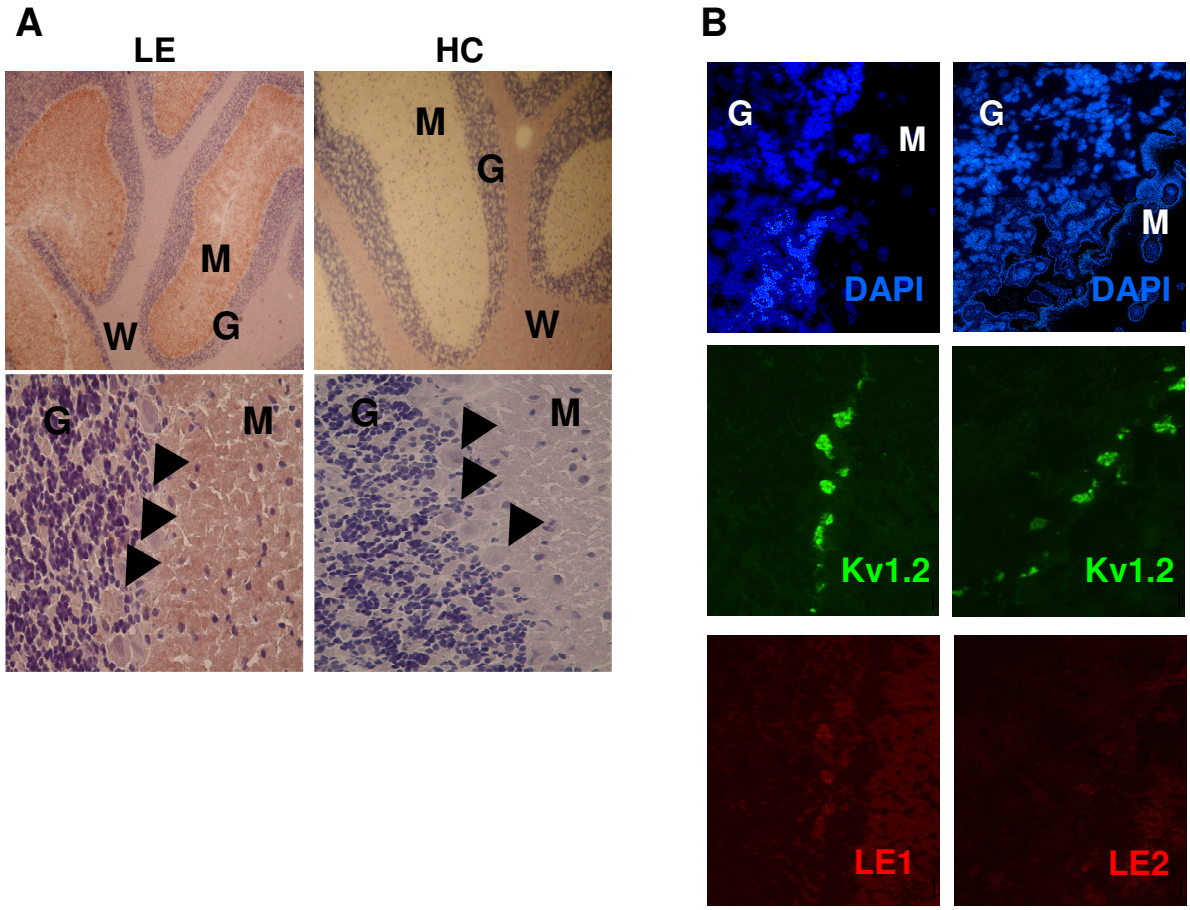


Figure 4.9. Cerebellar immunohistochemistry. A. LE patient (LE, left panels) with molecular layer preference within cerebellum. Clear sparing of Purkinje cells seen (arrowheads). No binding to the molecular layer with healthy controls (HC, right panel). Magnification: upper x 20; lower x 100. B. Two LE patients (red) and rabbit anti-Kv1.2 (green) showed some, albeit faint, co-localisation (left panel, LE1) and no co-localisation (right panel, LE2). DAPI highlighting granule cell layer. Magnification x 200. G=granule, M=molecular, W = white matter tracts. Counterstained with haemalun.

extracellular antigenic targets where intracellular targets offer limited insights into potential pathogenicity. Live hippocampal cultures were examined as a possible means to

overcome both of these problems and to compare Kv1 commercial antibody and patient IgG binding characteristics to native neural antigens. Initially, patient serum binding to

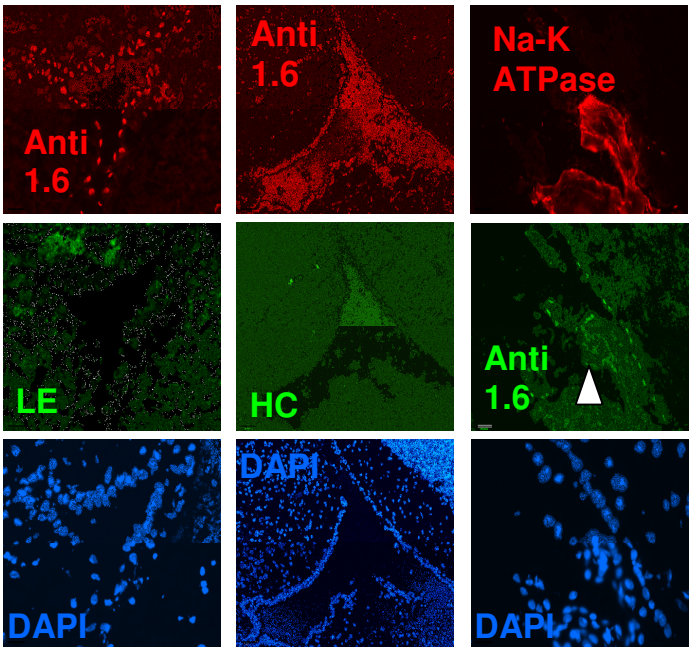


Figure 4.10. Ventricular immunohistochemistry. Anti-Kv1.6 antibodies (but not Kv1.1/1.2 antibodies – data not shown) bind intensely to the ventricular ependymal layer. LE/MoS sera (n=15) did not bind this cell population anymore strongly than healthy control sera (HC). This cell population were Na-K ATPase deficient, suggesting they did not lie on the apical membrane of the choroid plexus (arrowhead). Magnification x 100 (left and centre panels) and x 500 (right panel).

unfixed cells was not observed and cells were very briefly fixed. Fixed permeabilised cultured hippocampal tissue allowed visualisation of microtubule associated protein 2 (MAP2) and glial fibrillary associated protein (GFAP) expression within neurons and astrocytes, respectively (Figure 4.12, left panels). Clear co-localisation of patient sera and commercial Kv1 antibodies was not seen within neuronal populations (Figure 4.12, with two LE sera). It was later discovered (by Dr L Zulliani, within our laboratory) that initial fixation of hippocampal cultures caused slight cell permeabilisation. Nevertheless, the apparent surface staining seen with patient sera was not seen with the Kv1.1e antibody.

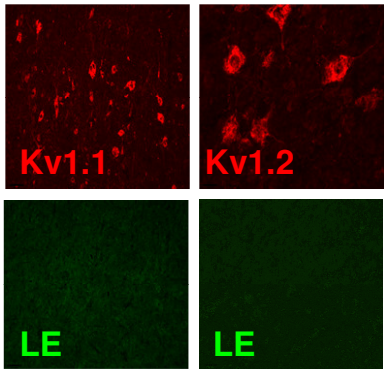


Figure 4.11. Brainstem immunohistochemistry. A subset of brainstem neurons were bound by Kv1.1 (x 50 magnification) and Kv1.2 (x 250 magnification) antibodies (red). Similar patterns were not seen with LE sera (green).

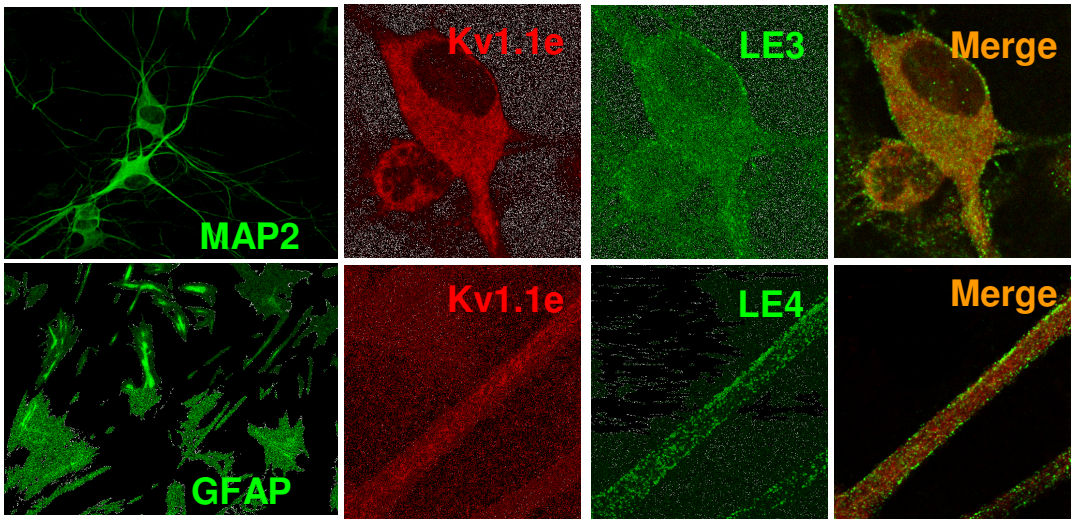


Figure 4.12. Hippocampal cultures. MAP2 (microtubule associated protein 2) positive and GFAP (glial fibrillary acidic protein) positive cells were identified within hippocampal culture preparations and showed neuronal and glial morphology, respectively (left panel, green, magnification x 400). LE sera (LE3 and LE4, green) bound in a punctate pattern towards the surface of neuronal somata (upper three panels, magnification x 1000) and axons (lower panels, magnification x 3000), in comparison to the more homogeneous binding of Kv1.1 (determined using Kv1.1e antibody directed against the extracellular domain of Kv1.1, red).

^{125}I-αDTX-labelled, Kv1-transfected HEK cell extracts are not precipitated by patient sera

Hence, clear discrepancies existed between the behaviour of commercial antibodies, representing Kv1 subunits, and patient sera in both brain and transfected HEK cells. The relative Kv1-quantities available in brain tissue suggested that patient sera did not bind a single Kv1-channel. However, patient sera do not bind heteromeric Kv1s expressed on the surface of HEK cells, where a commercial antibody allowed their detection. It was still possible that patient antibodies bound the intracellular aspect of Kv1 channels – and were hence not detected using unpermeabilised Kv1-transfected cells. The routine clinical radioimmunoassay is used to define VGKC-Abs. To mimic this assay as closely as possible, but specifically with over-expression of Kv1s, Kv1-transfected HEK cells were solubilised in 2% digitonin and extracts were labelled with ^{125}I-αDTX. This allowed us to examine all epitopes available in solution. Figures 4.13A to F show immunoprecipitation from extracts expressing different Kv1-combinations. Initially, it appeared that the extracts from cells only transfected with Kv1.1 were not precipitated by the anti-Kv1.1 commercial antibody (Figure 4.13A). This also seemed true for the Kv1.6 extract and antibody (Figure 4.13B). However, the Kv1.2 antibody precipitated appreciable ^{125}I-αDTX from the Kv1.2 extracts (Figure 4.13C). When Kv1.1, 1.2 and 1.6 were co-expressed in pairs (Figures 4.13D to F), only extracts with Kv1.2 present were successfully immunoprecipitated with commercial antibodies (although the first data set for Kv1.2 plus Kv1.6 (Figure 4.13E) showed only modest differences). These observations suggested ^{125}I-αDTX binding to Kv1 heteromers required the presence of the Kv1.2 subunit. To maximise the variety of available Kv1 epitopes in solution, and

include the obligatory Kv1.2, all the available Kv1s were expressed and the extract was

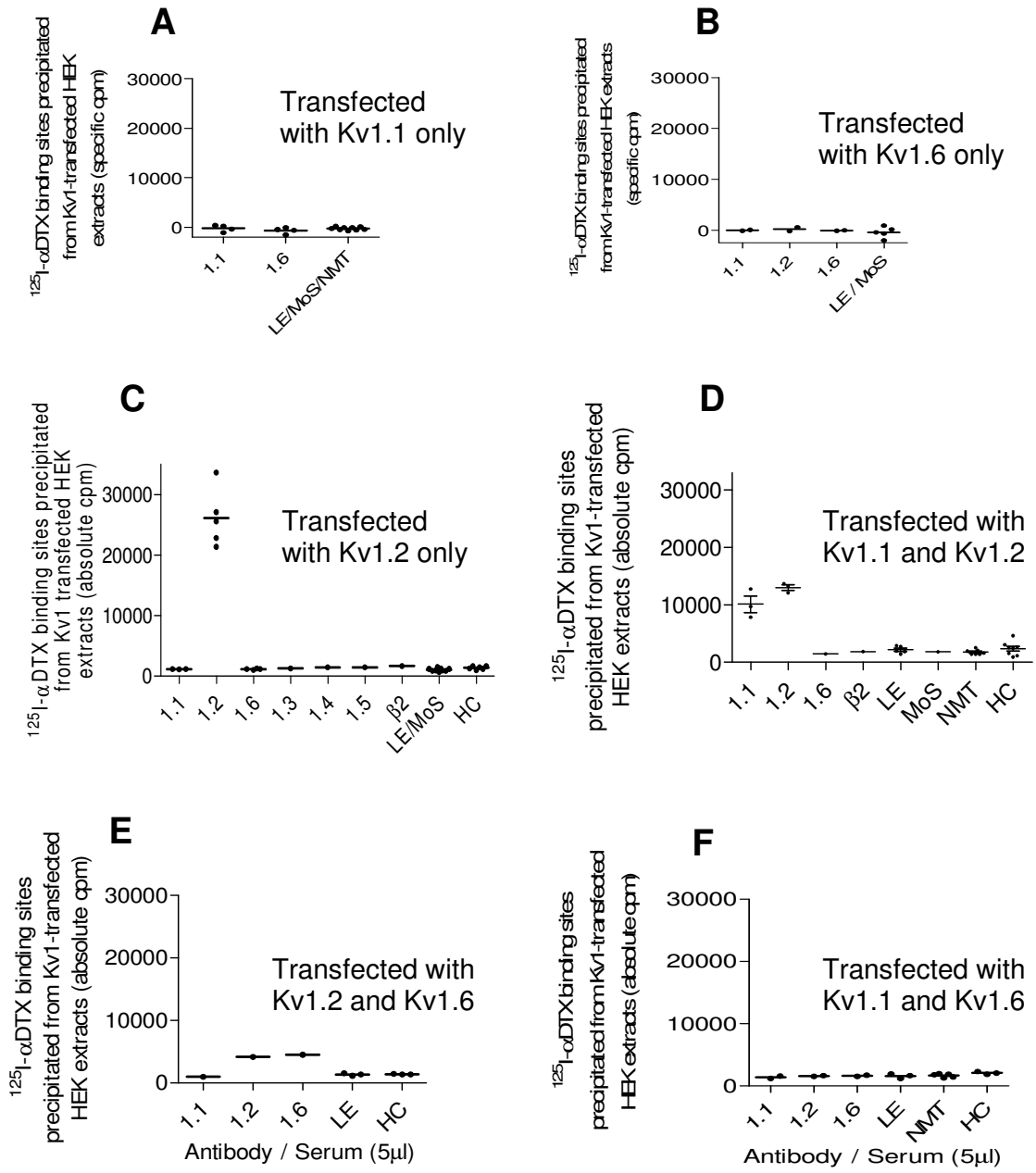


Figure 4.13. HEK-cell immunoprecipitations. ^{125}I-αDTX-labelled HEK cells transfected with either Kv1.1 (A), Kv1.6 (B) or Kv1.2 (C). D, E and F show data from co-transfections using Kv1.1 and 1.2 (D), Kv1.2 and 1.6 (E) and Kv1.1 and 1.6 (F). Immunoprecipitations were performed with rabbit antibodies against Kv1.1-1.6, Kvβ2, LE/MoS/NMT sera and healthy control sera (HC). A and B have had HC data subtracted.

labelled with ^{125}I-αDTX and precipitated from solution with Kv1 commercial antibodies (Figure 4.14A). However, surprisingly, none of the LE (n=15), possible MoS (n=13) or NMT (n=14) sera tested precipitated ^{125}I-αDTX above background levels (Figure 4.14A). It was possible that, although originally designed to resemble the diagnostic brain-based assay, this assay was not sufficiently sensitive to allow detection of patient antibodies. The main issue was the relative amount of ^{125}I-αDTX and Kv1 protein, which were arbitrarily chosen (at 50,000 cpm per 50µl of extract). Although commercial antibodies consistently precipitated large amounts of ^{125}I-αDTX in excess of background levels (for example Figure 4.14A), an excess of ^{125}I-αDTX is required to allow observation and detection of all the available, and labelled, Kv1s. The amount of ^{125}I-αDTX was titrated against a fixed amount of extract and showed that between 50,000 and 100,000 cpm, the Kv1.1/1.2 precipitation saturated. Therefore, with around 100,000 cpm ^{125}I-αDTX per 50µl of cell extract all the Kv1s were labelled in solution (Figure 4.14B).

Under these conditions, the specific Kv1-precipitation of the 113 sera with VGKC-Abs described in Chapter 3 were examined ('n=113', Figure 4.14C). Only three cases precipitated above background levels of ^{125}I-αDTX. These cases did not directly immunoprecipitate the ^{125}I-αDTX (Figure 4.14D). These three cases precipitated ^{125}I-αDTX from many combinations of Kv1-transfected cell extracts (Figure 4.15A) and from extracts that only contained Kv1.2 (Figure 4.15A, red bars). Particularly with high amounts of serum, the patient anti-Kv1.2 antibodies precipitated essentially all the available Kv1.2 (Figure 4.15B). Each of these three cases had multiple samples sent by their referring clinicians: VGKC-Ab titres (as determined by the routine

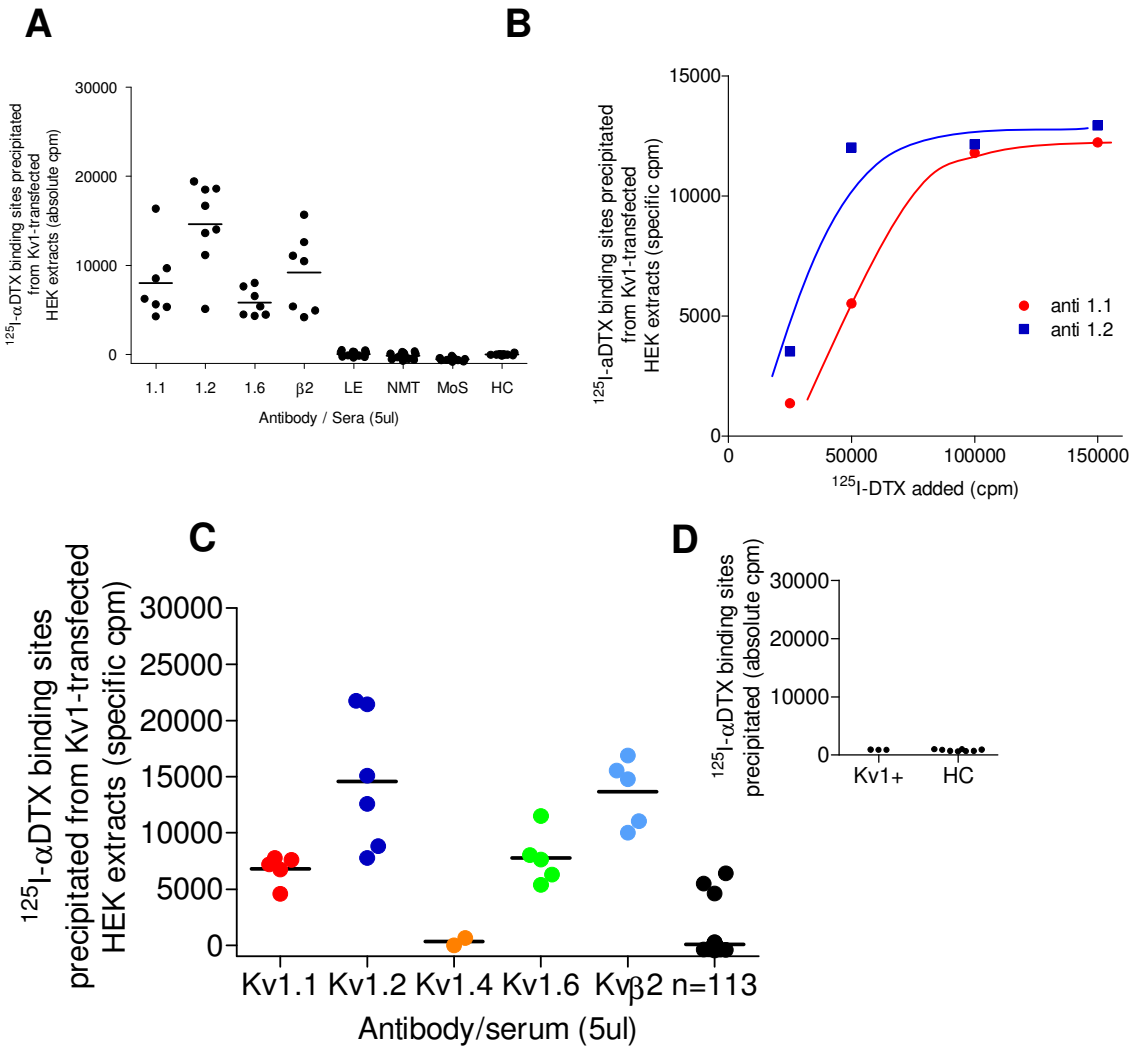


Figure 4.14. HEK-cell immunoprecipitations. A. 50,000cpm of ^{125}I-αDTX was used to label these co-transfected HEK cells. Immunoprecipitations were performed with rabbit anti-Kv antibodies, patient sera (LE (n=15), MoS (n=13), NMT (n=14)) and healthy control sera (HC). B. Toxin titration using increasing amounts of ^{125}I-αDTX were used to label 50µl of Kv1.1, 1.2, 1.4, 1.6, B2 co-transfected HEK cell extract and precipitated using rabbit anti-Kv1.1 and 1.2 antibodies. C. This assay was performed on the whole cohort of cases with clinical data available (n=113). D. The three cases which precipitated well above background levels (from Figure 4.14C, 'Kv1+') did not bind the toxin alone.

radioimmunoassay from rabbit brain extract) and Kv1.2-specific antibody titres (determined from Kv1.2-transfected HEK cells) were compared in each sample (Figure 4.15C). An excellent correlation was observed for each of the three patients (Spearman r

values 0.9, 1 and 1). This suggested these assays measured the same population of antibodies. Disappointingly, these three sera did not show detectable binding to non-

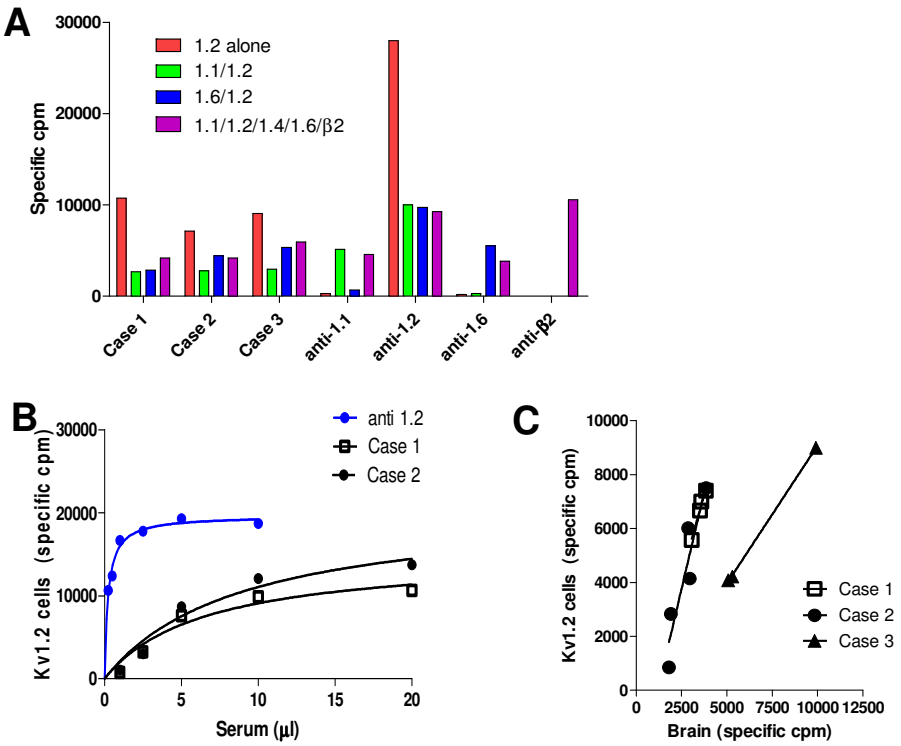


Figure 4.15. Kv1-antibody positive cases. A. The three cases (Case 1, 2 and 3) with above background precipitation of ^{125}I-αDTX-labelled Kv1.1/1.2/1.4/1.6/β2 from solution (purple) also precipitated Kv1.1/1.2 (green), Kv1.2/1.6 (blue) and Kv1.2 alone (red). B. Two cases with sufficient serum available showed non-saturating serum titrations up to 20µl. C. In comparison to the diagnostic brain-based 'VGKC'-Ab assay, there was a linear correlation between Kv1.2 precipitation and 'VGKC'-Ab titres (Spearman r values 0.9 (Case 1, open squares), 1 (Case 2, filled circles) and 1 (Case 3, filled triangles)). All y-axes represent ^{125}I-αDTX specific binding sites precipitated from Kv1-transfected HEK cell extracts.

permeabilised (similar to Figure 4.3, bottom panel) or permeabilised Kv1.2-transfected cells (Figure 4.16). To examine whether these sera bound the extracellular domain of the Kv1s in a ^{125}I-αDTX-based experiment, sera were applied to the outside of intact Kv1.2 or Kv1.1/1.2/1.6/β2 transfected cells. Excess serum was washed away after one hour, the cells were solubilised in 2% digitonin, labelled with ^{125}I-αDTX and precipitated. The

three 'Kv1.2 positive' sera did not precipitate above background levels of ^{125}I-αDTX (Figure 4.17). Of possible relevance to a likely intracellular epitope, patient VGKC/Kv1.2 titres were not very sensitive to immunotherapies and the modified Rankin Score only improved in one case after treatments (Figure 4.18; Case 2).

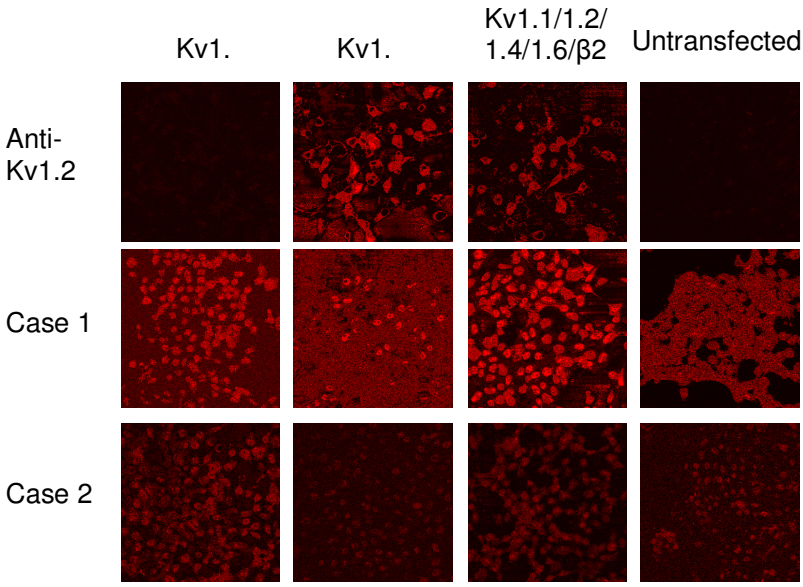


Figure 4.16. Permeabilised immunocytochemistry. Permeabilised cells with Kv1.2 expression demonstrated (anti-Kv1.2, top row). Patients that precipitate Kv1.2 (Case 1 and Case 2) do not show more than background binding to Kv1.2 (co-transfected cells. Data for non permeabilised binding to these cells were negative (as figure 4.3, lowest panel). Magnification x 200.

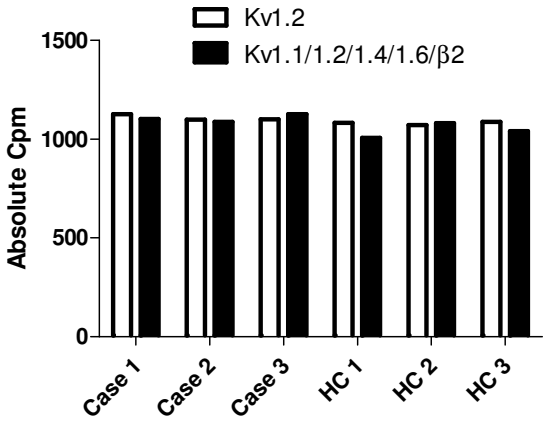


Figure 4.17. Sera do not immunoprecipitate above background levels when incubated with the extracellular aspect of HEK cells transfected with either Kv1.2 (white bars) or Kv1.1, 1.2, 1.6 and Kvβ2 (black bars), prior to membrane solubilisation and ^{125}I-αDTX labelling.

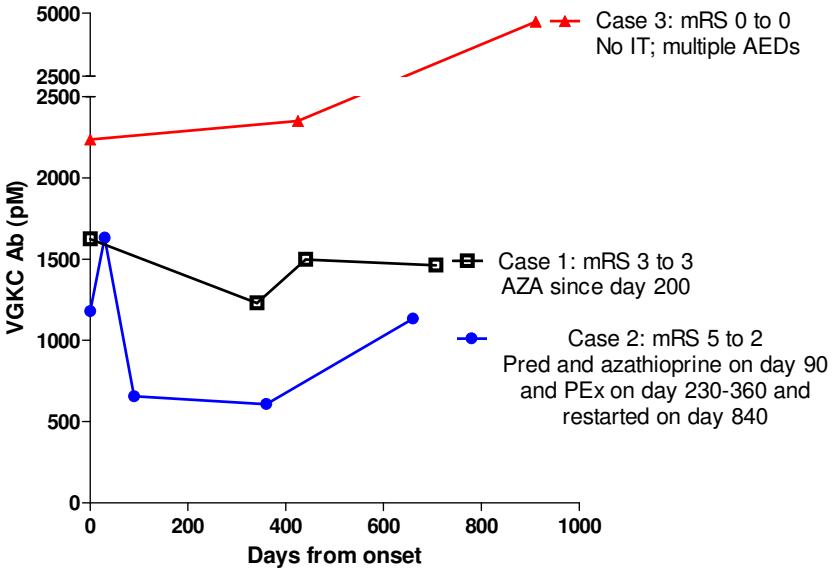


Figure 4.18. Kv1.2 antibody positive cases. VGKC-antibody or Kv1.2 antibody titres do not clearly fall with or without immunotherapy in the three patients with demonstrable Kv1.2 antibodies. Modified Rankin score (mRS) reduced in only case 2.

Summary

The above experiments have utilised a number of biochemical and histological techniques to identify which sera with VGKC-Abs, defined by ^{125}I-αDTX-precipitation from rabbit brain membranes, directly bound the DTX-sensitive VGKCs. Experiments initially showed that VGKC-Ab positive sera did not bind the surface of Kv1-transfected HEK cells, despite intensive optimisation of Kv1-expression at the cell surface. Subsequent experiments in brain tissue showed a marked absence of co-localisation between Kv1-antibodies and patient sera in multiple brain regions and on the surface of native hippocampal neurons, and that the population of VGKCs precipitated by patient sera was different to that precipitated by any Kv1-commercial antibody. Finally, an experiment that mimicked the routine brain assay, but did not contain neural Kv1-associated proteins, showed only three of 113 VGKC-Ab positive sera bound Kv1 epitopes available in solution.

However, a number of limitations applied to these approaches. While native Kv1-heteromers were expressed in all these assays, the observed DTX binding may prevent the detection of heteromers without Kv1.2, as Kv1.2 was present in most DTX-bound brain and Kv1-transfected HEK cell VGKCs (also see Scott et al 1994). Nevertheless, DTX Kv1.1 and 1.6 were able to show independent surface expression and were not bound by patient sera. The use of DTX in many experiments aimed to offset reliance on commercial antibodies which were more likely to detect linearised and non-conformationally active VGKCs. While previous studies never showed perfect co-localisation between Kv1 commercial antibodies and patient IgG (Buckley et al 2001; Ances et al 2005; Kleopa et al 2006), immunohistochemistry is inherently reliant upon

relative IgG concentrations, competition of antibodies and fixation techniques which may make individual studies difficult to compare. Potential competition of DTX with patient IgG in solution had been previously excluded within the laboratory (Clover and Vincent, unpublished observations). Finally, the most definitive experiment presented which mimicked the routine brain assay in Kv1-transfected cell extracts may not mimic the brain tissue adequately by precluding either post-transcriptional modifications (e.g. Shi and Trimmer 1999) or the presence of Kv1-accessory proteins which may alter Kv1-conformations.

Nevertheless, the above experiments have concentrated on the use of mammalian tissue and native, heteromerised antigen and have been unable to show direct VGKC binding in the vast majority of sera defined as VGKC-Ab positive by precipitation of VGKCs from ^{125}I-αDTX-labelled rabbit brain membranes. Therefore, if it is assumed that αDTX selectively binds VGKCs, and no other proteins, the original hypothesis must be modified. The novel hypothesis should explore the question of whether the 'VGKC'-Ab positive sera actually bind to a protein associated with VGKCs in mammalian brain membranes, not available in transfected HEK cells, which is not itself the VGKCs. This is directly addressed in the following chapter.

CHAPTER 5: LGI1, CASPR2 AND CONTACTIN-2 AS ANTIGENIC TARGETS

Chapter 4 showed dissociations between binding characteristics of patient sera and Kv1-commercial antibodies to various Kv1-containing preparations, including Kv1-expressing HEK cells and native neural tissue. As previously shown, VGKC-Abs are routinely diagnosed by precipitation of ^{125}I-αDTX-Kv1 complexes from rabbit brain membranes. It was possible that the patient sera bound a Kv1-associated protein that is complexed with Kv1s and therefore *co*immunoprecipitate both ^{125}I-αDTX and Kv1s. To investigate this hypothesis, the detergent sensitivities of the ^{125}I-αDTX-Kv1 complexes were explored.

Distinction between Kv1 channels and antigenic targets of patient sera: 'Stripping' experiments

The diagnostic assay uses 2% digitonin as this is considered a mild detergent (Privé 2007). When harsher detergents were used (Triton X100 and SDS) to solubilise brain membranes, anti-Kv1.1/1.2 commercial antibodies and patient sera all precipitated substantially less than from digitonin solubilised membranes (Figure 5.1A). This showed that the assay was sensitive to varying detergents. Therefore, SDS was used to dissociate the ^{125}I-αDTX-bound Kv1 proteins - as defined by the commercial antibodies - from the antigenic target of the patient sera. Digitonin-solubilised extracts were made and SDS was added for two hours at 4˚C to create the appropriate concentration in solution. With 0.01% and 0.025% SDS added to the 2% digitonin extract, clear differences in ^{125}I-αDTX precipitation were observed between the precipitation of the commercial antibodies and one LE patient serum (Figure 5.1B). In a larger experiment, four LE sera showed

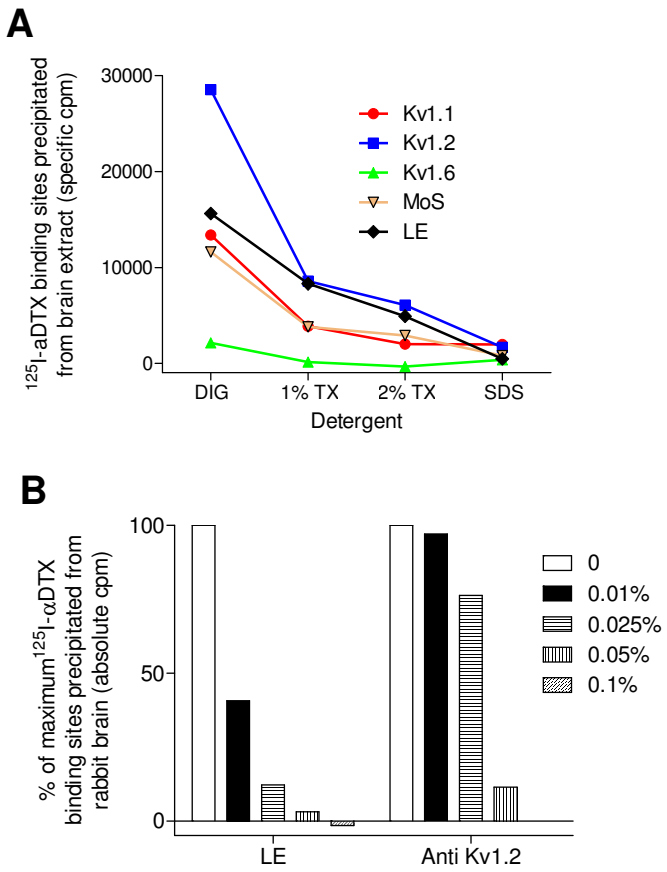


Figure 5.1. Detergent sensitivities of VGKC-antibodies. A. 2% digitonin (DIG) maintained precipitation of ^{125}I-αDTX-labelled rabbit brain membranes with LE (black) / MoS (peach) sera and antibodies to Kv1.1 (red), Kv1.2 (blue) and Kv1.6 (green), by contrast to 1-2% TritonX100 (TX) and 0.1% SDS. B. Titrated addition of SDS to digitonin solubilised ^{125}I-αDTX-labelled complexes from rabbit brain membranes to a final concentration of between 0 and 0.1% (see key). One patient serum (LE) showed markedly reduced precipitation when compared to anti-Kv1.2 antibodies at 0.01% and 0.025% SDS.

differential dissociation from the Kv1-bound ^{125}I-αDTX, as defined by Kv1.1 (n=5) and Kv1.2 (n=3) commercial antibodies (Figure 5.2A). Sera from three MoS cases showed a similar pattern to the LE sera (Figure 5.2B, peach). By contrast, five NMT sera lay closest to the Kv1 dissociation curve (Figure 5.2B, pink). These data showed a differential detergent sensitivity of many patient sera and the Kv1 commercial antibodies. This may be interpreted as evidence for the patient sera binding an accessory protein

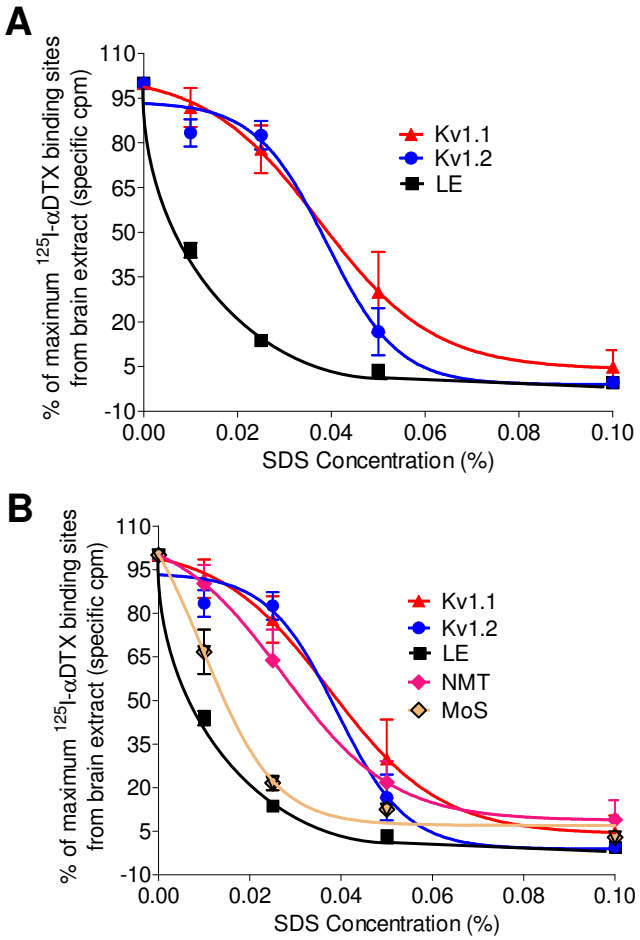


Figure 5.2A and B. 'Stripping' experiments. SDS addition (final concentration of 0.01-0.1%) to 2% digitonin-solubilised ^{125}I-αDTX-labelled complexes from rabbit brain membranes. Immunoprecipitations performed using LE (black, n=4) / MoS (peach, n=3) / NMT (pink, n=5) sera and commercial anti-Kv1.1 (n=5, red) and Kv1.2 (n=3, blue) antibodies.

present within digitonin-solubilised Kv1 complexes that are 'stripped' from ^{125}I-αDTX-bound Kv1s with the addition of low concentrations of SDS.

Which proteins, other than Kv1s, exist within ^{125}I-αDTX-bound Kv1-complexes?

To identify these candidate antigenic targets within the ^{125}I-αDTX-bound Kv1 complexes, immunoprecipitations were performed using multiple commercial antibodies

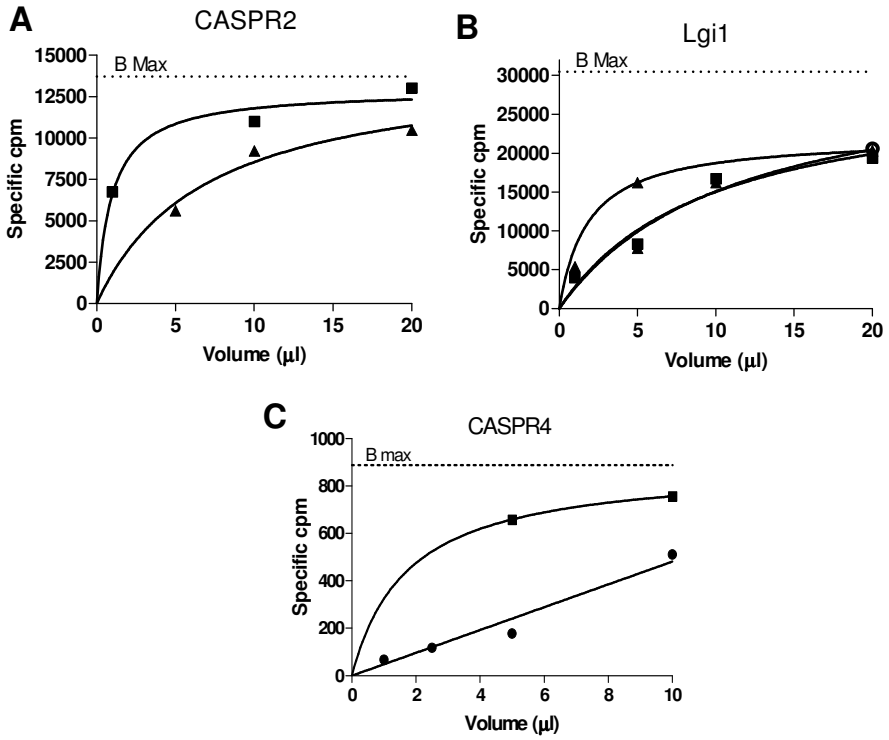


Figure 5.3. Commercial antibodies. Titration of commercial antibodies against CASPR2 (A), Lgi1 (B) and CASPR4 (C) using 2% digitonin solubilised ^{125}I-αDTX-labelled complexes from rabbit brain membranes (n=2). Predicted saturation levels (BMax, from one site hyperbola using GraphPad Prism) are plotted for CASPR2 (BMax derived from average of two titrations), Lgi1 (BMax derived from average of two titrations) and CASPR4 (using data from filled squares, as one of the two CASPR4 precipitations (circles) was unsaturated at maximal serum volumes used).

raised against a number of antigens that have previously been shown to associate with Kv1s or, by inference, may do so given these established interactions.

Where clear ^{125}I-αDTX precipitation above background was observed (> 800 cpm, once backgrounds of control antibodies had been subtracted), saturation points were calculated using a one binding-site hyperbola (BMax, Graph Pad Prism, Figure 5.3A and B). Where

values were low and quantities of serum were a limiting factor (for example, Figure 5.3C (circles)), the precipitation value at the maximal volume of serum was used.

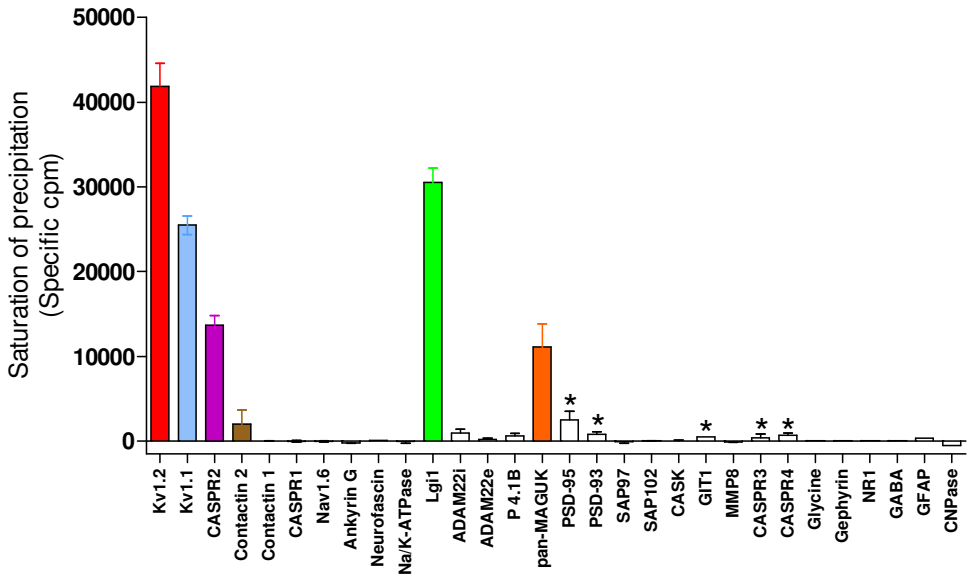


Figure 5.4. Antigens available in VGKC-complexes. Maximal precipitation of various commercial antibodies from digitonin solubilised ^{125}I-αDTX-labelled complexes from rabbit brain membranes. Saturation points (predicted from one site hyperbola, GraphPad Prism) or precipitation at largest serum volume if still unsaturated (*) are plotted below for a variety of commercial antibodies. N=2 for all except for Kv1.1, Kv1.2 and CASPR2 (n=3) and for GIT1, neurofascin, glycine, gephyrin, NR1, GFAP and CNPase (n=1).

All commercial antibodies used are shown in Figure 5.4: stars represent antibodies which showed linearity and did not clearly saturate with the sera volumes used. These immunoprecipitation experiments provided conclusions mainly confirming observations in the literature. Juxtaparanodal proteins were present at high levels in ^{125}I-αDTX-bound Kv1 complexes (CASPR2, TAG1/contactin 2 and Kv1s, Figure 5.5) and, somewhat reassuringly, no paranodal or nodal proteins were identified at high levels (Figure 5.5). Lgi1 and one of its receptors, ADAM22, were also seen: Lgi1 was found at substantially higher levels. Internodal CASPR3 and CASPR4 were seen at low (albeit non-saturated) levels (Figure 5.6A). The other 'peak' of proteins was the membrane associated

guanylate kinases (MAGUKs) including PSD93 and PSD95: these are known to be intracellular proteins (Figure 5.6B). Another intracellular protein seen above background was protein 4.1B. In summary, Lgi1, CASPR2 and Contactin2/TAG1 were the non-Kv1 proteins seen at the highest quantities: (Schulte et al 2006, Poliak et al 1999, Poliak et al 2003).

The number of αDTX bindings sites associated with CASPR2 and Lgi1 were most similar to saturation levels of the patients. Therefore, these were explored first (see Chapter 4, Figure 4.6B). Stripping experiments were performed with these commercial antibodies and showed similar patterns to the patient sera (compare Figures 5.2 and 5.7). Therefore, we directly asked whether these proteins were antigenic targets for LE/MoS/NMT sera.

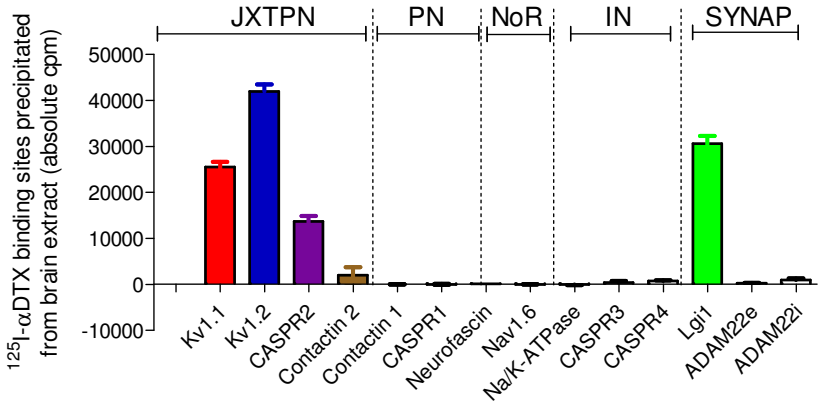


Figure 5.5. Precipitations of candidate proteins with extracellular domains distributed by subcellular localisation, from Figure 5.4. JXTPN=Juxtaparanode; PN=paranode; NoR=Node of Ranvier; IN=internode; SYNAP=Synaptic.

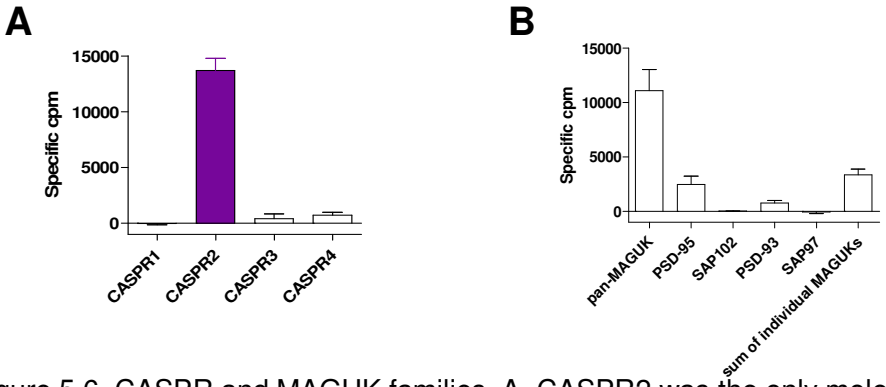


Figure 5.6. CASPR and MAGUK families. A. CASPR2 was the only molecule from the CASPR family found at high quantities (n=2). B. Membrane associated guanylate kinases (MAGUKs). A pan-MAGUK antibody precipitated >10000 cpm, much more than the sum of the known MAGUKs, of which PSD95 and PSD93 were found in the greatest quantities (n=2).

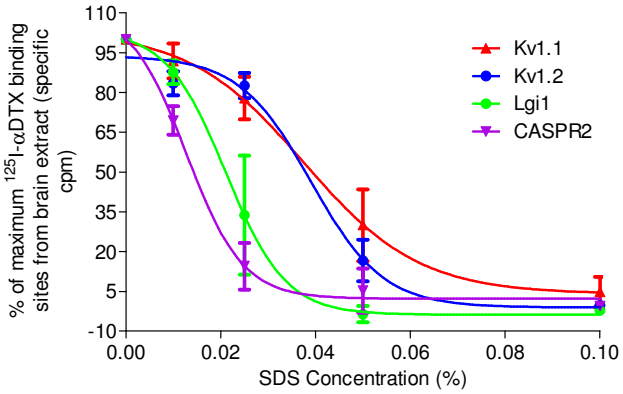


Figure 5.7. 'Stripping' experiments with commercial antibodies. Addition of SDS (0.01-0.1%) to digitonin solubilised ^{125}I-αDTX-labelled complexes from rabbit brain membranes. Immunoprecipitations performed using commercial antibodies against Kv1.1 (red, n=5), Kv1.2 (blue n=3), CASPR2 (purple, n=2) and Lgi1 (green, n=2).

CASPR2 is an antigenic target

To directly address this hypothesis, full length CASPR2-EGFP was transfected into HEK cells: clear, predominant surface expression was visualised as surface green fluorescence and confirmed with a commercial CASPR2 antibody that bound to the surface of these unpermeabilised cells (Figure 5.8 – upper panels). These cells were not bound by commercial antibodies against CASPR, the most homologous molecule to CASPR2 (Figure 5.8 – lower panels).

Next, a commercial CASPR2-antibody was used to precipitate from digitonin-solubilised CASPR2-EGFP-transfected HEK cells to understand how much initial CASPR2-EGFP extract would allow maximal precipitation efficiency (Figure 5.9). From these data, albeit

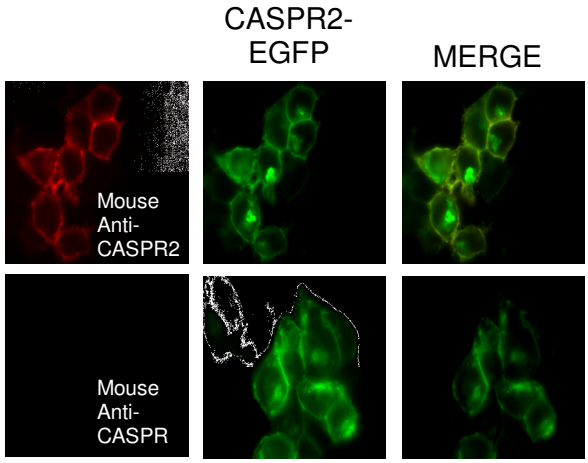


Figure 5.8. Surface expression of CASPR2. Mouse anti-CASPR2 antibody bound the surface of live, unpermeabilised HEK cells which expressed CASPR2-EGFP. Mouse anti-CASPR antibody shown as negative control. Magnification x 1000.

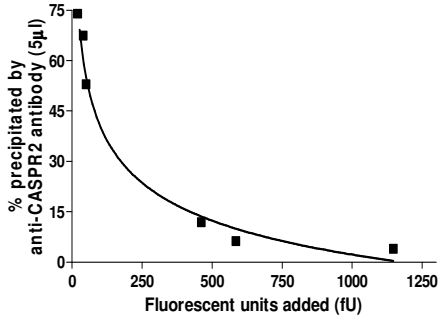


Figure 5.9. Fluorescent immunoprecipitation assay (FIPA). FIPA using digitonin-solubilised CASPR2-EGFP. Percentage of precipitated fluorescent units (fU, y-axis) against total fluorescent units (x-axis).

generated using a commercial antibody, 100fU was used for further experiments as this offered high precipitation efficiency. Next, HEK cells were co-transfected with CASPR2-EGFP and Kv1.1/1.2. These cells were solubilised in 2% digitonin – to recreate the conditions of the diagnostic assay – and neither did anti-Kv1 commercial antibodies precipitate CASPR2-EGFP, measured on a fluorescent plate reader (Figure 5.10A), nor did CASPR2 antibodies precipitate ^{125}I-αDTX-bound Kv1s (Figure 5.10B). Anti-Kv1.6 antibody was used as a negative control in these experiments. Therefore, CASPR2 did not interact in solution with Kv1s in digitonin-extracts from co-transfected HEK cells. A few 'VGKC'-Ab positive sera were subsequently tested for their ability to immunoprecipitate CASPR2-EGFP expressed alone in solution (the fluorescent immunoprecipitation assay (FIPA)). Although none of the initial LE/NMT cases precipitated more than background levels of CASPR2-EGFP, one MoS case precipitated levels comparable to or above that of the anti-CASPR2 antibody (Figure 5.11A). This serum also bound the surface of untransfected HEK cells (Figure 5.11B). Hence, this precipitation in solution may have been due to non-specific HEK-cell binding.

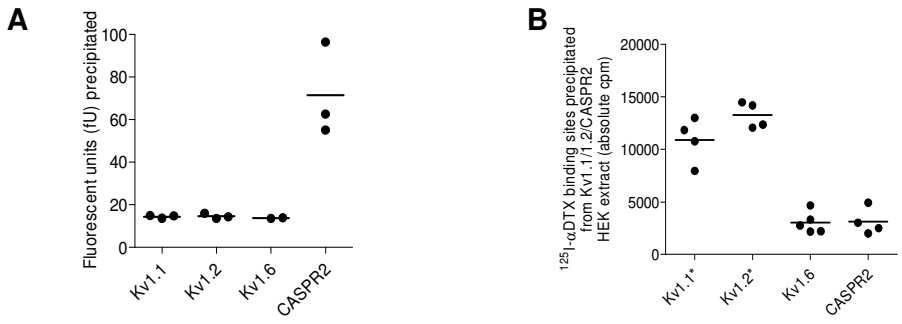


Figure 5.10. Co-transfection of CASPR2-EGFP, Kv1.1 and Kv1.2 in HEK cells. A. CASPR2-EGFP precipitation from solution was successful with a commercial antibody against CASPR2 but not with commercial antibodies against Kv1.1, Kv1.2 or Kv1.6. B. This CASPR2 antibody did not precipitate ^{125}I-αDTX-labelled digitonin-solubilised Kv1s-transfected HEK extracts from solution. 1µl (asterix) or 5µl of each antibody used.

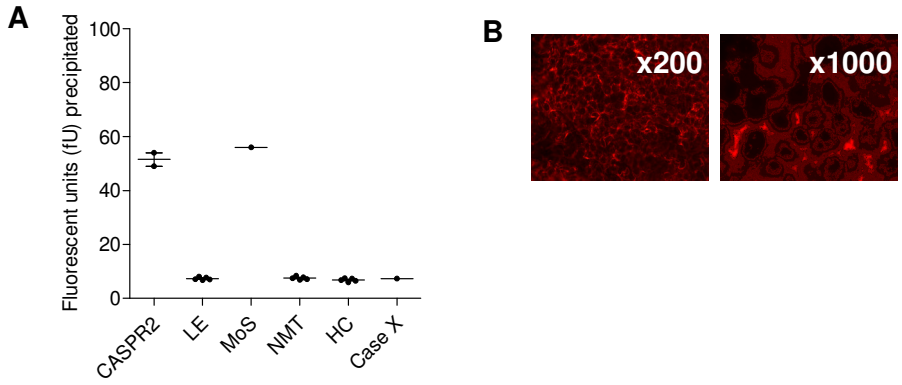


Figure 5.11. CASPR2 antibody in a Morvan's patient (MoS). A. One Morvan's case was found to precipitate CASPR2-EGFP from solution at a level similar to the anti-CASPR2 commercial antibody. B. This serum bound to the surface of untransfected HEK cells in a non-specific manner (magnification x200 and x1000). Case X, whose serum was without 'VGKC'-antibodies but also bound to all untransfected HEK cells, did not precipitate CASPR2-EGFP from solution.

Another patient (Case X, VGKC-Ab negative, Figure 5.12A) was identified whose serum also bound untransfected HEK cells and this case did not precipitate CASPR2-EGFP. Furthermore, the MoS serum did not precipitate $GABA_A$-EGFP or MuSK-EGFP, suggesting specificity for the CASPR2 moiety (Figure 5.12A, green bars). In addition, the

MoS serum showed a clear specific serum titration using the CASPR2-EGFP FIPA, and with high amounts of serum was able to precipitate all the available CASPR2-EGFP (Figure 5.12B, red). The FIPA results were very similar when 2% digitonin or Triton-X100 was used to solubilise transfected cells (data not shown).

Subsequently, the previously-described cohort of 113 VGKC-Ab positive cases were screened using the CASPR2-EGFP FIPA. Thirty cases (26%) precipitated CASPR2-EGFP at levels above background (10.4 fU), as determined by the mean plus three standard deviations from ten healthy controls. Other disease controls groups, including nine patients with thymomas (and myasthenia gravis), 50 with encephalopathies but negative 'VGKC'-Abs, 14 with multiple sclerosis and 34 with subacute onset dysautonomia, showed values below 10 fU (Figure 5.13). The mean plus three standard deviations from these disease cohorts was 9.97 fU. A selection of the CASPR2-anitbody positive sera, with high (>50 fU, red), medium (20-40 fU, blue), low (12-20 fU, green) and no positivity in the FIPA determined with 5µl serum, titrated clearly above background levels within the FIPA (Figure 5.14).

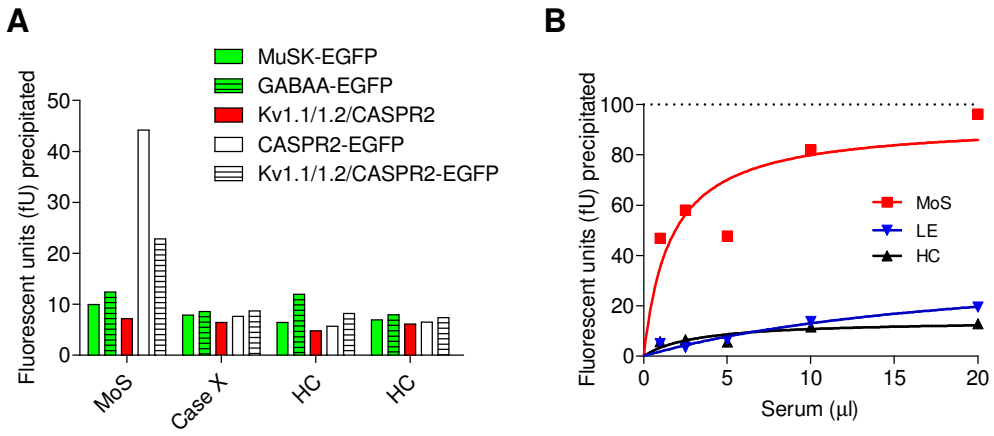


Figure 5.12. CASPR2-antibody in a Morvan's patient (MoS). A. One MoS patient that precipitated CASPR2-EGFP from solution did not precipitate MuSK-EGFP or $GABA_A$-EGFP. Another patient with antibodies similarly found to bind all HEK cells (Case X) did not precipitate CASPR2-EGFP. B. This MoS serum precipitate all the available CASPR2-EGFP (dotted line), in comparison to a healthy control (HC) and one LE patient.

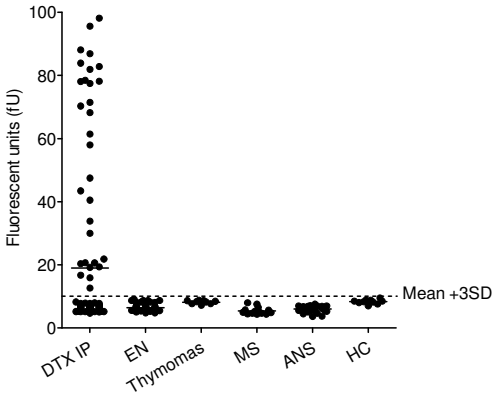


Figure 5.13. CASPR2-EGFP FIPA. CASPR2-EGFP fluorescent immunoprecipitation assay (FIPA) showed 30 of the 113 patients (26%) precipitated above background levels of CASPR2-EGFP (10.4 fU, determined from mean plus three standard deviations of ten healthy controls – HC). Patients with non-DTX precipitating encephalopathies (EN, n=50), myasthenic thymomas (Thymomas, n=9), multiple sclerosis (MS, n=14) and subacute onset dysautonomia (ANS, n=34) precipitated below background levels.

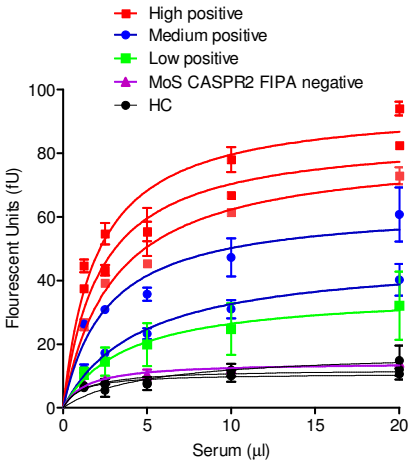


Figure 5.14. CASPR2-EGFP FIPA serum titration. Data shown from high (>40 fU with 5µl serum, n=3), medium (20-40 fU with 5µl serum, n=2) and low (<20 fU with 5µl serum, n=1) CASPR2-antibody positive sera, negative controls (CASPR2-FIPA negative MoS, n=1) and HC (n=3). Mean of two experiments for each case shown.

To determine whether this reactivity was directed towards the extracellular domain of CASPR2, these sera were tested using a CASPR2-cell-based assay. Sera from many healthy controls (1:20 dilution) bound the extracellular domain of CASPR2-EGFP transfected cells (Figure 5.15A). This binding was not seen in the healthy controls sera at 1:100 dilutions. Under these conditions, all the CASPR2 FIPA-positive sera bound strongly to unpermeabilised CASPR2-EGFP transfected cells (all showed score of 4 using a semi-quantitative assay with good interrater agreement, as used for aquaporin-4, acetylcholine receptor and N-methyl D-aspartate receptor antibodies within the laboratory; Waters et al 2008; Leite et al 2008; Irani et al 2010 (Appendix 1), respectively); MoS serum example in Figure 5.15B). None of these sera bound to MuSK-EGFP or Glycine α1 receptor–EGFP transfected cells (data not shown).

Linear ranges within the CASPR2-EGFP FIPA titrations (e.g. from Figure 5.14) were used to calculate CASPR2-antibody concentrations. When compared with 'VGKC'-Ab concentrations (performed simultaneously by Dr B Lang), as determined using the diagnostic brain-based assay, an excellent correlation was observed (Figure 5.16; $r = 0.88$, $p < 0.0001$, Spearman's rank correlation). In addition, limiting amounts of five CASPR2-antibody positive sera were immunoabsorbed against live HEK cells transfected with either CASPR2 or with Kv1.1/1.2 and 1.6. The sera were then tested for their ability to precipitate either ^{125}I-αDTX-labelled Kv1 complexes from brain tissue or CASPR2-EGFP from solution. The sera immunoabsorbed against CASPR2 were unable to precipitate above background levels from either assay, whereas the Kv1 immunoabsorbed sera retained their immunoprecipitation capacity in both assays (Figure

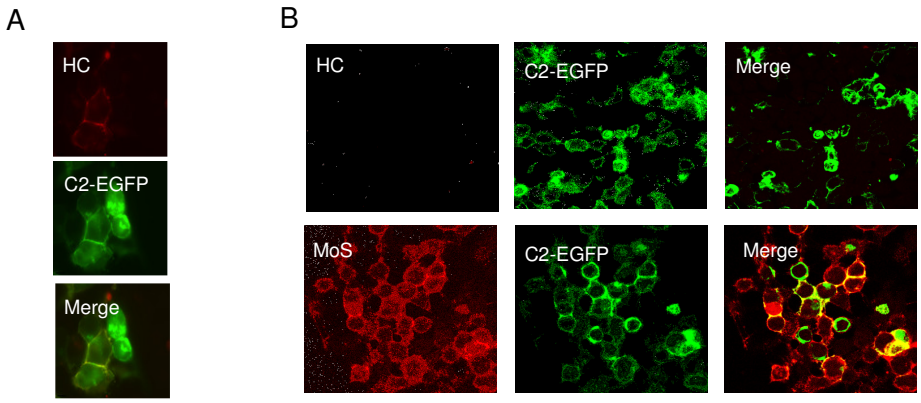


Figure 5.15A and B. CASPR2 cell-based assay. Healthy control sera faintly bound CASPR2-EGFP transfected HEK cells at 1:20 serum dilution (magnification x 1000). B. CASPR2 antibody cell-based assay. CASPR2-EGFP FIPA positive cases (with serum at 1:100 dilution, data shown for one MoS case, red) all bound the extracellular domain of CASPR2-EGFP transfected cells (C2-EGFP, green). 20 healthy controls (HC) did not bind at 1:100. Magnification x 400.

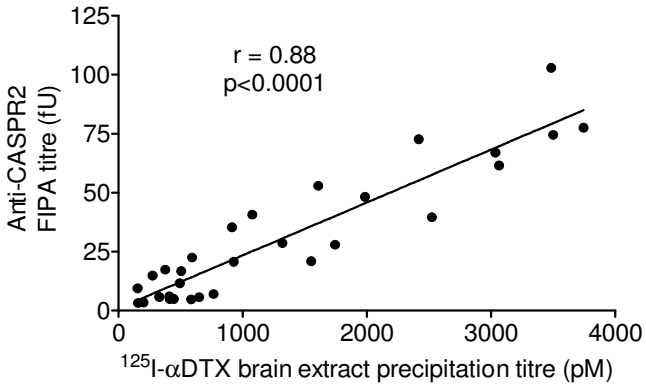


Figure 5.16. CASPR2-specific antibody Vs 'VGKC'-antibody titres. Titres of 'VGKC'-Abs as determined by the diagnostic assay (x-axis) against CASPR2-FIPA titres (fU, y-axis), determined from the linear aspect of titration curves (examples shown in Figure 5.14).

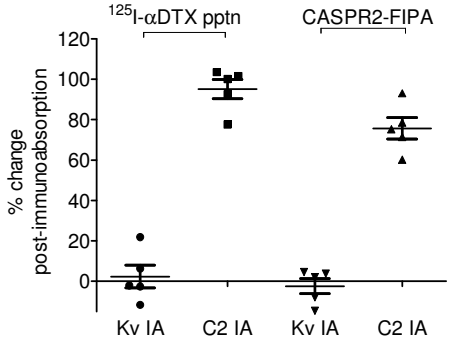


Figure 5.17. CASPR2-antibody immunoabsorption. Percentage change in ^{125}I-αDTX precipitation from rabbit brain membranes (^{125}I-αDTX pptn) and CASPR2-FIPA after serum immunoabsorption against Kv1-expressing and CASPR2-expressing cells (Kv IA and C2 IA, respectively).

5.17). The assays presented in figures 5.16 and 5.17 supported the hypothesis that CASPR2-specific antibodies bound the same population of ^{125}I-αDTX-labelled Kv1s precipitated by these sera from brain tissue.

To determine the IgG subclasses of CASPR2-antibodies, the cell-based assay technique was modified. After serum had been incubated with CASPR2-EGFP transfected cells, a subclass-specific secondary antibody was applied, followed by the appropriate conjugated fluorescent antibody. Three blinded observers graded cell fluorescence using 22 sera from zero to four. When averaged over the 22 cases, the majority of the antibodies were IgG4 and IgG1 (Figure 5.18A). There were low or absent levels of IgG2, IgG3 and IgM (Figure 5.18A). Given the prominence of IgG1, it was possible that CASPR2-antibodies fixed complement to produce complement end-products such as C3b and membrane attack complex (MAC). Therefore, CASPR2-antibodies were incubated with CASPR2-transfected HEK cells and provided with a fresh source of human complement. C3b and MAC deposition were seen on the surface of CASPR2-transfected cells using commercial antibodies (Figure 5.18B). The IgG1 CBA score correlated well with the C3b and MAC scores (Figure 5.18C). As expected, no correlation was seen when MAC/C3b scores were plotted against the IgG2 or 4 levels (data not shown).

CASPR2-antibodies bound more clearly to the extracellular domain of CASPR2-transfected cells than commercial anti-CASPR2 antibodies. This may be consistent with their preferential recognition of natively folded antigen. To investigate this further, CASPR2 (†) and Kv1 (*) HEK-cell extracts were run on denaturing SDS gels and probed

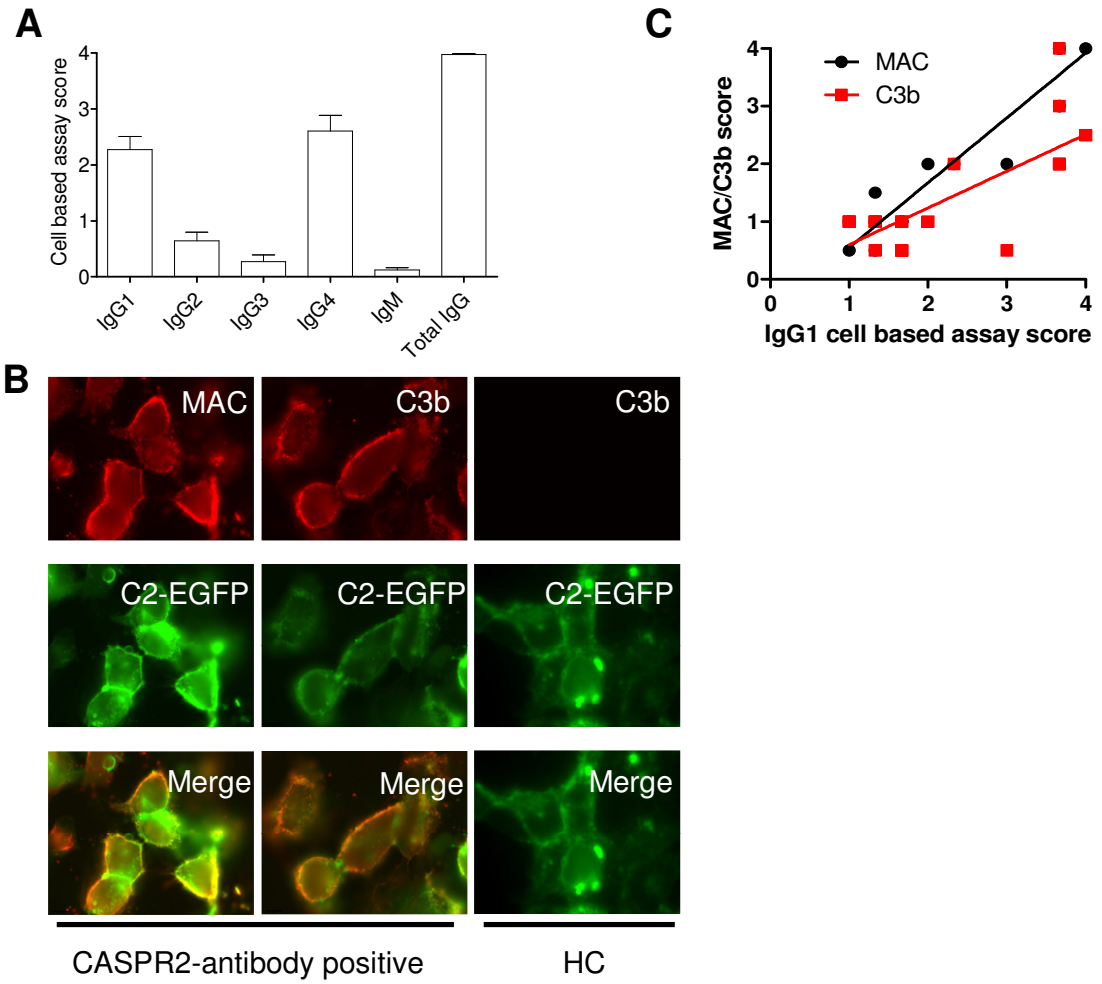


Figure 5.18. CASPR2 antibody subclasses and complement fixation. A. Subclasses of CASPR2-antibodies determined using subclass specific secondaries on CASPR2-EGFP transfected HEK cells (mean from three blinded observers). B. When provided with a source of human complement, CASPR2 antibodies activated deposition of both MAC (red, left) and C3b (red, centre) on CASPR2-EGFP (C2-EGFP, green) transfected HEK cells. Healthy control (HC) serum showed no C3b (right) or MAC (data not shown) deposition. C. The IgG1 cell-based assay score correlated well with both the degree of MAC (black) and C3b (red) deposition ($r=0.90$ ($p<0.0001$) and 0.64 ($p=0.0014$), respectively – Spearman correlations). Magnifications x 2000.

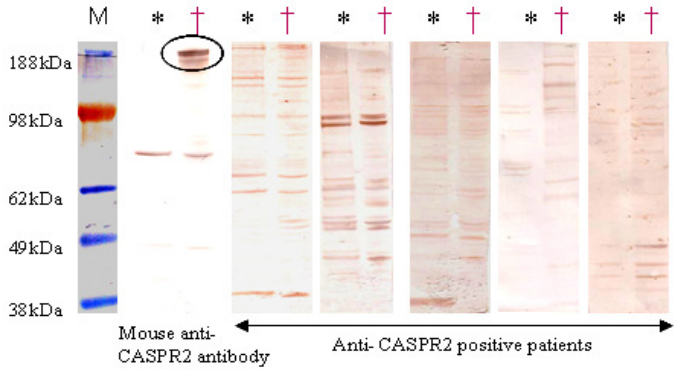


Figure 5.19. CASPR2 western blotting. CASPR2 (†) and Kv1.1/1.2/1.6 (*) extracts were run on denaturing Nu-PAGE SDS gels and probed with a commercial mouse CASPR2 antibody or CASPR2-FIPA/CBA positive sera (Anti-CASPR2 positive patients). The circled band shows the band likely to represent CASPR2 (predicted molecular weight of CASPR2 is 180kDa).

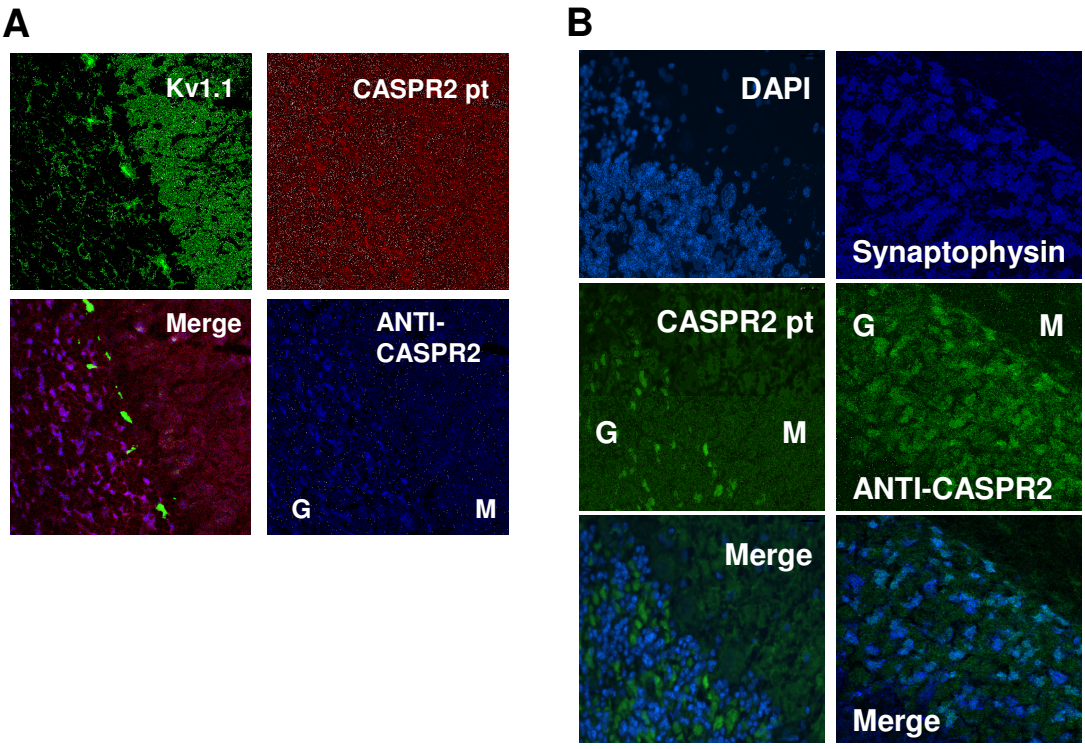


Figure 5.20 A and B. CASPR2, Kv1 and patient cerebellar immunofluorescence patterns. CASPR2-antibody positive sera (CASPR2 pt), mouse anti-CASPR2 antibodies (ANTI-CASPR2), rabbit anti-synaptophysin and rabbit anti-Kv1.1 antibodies. G = granule cell layer, M = molecular layer, DAPI = nuclear counterstain. Magnification x 200 (A) and x 400 (B).

with commercial CASPR2 antibodies and CASPR2-antibody positive patient sera. Whereas commercial anti-CASPR2 antibodies clearly recognised a band at 180 kDa (Figure 5.19, circled), none of the patient sera recognised a similar denatured band.

From Chapter 4, some clear dissociations between patient serum and Kv1-commercial antibody binding patterns were observed in cerebellar sections. To specifically investigate serum from patients now known to have CASPR2-antibodies, similar immunofluorescence studies were performed (Figure 5.20A). Modest CASPR2 expression was detected in the molecular layer of the cerebellum and none in the basket cells, similar to some of the previous 'VGKC'-Ab positive sera tested. A neuronal population within the granule cell layer that showed clear CASPR2 expression, without detectable Kv1 expression, was also identified. This cell population was consistently devoid of DAPI staining which was particularly remarkable given the high soma density within the granule cell layer (Figure 5.20B, left hand panels). Neuroanatomy literature suggested this binding may have represented the giant terminals of mossy fibres ('rosettes') that are seen in the cerebellar granule cell layer. Correspondingly, this CASPR2-positive, DAPI-negative population were labelled by a commercial antibody against synaptophysin (Figure 5.20B, right hand panels).

Contactin 2 / TAG-1 is an antigenic target

Contactin 2, the human homolog of rodent TAG-1, is a GPI anchored molecule and therefore lacks an intracellular domain but has a large extracellular domain (Traka et al 2003). Controversy exists regarding its detergent solubility (Prinetti et al 2001). For these reasons, a cell-based assay technique was used to look for contactin-2 antibodies in patient sera.

HEK cells co-transfected with contactin-2 cDNA (a kind gift from Dr D Karagenos) and EGFP cDNA were clearly bound by a commercial anti-contactin-2 antibody (Figure 5.21, horizontal middle panels). None of 20 healthy controls and 30 disease controls (ten MuSK-Ab-positive myasthenia gravis, ten NMDAR-Ab positive encephalitis and ten 'VGKC'-Ab negative encephalopathies) were found to bind to these contactin-2 transfected cells (for example Figure 5.21, lower horizontal panels, HC). Of the 113 'VGKC'-Ab positive sera within our cohort, seven cases were positive: only two of these seven did not have antibodies to other proteins (CASPR2, Kv1s or Lgi1 – see Chapter 6 for details). Contactin-2 antibody subclasses were always of the IgG1 subclass (scored between 1 and 4, Figure 5.22).

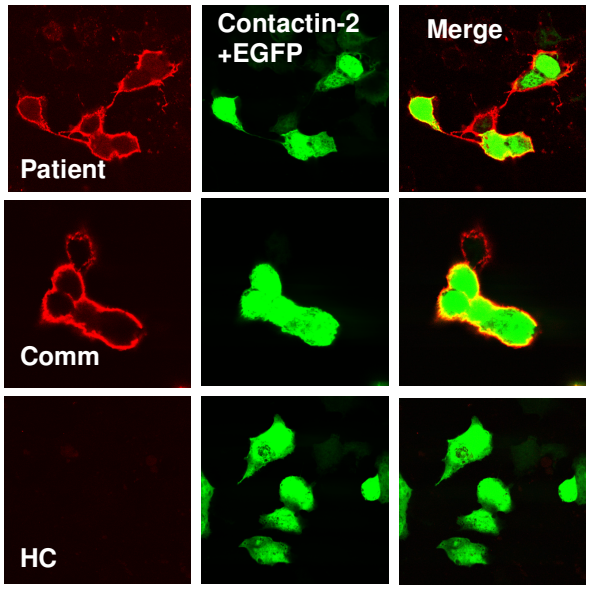


Figure 5.21. Contactin-2 antibody cell based assay. Unpermeabilised contactin-2 and EGFP co-transfected cells labelled by a few patient sera (Patient) and mouse anti-contactin-2 commercial antibody (Comm) but not by 20 healthy controls (HC) or 30 disease controls. Magnification x 800.

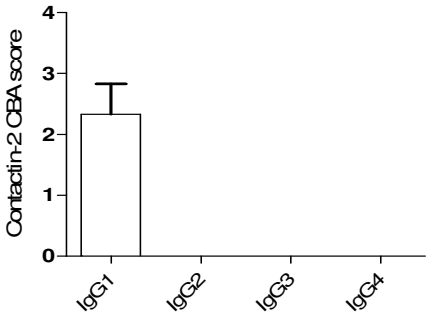


Figure 5.22. Contactin-2 IgG subclasses scored using CBA. Contactin-2 IgG were exclusively of the IgG1 subclass (n=6 sera, final positive serum no longer available).

Lgi1 (leucine-rich glioma-inactivated 1) is an antigenic target

The literature surrounding Lgi1 is controversial as to whether this molecule is predominantly secreted or membrane associated (Chapter 7 for further discussion, Sirerol-Piquer et al 2006, Fukata et al 2006, Schulte et al 2006). Recent data, however, suggest it is not considered an integral membrane protein (Schulte et al 2006).

Sera from a number of 'VGKC'-Ab positive patients bound to the surface of unpermeabilised Lgi1 and EGFP co-transfected HEK cells. However, the sera bound to all the cells – not just the subpopulation co-expressing EGFP (Figure 5.23 – top horizontal panels). To confirm this, Lgi1-EGFP cDNA (full-length Lgi1 tagged with either EGFP at its N or C-terminus) was used for transfection and cells bound by the patient sera were most commonly cells which did not express the Lgi1-EGFP fusion protein (Figure 5.23 – second horizontal panel, N-tagged Lgi1 shown). The patient binding was clearly localisable to the surface of the untransfected and transfected HEK cells (Figure 5.23 – third horizontal panel). No similar binding was seen with 20 healthy controls, ten cases of multiple sclerosis, ten MuSK-Ab-positive myasthenia gravis, ten with neuromyelitis optica, ten with NMDA-receptor antibodies or 30 with 'VGKC'-Ab negative encephalopathies (e.g. Figure 5.23 – lowest horizontal panel, healthy control (HC) shown). In addition, commercial antibodies against the signal peptide N-terminus (N-18) or distal C-terminal domain (C-19) of Lgi1 did not bind the surface of these cells (data not shown).

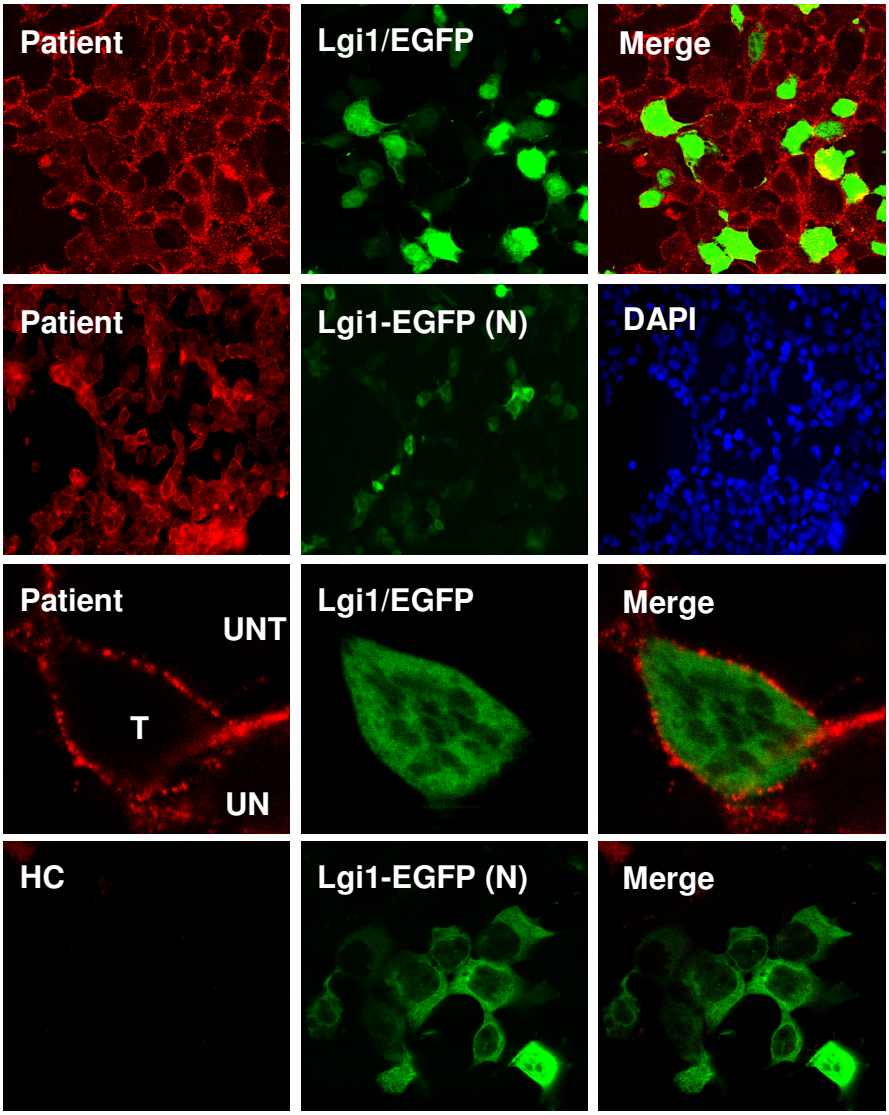


Figure 5.23. Lgi1-antibody cell-based assay. Live Lgi1-EGFP (N-terminally tagged; Lgi1-EGFP (N)) transfected and Lgi1/EGFP co-transfected HEK cells (middle panels) labelled with patient sera and are not bound by healthy control (HC) or disease control (data similar to HC) sera (red). DAPI = nuclear counterstain (blue). HC = healthy control. Magnifications x 400 (top row), x 100 (second row), x 3000 (third row) and x 800 (lowest row). T = transfected cell. UNT = untransfected cell.

To develop a more quantitative assay, an Lgi1-EGFP FIPA was attempted using full-length Lgi1 cDNA tagged with EGFP at its N-terminus ((Lgi1-EGFP (N)) or C-terminus (Lgi1-EGFP (C)). The antibody directed against the C-terminus (C-19) precipitated

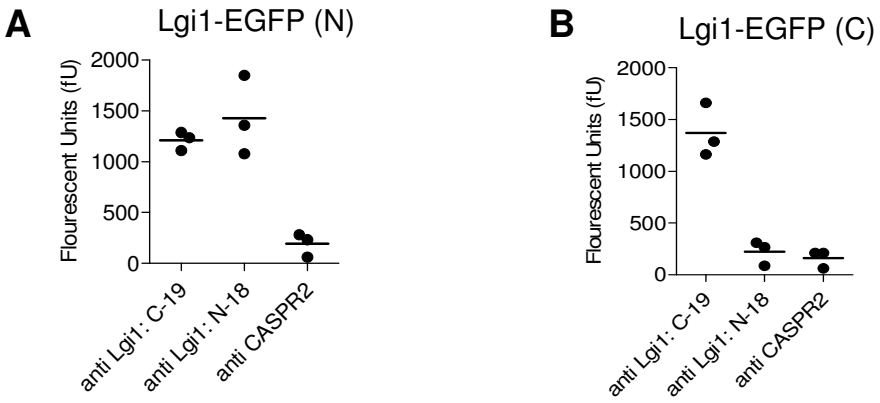


Figure 5.24. Lgi1-FIPA. Lgi1-EGFP fusion constructs were expressed in HEK cells, solubilised in 2% digitonin and precipitated with commercial antibodies directed against the N-and C-termini of Lgi1 (N-18, C-19, respectively) or CASPR2. These tagged constructs were either N-terminally or C-terminally tagged; (Lgi1-EGFP (N) and Lgi1-EGFP (C)).

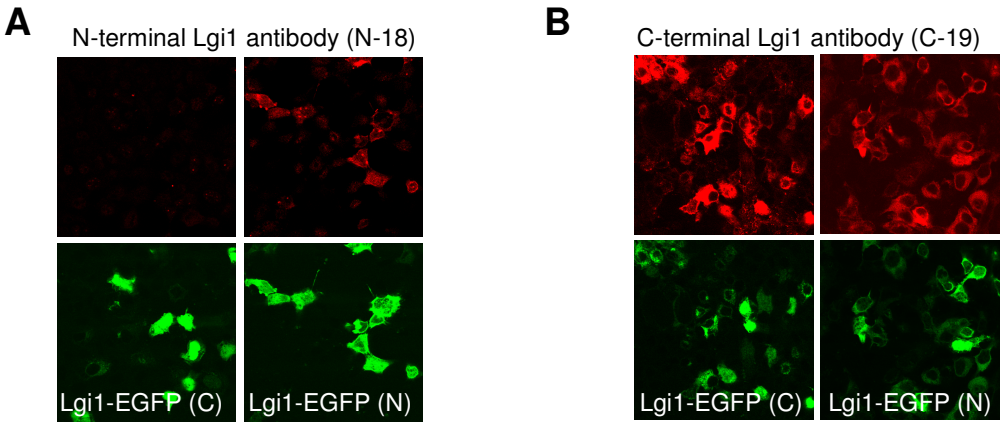


Figure 5.25. Lgi1 commercial antibody binding in cell-based assay. Permeabilised HEK cells transfected with either Lgi1-EGFP (C) or (N) stained with commercial antibodies directed against N-terminus (A, N-18) or C-terminus (B, C-19) of Lgi1. Commercial antibodies did not bind to non-permeabilised Lgi1-transfected cells. Magnification x 400.

EGFP from digitonin-extracts of both Lgi1-EGFP (N) and Lgi1-EGFP (C) transfected HEK cells. The N-terminal antibody (N-18) only precipitated the N-terminally tagged construct (Figures 5.24A and B).

In addition, the N-18 antibody only bound to the N-terminally tagged Lgi1-transfected permeabilised cells, whereas the C-19 antibody bound to permeabilised cells which expressed the N-terminally and C-terminally tagged Lgi1 proteins (Figure 5.25A and B). In agreement, western blotting showed that the antibody directed against the C-terminus (C-19) recognised Lgi1 in both tagged constructs and in the untagged construct and recognised cell-surface Lgi1 extracted with the alkaline (Na_2CO_3) elution that attempted to elute non-integral membrane proteins (Figure 5.26A). Whereas, the antibody directed against the N-terminus (N-18) only recognised the N-terminally tagged construct (Figure 5.26B). The recognised tagged constructs were consistently detected with molecular weight around 85kDa and the untagged constructs were seen within a band consistent with a molecular weight of around 55kDa.

As the N-terminally tagged protein appeared to represent non-modified, full-length Lgi1, the non-saturated linear range for Lgi1-EGFP (N) based precipitation was determined using the anti Lgi1 C-terminus (C-18) antibody (Figure 5.27A). A FIPA using 400 fUs of Lgi1-EGFP (N) (value from within the linear range derived in Figure 5.27A), showed that the sera which bound to Lgi1-transfected cells (Figures 5.27B and C, 'Lgi1-positive on CBA'), did not precipitate above background counts. This was also true for the C-terminally EGFP-tagged Lgi1 (Figures 5.27B and C). EGFP deposition on the surface of serum-bound cells was consistently absent from CBAs and EGFP was not detectable above background levels in the various media or Na_2CO_3 surface-elutions using a fluorescent plate reader (Figure 5.27D).

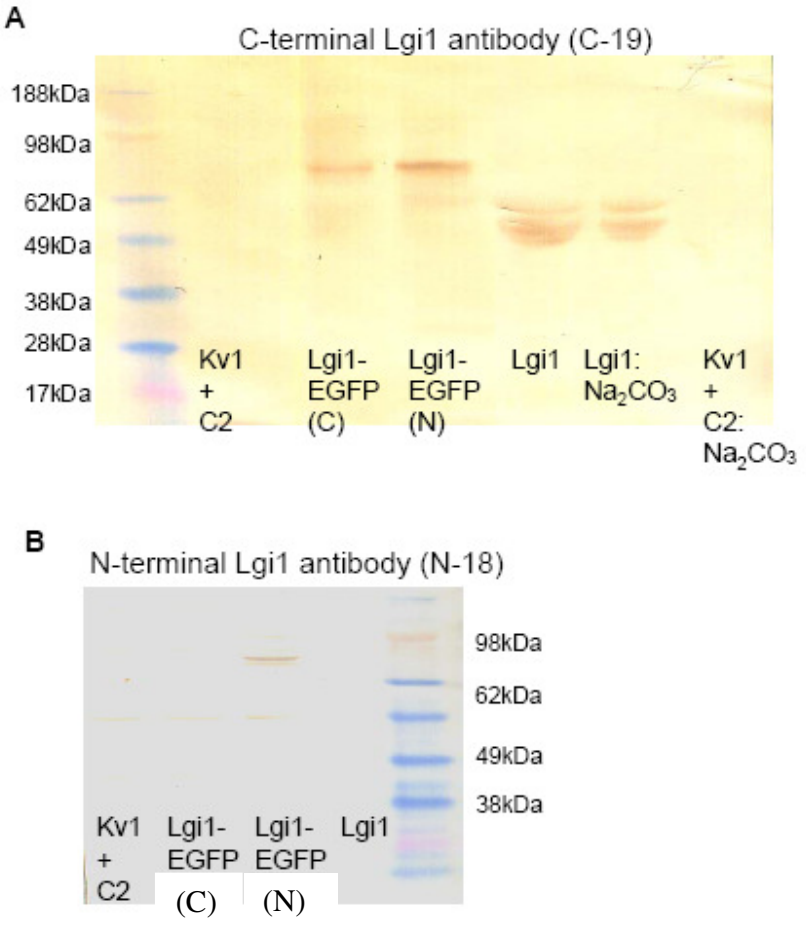


Figure 5.26. Lgi1 western blots. Gels were loaded with extracts from HEK cells transfected with Kv plus CASPR2 (Kv1+C2), Lgi1-EGFP (C, C-terminally tagged or N, N-terminally tagged), full-length untagged Lgi1 (Lgi1) and Na_2CO_3 elutions from either Lgi1-transfected cells (Lgi1: Na_2CO_3) or Kv1 plus CASPR2 transfected cells (Kv + C2: Na_2CO_3). These membranes were probed with antibodies to the C (C-19, Figure A) or N (N-18, Figure B) termini of Lgi1.

Hence, two possibilities arose to explain the mechanism by which sera bound Lgi1-transfected cells. It was possible that the patient sera were binding secreted Lgi1, which had been immobilised non-specifically at the charged cell surface or via an interaction with a known Lgi1-receptor (e.g. ADAM-22, Fukata et al 2006) endogenously expressed

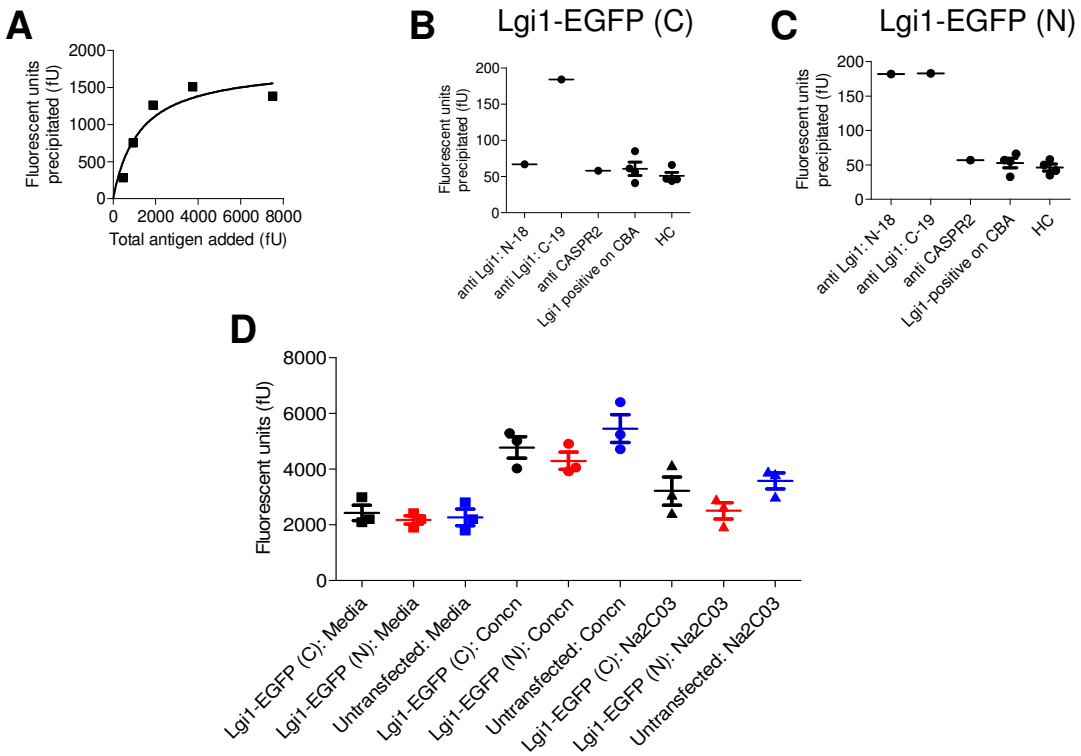


Figure 5.27. Lgi1-FIPA. A. Fluorescent units of Lgi1-EGFP added (x-axis) against amount precipitated (y-axis) using the Lgi1-EGFP (N) construct and N-terminal antibody (N-18). B. Only the commercial Lgi1 antibody directed against the C terminus (C-19) of Lgi1 precipitated C-terminally tagged Lgi1-EGFP (Lgi1-EGFP (C)) in a FIPA. C. Commercial Lgi1 antibodies directed against both the N-terminus (N-18) and C-terminus of Lgi1 (C-19) precipitated N-terminally tagged Lgi1 (Lgi1-EGFP (N)). 400 fU were added to each assay. Patient sera that bound to Lgi1-transfected cells (Lgi1-positive on CBA) did not show above background precipitation (B and C). HC = healthy control. D. Fluorescent plate reader measurements at EGFP emission wavelength in 50µl of media alone (squares), concentrated media (circles) and Na_2CO_3 elutions (triangles) from HEK cells which were transfected with the C-terminally tagged Lgi1 construct (Lgi1-EGFP (C), black), N-terminally tagged Lgi1-EGFP construct (Lgi1-EGFP (N), red) or from untransfected cells (blue).

by HEK cells. It was also possible that Lgi1 cDNA upregulated expression of a different protein which the patient sera bound, however this would have to be present in the majority cell population which were not expressing Lgi1-EGFP: the former was strongly

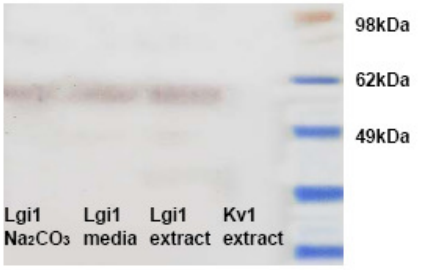


Figure 5.28. Lgi1 in intracellular, membrane and media compartments. Lgi1 or Kv1 extracts, Lgi1 media and Lgi1 Na_2CO_3 elution run on denaturing gels and probed with an antibody against the C-terminus of Lgi1 (C-19, 1:250).

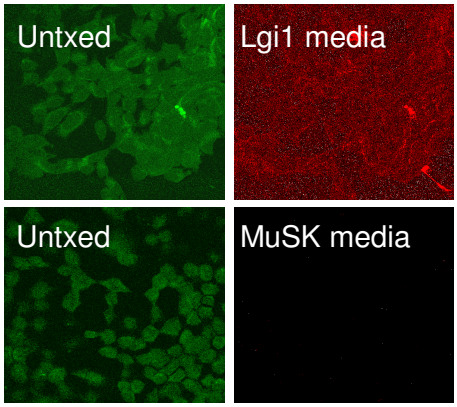


Figure 5.29. Lgi1 media can transfer serum binding properties. Lgi1 or MuSK cell transfected media was gathered and transferred to untransfected cells (Untxed). High power autofluorescence was used to identify cells as microscope did not have DAPI filter. Magnification x 400.

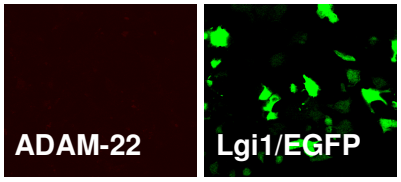


Figure 5.30. ADAM-22 is not present on Lgi1-transfected HEK cell surface. Lgi1/EGFP co-transfected cells were not bound by antibodies against an extracellular epitope of ADAM-22 (red). Magnification x 500.

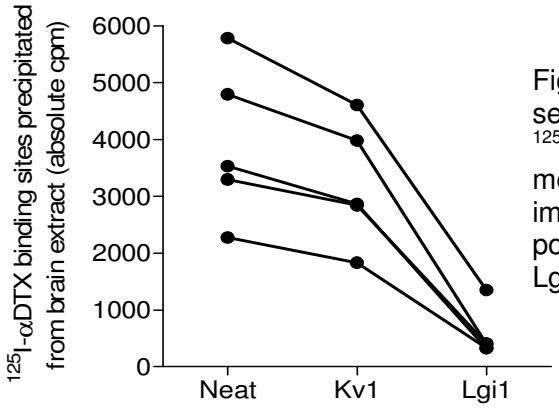


Figure 5.31. ^{125}I-αDTX precipitation is lost after serum absorption against Lgi1-transfected cells. ^{125}I-αDTX precipitation from rabbit brain membranes before (neat) and after immunoabsoprtion of five Lgi1-cell based assay positive sera against Kv1-transfected (Kv1) and Lgi1-transfected (Lgi1) HEK cells.

favoured. This hypothesis would suggest the likely possibility that secreted/bound Lgi1 was of a different conformation to cell-retained Lgi1.

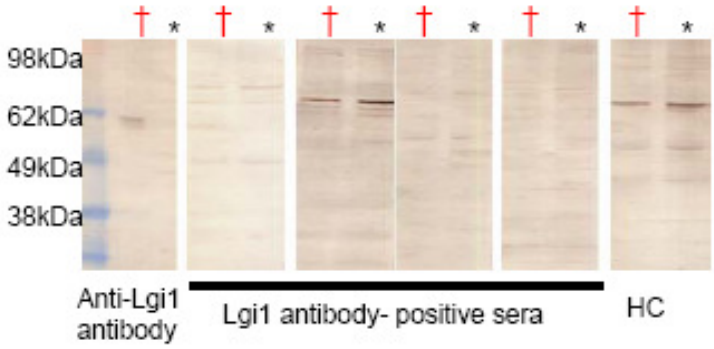


Figure 5.32. Lgi1 western blotting. Lgi1 transfected cell extracts (†) and Kv transfected cell extracts (*) were run on denaturing gels and transferred to membranes that were probed with anti-Lgi1 (C-19) antibody, Lgi1-antibody positive patient sera and healthy control sera (HC). All dilutions 1:200.

Indeed, secreted Lgi1 was detected in the media of Lgi1-transfected cells at a similar molecular weight to the band seen from the Lgi1-transfected whole cell extract and the band seen after sodium-carbonate (Na_2CO_3) elution of the membrane-associated (but not membrane integral) Lgi1 (Figure 5.28). To further this observation, media from Lgi1-transfected HEK cells was transferred to untransfected HEK cells. Two hours later, a cell-based assay on these cells showed the binding to Lgi1-transfected cells was reproduced, essentially identically, by transfer of the media (Figure 5.29). This was not seen with transfer of MuSK-transfected cell media. However, the major known receptor for Lgi1 – ADAM22 – was neither detected on blots of untransfected / Lgi1 transfected HEK cells (data not shown) nor was it detected using immunofluorescence with commercial antibodies against ADAM-22 (Figure 5.30).

To understand if Lgi1-Abs were the same antibodies as the 'VGKC'-Abs, precipitated from the brain complexes, a limiting amount of serum was immunoabsorbed against the surface of live Lgi1-transfected cells, having removed the media. Sera titrated as far as 0.5µl per Lgi1-transfected coverslip, the approximate equivalent of 2µl per well of a six-well plate. Therefore, 1µl of five sera were absorbed per six-well plate of Lgi1-transfected HEK cells and untransfected HEK cells and this was compared to the non-absorbed serum. A clear reduction in 'VGKC'-Abs in the sera that had been absorbed against Lgi1-transfected cells was detected, and a smaller reduction for the sera absorbed against untransfected HEK cells (Figure 5.31). Unsurprisingly, given the likely modified conformation of the secreted Lgi1-antigen, patient sera did not bind to western blots using Lgi1 whole cell extract (Figure 5.32).

Experiments to investigate the Lgi1-antibody subclasses were performed as for CASPR2 and contactin-2. However, as the Lgi1-antibody cell based assay was scored in a binary manner, the number of patients with IgG subclass binding were represented on the y-axis (Figure 5.33A and B).

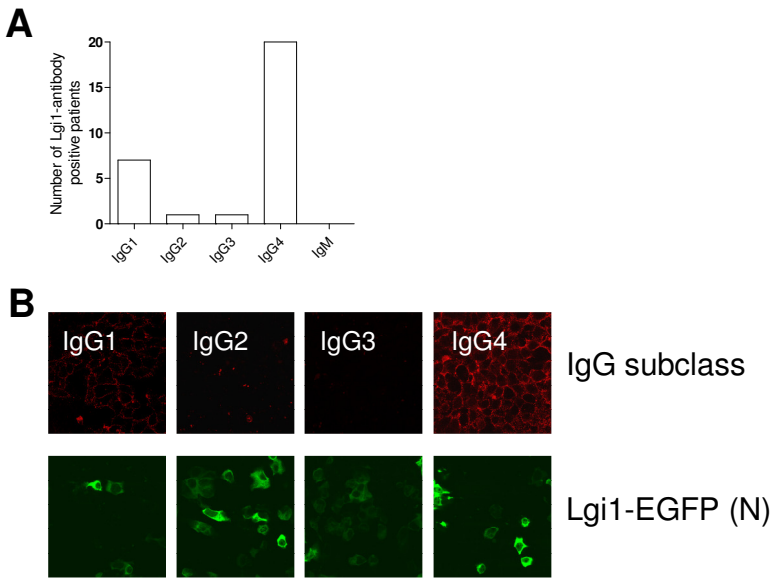


Figure 5.33. Lgi1-antibody subclasses. A. Number of twenty Lgi1-antibody positive patients with IgG1-4 or IgM subclasses detected. B. Representative images from a patient with LE and Lgi1-antibodies to show IgG4 predominance. Serum dilution = 1:20. Magnification x 400.

Using the non-quantitative cell-based Lgi1 assay, all 113 sera from patients with available clinical data were examined (1:20 dilution). Forty-nine (43%) of these cases had Lgi1 antibodies defined in this manner. Of these, none had CASPR2 antibodies and only one had contactin-2 antibodies. As described previously, none of these patients bound Kv1-transfected cells.

Retrospective blinded observations

Having identified patients with defined antigenic targets, Lgi1, CASPR2, Kv1.2 and contactin-2, a retrospective analysis of some of the earlier data from histological and 'stripping' experiments was reviewed (Chapter 4). At the time the experiments were performed, we knew only that many patients did not bind potassium channels expressed in solution or on the surface of HEK cells.

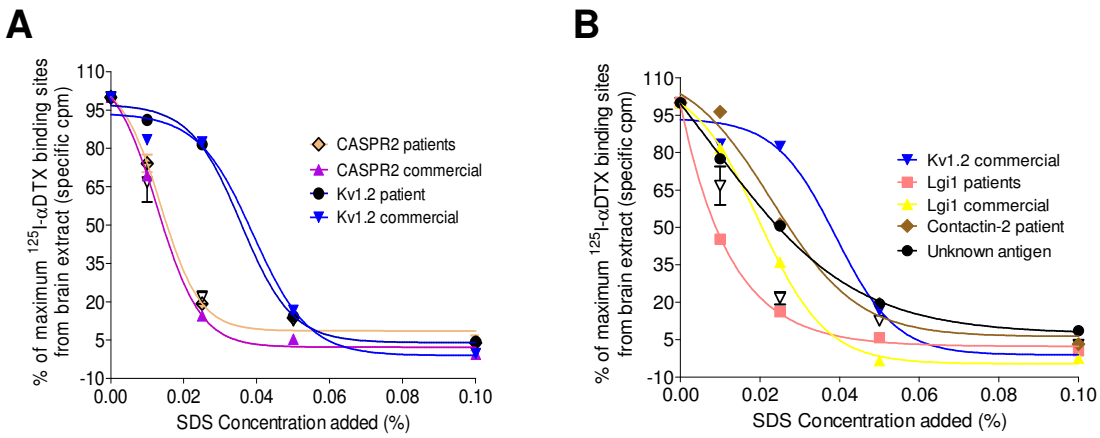


Figure 5.34 A and B. Retrospective analysis of stripping experiments. Previous stripping experiments now analysed with respect to subsequently determined antigenic specificities of individual cases. A. One case was found to have Kv1.2 antibodies and two to have CASPR2-antibodies. B. Four cases were found to have Lgi1 antibodies and one with contactin-2 antibodies. Cases with currently unknown antigen shown in black.

The sera which showed partial co-localisation with Kv1.1/2, within the cerebellar basket cell layer, were all found to be Lgi1-antibody positive cases (e.g. Figure 4.9B, Chapter 4, left hand panel). Furthermore, Dr K Kleopa (Cyprus) showed that all six of 14 blinded sera, which demonstrated binding to Lgi1-transfected cells, co-localised with Lgi1 expressed within the basket cells. In addition, the stripping data, which were previously grouped by clinical syndrome, are individualised by antigenic target (Figures 5.34A and B). The one patient tested, and subsequently found to have anti-Kv1.2 antibodies, strikingly matched the Kv1.2 stripping profile. The same was true for the two CASPR2 positive cases tested in early experiments. The Lgi1-antibody positive cases followed a pattern which was significantly different from the Kv1.2 commercial antibody and showed only a modest overlap with the line followed by the commercial Lgi1 antibody.

Data are also shown from the one contactin-2 antibody positive case and from the patients with an, as yet, unknown antigenic target (Figure 5.34A and B).

Summary and limitations

Within ^{125}I-αDTX-labelled brain membrane complexes, a differential SDS-detergent sensitivity between patient sera and Kv1-commercial antibodies is apparent. Although the Kv1-commercial antibodies are raised against linear epitopes, akin to those available in SDS-treated extracts, this observation was taken as evidence to support the hypothesis that patient antibodies may bind non-Kv1 proteins within the Kv1 digitonin-solubilised, ^{125}I-αDTX-labelled complexes.

Commercial antibodies to a variety of Kv1/nodal-associated proteins identified candidate antigens present in high quantities within ^{125}I-αDTX-labelled rabbit brain membranes. This methodology predominantly identified candidate antigens which had been previously established as Kv1-accessory proteins and reinforced the concept of the VGKC-*complex* as the target for patient antibodies. One method used to narrow-down the likeliest antigenic targets was to exclude proteins which were predominantly or entirely intracellular. This may have biased our results and certainly leaves the MAGUKs as potential antigenic targets to explore in the future. In addition, limited quantities of some antibodies meant titrations to clear saturation points were not always possible.

Nevertheless, this approach generated three possible candidate targets: CASPR2, Lgi1 and contactin-2. Sera traditionally considered to be directed against VGKCs were shown

to bind the extracellular domain of these three targets. CASPR2 patient antibodies consistently showed much more intense binding to live CASPR2-transfected HEK cells than commercial anti-CASPR2 antibodies, did not bind appreciably to denatured CASPR2, were of subclasses IgG1 and IgG4 and were able to activate complement deposition. In addition, a number of control cohorts showed no CASPR2-reactivity in both the cell based assay and fluorescent immunoprecipitation assays. These data seem highly robust.

Unlike CASPR2, Lgi1 was not precipitated by patient sera using a FIPA. Lgi1-Abs were not detected using whole-cell western blotting. A non-quantitative cell-based assay was used to determine Lgi1 antibodies. As the binding properties could be transferred with Lgi1-cell media to untransfected cells, the secreted then surface-bound Lgi1 appeared to be the antigenic target. This protein was found to be of the same length as the cell retained Lgi1, a contradictory finding to some of the literature which may simply represent the limited resolution of the gels used. How the Lgi1 molecules are retained at the cell surface despite washing without the demonstrable presence of ADAM-22, the confirmed Lgi1-ligand, is a question for future research. This may represent a non-specific interaction with the cell surface, for example via charge, or may be explained by the presence of other Lgi1-ligands expressed, probably constitutively, within our HEK cells (as suggested by Fukata et al (2006) and Sagane et al (2008)). In fact, Sirerol-Piquer et al (2006) described the same phenomenon with both PC12 cells and COS7 cells, suggesting the constitutive expression of Lgi1-receptors in both neural and non-neural

cells. The co-expression of Lgi1 with a putative Lgi1-receptor may present a more native conformation of the bound protein with greater antigenicity.

Only one experimental method has been used to demonstrate the presence of antibodies against contactin-2. As this molecule has no intracellular domain, an additional method may be to use fluorescent-activated cell sorting or to add an extracellular EGFP-moiety and perform a FIPA. The latter is a higher-risk strategy which may disrupt the epitope.

Yet, 26% of sera remain without a clear antigenic target. This may be due to the relative insensitivity of the current assays or imply alternative antigenic targets await discovery. Affinity purification of digitonin-solubilised brain membranes is the least biased method to understand whether other, as yet undiscovered, proteins exist in ^{125}I-αDTX-labelled rabbit brain complexes: this has been attempted once in the laboratory without clear results.

The main question posed at the start of the thesis was whether the antigenic specificities of the sera may explain the heterogeneity of the clinical syndromes. These clinico-serological correlations are presented in the following chapter.

CHAPTER 6: CLINICO-SEROLOGICAL CORRELATIONS

Introduction

With the discovery of a number of antigenic targets, the clinical data were revisited and analysed with respect to the single most important question posed at the beginning of the thesis: can the clinical heterogeneity be explained by the specific antigenic targets of the antibodies? The secondary question of whether any other specific clinical features are predicted by antibody specificities was also investigated.

Clinico-serological correlations

The four antibody targets discovered (Lgi1, CASPR2, Contactin-2 and Kv1.2), allowed a serological segregation of the 113 patients (Table 6.1). Twenty-nine cases (26%) remained without a determined antigenic target (no Ag). From the remaining 84 cases, 30 (27%) had CASPR2 antibodies, 49 (43%) had Lgi1 antibodies, seven (6%) had contactin-2 antibodies and three (3%) Kv1.2 antibodies. This totalled more than 100% because five contactin-2 antibody positive patients (4%) were found to have contactin-2 antibodies plus antibodies to one other target: CASPR2 (n=3), Lgi1 (n=1) and Kv1.2 (n=1). As the contactin-2 antibody positive group contained all the overlap cases, all these were returned to the cohorts of their other antigenic specificity and the two purely contactin-2 antibody positive cases were analysed within the contactin-2 antibody positive group.

	CASPR2	Lgi1	Pure contactin-2	Pure Kv1.2	No Ag
N (total = 113)	30	49	2	2	29
Age at onset (median and range)	63 (30-79)	63 (25-83)	40, 42	39, 77	54 (17-78)
VGKC-Ab titre (mean and range, pM)	1308 (154-3746)	2585 (637-8840)	470, 489	470, 910	808 (411-7607)
Male:Female	26:4	35:14	1:1	2:0	18:11
Tumour (N=15)	14	0	0	0	1
LE (N=74)	7	44	1	1	21
Epilepsy (N=4)	2	1	0	0	1
MoS (N=13)	11	2	0	0	0
NMT (N=17)	11	0	1	1	4
Other (N=5)	0	3	0	0	3
Infectious precipitant	1	1	1	0	8
Amnesia or confusion	17	46	1	1	22
Any neuropsychiatric features	17	46	1	1	24
Seizures	12	44	0	0	17
Hypersomnia	0	4	0	0	5
Insomnia	15	5	0	0	1
Hyperhidrosis	11	5	1	1	3
Any dysautonomia	15	7	1	1	3
Pain	16	5	0	0	2
Weight loss	11	1	0	0	2
Myasthenia gravis	8	0	0	0	1
MRI MTL high signal	4 of 21	26	0	0	12 of 27
Hyponatraemia	2	32	0	1	10
Fall in mRS (mean and range, see Figure 6.5A)	-0.04 (-4 to 5)	3.30 (-2 to 5)	NA	0, 3	1.9 (-1 to 5)
Death	11	1	0	0	0

Table 6.1. Clinical features of 113 'VGKC'-Ab positive cases divided by antibody specificities. No Ab = no antigenic target defined. NA = not applicable.

Overall clinical-serological correlations

When the 113 cases were segregated by antibody specificities, some clear correlations appeared. These have been summarised in Figures 6.1 and 6.2 and Tables 6.1 and 6.2. Briefly, 45 of the 78 (58%) LE/Epilepsy cases had Lgi1-antibodies, nine (12%) had CASPR2 antibodies, one had contactin-2 antibodies (1%) and one had Kv1.2 antibodies (1%). Eleven of 13 Morvan's cases (85%) had CASPR2 antibodies and two had Lgi1 antibodies (15%). 11 of 17 NMT cases (65%) had CASPR2 antibodies while one had contactin-2 and one had Kv1.2 antibodies. None of the NMT cases had Lgi1 antibodies. 'VGKC'-Ab titres were higher in the Lgi1-Ab positive cohort than the CASPR2-Ab positive patients or the patients without a known antigenic target (Figure 6.3; Kruskal-Wallis test, $p<0.0001$; Dunn's multiple comparison, $p<0.05$ for Lgi1 Vs CASPR2 and Lgi1 Vs no Ab). Age of onset modestly significantly differed across the groups (Figure 6.4; Kruskal-Wallis test $p=0.024$) but Dunn's multiple comparison revealed no differences between any two groups. Finally, the clinical improvements after treatments (as rated by the modified Rankin Score; mRS) were poorest in the CASPR2-Ab positive cohort (Figure 6.5A). However, this poor outcome was in the main restricted to the CASPR2-Ab positive cases with tumours (Figure 6.5B; Mann Whitney U test, $p=0.0002$). Table 6.2 highlights multiple statistical comparisons between four groups: those with and without CASPR2 antibodies, those with and without Lgi1 antibodies, CASPR2 and Lgi1 antibody positive groups and, finally, Lgi1-antibody positive cases and those without a defined antigenic target.

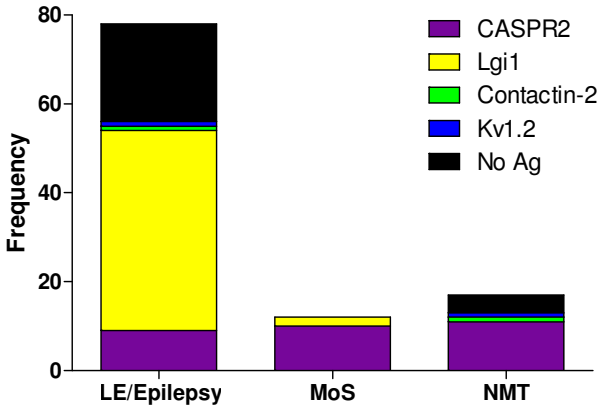


Figure 6.1. Determined antigenic targets within clinical syndrome classifications (LE/Epilepsy, MoS and NMT). No Ag = no antigenic target defined.

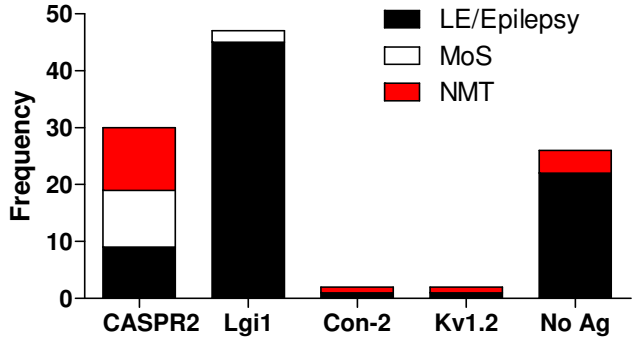


Figure 6.2. Clinical syndromes (LE/Epilepsy, MoS and NMT) by antigenic targets. Con-2 = contactin-2; No Ag = no antigenic target defined.

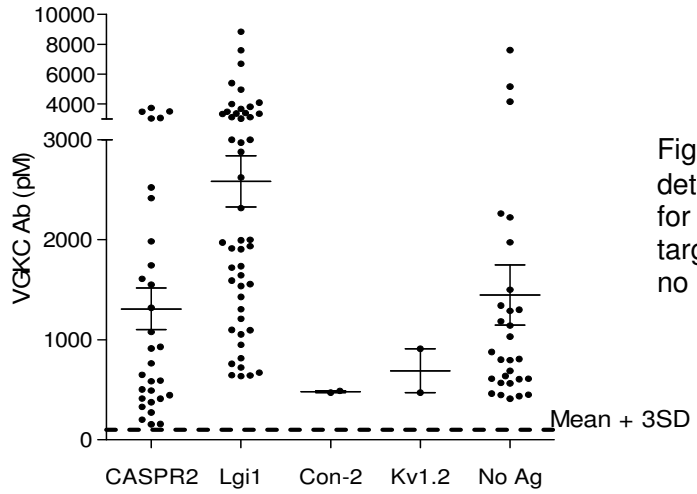


Figure 6.3. 'VGKC'-Ab titres determined by the diagnostic assay for groups defined by antigenic target. Con-2 = contactin-2. No Ag = no antigenic target defined.

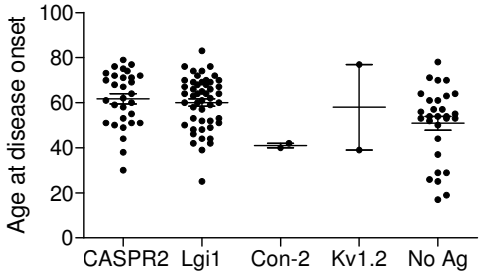


Figure 6.4. Age of onset divided by antigenic target. Contactin-2 =Con-2; No Ag = no antigenic target defined.

Clinical features of CASPR2-Ab positive cases

CASPR2 was the first antigenic target discovered and clinical features of CASPR2-Ab positive cases will be described below. Table 6.1 compares the CASPR2-Ab positive and negative patients (statistics for multiple comparisons in Table 6.2). Demographically, while the age range defined by CASPR2-Ab positivity was unremarkable, there was a non-significant predilection for males within the CASPR2-Ab positive group (87% Vs 67% for CASPR2-Ab positive Vs negative cases, Fisher's t test p=0.06). Interestingly, 'VGKC'-Ab levels were significantly lower in CASPR2-Ab positive cases (Figure 6.3). CASPR2-Ab positive cases showed a massive overrepresentation of MoS and NMT. Infact, CASPR2-Abs accounted for 11 of 13 with MoS (85%) and 11 of 17 with NMT (65%). Whereas, only seven of 74 (9%) with LE were found to be CASPR2-Ab positive. Although small numbers were available, two of the four patients with pure epilepsy (50%) were found to be CASPR2-Ab positive. The single most impressive and probably most clinically relevant finding was that 14 of the 15 tumours (12 thymomas, one endometrial adenocarcinoma and one non-small cell lung cancer) fell into the CASPR2-Ab positive cohort (Fisher's t test, $p<0.0001$; one serum from a NMT patient with a resected, non-metastatic thymoma was CASPR2-Ab negative). This generated an odds ratio of 71.8 (8.8 to 585.2) and a negative predictive value of 99%, for CASPR2-Ab seropositivity as a paraneoplastic predictor. However, as 16 of the CASPR2-Ab positive cases had no tumour detected, the positive predictive value was only 47%. In addition, from the 98 cases without active tumours, only two cases (one LE and one MoS) had body-imaging defined regression of small mediastinal lymph nodes: both of these were CASPR2-Ab positive.

	CASPR2 positive Vs CASPR2 negative	Lgi1 positive Vs Lgi1 negative	Lgi1 positive Vs No antigen	CASPR2 positive Vs Lgi1 positive
VGKC-Ab titre (mean and range, pM)*	0.0105	<0.0001	<0.0001	0.0002
Male : Female*	NS	NS	0.0391	NS
Tumour	< 0.0001	0.0001	NS	<0.0001
LE	< 0.0001	< 0.0001	NS	<0.0001
Epilepsy	NS	NS	NS	NS
MoS	< 0.0001	NS	NS	0.0003
NMT	0.0008	< 0.0001	0.0167	<0.0001
Other	NS	NS	NS	NS
Infectious precipitant	NS	0.0221	0.0012	NS
Amnesia or confusion	0.0044	0.0002	0.0338	0.0001
Any neuropsychiatric features	0.0013	0.0005	NS	0.0001
Seizures	0.0016	< 0.0001	0.0035	<0.0001
Hypersomnia	NS	NS	NS	NS
Insomnia	< 0.0001	NS	NS	0.0001
Hyperhidrosis	0.0054	NS	NS	0.0081
Any dysautonomia	0.0003	0.0456	NS	0.0015
Pain	< 0.0001	0.0203	NS	<0.0001
Weight loss	< 0.0001	0.0033	NS	<0.0001
Myasthenia gravis	< 0.0001	0.005	NS	0.0002
MRI MTL high signal	0.0237	0.0428	NS	0.0095
Hyponatraemia	< 0.0001	< 0.0001	0.0104	<0.0001
Death	< 0.0001	0.0118	NS	<0.0001

Table 6.2. Fisher's t-tests comparing individual features across a number of subgroups defined by their serological specificities. Features overrepresented in the CASPR2-Ab positive group are highlighted in red and those seen more commonly in the Lgi1-Ab positive group in blue. Neuropsychiatric features included amnesia, confusion, depression, psychosis and anxiety. Multiple comparisons would necessitate a significance level of p=0.002. * = Mann Whitney U test used. MTL = medial temporal lobe

Consistent with the MoS overrepresentation, analysis of the individual clinical features showed that amnesia/confusion were significantly underrepresented in the CASPR2-Ab positive group ($p=0.004$) and the presence of any neuropsychiatric features (amnesia, confusion, psychosis, depressive, anxiety, $p=0.0013$), seizures ($p=0.0016$) and serum hyponatraemia ($p<0.0001$) were also more common in the CASPR2-Ab negative group. Features which were seen more frequently in the CASPR2-Ab positive cases were insomnia ($p<0.0001$), hyperhidrosis ($p=0.0054$), dysautonomia ($p=0.0003$), pain ($p<0.0001$), weight loss ($p<0.0001$), a past history of myasthenia gravis ($p<0.0001$) and normal brain MRI ($p=0.003$). Cardiac arrhythmias or tachycardia were noted in seven cases with MoS, of whom six had CASPR2 antibodies. Interestingly, QT-interval prolongation was the only specific ECG abnormality reported. In addition, the CASPR2-Ab positive group contained 11 of 12 deaths ($p<0.0001$) and no median improvement in their mRS, in comparison to clinical improvements in most other cases (Figure 6.5A). This was likely due to the tumour burden in this group (Figure 6.5B): an example of the radiological appearance of the commonly metastatic thymic pathology is demonstrated in Figures 6.6A and B from a patient with MoS.

Serological value over clinical segregations

Table 6.3 shows the percentage of patients with the designated clinical feature (within rows) divided by the clinical diagnosis with or without their CASPR2-Ab status (within columns). The percentage of the group that contained the feature specified in the row and in the column are shown sequentially within the brackets. This table showed the associations of dysautonomia, insomnia, pain and weight loss across the spectrum of

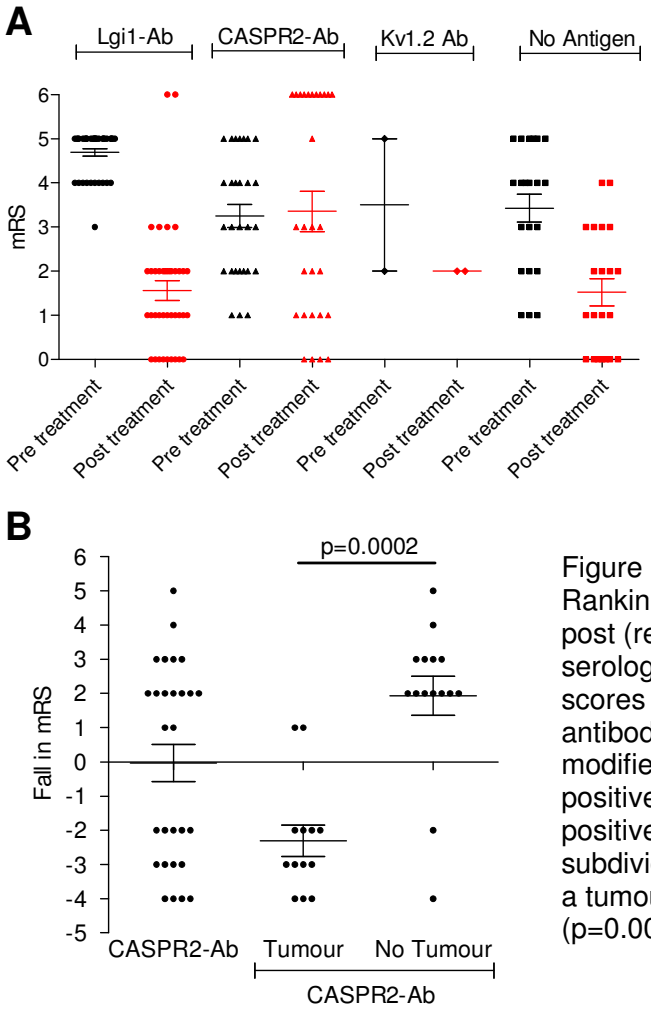


Figure 6.5 A and B. A. modified Rankin score (mRS) pre (black) and post (red) treatments, divided by serological specificity. No mRS scores available for contactin-2 antibody positive cases. B. Fall in modified Rankin score in CASPR2-Ab positive cases: all CASPR2-Ab positive cases and subsequently subdivided into those with and without a tumour. Mann Whitney U test (p=0.0002).

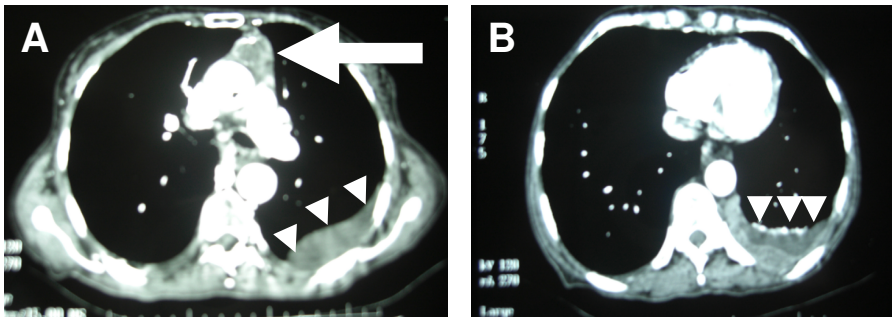


Figure 6.6A and B. Thymic metastases in 51 year-old female with CASPR2 antibodies and Morvan's syndrome. A. Plain computerised tomography of the chest. Arrow = anterior mediastinal mass with some superficial calcification. B. Metastases with contrast rim enhancement (arrowheads) and multiple densities within the mass.

(% of total in row; % of total in column)	LE / Epilepsy (N=78)	MoS (N=13)	NMT (N=17)	MoS plus NMT (N=30)	CASPR2-Ab positive (N=30)	CASPR2-Ab positive *and* MoS/NMT (N=21)	CASPR2-Ab negative (N=83)
Dysautonomia (N=27)	7 (26;9)	12 (44;92)	8 (30;47)	20 (74;67)	15 (56; 50)	12 (44;57)	12 (44;14)
Insomnia (N=21)	6 (29;8)	13 (62;100)	2 (10;12)	15 (71;50)	15 (71;50)	13 (62;62)	6 (29;7)
Weight loss (N=14)	2 (14;3)	8 (57;62)	4 (29;24)	12 (86;40)	11 (79;37)	11 (79;52)	3 (21;4)
Pain (N=23)	3 (13;4)	12 (52;92)	7 (30;41)	19 (83;63)	16 (70;53)	16 (70;76)	7 (30;8)
Tumour (N=15)	0 (0;0)	8 (53;62)	7 (47;41)	15 (100;50)	14 (93;47)	14 (93;67)	1 (7;1)
Death (N=12)	0 (0;0)	8 (67;62)	4 (33;24)	12 (100;40)	11 (92;37)	11 (92;52)	1 (8;1)

Table 6.3. CASPR2-Ab subgroup analysis. Groups with the highest representations are highlighted in red. Brackets denote the proportion of cases with each clinical feature (in rows) within a subgroup; the percentage of the subgroup with the relevant clinicoserological status (in columns).

'VGKC'-Ab associated disorders (LE, MoS and NMT). It also, somewhat disappointingly, showed that CASPR2-Ab positivity across the whole cohort or exclusively in the cases with MoS/NMT (N=21) does not confer a higher strength in the prediction of individual clinical features than categorization of cases as simply 'with NMT' (i.e. MoS plus NMT). In summary, the clinical group defined purely as MoS plus NMT consistently contained the most cases with features which were overrepresented by CASPR2-Ab positivity.

Overall, the CASPR2 patients had a poor outcome and the Lgi1 positive patients a good prognosis. However, within the CASPR2-Ab positive group, the presence of a tumour

clearly affected the prognosis (Figure 6.5B). How did the clinical classifications modify these findings? Figure 6.7 suggested that the CASPR2-positivity conferred a marginally poorer prognosis in MoS and NMT subgroups, but not within the LE subgroup.

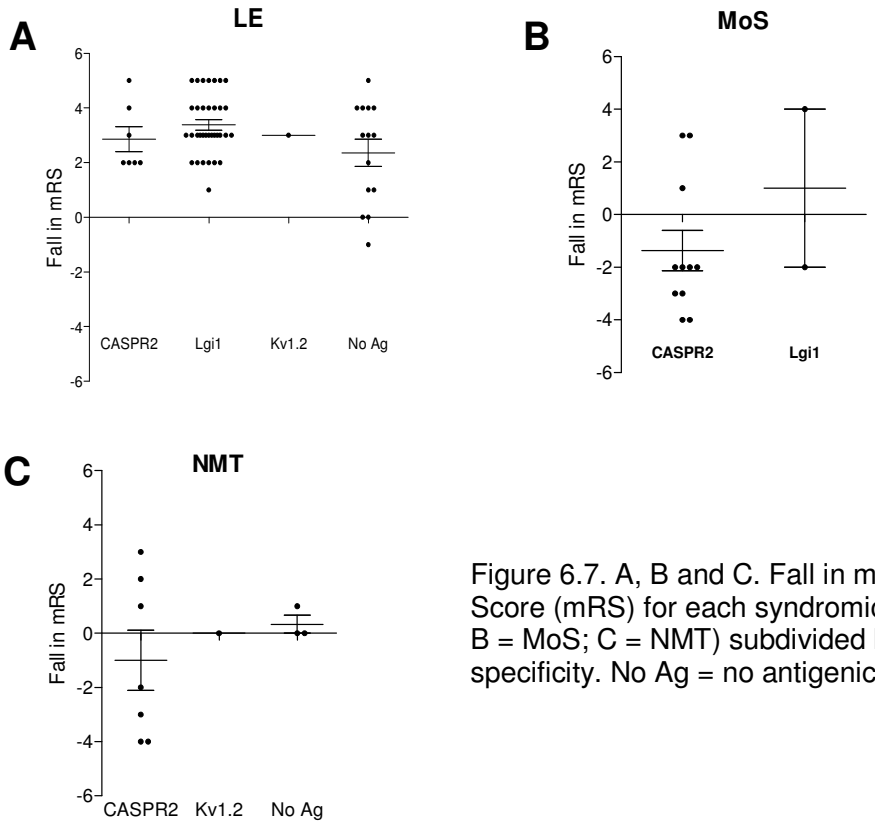


Figure 6.7. A, B and C. Fall in modified Rankin Score (mRS) for each syndromic group (A = LE; B = MoS; C = NMT) subdivided by antibody specificity. No Ag = no antigenic target defined.

Clinical features of Lgi1-antibody positive cases

The next antigen discovered was Lgi1. Lgi1-Abs were found in 44 of 74 (59%) LE cases, the two non-CASPR2 positive cases of MoS (15%) and one case with epilepsy (25%). Interestingly, none of the NMT cases showed Lgi1-Ab positivity. Also, from the other cohort of 42 cases with NMT, none had Lgi1-Ab positivity. In other words, of the Lgi1-Ab positive sera, LE/Epilepsy cases accounted for 92%, 4% had MoS and 4% had other syndromes – including a fixed dystonia and a diffuse pain syndrome. Lgi1-Ab positive

cases had higher 'VGKC'-Ab levels when compared to Lgi1-Ab negative cases (Figure 6.3) and, overall, had a better prognosis with a clinical deterioration recorded only in two cases (Figure 6.5A). The important differences between Lgi1-Ab positive and negative cases broadly reflected the converse features of the CASPR2-Ab positive group (Table 6.2, second column). Therefore Lgi1-Ab positive cases reflected an absence of active tumours, higher representation of neuropsychiatric features, seizures, medial temporal lobe MRI changes and hyponatraemia.

In addition, 17 of the 24 (71%) patients with dystonic seizures and positive 'VGKC'-Abs had Lgi1-Abs. Two had contactin-2 antibodies, one in addition to Lgi1-Abs. None of these cases had CASPR2-Abs.

Clinical features of Contactin-2 antibody positive cases

Of the two cases purely with contactin-2 antibodies, one 42 year-old female, with a past history of thyrotoxicosis, had neuromyotonia with an initial 'VGKC'-Ab titre of 489pM and one 40 year-old male had a limbic encephalitis concomitant with a salmonella sepsis and a 'VGKC'-Ab titre of 470pM. He had a past history of thyroid eye disease, normal brain imaging and serum sodium. Neither of these cases had malignancies detected after full body CT imaging.

Clinical features of Kv1.2 antibody positive cases

Three cases had Kv1.2 antibodies: one of these also had contactin-2 antibodies. Of the two male cases purely with Kv1.2 antibodies, one had LE and one had NMT. The 77-

year-old male with LE ('VGKC'-Ab titre = 470pM) developed amnesia and confusion without seizures. He was ataxic with myelopathic signs and a peripheral neuropathy. He had normal brain imaging and showed a partial response to immunotherapy (prednisolone and plasma exchange). The 39-year-old male with NMT ('VGKC'-Ab titre = 910pM) had a 15 year history of non-progressive prostate cancer and severe constipation. He has had little response to azathioprine. The female, with both Kv1.2 and contactin-2 antibodies detected, had EMG-proven periocular NMT without improvement after multiple antiepileptics. None of these three cases had relevant detectable tumours after body imaging.

Clinical features of cases with no confirmed antigenic target

Within the patients that remained without a defined antigenic target, 21 of 29 cases (72%) had LE and four (14%) had NMT (see Table 6.1). Probably as a reflection of this LE bias, the overall distribution of clinical features within this group was similar to the Lgi1-Ab positive patients. However, there was one important exception to this rule: of the 11 patients with an infectious prodrome, eight of them were within the 'no-antibody' group (Fisher's t test, p=0.0005).

Neuromyotonia cohort with low positive VGKC-Ab titres

The CBA scores for all but one of the 30 CASPR2-Ab FIPA-positive cases were '4', this suggested that the high VGKC-Ab positive cases (>400pM) may saturate the CASPR2-Ab cell based assay. Therefore, a 'low-positive' VGKC-Ab cohort may provide an opportunity to compare the relative sensitivity and specificity of cell-based assays for the

newly defined antigenic targets with the diagnostic brain-based 'VGKC'-Ab assay. The cell-based assay results from 42 cases with neuromyotonia (collected by Prof M Kiernan (n=17) and the late Dr I Hart (n=25)) are summarised below and in Figure 6.8 and 6.9.

Thirty of these 42 cases had undetectable 'VGKC'-Abs, using the diagnostic assay (<100 pM). Of the 42 cases, 12 cases had CASPR2-Abs detected by a cell-based assay: all had <200 pM of 'VGKC'-Abs and eight had undetectable 'VGKC'-Abs. When CBA scores were plotted against 'VGKC'-Ab titres, it appeared that the cell-based assay conferred greater sensitivity than the routine 'VGKC'-Ab assay (Figure 6.8). Of the five contactin-2 antibody positive cases, four had undetectable 'VGKC'-Abs. Three of the CASPR2-Ab positive cases also had contactin-2 reactivity. Six cases had Kv1-antibodies as determined by significant precipitation from ^{125}I-αDTX-labelled HEK-expressed Kv1s. Five of these six had <200 pM of detected 'VGKC'-Abs, with two samples at undetectable levels (<100 pM). None of these 42 cases had Lgi1 reactivity. These data are summarised in Figure 6.9. Hence, it would appear that these assays, while maintaining specificity – see negative and disease control data presented earlier – provided some increased sensitivity.

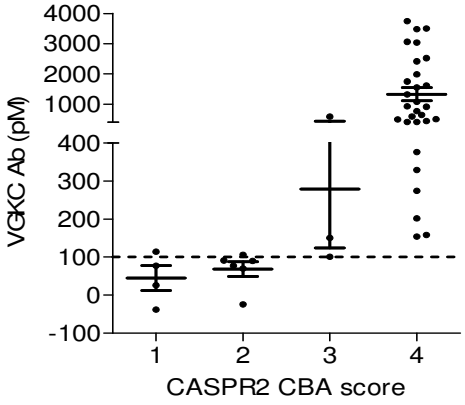


Figure 6.8. CASPR2-cell based assay (CBA) score against VGKC-Ab titre plotted for 30 patients from main study and 13 from the two neuromyotonia cohorts which were positive on a CASPR2 cell-based assay. Dashed line shows cut-off value for 'VGKC'-Ab determined positivity (100 pM).

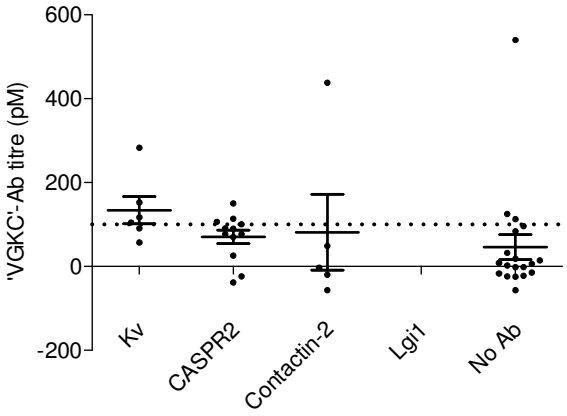


Figure 6.9. Distribution of antigenic targets in unselected cohort of 42 cases with neuromyotonia.

Summary and limitations

The correlations of clinical and serological data revealed some original and very exciting findings with implications for diagnostic assay development, prediction of clinical features – in particular tumours – and understanding the biology of these diseases.

Despite the limitations of the clinical data ascertainment, as outlined in the summary of Chapter 3, the cohort with CASPR2-Abs had some notable clinical consistencies. There was a clear over-representation of the MoS and NMT populations. However, analysis of the individual clinical features may be less biased than the possible more arbitrary syndromic classifications. This proved a clear bias towards insomnia, pain and dysautonomia within the CASPR2-Ab positive cohort. But of greatest importance was the finding that CASPR2-Abs had a 99% negative predictive value for tumours. This was

also interesting in the only two cases with mediastinal lymph node regression, whose sera were CASPR2-Ab positive. This is of importance not least given the initial absence of tumours detected by imaging in three of the 14 CASPR2-Ab cases who eventually had clear evidence of tumours. The presence of these tumours predominates in determining the poor overall prognosis of the CASPR2-Ab positive group. However, the non-paraneoplastic, CASPR2-Ab positive cases still had a worse outcome when compared to the Lgi1-Ab positive cases (Mann Whitney U test, p=0.0089, compare Figures 6.5A and B). CASPR2 seropositivity did not seem to offer predictive value over the clinical segregations. Further data from LE cases with tumours are required before the 'onconeural' value of CASPR2-Ab positivity is fully established.

By contrast, the Lgi1-Ab positive cases were biased towards features consistent with limbic encephalitis: seizures, amnesia/confusion, hyponatraemia, medial temporal lobe MRI abnormalities and a good prognosis. These cases had no tumours detected. In addition, two of 13 MoS cases and none of the neuromyotonia cases had Lgi1-Abs.

One problem occurred when classifying the serology of the seven patients with contactin-2 antibodies. As these were the only antibodies sharing overlaps with others, all overlapping cases were returned to their non-contactin-2 positive groups. It may be that these antibodies are epiphenomena, possibly generated via epitope spread, and are better excluded entirely. Of the five cases with Kv1.2 or contactin-2 antibodies, two had LE and three had NMT. In none was a tumour detected.

Assay optimisation could have been pursued further within this thesis. It may still be that some of the 26% with positive 'VGKC'-Abs but currently without defined antigenic targets may still have Lgi1 or CASPR2 positivity which is not detectable using the current assays. The absence of a quantifiable assessment of Lgi1 antibodies and the absence of a second confirmatory assay is suboptimal. As shown in the low-positive NMT cohort, these cell-based assays have the potential to offer increased sensitivity over the current assay. However, further assessments of healthy controls and disease controls are required to confirm this initial observation in the neuromyotonia cohort with some of the lowest 'VGKC'-Abs.

CHAPTER 7: DISCUSSION

Introduction

In this body of work, Kv1 channels have been shown to be very uncommon target of 'VGKC'-antibodies. Three novel antigenic targets of these antibodies, all tightly associated with Kv1s in brain membranes, have been identified and have explained the majority of the clinical phenotypic heterogeneity in the largest reported 'VGKC-complex' antibody positive cohort. The two major novel antigenic targets – Lgi1 and CASPR2 – account for 70% of the cohort. The antigen-specific modulation of Lgi1 seems to commonly elicit a novel clinical phenotype as defined by frequent, brief late-onset faciobrachial dystonic seizures.

These findings have major implications within the field. Firstly, they may offer more specific examination and prediction of individual features, most importantly tumours but also pain, insomnia and cardiac arrhythmias. Secondly, the expression of a specific antigenic target may offer increased sensitivity when compared to brain tissue-based assays. This may be especially useful when examining patients with low-antibody titres. Finally, in combination with knowledge about the very similar phenotypes derived from genetic mutations of these antigenic targets, the 'immunophenocopies' offer opportunities to further our understanding regarding the biology, in particular the aetiology, of these diseases. Nevertheless, some of the results of studies that examined the effect of 'VGKC'-antibodies in the context of neural tissue or in vivo (e.g. Sinha et al 1991; Shilitto et al 1995) are still important and valid. By contrast, studies suggesting direct

binding to Kv1s (e.g. Hart et al 1997; Nagado et al 1999; Kleopas et al 2006) may not stand the test of time. Although it is possible that such studies, using low positive 'VGKC'-Ab positive sera have different characteristics to the high-positive sera focussed upon within this thesis.

Below, the molecular characteristics of the novel identified antigenic targets will be discussed with particular reference to established genetic models of their malfunction. These data will be used to hypothesise aetiological mechanisms for their roles in the aetiology of LE, MoS and NMT.

Kv1-associating molecules around the node of Ranvier: an overview

These molecules directly modulate the biology of Kv1s and allow understanding of the subcellular neuronal domains which have clear structural and functional differentiation. Many of the salient features regarding individual Kv1s and Kv1-associated molecules are shown in Table 7.1. Kv1s were also reviewed in Chapter 1.

Three main axonal divisions have been established around nodes of Ranvier. These are the paranode (adjacent to the node), the juxtaparanode (JXTPN) and the internode as reviewed by Peles and Salzer 2000 and Rosenbluth 2009 (also see Figure 1.2 and 1.3A). The node harbours voltage-gated sodium channels (particularly Nav1.6) and therefore determines action potential generation/propagation. Neurofascin 186 (NF186) also resides at the nodes. The paranode flanks the node and contains axonal CASPR and axonal contactin interacting with glial neurofascin 155 (NF155). At the paranode, the

myelin sheath is known to make direct contact with the neuron – via the CASPR/contactin/NF155 complex. The contacts formed produce a series of septate-like junctions that spiral around the axon. The juxtaparanode lies lateral to the paranode (further away from the node of Ranvier) and contains voltage-gated potassium channels (Kv1s), CASPR2 and TAG-1 (human homolog known as contactin-2). The potassium channels function to repolarise the depolarised membrane. The internode contains some Kv1s and the sodium-potassium ATPase, which work to restore the ionic balance after depolarisation. Hence, the structural divisions (shown in Figure 1.3) have clear functional implications including propagation of the action potential, restriction of molecule diffusion and axo-glial adhesion.

During early mouse development (around postnatal day five), Kv1s/CASPR2 are seen in unison but at the paranode. Whereas CASPR/contactin – again in unison - are nearer the node of Ranvier (Traka et al 2003). The migration of both these two 'complexes' to the juxtaparanodal and paranodal regions, respectively, has been shown to occur at around postnatal day eight. Mice deficient in galactolipids, which are a major constituent of the myelin at the septate junctions (e.g. CGT knockout mice), lack the paranodal septate bands (Poliak et al 2001). These mice showed severely disorganised paranodes with almost undetectable levels of contactin-1, CASPR and NF155. By contrast, the Kv1 and CASPR2 quantities were normal but these molecules had moved into paranodal regions (Poliak et al 2001). The nodes showed normal Na_vs and NF186 expression. Hence, despite selective genetic modulation of the paranodal architecture, the paranode and the

Molecule	Structure/biology including extent of extracellular domains	Localisation: macroscopic and subcellular	Functional interaction with Kv1.1	Human mutations	Animal mutations
Kv1.1, 1.2 and 1.6	Six transmembrane domains in each of four alpha-subunits. Four small extracellular loops (each from 43-72 amino acids).	Hippocampus, cortex and multiple subcortical structures. Juxtaparanodes of Ranvier, axon initial segment and presynaptic terminals.	NA	Autosomal dominant Kv1.1 mutations produce neuromyotonia and increased frequency of epilepsy	Knockout mice show spontaneous seizures and truncations produce megancephaly. Auditory startle responses seen in both mice.
Lgi1	Principally secreted and only partially membrane retained; 522 amino acids are secreted.	Hippocampus, cerebellum, amygdale and cortex. Presynaptic neuronal localisation.	Prevents Kvβ1-mediated inactivation	Autosomal dominant lateral temporal lobe epilepsy with auditory features	Increased seizure susceptibility and spontaneous myoclonic seizures in null mutant mice with reduced seizure threshold in heterozygote mutants
CASPR2	Single transmembrane cell-adhesion protein. 1281 extracellular amino acids.	Hippocampus, cerebellum, amygdale, cortex and striatum. Juxtaparanodes of Ranvier and axon initial segment.	Maintains Kv1 and contactin-2/TAG-1 localisation at juxtaparanodes.	Autosomal recessive cortical dysplasia with focal epilepsy and absent tendon reflexes. Polymorphisms associated with autism, mental retardation and epilepsy/schizophrenia	Knockout mice show normal phenotype but lack of Kv1 clustering at juxtaparanodes
Contactin-2 / TAG-1	GPI-linked cell adhesion molecule with multiple Ig-like domains. 1040 extracellular amino acids.	Cerebellum, hippocampus, olfactory bulb and white matter tracts. Juxtaparanodes of Ranvier, axon initial segment and opposing oligodendrocytes / Schwann cells.	Maintains Kv1 and CASPR2 localisation at juxtaparanodes.	Polymorphisms associated with good intravenous immunoglobulin response in CIDP.	Increased seizure susceptibility and lack of CASPR2/Kv1 clustering in knockout mice. One study also shows increased latency to noxious stimuli and working memory difficulties

Table 7.1. Pathophysiological summaries of Kv1s and associated molecules.

juxtaparanode were significantly disrupted. These observations demonstrated the importance of the axo-glial interactions in maintaining the juxtaparanodal structure. Examination of human brains has shown that aberrant organisation of these molecules is apparent in some pathological states known to associate with axonal degeneration, such as multiple sclerosis (Coman et al 2006).

PDZ-domain containing molecules

As reviewed by Kim and Sheng (2004), PDZ-domains are protein interaction modules found as part of molecular complexes which are seen prominently at the post-synaptic densities (PSDs). PSD molecules each have three distinct PDZ domains that have been implicated in the clustering of ion channels and receptors such as Kv1, NMDA, nAChR, beta-adrenergic and 5-HT2A/C. Each of the three PDZ domains has differing affinities for interacting proteins.

CASPR2 (CONTACTIN-ASSOCIATED PROTEIN 2)

Molecular characteristics

CASPR2 is a member of the neurexin superfamily, a group of transmembrane proteins which mediate cell-cell interactions in the nervous system. Five CASPR molecules exist (CASPR1-5) maintaining >37% homology with each other and 97% identity between human and mouse. Of these, CASPR2 is most closely associated with Kv1 channels. CASPR2 has a molecular weight of 180kDa containing 1331 amino acids. Fifty of these amino acids are intracellular. The extracellular region is divided into an N-terminal signal peptide, one discoidin-like, four laminin-G and two epidermal growth factor-like domains

(www.hprd.org). The intracellular region has a PDZ-binding domain at the C-terminus and a protein 4.1B binding domain adjacent to the plasma membrane. Protein 4.1B can associate independently with CASPR2 and also interacts directly with cytoskeletal actin and spectrin (Denisenko-Nehrbrass et al 2003, Horresh et al 2010). CASPR2 expression appears at day E15 and increases until adulthood. CASPR2 transcripts are detected predominantly in the nervous system, with very low levels in the ovary and prostate (Poliak et al 1999).

The main subcellular site of CASPR2 expression is within the juxtaparanodes, especially those of larger diameter myelinated neurons, with a higher expression towards the paranodal region. It is estimated that 15% of juxtaparanodes contain CASPR2, suggesting that other molecules may be playing a similar role at the remaining 85% (Poliak et al 1999). CASPR2 is expressed in the hippocampus – especially within the dentate gyrus – as well as in the amygdala, neocortex and striatum. There is also some CASPR2 in oligodendrocytes, but not Schwann cells (Poliak et al 1999).

CASPR2-Kv1 interactions

In mammalian brain tissue, CASPR2 clearly co-precipitates with Kv1s and the intracellular tail of CASPR2 is sufficient to mediate this observation. CASPR2 can be precipitated in the reverse experiment, performed with the C-terminal of Kv1.2 as bait. However, only a very small proportion of the total Kv1.2 is said to be associated with CASPR2 (estimates range between 0.5% and 5%, Poliak et al 1999; Horresh et al 2008). Despite the CASPR2-Kv1 co-precipitation noted in brain tissue in many publications

(Poliak et al 1999; Poliak et al 2003; Traka et al 2003; Horresh et al 2008), this has not been convincingly reproduced in co-transfected mammalian cells (Tzimourakas et al 2007). Hence, it was assumed that the PDZ domains on CASPR2 and Kv1s were linked by a MAGUK molecule, to account for the co-precipitation of these two molecules from brain tissue. However, further to Rasband et al (2002), it was found that a mouse with knockout of both PSD93 (chapsyn110) and PSD95 (SAP90) maintained normal Kv1 clusters at the juxtaparanodes (Horresh et al 2008). In addition, transgenic mice that expressed CASPR2 without its PDZ binding domain maintained both Kv1 clustering at juxtaparanodes and CASPR2-Kv1 co-immunoprecipitation. But in transgenic mice that expressed CASPR2 without its intracellular domain, CASPR2 was no longer able to closely associate with Kv1s (Horresh et al 2008). All these studies were performed by examining the subset of Kv1s at the juxtaparanodes. When the axon initial segment was assessed, CASPR2 knockout mice showed a normal Kv1 distribution, but PSD93 knockout mice show dispersed Kv1s (Ogawa et al 2008). Hence, future research will aim to determine the non-PSD mechanisms which allow interaction of CASPR2 and Kv1 at the juxtaparanodes and may generate further potential antigenic targets.

In a separate approach to answer this question, Horresh et al (2008) used the cytoplasmic tail of CASPR2 as bait and found by mass spectrometry that a number of scaffolding proteins from brain tissue bound this tail. These included MPP2, 3, 5, 6, CASK and MUPP1: these associations were maintained in co-transfected HEK cells. However, whether any of these are sufficient to maintain a CASPR2-Kv1 interaction in brain tissue

was unstated. One separate mass spectrometry experiment identified carboxypeptidase E as a protein which directly interacts with CASPR2 (Oiso et al 2009).

Very few of these experiments showed data regarding Kv1.4 or Kv1.6. This conspicuous absence is a limitation of such studies which may suggest low or no expression of these proteins at the juxtaparanodes.

CASPR2 mutations in animals

CASPR2 knock-out mice were noted to be smaller until month three but to subsequently show an entirely normal phenotype. They had normal Nav, CASPR and contactin distributions and normal gross morphology of their CNS until 20 months of age. However, consistent with the regimented structural organisation within the juxtaparanodal domain, Kv1.1/1.2 and contactin-2 proteins were scarcely seen at juxtaparanodes in the PNS and CNS of CASPR2-/- mice (Poliak et al 2003; Traka et al 2003). However, internodal Kv1 expression was preserved and PSD93 and PSD95 were redistributed to the nodes of Ranvier (Horresh et al 2008). Whilst the total quantity of Kv1s was only slightly reduced, TAG-1 was not detected in these knockout mice. Despite these marked molecular alterations, the sciatic nerves of these animals had normal conduction velocities, compound action potentials, no spontaneous repetitive discharges and no cooling-induced hyperexcitability, in comparison to the Kv1.1 knockout mice (Zhou et al 1998). The lack of a clear phenotype in CASPR2-/- mice may be due to the residual activity of the internodal Kv1s or due to the compensatory upregulation of other Kv1s/CASPRs.

CASPR2 mutations in humans

Human mutations in CNTNAP2, the gene encoding CASPR2, were first reported in 2006 (Strauss et al 2006). This article described nine children within an Amish family with an autosomal recessive pattern of inheritance. The cases developed cortical focal dysplasia with mental retardation (100%), intractable focal epilepsy (100%), macrocephaly and absent tendon reflexes (89%). The CNTNAP2 mutation introduced a premature stop codon with subsequent loss of the intracellular C-terminus. Histologically, the brains showed diffuse abnormalities including abnormal organisation of neurons (with rounded and binucleate cells) and reactive enlarged astrocytes. Most interestingly, there was evidence of reduced Kv1.1 expression along axons with normal expression within somae. This finding, although only examined in a few brains, would support the in vitro data that suggested CASPR2 was critical to Kv1 localisation along axons. The observations of cortical dysplasia and neurons arranged in clusters or radial columns, suggested a possible role of CASPR2 in neuronal migration. In an effort to generalise this observation to the more common, and at least partially congenital, syndromes of epilepsy and schizophrenia, one group reported CASPR2 gene dosage variations (Friedman et al 2010). In addition, an insertion within the CASPR2 gene was noted in a family with Gilles de la Tourette syndrome and obsessive compulsive disorder, although no functional studies were presented to examine the pathogenicity of this mutation (Verkerk et al 2003). More recently, four separate publications have linked CASPR2 gene polymorphisms and heritability patterns with autism spectrum disorders (Alarcon et al 2008; Arking et al 2008; Bakkaloglu et al 2008; Vernes et al 2008).

CASPR and contactin

CASPR shares 45% identity with CASPR2. It contains a protein 4.1 binding region but notably lacks a PDZ-binding domain. Axonal paranodal CASPR has been shown to directly interact with both glial neurofascin 155 and axonal contactin (Gollan et al 2003). CASPR knockout mice developed ataxia and tremor (Bhat et al 2001). Contactin is a glycosylphosphatidylinositol (GPI)-linked molecule which is a member of the immunoglobulin superfamily (as contactin-2, see below).

CASPR3, 4 and 5

Very little is known about these three proteins. One study investigated the PNS and CNS distributions of CASPR3 and 4 (Speigel et al 2002) and concluded that CASPR3 was present in axons – although not clearly juxtaparanodal - and oligodendrocytes, whereas CASPR4 was seen in the somatodendritic compartments of CNS neurons only. Both CASPR3 and 4 have PDZ-binding domains. No similar information is yet available for CASPR5 (Traut et al 2006).

CONTACTIN-2/TAG-1

Molecular characteristics

TAG-1 is the rodent homolog of the human contactin-2 molecule. Contactin-2 is a large GPI-linked cell adhesion molecule (110kDa) closely related to contactin (48% identity) and is a member of the immunoglobulin superfamily. It has six immunoglobulin-like domains and four fibronectin III domains. TAG-1 is expressed by oligodendrocytes and

myelinated Schwann cells as well as within the juxtaparanodal domains of neurons. Its role in the CNS has mainly thought to be during development where it has been ascribed functions such as axonal outgrowth, neurite extension and neuronal migration (Karagogenos 2003). Its high homology to contactin and its localisation at some juxtaparanodes, suggested it may be part of the Kv1-CASPR2 complex.

Indeed, in two simultaneously published studies Kv1.1/1.2, CASPR2 and TAG-1 were found to exist in a tripartite complex within brain tissue (Traka et al 2003; Poliak et al 2003). In addition, CASPR2 and TAG-1 could be co-immunoprecipitated from co-transfected HEK cells, which suggested a direct interaction. This interaction was maintained both in cis (on the same plasma membrane) and in trans (on adjacent cells). Only one paper claims to have been able to co-precipitate TAG-1, CASPR2 and Kv1 from co-transfected HEK cells (Tzimourakas et al 2007) but this has not been reproduced and more recently has been firmly contradicted by more definitive experiments from a collaboration between three other groups (e.g. Horresh et al 2008, Ogawa et al 2008).

Contactin-2/TAG-1 mutations in animals

As with the CASPR2 knockout animals, TAG-1 knockout animals show no gross CNS morphological changes and normal peripheral nerve conduction velocities/compound muscle action potentials (Traka et al 2003, Poliak et al 2003). Again consistently, they show normal paranodal CASPR and contactin and normal nodal sodium channel accumulation. Their Kv1.1/1.2 and CASPR2 molecules are not concentrated at the juxtaparanode and are dispersed to the internode. However, the total levels of CASPR2

and Kv1.1/1.2 are only slightly reduced in the CNS and PNS. A more detailed analysis of the phenotype of these mice showed some impairments in Morris water maze and gait coordination with reduced spontaneous activity and an increased latency to noxious stimuli (Savvaki et al 2008). These findings were interpreted as a demonstration of both CNS and PNS phenotypes. In this study, the TAG-1 heterozygote had a normal phenotype. In a separate study, TAG-1 knockout mice showed an increased sensitivity to proconvulsant agents (Fukamauchi et al 2001).

Contactin-2/TAG1 polymorphisms and antibodies in humans

Recently, it has been shown that single nucleotide polymorphisms in TAG-1 are related to IvIg responsiveness in Japanese patients with an inflammatory neuropathy (chronic inflammatory demyelinating polyneuropathy, CIDP; Iijima et al 2009).

The immunological role of TAG-1 has also been studied in humans with multiple sclerosis (MS; Derfuss et al 2009). In this study, patient sera were used to probe human myelin glycoproteins run on denaturing 2D gels. Mass spectrometry identified some spots, which MS patient antibodies bound, as contactin-2/TAG-1. The authors concluded that contactin-2 specific IgG and contactin-2 specific T cells were present in MS patients, despite only a very small response of MS T cells to the contactin-2 antigen and an ELISA with recombinant contactin-2 showing little or no specific reactivity of patient sera. This study is very unlikely to generate clinical utility and we have found no contactin-2 antibodies in 20 MS sera using a cell-based assay (Irani and Vincent, unpublished).

LGI1 (LEUCINE-RICH GLIOMA INACTIVATED 1)

Molecular characteristics

Lgi1 is a glycoprotein predicted to have a molecular weight of 64kDa (557 amino acids). It has an N-terminal signal peptide (the first 35 amino acids), three leucine-rich regions and seven epitempin (EPTP) repeats. There is 97% identity between the mouse and human homologues (both are 557 amino acids in length). Lgi1-4 have been described and all have predominant neural expression profiles, although a splice-variant of Lgi1 has been described in skeletal muscle (Furlan et al 2006). Lgi4 mutations have been associated with a peripheral demyelination syndrome in mice (Bermingham et al 2006).

Although molecular prediction models originally suggested Lgi1 contained two transmembrane domains, advances in this technology mean that Lgi1 is now considered to have no transmembrane domains and to be a predominantly secreted protein. The four major studies which experimentally addressed this question showed that Lgi1 is secreted from transfected HEK, COS, CHO and PC12 cells (Senechal et al 2005; Sirerol-Piquer et al 2006; Furlan et al 2006; Fukata et al 2006). The secreted product was able to bind to native brain tissue, NGF-differentiated PC12 cells and COS7 cells (Sirerol-Piquer et al 2006; Fukata et al 2006). Fukata et al (2006) identified ADAM22, a disintegrin, as a receptor for the secreted Lgi1. Although this is not a specific relationship, as ADAM23 and ADAM11 have also been reported to bind Lgi1 (Fukata et al 2006; Sagane et al 2008) and it is possible that other receptors will be discovered. The addition of soluble Lgi1 to brain sections modulated excitatory neurotransmission (Fukata et al 2006). Hence, Lgi1 is believed to have a role as a putative neurotransmitter with a functional

role in neurons. However, it is a rather large molecule in comparison to other conventional neurotransmitters and may better be termed a neuromodulator.

Cerebral localisation of Lgi1 has been investigated in rat/mouse brain sections which have shown Lgi1 expression in the neocortex (including the lateral temporal lobe), thalamic nuclei, hippocampus and the cerebellum (Schulte et al 2006). Within the hippocampus, Lgi1 has been shown to be expressed in the outer and middle molecular layers of the dentate gyrus, CA1/3 pyramidal cells and the mossy fibre pathway. This is particularly interesting given the demonstration of 'VGKC'-Abs binding to the outer and middle molecular layers in a very different study (Ances et al 2005). Within the cerebellum, Lgi1 expression was apparent in the molecular and granule cell layers with exclusion of the Purkinje cells. Expression in glia has been reported, although at much lower levels than within neurons (Senechal et al 2005).

Within neurons, Lgi1 has been shown to have a presynaptic localisation and function. Specifically, a neurotoxic lesion to entorhinal cortex (the main source of hippocampal neurons) abolished much of the hippocampal immunoreactivity seen with an Lgi1 antibody, although activity-dependent adaptations could be responsible (Schulte et al (2006)). This paper also showed that Lgi1 could be co-immunoprecipitated from mouse brain tissue with a Kv1.1 antibody. In addition, this approach identified a number of other molecules known to be associated with Kv1s, such as CASPR2, PSD95/93 and ADAM22. It is of interest that ADAM22 was identified in this experiment as it may imply the Lgi1-ADAM22 interaction is not readily reversible with direct relevance to our

Lgi1-Ab cell based assay. Rat brain membrane Lgi1 could be solubilised at pH 11, which suggested it was not an integral membrane protein but 'membrane-associated' (Schulte et al 2006).

Schulte et al (2006) is the only study to date to show a functional interaction between any Kv1 (Kv1.1) and Lgi1: electrophysiological data in Xenopus oocytes supported the notion that Lgi1 removed the Kvβ1-mediated inactivation of the Kv1.1. This was not seen with Kv1.2 or 1.6 or with Kvβ2. One recent study has shown that brains from mice over-expressing Lgi1 showed abnormal glutamate release, again implicating a presynaptic function (Zhou et al 2009).

Lgi1 mutations in humans

Lgi1 was initially identified as a tumour suppressor gene, in a glioma cell line (Chernova et al 1998). More recently this function has been questioned (Piepoli et al 2006). Of greater interest to neurologists, 25 different Lgi1 truncation and missense mutations have been demonstrated in around half of the cases with autosomal dominant partial epilepsy with auditory features (ADPEAF, Nobile et al 2009). The 25 mutations have been identified throughout the molecule. ADPEAF commonly presents in late adolescence and manifests with simple and complex auditory hallucinations, although visual and sensory hallucinations have been described more rarely. Around 70% penetrance is demonstrated in affected families and more recently de novo mutations have been detected in around 2% of non-familial cases with idiopathic PEAF (Nobile et al 2009). Routine MRI is often unremarkable but subtle left temporal lobe abnormalities have been demonstrated with

the use of more sophisticated imaging techniques. Approximately half of the cases show epileptic electroencephalographic abnormalities. This condition is usually highly-responsive to antiepileptic medications. One interesting exception to this case is the proband in one Italian family who had a high frequency of drug-resistant seizures and status epilepticus (Di Bonaventura et al 2009). Therefore, this family bear a strong clinical resemblance to the cases with Lgi1 antibodies and dystonic seizures (Irani et al 2008 and Chapter 3).

Many studies have examined the effect of ADPEAF mutations on the function of Lgi1. These studies have shown a lack of Lgi1 secretion from heterologous cell lines (Sirerol-Piquer et al 2006; Fukata et al 2006) and an exaggerated Kvβ1-mediated inactivation (Schulte et al 2006).

Lgi1 mutations in animals

Mice with upregulated Lgi1 showed abnormalities in dendritic branching/pruning expressing and, possibly consequential, increased seizure susceptibility to a GABA antagonist (Zhou et al 2009). Lgi1 null mice have very recently been described to have spontaneous myoclonic seizures after 12 to 18 days of age followed by death (Yu et al 2010). These findings have been reproduced by another group and the phenotype can be rescued by the Lgi1 transgene.

In summary, Lgi1 is a secreted glycoprotein with dense expression within the temporal lobe that has been shown to interact with both Kv1.1 and ADAM22. The presynaptic

detection of Lgi1 may be dependent upon interactions with these molecules. Human mutations in Lgi1 cause a lateral temporal lobe partial epilepsy syndrome. In vitro studies and animal models show these mutations impair the secretion of Lgi1 and increase neuronal excitability.

VGKC-COMPLEX ANTIBODY ASSOCIATED CLINICAL SYNDROMES

The classification of the clinical syndromes was the basis for much of the data generated by the antibody specificities. However, the three traditional syndromes (LE, MoS and NMT) have many features in common. Insomnia, pain and florid dysautonomia appear in all categories but are the hallmarks of MoS. Hence, the serological overlap between these conditions is of interest in future disease classifications. By contrast, there are some clear differences between the CNS-features seen in LE and MoS, notably seizures, hallucinations and insomnia, suggestive of differing pathophysiology, disease localisation and antigenic specificities.

CASPR2-antibodies

Currently accepted clinical definitions segregate these syndromes based on the presence of central nervous system features and neuromyotonia. These features clearly have some predictive value. Most notably, no tumours were detected in the absence of neuromyotonia. However, the CASPR2-Ab positivity may offer further information such as which patients within the NMT and MoS groups are at highest risk of malignancies. This will allow more intensive and appropriately tailored investigations for underlying tumours. Conversely, it is important to understand that the majority of CASPR2-Ab

positive cases did not have a tumour: positive predictive value was 46%. Of the other clinical features, there is less clinical utility in their prediction. However, understanding which patients may have dysautonomia (in particular arrhythmias), seizures, weight loss, sleep problems and pain syndromes may conceivably allow early initiation of potentially prophylactic treatments or allow intensive observation / investigations to assess these features in some detail. In particular, the data from cardiac investigations showed QT interval prolongation was the only consistently recognised ECG change and this would be consistent with potassium channel dysfunction (e.g. KCNQ1, Peroz et al 2008). These specific findings may further widen the phenotypes associated with these antibodies: maybe the presence of CASPR2-antibodies should be investigated in patients with isolated QT interval disorders.

The occurrence of aggressive, often recurrent, tumours is associated with CASPR2-Abs. This is an uncommon phenomenon, especially given the atrophic or clearly benign nature of the tumours of those when initially resected. Therefore, one important question is whether CASPR2-Abs are generated prior to the onset of the tumour – and are even possibly involved in the aetiology of the tumour – or whether CASPR2 is expressed at high levels within thymomas and the subsequent development of CASPR2-Abs mediates the onset of the clinical syndrome. The latter hypothesis is certainly augmented by the clinical observation of syndrome onset a few days after the thymectomy, in two cases (also described by Cottrell et al 2004). It would be of particular interest to know whether CASPR2 is expressed in thymomas of patients with myasthenia, without myasthenia and

with NMT/MoS. The cell-cell adhesion function of CASPR2 may confer tumours with an invasive property.

Lgi1-antibodies

The Lgi1-Ab positive group, other than two cases with MoS, are found in patients with a CNS-only syndrome, mainly LE. However, the two Lgi1-Ab positive MoS cases did not have a tumour (0/2 Vs 8/11: p=0.12) or myasthenia gravis (0/2 Vs 8/11; p=0.12) but did have seizures (2/2 Vs 2/11, p= 0.08; Fisher's t-test) and a better prognosis. Hence, within the MoS cohort serologically-defined subgroups of potential interest are apparent, albeit very small numbers are available. The low rate of seizures in the CASPR2-Ab positive MoS group, compared to the Lgi1-Ab positive MoS group, is potentially very interesting and may suggest even in clinically similar cases the biology of the disease may be predicted by the modulated antigen. In addition, the presence of Lgi1 antibodies in cases with MoS suggests there may be some low level Lgi1 expression in neural juxtaparanodes as suggested by Ogawa et al (2010).

No antibody group

Despite the above laboratory observations, antigenic targets are not apparent in 26% of cases. It may be that an increased sensitivity of the current assays would be sufficient to account for a number of these cases. This concept is supported by the observed partial dissociation of CASPR2 and Kv1 localisations within neural tissue, which has also been observed with Lgi1 (Dr K Kleopa, Cyprus). This dissociation implies that the ^{125}I-αDTX-labelled rabbit brain tissue may not be detecting precipitation of all available CASPR2 or

Lgi1, whereas the cell-based assay may afford this increased sensitivity. This notion is supported by the observation of clear cell-based assay positivity in cases with only low ^{125}I-αDTX-precipitation from labelled rabbit brain tissue (often <100 pM).

Novel diagnostic assays may allow detection of these cases. The expression of Lgi1 together with a putative receptor (e.g. ADAM22) may allow more Lgi1 to be retained on the cell surface and hence detected by the patient antibodies. Recently, Lgi1 has been shown to be retained at the membrane when anchored to the tail of CASPR2 (Dr P Waters, Neurosciences Group). Expression of this form of Lgi1 allows detection of Lgi1-Abs in eight cases presented as seronegative within this thesis, including one case with NMT (Irani et al, in press). More simplistically, a higher concentration of serum may be required to detect the binding of the currently seronegative cases.

However, a novel antigenic target seems possible in at least a proportion of these patients as the clinical observation that this group contains eight of the 11 cases with infectious precipitants suggests an epitope with molecular resemblance to an infectious agent, as has been most elegantly demonstrated in Guillian-Barré syndrome (Willison and Yuki 2002). This is in marked contrast to the CASPR2-Ab positive group with only one infectious prodrome but 14 tumours, suggesting ectopic tumour expression of CASPR2 is likely to be the event initiating CASPR2-Ab generation.

Nevertheless, a number of candidate and potential antigenic targets surely remain. The potential targets may be proteins awaiting discovery: this is suggested by two major lines

of evidence. Firstly, our experimental data, and that of others, suggest that although CASPR2/Lgi1/contactin-2 co-precipitate with Kv1s from brain tissue they do not co-precipitate when co-expressed in HEK cells. These data are taken to implicate a further protein(s) in the CASPR2/Lgi1/Contactin-2 interaction with Kv1s. However, our cell-surface expression data did suggest a direct functional effect of Lgi1 and PSD95 on Kv1 expression in HEK cells, which may mediate a functional interaction without co-precipitation. Secondly, mice that express CASPR2 without its PDZ-binding domain showed no abnormal localisation of CASPR2 or Kv1s away from the juxtaparanodes, again implicating as yet undiscovered molecules mediating Kv1 – CASPR2 interactions. Candidate antigens have been highlighted by our immunoprecipitation data using specific commercial antibodies and by the more broad-brush, less-biased mass spectrometry approaches of others. Lgi1 is the only Kv1-co-precipitating molecule with a large putative extracellular domain that has been elucidated using a mass spectrometry approach (Schulte et al 2006). However, the paucity of likely candidate antigenic targets developed via this approach is mainly dependent on experimental designs which aimed to examine the intracellular interactions of these proteins, for example using the intracellular domain of CASPR2 as bait (Horresh et al 2008). Hence, this technique surely holds promise for the future. Experiments presented within this thesis which use commercial antibodies have generated a few targets which have not yet been investigated. One possibility is that intracellular molecules are antigenic targets. Our data would specifically implicate MAGUKs (including known and unknown PSD molecules) and protein 4.1B. As the pan-MAGUK antibody precipitated markedly more than the sum of the antibodies to known MAGUK proteins, our data suggest other MAGUKs exist in the

αDTX-complexes. However, this hypothesis is strongly countered by the extracellular epitopes of the main three novel antigenic targets and by the excellent immunotherapy response correlating with substantial reductions in antibody titres in the currently seronegative patients. Many examples of such recoveries are shown in Chapter 3 when describing the patients with dystonic seizures. Another hypothesis is that the molecules CASPR3, CASPR4 and ADAM22 are antigenic targets for some of the remaining sera. This is supported by the marked homology between the CASPRs 2, 3 and 4 and as ADAM-22 is the established receptor for Lgi1. However, these proteins were found at very low levels within the ^{125}I-αDTX-labelled rabbit brain tissue which argues against this possibility. Direct expression methods could formally answer this question in the future. A very recent report, published during completion of this discussion, has indeed suggested ADAM22 is closely linked with Kv1.1 in peripheral nerve and brain tissue, and they may interact via PSD proteins in HEK cells (Ogawa et al 2010). Two other potential targets which have been associated, albeit rather rarely, with Kv1s are members of the connexin family, in particular connexin-29 (Altevogt et al 2002) and stargazin (Fukata et al 2006).

PATHOPHYSIOLOGY OF CASPR2, LGI1 AND CONTACTIN-2 ANTIBODY ASSOCIATED DISEASES

The serological data have provided some clear clinical correlates which provide some much required rationale for the possible pathophysiological mechanisms of these diseases.

A 'systems' perspective

At a basic level, it is of great satisfaction that the antigenic targets express uniquely in the areas of disease burden. This is not a necessary prerequisite for pathogenicity, as shown by the expression of aquaporin-4 in stomach and renal tissue (Lennon et al 2005), but yet holds much weight in such an argument. The wide tissue expression profile of Kv1s and the presence of Kv1.1, 1.2 and 1.6 in both the central and peripheral nervous systems provided little room for antigenic preference to be paramount in determining the disease phenotype. By contrast, only the peripheral nerve and central nervous system are known to express CASPR2 and therefore it is more logical that serum antibodies to CASPR2 determine 85% of MoS and 61% of NMT. Similarly, Lgi1 only has its major expression in the CNS and 96% of Lgi1-Ab positive cases have a CNS-restricted phenotype. These pleasingly simple explanations do not account for the 9% of LE cases with CASPR2-Abs and the 4% of Lgi1-Ab positive cases with MoS. It is plausible that a CNS-specific isoform of CASPR2 accounts for this minority of cases and that the low level Lgi1 expression in the PNS is sufficient for antibodies to mediate an effect. In summary, the antigen distribution accounts for the majority of the disease phenotype (summarised in Figure 7.1).

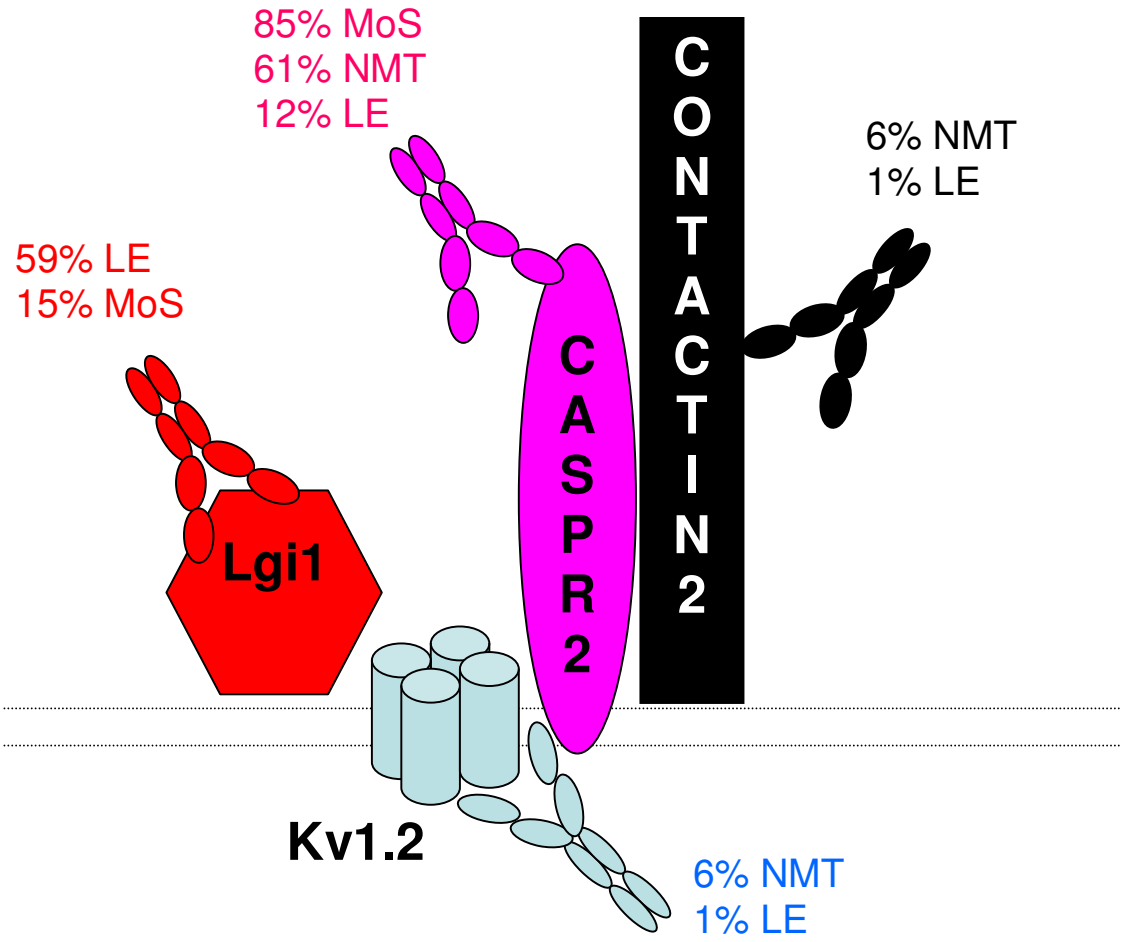


Figure 7.1. Summary of clinico-serological correlations

These observations largely account for the 'hierarchy' of 'VGKC'-Ab titres seen in moving from LE down to MoS to NMT (Chapter 3, Vincent et al 2004) and do not require a blood-brain barrier (BBB) to be formally evoked as a very important factor in the development of one syndrome over another. Although the role of the BBB in antibody or B-cell trafficking is still clearly crucial in the development of these CNS-syndromes. It may be of particular importance in the patients with infectious prodromes, as lipopolysaccharide is known to disrupt the BBB (e.g. Kowal et al 2004). Consistent with this is the observation that the neuromyotonic population have the lowest age of

onset and their blood-brain barrier may still be impermeable, for example to CASPR2-Abs.

These broadly satisfactory explanations regarding pathophysiology do not account for the absent CSF changes in 71% of patients with CNS syndromes and the rather modest changes observed in the majority of the remaining 29%. It may be that only small numbers of plasma/B-cells are required to reach the thecal compartment before antibody levels achieve pathological concentrations. Although CASPR2, Lgi1 and contactin-2 IgG1 subclasses exist, complement activation and consequent inflammation may not play a major role in the in vivo pathology of this disease. However, the inflammation shown by T2-high hippocampal signal and the serum hyponatraemia (where examined due to a SIADH pattern) would suggest a diffuse inflammatory brain insult is operating. Then again, the SIADH may be a specific action of the antibody - almost always targeting Lgi1 – operating on the hypothalamic-pituitary axis. The degree of inflammation operating in this condition and the consequent CSF changes are somewhat discrepant and would be best investigated in detail in some prospectively studied patients.

The medial temporal lobe MRI signal change is considered a characteristic feature of this condition. However, only 53% of patients with a CNS syndrome showed more than age-related MRI changes. This is a likely reason for the probable ongoing under-recognition of the syndrome. Another example of this under-recognition is seen in the cases with dystonic seizures that were not appreciated to have a VGKC-Ab associated syndrome.

One final reason may be the striking 2.5:1 ratio of males to females in an autoimmune condition and the rare finding of concomitant autoimmune diseases.

Does knowledge of the precise antigenic targets help explain some of the most characteristic features associated with these conditions? The main features which fall into this category are the neuropathic pain, sleep disturbances and the dysautonomia. The pain syndrome, mainly seen in the CASPR2-Ab positive cohort, was predominantly neuropathic in description with a lower limb, and more occasionally lower back, predilection. The back pain may be suggestive of a radiculitis, akin to the back pain seen commonly in Guillian-Barré syndrome, whereas the lower limb pain is most similar to that associated with small-fibre peripheral neuropathies. The blood-nerve barrier deficient, unmyelinated Kv1-rich nerve terminals are a highly plausible site of CASPR2 expression and hence antibody action but would not account for the probable radiculitis. The serological and syndromic dichotomy in the nature of the sleep disturbances was striking: 50% of CASPR2-Ab positive cases had insomnia whereas none had hypersomnia. By contrast, of the Lgi1-Ab positive cases, hypersomnolence was seen in 8% and insomnia 10%. Our initial hypothesis was that the MoS patients had relatively intact BBBs and developed insomnia via antibody access to the circumventricular-diencephalic region. Although still plausible, it seems more likely that this is an antigen-specific effect which may be determined by relative regional expression levels. For example, maybe CASPR2 is highly expressed in the hypothalamic region. Interestingly, as with NMDAR-Abs (Irani et al 2010 in Appendix 1), there was a dichotomy between putative mechanisms producing insomnia and hypersomnia. The relevance of the

hypothalamus as a CNS orchestrator of autonomic function may justify a similar anatomical explanation.

A molecular perspective

At the molecular level, there are three main possible modes of action of pathogenic antibodies. The likeliest, and proven for AQP4, NMDAR and AMPAR antibodies, is cross-linking and subsequent downregulation of the surface protein. This is clearly only possible if antibodies target the extracellular aspect of the protein, a necessity if they are to fulfil Witebsky's postulates. If this occurred in neuronal tissue in vitro, it could mediate an effect via two theoretical mechanisms. Firstly, downregulation of, for example, CASPR2 could internalise this molecule and, assuming insufficient compensation, mean that contactin-2-CASPR2 interactions are weakened, possibly resulting in disruption of the neural architecture and subsequent functional impairment. If CASPR2 has as yet unknown function(s), internalisation of CASPR2 may mediate other direct functional effect(s). Alternatively, particularly in neural regions where Kv1s and CASPR2 are co-expressed, downregulation of CASPR2 may 'co-internalise' Kv1s, which would produce repolarisation abnormalities resulting in neuronal hyperexcitability. In the juxtaparanodal region, however, it is still not proven whether these antibodies may gain access below the myelin sheath. This may not always be necessary as CASPR2 (and Kv1s) are known to take-up other subcellular localisations, despite the juxtaparanode being the best studied region. In summary, it is possible that CASPR2/Lgi1/contactin-2 antibodies mediate an antigen-specific effect or utilise Kv1s as their final common pathway to create a functional disruption of neuronal excitability. The fundamental

observation that αDTX-labelled brain tissue allowed antibody detection is likely to be no coincidence and supports the possibility that Kv1s still play an important functional role in these syndromes (as in Shilitto et al 1995).

Secondly, it is possible that the IgG1 subclass of all these antibodies is able to bind its target in vitro and fix complement to initiate the complement cascade: as demonstrated in vitro with CASPR2 antibodies. However, although complement is produced by astrocytes and neurons, the controversial evidence for CNS inflammation in VGKC-Ab associated diseases (see above) may reduce the likelihood of this mechanism being of importance in vivo. In particular, the bias of Lgi1-antibodies towards the IgG4 subclass may suggest a less inflammatory pathology in LE. By contrast, the animal model paradigm from neuromyelitis optica has shown that human complement is required in addition to aquaporin-4 IgG for the development of characteristic cerebral lesions (Saadoun et al 2010). However, in NMO there is a common CSF lymphocytosis and strong evidence for complement deposition in post-mortem tissue (Lucchinetti et al 2002).

Finally it is conceivable, although has only very rarely been proven, that antibodies may act as direct agonists or antagonists towards their intended target. This is particularly relevant to ion channel targets, which have not been discovered in this thesis.

Novel phenotypes generated by novel pathological mechanisms

The characteristic brief, dystonic seizures as described in Chapter 3, are not seen in other conditions and seem to be relatively common and under-recognised manifestations of

'VGKC'-Ab positive patients. Their clear, albeit not universal, association with Lgi1-antibodies may suggest that the pathway(s) modulated/lesioned by Lgi1-antibodies or the mechanism of this lesion is not mimicked by other conditions. This unique clinical phenotype is analogous to the movement disorder seen in patients with NMDAR-Abs, which is considered to be essentially pathognomic for this disorder. It is likely that as novel antigenic targets are discovered, careful and thoughtful clinical studies will help elucidate further specific, possibly pathognomic, phenotypes.

The hypothesis that these undoubtedly dystonic events are seizures is supported by the frequent loss of consciousness, presence of other seizure semiologies, and the noted, albeit infrequent, ictal EEG changes. Further support for an epileptic aetiology, and specifically the notion of a frontal focus, come from the very frequent, brief episodes with rapid recovery and a prominent startle trigger (Manford et al 1996). In addition, truncal turning has been observed in a number of patients with medial frontal lobe epilepsy (Leung et al 2008). Subcortical (particularly striatal), extratemporal neocortical hypometabolism have been associated with dystonic posturing (Dupont et al 1998; Rusu et al 2005). A deep frontal seizure focus would be consistent with the low frequency of EEG changes and the observed clinical semiology/syndrome.

FUTURE DIRECTIONS

This research generates a number of important and interesting future research questions that require further clinical examination of these patients, investigations into the basic

biology of the antigenic molecules and their relationship to the in vivo pathology. The main pertinent questions which merit further attention are described below.

Basic biology

One important question is whether low-level Lgi1 expressed in peripheral nerve is sufficient to account for pathogenicity in the two MoS cases or whether these cases have other, as yet undiscovered, serological specificities. For Lgi4, the data suggest clear peripheral nerve expression and mutations generated the 'claw-paw' phenotype due to peripheral nerve demyelination (Bermingham et al 2006). Dr K Kleopa (Cyprus) has shown faint but above background binding of the Lgi1 commercial antibody to the juxtaparanode in teased sciatic fibres (Irani et al 2010, in press). This also generates the question of whether the juxtaparanodes always contain Lgi1 *and* CASPR2. More commonly, where Lgi1 is likely to be a presynaptic protein the consistency and frequency of its relationship with Kv1s should be further investigated. It is possible that many Lgi1 molecules exist independent of Kv1s in our brain complexes. The same may be true of CASPR2. The extent of the co-localisation could be investigated using specific immunoprecipitations and subsequent immunoblots and with live tissue co-immunostaining.

One other major question will be whether CASPR2 is expressed in thymic tissue of normal, myasthenic, non-myasthenic and MoS/NMT thymomas. CASPR2 expression, and the subsequent CASPR2-Ab generation, could cause thymomas to develop malignant/metastatic potential and the presence of CASPR2 in thymomas may denote a

poor prognosis. This is particularly true regarding the thymomas which were initially removed, appeared benign and subsequently recurred: maybe these recurrences could be predicted.

Clinico-scientific questions

Important future questions include whether the characteristic dystonic seizures can be treated when recognised in prospective cases, whether observation and subsequent early treatment retards or prevents the onset of amnesia and what the frequency of these events is in VGKC-Ab positive cases? The question of whether the pure-seizure phase is a 'window of opportunity' to prevent a 'full-blown' LE can be addressed in prospective cases. The other major clinical observation concerns the mechanism(s) for the apparent switch between epilepsy and limbic encephalitis, which may coincide with the development of hyponatraemia. These questions will be best answered with careful and thoughtful clinical observations in a few cases studied in great detail.

Using the data from the main cohort of 113 cases, and the cases with dystonic seizures, more evidence-based recommendations for optimal treatments can be made. On the contrary, the intriguing possibility that early steroids may be associated with neuronal atrophy – substantiated by preclinical observations (e.g. Wellman 2001) - still remains an important aspect of this research. Our data come from two retrospective studies: a prospective treatment trial would allow a more rigorous data set to be gathered.

For many of the analysed data, individual Fisher's t-tests and a correction for multiple comparisons have been used. To perform a more detailed statistical analysis of the data, in the future, multiple regression analysis could be used to account for each variable – e.g. clinical syndrome, serology – or a cluster analysis could be attempted to identify features which co-associate. Nevertheless, a more crude appreciation of the raw data has proven very useful.

To have an impact on future clinical therapeutics, it will be important to formally demonstrate in vivo pathogenicity of the antibodies. To date, in a series of small experiments, this has proven unsuccessful both with passive transfer of IgG from a patient subsequently found to have CASPR2-Abs (Liguori et al 2001) and with active immunisations using Kv1.1, 1.2 and 1.6. It may be that active immunisations using Lgi1/CASPR2 generate clearer clinical phenotypes, possibly via a Kv1-independent mechanism.

These in vivo approaches, combined with in vitro work – maybe using myelinated neuronal cultures – may elucidate whether these antibodies may access their neuronal targets at the juxtaparanodes, below the myelin sheath. This important question could also be investigated with the above in vivo immunisation models.

REFERENCES

Agius, M.A., Zhu, S., Lee, E.K., Aarli, J.A., Kirvan, C., Fairclough, R.H., and Maselli, R. (1998). Antibodies to AChR, synapse-organizing proteins, titin, and other muscle proteins in Morvan's fibrillary chorea. Annals of the New York Academy of Sciences *841*, 522-524.

Alarcon, M., Abrahams, B.S., Stone, J.L., Duvall, J.A., Perederiy, J.V., Bomar, J.M., Sebat, J., Wigler, M., Martin, C.L., Ledbetter, D.H.*, et al.* (2008). Linkage, association, and gene-expression analyses identify CNTNAP2 as an autism-susceptibility gene. American journal of human genetics *82*, 150-159.

Altevogt, B.M., Kleopa, K.A., Postma, F.R., Scherer, S.S., and Paul, D.L. (2002). Connexin29 is uniquely distributed within myelinating glial cells of the central and peripheral nervous systems. J Neurosci *22*, 6458-6470.

Ances, B.M., Vitaliani, R., Taylor, R.A., Liebeskind, D.S., Voloschin, A., Houghton, D.J., Galetta, S.L., Dichter, M., Alavi, A., Rosenfeld, M.R., and Dalmau, J. (2005). Treatment-responsive limbic encephalitis identified by neuropil antibodies: MRI and PET correlates. Brain *128*, 1764-1777.

Antel J, Birnbaum H, Hartung P and Vincent A (2005). Clinical Neuroimmunology, 2nd edition. ISBN13: 9780198510680.

Antozzi, C., Binelli, S., Frassoni, C., Ciano, C., Vincent, A., Andreetta, F., Panzica, F., Franceschetti, S., Confalonieri, P., and Mantegazza, R. (2007). Immunotherapy responsive startle with antibodies to voltage gated potassium channels. Journal of neurology, neurosurgery, and psychiatry *78*, 1281-1290.

Arimura, K., Watanabe, O., Kitajima, I., Suehara, M., Minato, S., Sonoda, Y., Higuchi, I., Takenaga, S., Maruyama, I., and Osame, M. (1997). Antibodies to potassium channels of PC12 in serum of Isaacs' syndrome: Western blot and immunohistochemical studies. Muscle & nerve *20*, 299-305.

Arking, D.E., Cutler, D.J., Brune, C.W., Teslovich, T.M., West, K., Ikeda, M., Rea, A., Guy, M., Lin, S., Cook, E.H., and Chakravarti, A. (2008). A common genetic variant in the neurexin superfamily member CNTNAP2 increases familial risk of autism. American journal of human genetics *82*, 160-164.

Azimi, S., Ludwig, A., Thevenot, D.R., and Colin, J.L. (2003). Trace metal determination in total atmospheric deposition in rural and urban areas. The Science of the total environment *308*, 247-256.

Badruddin, A., Menon, R.S., and Reder, A.T. (2009). 4-Aminopyridine toxicity mimics autoimmune-mediated limbic encephalitis. Neurology *72*, 1100-1101.

Bajaj, B.K., and Shrestha, S. (2007). An interesting case report of Morvan's syndrome from the Indian subcontinent. Neurology India *55*, 67-69.

Bakkaloglu, B., O'Roak, B.J., Louvi, A., Gupta, A.R., Abelson, J.F., Morgan, T.M., Chawarska, K., Klin, A., Ercan-Sencicek, A.G., Stillman, A.A.*, et al.* (2008). Molecular cytogenetic analysis and resequencing of contactin associated protein-like 2 in autism spectrum disorders. American journal of human genetics *82*, 165-173.

Barajas, R.F., Collins, D.E., Cha, S., and Geschwind, M.D (2009). Adult-onset drug-refractory seizure disorder associated with anti-voltage-gated potassium-channel antibody. Epilepsia *51*, 473-477.

Barber, P.A., Anderson, N.E., and Vincent, A. (2000). Morvan's syndrome associated with voltage-gated K+ channel antibodies. Neurology *54*, 771-772.

Bataller, L., Kleopa, K.A., Wu, G.F., Rossi, J.E., Rosenfeld, M.R., and Dalmau, J. (2007). Autoimmune limbic encephalitis in 39 patients: immunophenotypes and outcomes. Journal of neurology, neurosurgery, and psychiatry *78*, 381-385.

Bennett, J.L., Lam, C., Kalluri, S.R., Saikali, P., Bautista, K., Dupree, C., Glogowska, M., Case, D., Antel, J.P., Owens, G.P.*, et al.* (2009). Intrathecal pathogenic anti-aquaporin-4 antibodies in early neuromyelitis optica. Annals of neurology *66*, 617-629.

Bermingham, J.R., Jr., Shearin, H., Pennington, J., O'Moore, J., Jaegle, M., Driegen, S., van Zon, A., Darbas, A., Ozkaynak, E., Ryu, E.J.*, et al.* (2006). The claw paw mutation reveals a role for Lgi4 in peripheral nerve development. Nature neuroscience *9*, 76-84.

Bhat, M.A., Rios, J.C., Lu, Y., Garcia-Fresco, G.P., Ching, W., St Martin, M., Li, J., Einheber, S., Chesler, M., Rosenbluth, J.*, et al.* (2001). Axon-glia interactions and the domain organization of myelinated axons requires neurexin IV/Caspr/Paranodin. Neuron *30*, 369-383.

Bien, C.G., and Elger, C.E. (2007). Limbic encephalitis: a cause of temporal lobe epilepsy with onset in adult life. Epilepsy Behav *10*, 529-538.

Bien, C.G., Schulze-Bonhage, A., Deckert, M., Urbach, H., Helmstaedter, C., Grunwald, T., Schaller, C., and Elger, C.E. (2000). Limbic encephalitis not associated with neoplasm as a cause of temporal lobe epilepsy. Neurology *55*, 1823-1828.

Brain, L., P. B. Croft, et al. (1965). Motor neurone disease as a manifestation of neoplasm (with a note on the course of classical motor neurone disease). Brain 88(3): 479-500.

Brierley JB, Corsellis JAN, Hierons R and Nevin S (1960). Subacute encephalitis of later adult life mainly affecting the limbic areas. Brain: 83 (3);357-368

Browne, D.L., Gancher, S.T., Nutt, J.G., Brunt, E.R., Smith, E.A., Kramer, P., and Litt, M. (1994). Episodic ataxia/myokymia syndrome is associated with point mutations in the human potassium channel gene, KCNA1. Nature genetics *8*, 136-140.

Buckley, C., Oger, J., Clover, L., Tuzun, E., Carpenter, K., Jackson, M., and Vincent, A. (2001). Potassium channel antibodies in two patients with reversible limbic encephalitis. Ann Neurol *50*, 73-78.

Castillo, P., Woodruff, B., Caselli, R., Vernino, S., Lucchinetti, C., Swanson, J., Noseworthy, J., Aksamit, A., Carter, J., Sirven, J.*, et al.* (2006). Steroid-responsive encephalopathy associated with autoimmune thyroiditis. Archives of neurology *63*, 197-202.

Cheong, A., Dedman, A.M., and Beech, D.J. (2001). Expression and function of native potassium channel [K(V)alpha1] subunits in terminal arterioles of rabbit. The Journal of physiology *534*, 691-700.

Chernova, O.B., Somerville, R.P., and Cowell, J.K. (1998). A novel gene, LGI1, from 10q24 is rearranged and downregulated in malignant brain tumors. Oncogene *17*, 2873-2881.

Chung, Y.H., Joo, K.M., Nam, R.H., Kim, Y.S., Lee, W.B., and Cha, C.I. (2005). Immunohistochemical study on the distribution of the voltage-gated potassium channels in the gerbil cerebellum. Neuroscience letters *374*, 58-62.

Chung, Y.H., Shin, C., Kim, M.J., Lee, B.K., and Cha, C.I. (2001). Immunohistochemical study on the distribution of six members of the Kv1 channel subunits in the rat cerebellum. Brain research *895*, 173-177.

Coleman, S.K., Newcombe, J., Pryke, J., and Dolly, J.O. (1999). Subunit composition of Kv1 channels in human CNS. J Neurochem *73*, 849-858.

Coman, I., Aigrot, M.S., Seilhean, D., Reynolds, R., Girault, J.A., Zalc, B., and Lubetzki, C. (2006). Nodal, paranodal and juxtaparanodal axonal proteins during demyelination and remyelination in multiple sclerosis. Brain *129*, 3186-3195.

Corsellis, J.A., Goldberg, G.J., and Norton, A.R. (1968). Limbic encephalitis and its association with carcinoma. Brain *91*, 481-496.

Cottrell, D.A., Blackmore, K.J., Fawcett, P.R., Birchall, D., Vincent, A., Barnard, S., and Walls, T.J. (2004). Sub-acute presentation of Morvan's syndrome after thymectomy. Journal of neurology, neurosurgery, and psychiatry *75*, 1504-1505.

Dale, R.C., Irani, S.R., Brilot, F., Pillai, S., Webster, R., Gill, D., Lang, B., and Vincent, A. (2009). N-methyl-D-aspartate receptor antibodies in pediatric dyskinetic encephalitis lethargica. Annals of neurology *66*, 704-709.

Dalmau, J., Gleichman, A.J., Hughes, E.G., Rossi, J.E., Peng, X., Lai, M., Dessain, S.K., Rosenfeld, M.R., Balice-Gordon, R., and Lynch, D.R. (2008). Anti-NMDA-receptor encephalitis: case series and analysis of the effects of antibodies. Lancet neurology *7*, 1091-1098.

Dalmau, J., and Rosenfeld, M.R. (2008). Paraneoplastic syndromes of the CNS. Lancet neurology *7*, 327-340.

Dalmau, J., Tuzun, E., Wu, H.Y., Masjuan, J., Rossi, J.E., Voloschin, A., Baehring, J.M., Shimazaki, H., Koide, R., King, D.*, et al.* (2007). Paraneoplastic anti-N-methyl-D-aspartate receptor encephalitis associated with ovarian teratoma. Annals of neurology *61*, 25-36.

Darnell, R.B., and Posner, J.B. (2003). Paraneoplastic syndromes involving the nervous system. The New England journal of medicine *349*, 1543-1554.

Davies, G., Irani, S.R., Coltart, C., Ingle, G., Amin, Y., Taylor, C., Radcliffe, J., Hirsch, N.P., Howard, R.S., Vincent, A., and Kullmann, D.M (2009). Anti-N-methyl-D-aspartate receptor antibodies: a potentially treatable cause of encephalitis in the intensive care unit. Critical care medicine *38*, 679-682.

DeGiorgio, L.A., Konstantinov, K.N., Lee, S.C., Hardin, J.A., Volpe, B.T., and Diamond, B. (2001). A subset of lupus anti-DNA antibodies cross-reacts with the NR2 glutamate receptor in systemic lupus erythematosus. Nature medicine *7*, 1189-1193.

del Zoppo, G.J., and Milner, R. (2006). Integrin-matrix interactions in the cerebral microvasculature. Arteriosclerosis, thrombosis, and vascular biology *26*, 1966-1975.

Denisenko-Nehrbass, N., Oguievetskaia, K., Goutebroze, L., Galvez, T., Yamakawa, H., Ohara, O., Carnaud, M., and Girault, J.A. (2003). Protein 4.1B associates with both Caspr/paranodin and Caspr2 at paranodes and juxtaparanodes of myelinated fibres. The European journal of neuroscience *17*, 411-416.

Derfuss, T., Parikh, K., Velhin, S., Braun, M., Mathey, E., Krumbholz, M., Kumpfel, T., Moldenhauer, A., Rader, C., Sonderegger, P.*, et al.* (2009). Contactin-2/TAG-1-directed autoimmunity is identified in multiple sclerosis patients and mediates gray matter pathology in animals. Proceedings of the National Academy of Sciences of the United States of America *106*, 8302-8307.

Deymeer, F., Akca, S., Kocaman, G., Parman, Y., Serdaroglu, P., Oktem-Tanor, O., Coban, O., and Vincent, A. (2005). fasciculations, autonomic symptoms and limbic encephalitis: a thymoma-associated Morvan's-like syndrome. Eur Neurol *54*, 235-237.

Di Bonaventura, C., Carni, M., Diani, E., Fattouch, J., Vaudano, E.A., Egeo, G., Pantano, P., Maraviglia, B., Bozzao, L., Manfredi, M.*, et al.* (2009). Drug resistant ADLTE and recurrent partial status epilepticus with dysphasic features in a family with a novel LGI1mutation: electroclinical, genetic, and EEG/fMRI findings. Epilepsia *50*, 2481-2486.

Diaz-Manera, J., Rojas-Garcia, R., Gallardo, E., Juarez, C., Martinez-Domeno, A., Martinez-Ramirez, S., Dalmau, J., Blesa, R., and Illa, I. (2007). Antibodies to AChR, MuSK and VGKC in a patient with myasthenia gravis and Morvan's syndrome. Nature clinical practice *3*, 405-410.

Dolly, J.O., and Parcej, D.N. (1996). Molecular properties of voltage-gated K+ channels. Journal of bioenergetics and biomembranes *28*, 231-253.

Donadio, V., Montagna, P., Pennisi, M., Rinaldi, R., Di Stasi, V., Avoni, P., Bugiardini, E., Giannoccaro, M.P., Cortelli, P., Plazzi, G.*, et al.* (2009). Agrypnia Excitata: a microneurographic study of muscle sympathetic nerve activity. Clin Neurophysiol *120*, 1139-1142.

Dorandeu, F., Wetherell, J., Pernot-Marino, I., Tattersall, J.E., Fosbraey, P., and Lallement, G. (1997). Effects of excitatory amino acid antagonists on dendrotoxin-induced increases in neurotransmitter release and epileptiform bursting in rat hippocampus in vitro. Journal of neuroscience research *48*, 499-506.

Dunstan, E.J., and Winer, J.B. (2006). Autoimmune limbic encephalitis causing fits, rapidly progressive confusion and hyponatraemia. Age and ageing *35*, 536-537.

Dupont, S., Semah, F., Baulac, M., and Samson, Y. (1998). The underlying pathophysiology of ictal dystonia in temporal lobe epilepsy: an FDG-PET study. Neurology *51*, 1289-1292.

Fletcher, H.M. (1910). Symmetrical Trophic Lesions of the Extremities in a Child. Syringomyelia (Morvan's Type). Proceedings of the Royal Society of Medicine *3*, 98-104.

Florance, N.R., Davis, R.L., Lam, C., Szperka, C., Zhou, L., Ahmad, S., Campen, C.J., Moss, H., Peter, N., Gleichman, A.J.*, et al.* (2009). Anti-N-methyl-D-aspartate receptor (NMDAR) encephalitis in children and adolescents. Annals of neurology *66*, 11-18.

Friedman, J.I., Vrijenhoek, T., Markx, S., Janssen, I.M., van der Vliet, W.A., Faas, B.H., Knoers, N.V., Cahn, W., Kahn, R.S., Edelmann, L.*, et al.* (2008). CNTNAP2 gene dosage variation is associated with schizophrenia and epilepsy. Molecular psychiatry *13*, 261-266.

Fukamauchi, F., Aihara, O., Wang, Y.J., Akasaka, K., Takeda, Y., Horie, M., Kawano, H., Sudo, K., Asano, M., Watanabe, K., and Iwakura, Y. (2001). TAG-1-deficient mice have marked elevation of adenosine A1 receptors in the hippocampus. Biochemical and biophysical research communications *281*, 220-226.

Fukata, Y., Adesnik, H., Iwanaga, T., Bredt, D.S., Nicoll, R.A., and Fukata, M. (2006). Epilepsy-related ligand/receptor complex LGI1 and ADAM22 regulate synaptic transmission. Science (New York, N.Y *313*, 1792-1795.

Fukata, Y., Lovero, K.L., Iwanaga, T., Watanabe, A., Yokoi, N., Tabuchi, K., Shigemoto, R., Nicoll, R.A., and Fukata, M (2010). Disruption of LGI1-linked synaptic complex causes abnormal synaptic transmission and epilepsy. Proceedings of the National Academy of Sciences of the United States of America *107*, 3799-3804.

Fukushima, K., Yasaki, M., Kaneko, K., Fushimi, T., Yamamoto, K., Hashimoto, T., Oguchi, K., and Ikeda, S. (2005). Nonparaneoplastic, nonherpetic limbic encephalitis with severe episodic hypothermia: a case report. European neurology *54*, 170-174.

Furlan, S., Roncaroli, F., Forner, F., Vitiello, L., Calabria, E., Piquer-Sirerol, S., Valle, G., Perez-Tur, J., Michelucci, R., and Nobile, C. (2006). The LGI1/epitempin gene encodes two protein isoforms differentially expressed in human brain. Journal of neurochemistry *98*, 985-991.

Geschwind, M.D., Tan, K.M., Lennon, V.A., Barajas, R.F., Jr., Haman, A., Klein, C.J., Josephson, S.A., and Pittock, S.J. (2008). Voltage-gated potassium channel autoimmunity mimicking creutzfeldt-jakob disease. Archives of neurology *65*, 1341-1346.

Goldberg, R.J. (2008). Sound-alike syndromes: first report of Morvan's, and not Marfan's, syndrome. Journal of the American Geriatrics Society *56*, 774-776.

Gollan, L., Salomon, D., Salzer, J.L., and Peles, E. (2003). Caspr regulates the processing of contactin and inhibits its binding to neurofascin. The Journal of cell biology *163*, 1213-1218.

Graus, F., Delattre, J.Y., Antoine, J.C., Dalmau, J., Giometto, B., Grisold, W., Honnorat, J., Smitt, P.S., Vedeler, C., Verschuuren, J.J.*, et al.* (2004). Recommended diagnostic criteria for paraneoplastic neurological syndromes. Journal of neurology, neurosurgery, and psychiatry *75*, 1135-1140.

Graus, F., Keime-Guibert, F., Rene, R., Benyahia, B., Ribalta, T., Ascaso, C., Escaramis, G., and Delattre, J.Y. (2001). Anti-Hu-associated paraneoplastic encephalomyelitis: analysis of 200 patients. Brain *124*, 1138-1148.

Graus, F., Saiz, A., and Dalmau, J (2009). Antibodies and neuronal autoimmune disorders of the CNS. Journal of neurology *257*, 509-517.

Graus, F., Saiz, A., Lai, M., Bruna, J., Lopez, F., Sabater, L., Blanco, Y., Rey, M.J., Ribalta, T., and Dalmau, J. (2008). Neuronal surface antigen antibodies in limbic encephalitis: clinical-immunologic associations. Neurology *71*, 930-936.

Grosse, G., Draguhn, A., Hohne, L., Tapp, R., Veh, R.W., and Ahnert-Hilger, G. (2000). Expression of Kv1 potassium channels in mouse hippocampal primary cultures: development and activity-dependent regulation. J Neurosci *20*, 1869-1882.

Gultekin, S.H., Rosenfeld, M.R., Voltz, R., Eichen, J., Posner, J.B., and Dalmau, J. (2000). Paraneoplastic limbic encephalitis: neurological symptoms, immunological findings and tumour association in 50 patients. Brain *123 (Pt 7)*, 1481-1494.

Halbach, M., Homberg, V., and Freund, H.J. (1987). Neuromuscular, autonomic and central cholinergic hyperactivity associated with thymoma and acetylcholine receptor-binding antibody. Journal of neurology *234*, 433-436.

Hart, I.K., Maddison, P., Newsom-Davis, J., Vincent, A., and Mills, K.R. (2002). Phenotypic variants of autoimmune peripheral nerve hyperexcitability. Brain *125*, 1887-1895.

Hart, I.K., Waters, C., Vincent, A., Newland, C., Beeson, D., Pongs, O., Morris, C., and Newsom-Davis, J. (1997). Autoantibodies detected to expressed K+ channels are implicated in neuromyotonia. Annals of neurology *41*, 238-246.

Haug, B.A., Schoenle, P.W., Karch, B.J., Bardosi, A., and Holzgraefe, M. (1989). Morvan's fibrillary chorea. A case with possible manganese poisoning. Clinical neurology and neurosurgery *91*, 53-59.

Heidenreich, F., and Vincent, A. (1998). Antibodies to ion-channel proteins in thymoma with myasthenia, neuromyotonia, and peripheral neuropathy. Neurology *50*, 1483-1485.

Holley, E.B. (1947). Syringomyelia, Morvan's syndrome. The Journal of pediatrics *30*, 96-101.

Horio, Y. (2001). Potassium channels of glial cells: distribution and function. Japanese journal of pharmacology *87*, 1-6.

Horresh, I., Bar, V., Kissil, J.L., and Peles, E (2010). Organization of myelinated axons by Caspr and Caspr2 requires the cytoskeletal adapter protein 4.1B. J Neurosci *30*, 2480-2489.

Horresh, I., Poliak, S., Grant, S., Bredt, D., Rasband, M.N., and Peles, E. (2008). Multiple molecular interactions determine the clustering of Caspr2 and Kv1 channels in myelinated axons. J Neurosci *28*, 14213-14222.

Hudson, L.A., Rollins, Y.D., Anderson, C.A., Johnston-Brooks, C., Tyler, K.L., and Filley, C.M. (2008). Reduplicative paramnesia in Morvan's syndrome. Journal of the neurological sciences *267*, 154-157.

Hutchinson, M., Waters, P., McHugh, J., Gorman, G., O'Riordan, S., Connolly, S., Hager, H., Yu, P., Becker, C.M., and Vincent, A. (2008). Progressive encephalomyelitis, rigidity, and myoclonus: a novel glycine receptor antibody. Neurology *71*, 1291-1292.

Iijima, M., Tomita, M., Morozumi, S., Kawagashira, Y., Nakamura, T., Koike, H., Katsuno, M., Hattori, N., Tanaka, F., Yamamoto, M., and Sobue, G. (2009). Single nucleotide polymorphism of TAG-1 influences IVIg responsiveness of Japanese patients with CIDP. Neurology *73*, 1348-1352.

Irani, S., and Lang, B. (2008). Autoantibody-mediated disorders of the central nervous system. Autoimmunity *41*, 55-65.

Irani, S.R., Bera, K., Waters, P., Zuliani, L., Maxwell, S., Zandi, M.S., Friese, M.A., Galea, I., Kullmann, D.M., Beeson, D.*, et al* (2010). N-methyl-D-aspartate antibody encephalitis: temporal progression of clinical and paraclinical observations in a predominantly non-paraneoplastic disorder of both sexes. Brain *133*, 1655-1667.

Irani, S.R., Buckley, C., Vincent, A., Cockerell, O.C., Rudge, P., Johnson, M.R., and Smith, S. (2008). Immunotherapy-responsive seizure-like episodes with potassium channel antibodies. Neurology *71*, 1647-1648.

Irani, S.R., Fukushima, K., Yazaki, M., and Vincent, A. (2007). Limbic encephalitis: under-recognition of voltage-gated potassium channel antibodies. European neurology *58*, 184.

Iranzo, A., Graus, F., Clover, L., Morera, J., Bruna, J., Vilar, C., Martinez-Rodriguez, J.E., Vincent, A., and Santamaria, J. (2006). Rapid eye movement sleep behavior disorder and potassium channel antibody-associated limbic encephalitis. Ann Neurol *59*, 178-181.

Jacob, S., Irani, S.R., Rajabally, Y.A., Grubneac, A., Walters, R.J., Yazaki, M., Clover, L., and Vincent, A. (2008). Hypothermia in VGKC antibody-associated limbic encephalitis. Journal of neurology, neurosurgery, and psychiatry *79*, 202-204.

Johnson, N.C., and Morgan, M.W. (2006). An unusual case of 4-aminopyridine toxicity. The Journal of emergency medicine *30*, 175-177.

Josephs, K.A., Silber, M.H., Fealey, R.D., Nippoldt, T.B., Auger, R.G., and Vernino, S. (2004). Neurophysiologic studies in Morvan syndrome. J Clin Neurophysiol *21*, 440-445.

Kapina, V., Vargas, M.I., Vulliemoz, S., Landis, T., Picard, F., and Lalive, P.H (2009). VGKC antibody-associated encephalitis, microbleeds and progressive brain atrophy. Journal of neurology *257*, 466-468.

Karagogeos, D. (2003). Neural GPI-anchored cell adhesion molecules. Front Biosci *8*, s1304-1320.

Khan, N.L., Jeffree, M.A., Good, C., Macleod, W., and Al-Sarraj, S. (2009). Histopathology of VGKC antibody-associated limbic encephalitis. Neurology *72*, 1703-1705.

Kim, E., and Sheng, M. (1996). Differential K+ channel clustering activity of PSD-95 and SAP97, two related membrane-associated putative guanylate kinases. Neuropharmacology *35*, 993-1000.

Kim, E., and Sheng, M. (2004). PDZ domain proteins of synapses. Nature reviews *5*, 771-781.

Kleopa, K.A., Elman, L.B., Lang, B., Vincent, A., and Scherer, S.S. (2006). Neuromyotonia and limbic encephalitis sera target mature Shaker-type K+ channels: subunit specificity correlates with clinical manifestations. Brain *129*, 1570-1584.

Koch, R.O., Wanner, S.G., Koschak, A., Hanner, M., Schwarzer, C., Kaczorowski, G.J., Slaughter, R.S., Garcia, M.L., and Knaus, H.G. (1997). Complex subunit assembly of neuronal voltage-gated K+ channels. Basis for high-affinity toxin interactions and pharmacology. The Journal of biological chemistry *272*, 27577-27581.

Kowal, C., DeGiorgio, L.A., Nakaoka, T., Hetherington, H., Huerta, P.T., Diamond, B., and Volpe, B.T. (2004). Cognition and immunity; antibody impairs memory. Immunity *21*, 179-188.

Kurono, A., Arimura, K., Watanabe, O., Tomimitsu, H., Nagado, T., Sonoda, Y., Kameyama, M., and Osame, M. (2006). IgM-containing fraction suppressed voltage-gated potassium channels in acquired neuromyotonia. Acta neurologica Scandinavica *113*, 185-188.

Lai, M., Hughes, E.G., Peng, X., Zhou, L., Gleichman, A.J., Shu, H., Mata, S., Kremens, D., Vitaliani, R., Geschwind, M.D.*, et al.* (2009). AMPA receptor antibodies in limbic encephalitis alter synaptic receptor location. Annals of neurology *65*, 424-434.

Lancaster, E., Lai, M., Peng, X., Hughes, E., Constantinescu, R., Raizer, J., Friedman, D., Skeen, M.B., Grisold, W., Kimura, A.*, et al* (2010). Antibodies to the GABA(B) receptor in limbic encephalitis with seizures: case series and characterisation of the antigen. Lancet neurology *9*, 67-76.

Lapteva, L., Nowak, M., Yarboro, C.H., Takada, K., Roebuck-Spencer, T., Weickert, T., Bleiberg, J., Rosenstein, D., Pao, M., Patronas, N.*, et al.* (2006). Anti-N-methyl-D-aspartate receptor antibodies, cognitive dysfunction, and depression in systemic lupus erythematosus. Arthritis and rheumatism *54*, 2505-2514.

Lee, E.K., Maselli, R.A., Ellis, W.G., and Agius, M.A. (1998). Morvan's fibrillary chorea: a paraneoplastic manifestation of thymoma. Journal of neurology, neurosurgery, and psychiatry *65*, 857-862.

Leite, M.I., Jacob, S., Viegas, S., Cossins, J., Clover, L., Morgan, B.P., Beeson, D., Willcox, N., and Vincent, A. (2008). IgG1 antibodies to acetylcholine receptors in 'seronegative' myasthenia gravis. Brain *131*, 1940-1952.

Lennon, V.A., Kryzer, T.J., Pittock, S.J., Verkman, A.S., and Hinson, S.R. (2005). IgG marker of optic-spinal multiple sclerosis binds to the aquaporin-4 water channel. The Journal of experimental medicine *202*, 473-477.

Leung, H., Schindler, K., Clusmann, H., Bien, C.G., Popel, A., Schramm, J., Kwan, P., Wong, L.K., and Elger, C.E. (2008). Mesial frontal epilepsy and ictal body turning along the horizontal body axis. Archives of neurology *65*, 71-77.

Li, Y., Wang, P., Xu, J., and Desir, G.V. (2006). Voltage-gated potassium channel Kv1.3 regulates GLUT4 trafficking to the plasma membrane via a Ca2+-dependent mechanism. American journal of physiology *290*, C345-351.

Liguori, R., Vincent, A., Clover, L., Avoni, P., Plazzi, G., Cortelli, P., Baruzzi, A., Carey, T., Gambetti, P., Lugaresi, E., and Montagna, P. (2001). Morvan's syndrome: peripheral and central nervous system and cardiac involvement with antibodies to voltage-gated potassium channels. Brain *124*, 2417-2426.

London, B., Jeron, A., Zhou, J., Buckett, P., Han, X., Mitchell, G.F., and Koren, G. (1998). Long QT and ventricular arrhythmias in transgenic mice expressing the N terminus and first transmembrane segment of a voltage-gated potassium channel. Proceedings of the National Academy of Sciences of the United States of America *95*, 2926-2931.

Loscher, W.N., Wanschitz, J., Reiners, K., and Quasthoff, S. (2004). Morvan's syndrome: clinical, laboratory, and in vitro electrophysiological studies. Muscle & nerve *30*, 157-163.

Lucchinetti, C.F., Mandler, R.N., McGavern, D., Bruck, W., Gleich, G., Ransohoff, R.M., Trebst, C., Weinshenker, B., Wingerchuk, D., Parisi, J.E., and Lassmann, H. (2002). A role for humoral mechanisms in the pathogenesis of Devic's neuromyelitis optica. Brain *125*, 1450-1461.

Maddison, P. (2006). Neuromyotonia. Clin Neurophysiol *117*, 2118-2127.

Madrid, A., Gil-Peralta, A., Gil-Neciga, E., Gonzalez, J.R., and Jarrin, S. (1996). Morvan's fibrillary chorea: remission after plasmapheresis. Journal of neurology *243*, 350-353.

Majoie, H.J., de Baets, M., Renier, W., Lang, B., and Vincent, A. (2006). Antibodies to voltage-gated potassium and calcium channels in epilepsy. Epilepsy research *71*, 135-141.

Malter, M.P., Helmstaedter, C., Urbach, H., Vincent, A., and Bien, C.G (2010). Antibodies to glutamic acid decarboxylase define a form of limbic encephalitis. Annals of neurology *67*, 470-478.

Manganas, L.N., and Trimmer, J.S. (2000). Subunit composition determines Kv1 potassium channel surface expression. The Journal of biological chemistry *275*, 29685-29693.

Maselli, R.A., Agius, M., Lee, E.K., Bakshi, N., Mandler, R.N., and Ellis, W. (1998). Morvan's fibrillary chorea. Electrodiagnostic and in vitro microelectrode findings. Annals of the New York Academy of Sciences *841*, 497-500.

McKnight, K., Jiang, Y., Hart, Y., Cavey, A., Wroe, S., Blank, M., Shoenfeld, Y., Vincent, A., Palace, J., and Lang, B. (2005). Serum antibodies in epilepsy and seizure-associated disorders. Neurology *65*, 1730-1736.

Modoni, A., Masciullo, M., Spinelli, P., Marra, C., Tartaglione, T., Andreetta, F., Tonali, P., and Silvestri, G. (2009). Successful treatment of acute autoimmune limbic encephalitis with negative VGKC and NMDAR antibodies. Cogn Behav Neurol *22*, 63-66.

Monaghan, M.M., Trimmer, J.S., and Rhodes, K.J. (2001). Experimental localization of Kv1 family voltage-gated K+ channel alpha and beta subunits in rat hippocampal formation. J Neurosci *21*, 5973-5983.

Morvan (1890): Chorée fibrillaire. Gaz Hebd de Médet Chir 27, 173-200.

Mullen, K.M., Rozycka, M., Rus, H., Hu, L., Cudrici, C., Zafranskaia, E., Pennington, M.W., Johns, D.C., Judge, S.I., and Calabresi, P.A. (2006). Potassium channels Kv1.3 and Kv1.5 are expressed on blood-derived dendritic cells in the central nervous system. Annals of neurology *60*, 118-127.

Nagado, T., Arimura, K., Sonoda, Y., Kurono, A., Horikiri, Y., Kameyama, A., Kameyama, M., Pongs, O., and Osame, M. (1999). Potassium current suppression in patients with peripheral nerve hyperexcitability. Brain *122 (Pt 11)*, 2057-2066.

Newsom-Davis, J., and Mills, K.R. (1993). Immunological associations of acquired neuromyotonia (Isaacs' syndrome). Report of five cases and literature review. Brain *116 (Pt 2)*, 453-469.

Nobile, C., Michelucci, R., Andreazza, S., Pasini, E., Tosatto, S.C., and Striano, P. (2009). LGI1 mutations in autosomal dominant and sporadic lateral temporal epilepsy. Human mutation *30*, 530-536.

Ogawa, Y., Horresh, I., Trimmer, J.S., Bredt, D.S., Peles, E., and Rasband, M.N. (2008). Postsynaptic density-93 clusters Kv1 channels at axon initial segments independently of Caspr2. J Neurosci *28*, 5731-5739.

Ogawa, Y., Oses-Prieto, J., Kim, M.Y., Horresh, I., Peles, E., Burlingame, A.L., Trimmer, J.S., Meijer, D., and Rasband, M.N (2010). ADAM22, a Kv1 channel-interacting protein, recruits membrane-associated guanylate kinases to juxtaparanodes of myelinated axons. J Neurosci *30*, 1038-1048.

Ohshita, T., Kawakami, H., Maruyama, H., Kohriyama, T., Arimura, K., and Matsumoto, M. (2006). Voltage-gated potassium channel antibodies associated limbic encephalitis in a patient with invasive thymoma. Journal of the neurological sciences *250*, 167-169.

Oiso, S., Takeda, Y., Futagawa, T., Miura, T., Kuchiiwa, S., Nishida, K., Ikeda, R., Kariyazono, H., Watanabe, K., and Yamada, K. (2009). Contactin-associated protein (Caspr) 2 interacts with carboxypeptidase E in the CNS. Journal of neurochemistry *109*, 158-167.

Park, D.C., Murman, D.L., Perry, K.D., and Bruch, L.A. (2007). An autopsy case of limbic encephalitis with voltage-gated potassium channel antibodies. Eur J Neurol *14*, e5-6.

Parthasarathi, U.D., Harrower, T., Tempest, M., Hodges, J.R., Walsh, C., McKenna, P.J., and Fletcher, P.C. (2006). Psychiatric presentation of voltage-gated potassium channel antibody-associated encephalopathy. Case report. Br J Psychiatry *189*, 182-183.

Peles, E., and Salzer, J.L. (2000). Molecular domains of myelinated axons. Current opinion in neurobiology *10*, 558-565.

Pernet, G. (1917). Case of Morvan's Disease (Syringomyelia). Proceedings of the Royal Society of Medicine *10*, 105-107.

Peroz, D., Rodriguez, N., Choveau, F., Baro, I., Merot, J., and Loussouarn, G. (2008). Kv7.1 (KCNQ1) properties and channelopathies. The Journal of physiology *586*, 1785-1789.

Petersson, S., Persson, A.S., Johansen, J.E., Ingvar, M., Nilsson, J., Klement, G., Arhem, P., Schalling, M., and Lavebratt, C. (2003). Truncation of the Shaker-like voltage-gated potassium channel, Kv1.1, causes megencephaly. The European journal of neuroscience *18*, 3231-3240.

Piepoli, T., Jakupoglu, C., Gu, W., Lualdi, E., Suarez-Merino, B., Poliani, P.L., Cattaneo, M.G., Ortino, B., Goplen, D., Wang, J.*, et al.* (2006). Expression studies in gliomas and glial cells do not support a tumor suppressor role for LGI1. Neuro-oncology *8*, 96-108.

Plazzi, G., Montagna, P., Meletti, S., and Lugaresi, E. (2002). Polysomnographic study of sleeplessness and oneiricisms in the alcohol withdrawal syndrome. Sleep medicine *3*, 279-282.

Poliak, S., Gollan, L., Martinez, R., Custer, A., Einheber, S., Salzer, J.L., Trimmer, J.S., Shrager, P., and Peles, E. (1999). Caspr2, a new member of the neurexin superfamily, is localized at the juxtaparanodes of myelinated axons and associates with K+ channels. Neuron *24*, 1037-1047.

Poliak, S., Gollan, L., Salomon, D., Berglund, E.O., Ohara, R., Ranscht, B., and Peles, E. (2001). Localization of Caspr2 in myelinated nerves depends on axon-glia interactions and the generation of barriers along the axon. J Neurosci *21*, 7568-7575.

Poliak, S., Salomon, D., Elhanany, H., Sabanay, H., Kiernan, B., Pevny, L., Stewart, C.L., Xu, X., Chiu, S.Y., Shrager, P.*, et al.* (2003). Juxtaparanodal clustering of Shaker-like K+ channels in myelinated axons depends on Caspr2 and TAG-1. The Journal of cell biology *162*, 1149-1160.

Polman, C.H., O'Connor, P.W., Havrdova, E., Hutchinson, M., Kappos, L., Miller, D.H., Phillips, J.T., Lublin, F.D., Giovannoni, G., Wajgt, A.*, et al.* (2006). A randomized, placebo-controlled trial of natalizumab for relapsing multiple sclerosis. The New England journal of medicine *354*, 899-910.

Pozo-Rosich, P., Clover, L., Saiz, A., Vincent, A., and Graus, F. (2003). Voltage-gated potassium channel antibodies in limbic encephalitis. Ann Neurol *54*, 530-533.

Prinetti, A., Prioni, S., Chigorno, V., Karagogeos, D., Tettamanti, G., and Sonnino, S. (2001). Immunoseparation of sphingolipid-enriched membrane domains enriched in Src family protein tyrosine kinases and in the neuronal adhesion molecule TAG-1 by anti-GD3 ganglioside monoclonal antibody. Journal of neurochemistry *78*, 1162-1167.

Prive, G.G. (2007). Detergents for the stabilization and crystallization of membrane proteins. Methods (San Diego, Calif *41*, 388-397.

Rajakulendran, S., Schorge, S., Kullmann, D.M., and Hanna, M.G. (2007). Episodic ataxia type 1: a neuronal potassium channelopathy. Neurotherapeutics *4*, 258-266.

Rasband, M.N., Park, E.W., Zhen, D., Arbuckle, M.I., Poliak, S., Peles, E., Grant, S.G., and Trimmer, J.S. (2002). Clustering of neuronal potassium channels is independent of their interaction with PSD-95. The Journal of cell biology *159*, 663-672.

Reeback, J., Benton, S., Swash, M., and Schwartz, M.S. (1979). Penicillamine-induced neuromyotonia. British medical journal *1*, 1464-1465.

Reid, J.M., Foley, P., and Willison, H.J. (2009). Voltage-gated potassium channel-associated limbic encephalitis in the West of Scotland: case reports and literature review. Scottish medical journal *54*, 27-31.

Rhodes, K.J., Monaghan, M.M., Barrezueta, N.X., Nawoschik, S., Bekele-Arcuri, Z., Matos, M.F., Nakahira, K., Schechter, L.E., and Trimmer, J.S. (1996). Voltage-gated K+ channel beta subunits: expression and distribution of Kv beta 1 and Kv beta 2 in adult rat brain. J Neurosci *16*, 4846-4860.

Rinaldi, C., Russo, C.V., Filla, A., De Michele, G., and Marano, E. (2009). Course and outcome of a voltage-gated potassium channel antibody negative Morvan's syndrome. Neurol Sci *30*, 237-239.

Rose, N.R., and Bona, C. (1993). Defining criteria for autoimmune diseases (Witebsky's postulates revisited). Immunology today *14*, 426-430.

Rosenbluth, J. (2009). Multiple functions of the paranodal junction of myelinated nerve fibers. Journal of neuroscience research *87*, 3250-3258.

Rusu, V., Chassoux, F., Landre, E., Bouilleret, V., Nataf, F., Devaux, B.C., Turak, B., and Semah, F. (2005). Dystonic posturing in seizures of mesial temporal origin: electroclinical and metabolic patterns. Neurology *65*, 1612-1619.

Saadoun, S., Waters P, Bell BA, Vincent A, Verkman AS and Papadopoulos, M.C. (2010). Intra-cerebral injection of neuromyelitis optica immunoglobin G and human complement produces neuromyelitis optica lesions in mice. Brain 133, 349-61

Samarasekera, S.R., Vincent, A., Welch, J.L., Jackson, M., Nichols, P., and Griffiths, T.D. (2007). Course and outcome of acute limbic encephalitis with negative voltage-gated potassium channel antibodies. Journal of neurology, neurosurgery, and psychiatry *78*, 391-394.

Sagane, K., Ishihama, Y., and Sugimoto, H. (2008). LGI1 and LGI4 bind to ADAM22, ADAM23 and ADAM11. International journal of biological sciences *4*, 387-396.

Savvaki, M., Panagiotaropoulos, T., Stamatakis, A., Sargiannidou, I., Karatzioula, P., Watanabe, K., Stylianopoulou, F., Karagogeos, D., and Kleopa, K.A. (2008). Impairment of learning and memory in TAG-1 deficient mice associated with shorter CNS internodes and disrupted juxtaparanodes. Molecular and cellular neurosciences *39*, 478-490.

Schott, B., Fischer-Perroudon, C., and Boucher, M. (1996). From Morvan's fibrillary chorea to the "mal des ardents". Journal of the history of the neurosciences *5*, 265-273.

Schott, J.M., Harkness, K., Barnes, J., della Rocchetta, A.I., Vincent, A., and Rossor, M.N. (2003). Amnesia, cerebral atrophy, and autoimmunity. Lancet *361*, 1266.

Schulte, U., Thumfart, J.O., Klocker, N., Sailer, C.A., Bildl, W., Biniossek, M., Dehn, D., Deller, T., Eble, S., Abbass, K.*, et al.* (2006). The epilepsy-linked Lgi1 protein assembles into presynaptic Kv1 channels and inhibits inactivation by Kvbeta1. Neuron *49*, 697-706.

Scott, V.E., Muniz, Z.M., Sewing, S., Lichtinghagen, R., Parcej, D.N., Pongs, O., and Dolly, J.O. (1994). Antibodies specific for distinct Kv subunits unveil a heterooligomeric basis for subtypes of alpha-dendrotoxin-sensitive K+ channels in bovine brain. Biochemistry *33*, 1617-1623.

Sekiguchi, Y., Takahashi, H., Mori, M., Ito, S., Shimada, H., Hattori, T., and Kuwabara, S. (2008). Potassium channel antibody-associated encephalitis with hypothalamic lesions and intestinal pseudo-obstruction. Journal of the neurological sciences *269*, 176-179.

Senechal, K.R., Thaller, C., and Noebels, J.L. (2005). ADPEAF mutations reduce levels of secreted LGI1, a putative tumor suppressor protein linked to epilepsy. Human molecular genetics *14*, 1613-1620.

Shamotienko, O.G., Parcej, D.N., and Dolly, J.O. (1997). Subunit combinations defined for K+ channel Kv1 subtypes in synaptic membranes from bovine brain. Biochemistry *36*, 8195-8201.

Shi, G., Nakahira, K., Hammond, S., Rhodes, K.J., Schechter, L.E., and Trimmer, J.S. (1996). Beta subunits promote K+ channel surface expression through effects early in biosynthesis. Neuron *16*, 843-852.

Shi, G., and Trimmer, J.S. (1999). Differential asparagine-linked glycosylation of voltage-gated K+ channels in mammalian brain and in transfected cells. The Journal of membrane biology *168*, 265-273.

Shillito, P., Molenaar, P.C., Vincent, A., Leys, K., Zheng, W., van den Berg, R.J., Plomp, J.J., van Kempen, G.T., Chauplannaz, G., Wintzen, A.R., and et al. (1995). Acquired neuromyotonia: evidence for autoantibodies directed against K+ channels of peripheral nerves. Annals of neurology *38*, 714-722.

Shimazaki, H., Ando, Y., Nakano, I., and Dalmau, J. (2007). Reversible limbic encephalitis with antibodies against the membranes of neurones of the hippocampus. Journal of neurology, neurosurgery, and psychiatry *78*, 324-325.

Sinha, S., Newsom-Davis, J., Mills, K., Byrne, N., Lang, B., and Vincent, A. (1991). Autoimmune aetiology for acquired neuromyotonia (Isaacs' syndrome). Lancet *338*, 75-77.

Sirerol-Piquer, M.S., Ayerdi-Izquierdo, A., Morante-Redolat, J.M., Herranz-Perez, V., Favell, K., Barker, P.A., and Perez-Tur, J. (2006). The epilepsy gene LGI1 encodes a secreted glycoprotein that binds to the cell surface. Human molecular genetics *15*, 3436-3445.

Smart, S.L., Lopantsev, V., Zhang, C.L., Robbins, C.A., Wang, H., Chiu, S.Y., Schwartzkroin, P.A., Messing, A., and Tempel, B.L. (1998). Deletion of the K(V)1.1 potassium channel causes epilepsy in mice. Neuron *20*, 809-819.

Sokolov, M.V., Shamotienko, O., Dhochartaigh, S.N., Sack, J.T., and Dolly, J.O. (2007). Concatemers of brain Kv1 channel alpha subunits that give similar K+ currents yield pharmacologically distinguishable heteromers. Neuropharmacology *53*, 272-282.

Sonoda, Y., Arimura, K., Kurono, A., Suehara, M., Kameyama, M., Minato, S., Hayashi, A., and Osame, M. (1996). Serum of Isaacs' syndrome suppresses potassium channels in PC-12 cell lines. Muscle & nerve *19*, 1439-1446.

Speake, T., Kibble, J.D., and Brown, P.D. (2004). Kv1.1 and Kv1.3 channels contribute to the delayed-rectifying K+ conductance in rat choroid plexus epithelial cells. American journal of physiology *286*, C611-620.

Spiegel, I., Salomon, D., Erne, B., Schaeren-Wiemers, N., and Peles, E. (2002). Caspr3 and caspr4, two novel members of the caspr family are expressed in the nervous system and interact with PDZ domains. Molecular and cellular neurosciences *20*, 283-297.

Spinazzi, M., Argentiero, V., Zuliani, L., Palmieri, A., Tavolato, B., and Vincent, A. (2008). Immunotherapy-reversed compulsive, monoaminergic, circadian rhythm disorder in Morvan syndrome. Neurology *71*, 2008-2010.

Strauss, K.A., Puffenberger, E.G., Huentelman, M.J., Gottlieb, S., Dobrin, S.E., Parod, J.M., Stephan, D.A., and Morton, D.H. (2006). Recessive symptomatic focal epilepsy and mutant contactin-associated protein-like 2. The New England journal of medicine *354*, 1370-1377.

Takahashi, H., Mori, M., Sekiguchi, Y., Misawa, S., Sawai, S., Hattori, T., and Kuwabara, S. (2008). Development of Isaacs' syndrome following complete recovery of voltage-gated potassium channel antibody-associated limbic encephalitis. Journal of the neurological sciences *275*, 185-187.

Takahashi, Y., Mori, H., Mishina, M., Watanabe, M., Fujiwara, T., Shimomura, J., Aiba, H., Miyajima, T., Saito, Y., Nezu, A.*, et al.* (2003). Autoantibodies to NMDA receptor in patients with chronic forms of epilepsia partialis continua. Neurology *61*, 891-896.

Takahashi, Y., Mori, H., Mishina, M., Watanabe, M., Kondo, N., Shimomura, J., Kubota, Y., Matsuda, K., Fukushima, K., Shiroma, N.*, et al.* (2005). Autoantibodies and cell-mediated autoimmunity to NMDA-type GluRepsilon2 in patients with Rasmussen's

encephalitis and chronic progressive epilepsia partialis continua. Epilepsia *46 Suppl 5*, 152-158.

Tan, K.M., Lennon, V.A., Klein, C.J., Boeve, B.F., and Pittock, S.J. (2008). Clinical spectrum of voltage-gated potassium channel autoimmunity. Neurology *70*, 1883-1890.

Tanosaki, M., Baba, M., Miura, H., Matsunaga, M., and Arimura, K. (1999). Reversible F-wave hyperexcitability associated with antibodies to potassium channels in Isaacs' syndrome. Eur J Neurol *6*, 95-98.

Thieben, M.J., Lennon, V.A., Boeve, B.F., Aksamit, A.J., Keegan, M., and Vernino, S. (2004). Potentially reversible autoimmune limbic encephalitis with neuronal potassium channel antibody. Neurology *62*, 1177-1182.

Tiffany, A.M., Manganas, L.N., Kim, E., Hsueh, Y.P., Sheng, M., and Trimmer, J.S. (2000). PSD-95 and SAP97 exhibit distinct mechanisms for regulating K(+) channel surface expression and clustering. The Journal of cell biology *148*, 147-158.

Tomimitsu, H., Arimura, K., Nagado, T., Watanabe, O., Otsuka, R., Kurono, A., Sonoda, Y., Osame, M., and Kameyama, M. (2004). Mechanism of action of voltage-gated K+ channel antibodies in acquired neuromyotonia. Annals of neurology *56*, 440-444.

Toosy, A.T., Burbridge, S.E., Pitkanen, M., Loyal, A.S., Akanuma, N., Laing, H., Kopelman, M.D., and Andrews, T.C. (2008). Functional imaging correlates of fronto-temporal dysfunction in Morvan's syndrome. Journal of neurology, neurosurgery, and psychiatry *79*, 734-735.

Traka, M., Goutebroze, L., Denisenko, N., Bessa, M., Nifli, A., Havaki, S., Iwakura, Y., Fukamauchi, F., Watanabe, K., Soliven, B., *et al.* (2003). Association of TAG-1 with Caspr2 is essential for the molecular organization of juxtaparanodal regions of myelinated fibers. The Journal of cell biology *162*, 1161-1172.

Traut, W., Weichenhan, D., Himmelbauer, H., and Winking, H. (2006). New members of the neurexin superfamily: multiple rodent homologues of the human CASPR5 gene. Mamm Genome *17*, 723-731.

Tuzun, E., Zhou, L., Baehring, J.M., Bannykh, S., Rosenfeld, M.R., and Dalmau, J. (2009). Evidence for antibody-mediated pathogenesis in anti-NMDAR encephalitis associated with ovarian teratoma. Acta neuropathologica.

Tytgat, J., Debont, T., Carmeliet, E., and Daenens, P. (1995). The alpha-dendrotoxin footprint on a mammalian potassium channel. The Journal of biological chemistry *270*, 24776-24781.

Tzimourakas, A., Giasemi, S., Mouratidou, M., and Karagogeos, D. (2007). Structure-function analysis of protein complexes involved in the molecular architecture of juxtaparanodal regions of myelinated fibers. Biotechnology journal *2*, 577-583.

Vacher, H., Mohapatra, D.P., Misonou, H., and Trimmer, J.S. (2007). Regulation of Kv1 channel trafficking by the mamba snake neurotoxin dendrotoxin K. Faseb J *21*, 906-914.

Verkerk, A.J., Mathews, C.A., Joosse, M., Eussen, B.H., Heutink, P., and Oostra, B.A. (2003). CNTNAP2 is disrupted in a family with Gilles de la Tourette syndrome and obsessive compulsive disorder. Genomics *82*, 1-9.

Vernay, D., Dubost, J.J., Thevenet, J.P., Sauvezie, B., and Rampon, S. (1986). "Choree fibrillaire de Morvan" followed by Guillain-Barre syndrome in a patient receiving gold therapy. Arthritis and rheumatism *29*, 1413-1414.

Vernes, S.C., Newbury, D.F., Abrahams, B.S., Winchester, L., Nicod, J., Groszer, M., Alarcon, M., Oliver, P.L., Davies, K.E., Geschwind, D.H.*, et al.* (2008). A functional genetic link between distinct developmental language disorders. The New England journal of medicine *359*, 2337-2345.

Vetrugno, R., Liguori, R., Provini, F., Plazzi, G., and Montagna, P. (2005). Continuous motor unit activity syndromes: a video-polysomnographic study. Clin Neurophysiol *116*, 2533-2541.

Vincent, A., Buckley, C., Schott, J.M., Baker, I., Dewar, B.K., Detert, N., Clover, L., Parkinson, A., Bien, C.G., Omer, S.*, et al.* (2004). Potassium channel antibody-associated encephalopathy: a potentially immunotherapy-responsive form of limbic encephalitis. Brain *127*, 701-712.

Vincent, A., Irani, S.R., and Lang, B. The growing recognition of immunotherapy-responsive seizure disorders with autoantibodies to specific neuronal proteins. Current opinion in neurology *23*, 144-150.

Vincent A, Buckley C, Lang B, Irani S, Pittock SJ and Tan KM. Clinical spectrum of voltage-gated potassium channel autoimmunity Neurology 2009;72;99-100

Wang, F.C., Bell, N., Reid, P., Smith, L.A., McIntosh, P., Robertson, B., and Dolly, J.O. (1999a). Identification of residues in dendrotoxin K responsible for its discrimination between neuronal K+ channels containing Kv1.1 and 1.2 alpha subunits. European journal of biochemistry / FEBS *263*, 222-229.

Wang, F.C., Parcej, D.N., and Dolly, J.O. (1999b). alpha subunit compositions of Kv1.1-containing K+ channel subtypes fractionated from rat brain using dendrotoxins. European journal of biochemistry / FEBS *263*, 230-237.

Watanabe O, Nagado T, Matsuura E, Osame M, Arimura K. Anti-voltage gated potassium channel (VGKC) antibodies associated limbic encephalitis in Japan: Clinical presentation and patch-clamp study. Clinical Neurophysiology 117 (2006) S49–S111 (FC29.1)

Waters, P., Jarius, S., Littleton, E., Leite, M.I., Jacob, S., Gray, B., Geraldes, R., Vale, T., Jacob, A., Palace, J.*, et al.* (2008). Aquaporin-4 antibodies in neuromyelitis optica and longitudinally extensive transverse myelitis. Archives of neurology *65*, 913-919.

Wellman, C.L. (2001). Dendritic reorganization in pyramidal neurons in medial prefrontal cortex after chronic corticosterone administration. Journal of neurobiology *49*, 245-253.

Willison, H.J., and Yuki, N. (2002). Peripheral neuropathies and anti-glycolipid antibodies. Brain *125*, 2591-2625.

Winger, D.I., Spiegler, P., Trow, T.K., Goyal, A., Yu, H., Yung, E., and Katz, D.S. (2007). Radiology-Pathology Conference: pulmonary hyalinizing granuloma associated with lupus-like anticoagulant and Morvan's Syndrome. Clinical imaging *31*, 264-268.

www.hprd.org. Human protein reference database.

Yealland, L. (1925). Case of Syringomyelia (Morvan's Type). Proceedings of the Royal Society of Medicine *18*, 7.

Yu, Y.E., Wen, L., Silva, J., Li, Z., Head, K., Sossey-Alaoui, K., Pao, A., Mei, L., and Cowell, J.K (2010). Lgi1 null mutant mice exhibit myoclonic seizures and CA1 neuronal hyperexcitability. Human molecular genetics *19*, 1702-1711.

Zandi, M.S., Irani, S.R., Follows, G., Moody, A.M., Molyneux, P., and Vincent, A. (2009). Limbic encephalitis associated with antibodies to the NMDA receptor in Hodgkin lymphoma. Neurology *73*, 2039-2040.

Zhou, L., Zhang, C.L., Messing, A., and Chiu, S.Y. (1998b). Temperature-sensitive neuromuscular transmission in Kv1.1 null mice: role of potassium channels under the myelin sheath in young nerves. J Neurosci *18*, 7200-7215.

Zhou, Y.D., Lee, S., Jin, Z., Wright, M., Smith, S.E., and Anderson, M.P. (2009). Arrested maturation of excitatory synapses in autosomal dominant lateral temporal lobe epilepsy. Nature medicine *15*, 1208-1214.

Zisfein, J., Sivak, M., Aron, A.M., and Bender, A.N. (1983). Isaacs' syndrome with muscle hypertrophy reversed by phenytoin therapy. Archives of neurology *40*, 241-242.

Zuberi, S.M., Eunson, L.H., Spauschus, A., De Silva, R., Tolmie, J., Wood, N.W., McWilliam, R.C., Stephenson, J.B., Kullmann, D.M., and Hanna, M.G. (1999). A novel

mutation in the human voltage-gated potassium channel gene (Kv1.1) associates with episodic ataxia type 1 and sometimes with partial epilepsy. Brain *122 (Pt 5)*, 817-825.

APPENDIX 1: N-METHYL-D-ASPARTATE ANTIBODY ENCEPHALITIS: TEMPORAL PROGRESSION OF CLINICAL AND PARACLINICAL OBSERVATIONS IN A PREDOMINANTLY NON-PARANEOPLASTIC DISORDER OF BOTH SEXES

doi:10.1093/brain/awq113 Brain 2010: 133; 1655–1667 | 1655

BRAIN
A JOURNAL OF NEUROLOGY

N-methyl-D-aspartate antibody encephalitis: temporal progression of clinical and paraclinical observations in a predominantly non-paraneoplastic disorder of both sexes

Sarosh R. Irani,[1] Katarzyna Bera,[1] Patrick Waters,[1] Luigi Zuliani,[1] Susan Maxwell,[1] Michael S. Zandi,[2] Manuel A. Friese,[1,3] Ian Galea,[4] Dimitri M. Kullmann,[5] David Beeson,[1] Bethan Lang,[1] Christian G. Bien[6] and Angela Vincent[1]

1 Department of Clinical Neurology, John Radcliffe Hospital, University of Oxford, Oxford OX3 9DU, UK
2 Department of Neurology, Box 165, Addenbrooke's Hospital, Cambridge CB2 2QQ, UK
3 Institut für Neuroimmunologie und Klinische Multiple Sklerose-Forschung, Zentrum für Molekulare Neurobiologie, Universitätsklinikum Hamburg-Eppendorf, D-20251 Hamburg, Germany
4 Division of Clinical Neurosciences, School of Medicine, University of Southampton, Southampton SO17 1BJ, UK
5 Institute of Neurology, University College London, Queen Square, London WC1N 3BG, UK
6 Department of Epileptology, University of Bonn Medical Centre, Sigmund-Freud Str. 25, 53105, Bonn, Germany

Correspondence to: Prof. Angela Vincent,
Department of Clinical Neurology,
L6 West Wing,
John Radcliffe Hospital,
University of Oxford,
Oxford OX3 9DU, UK
E-mail: angela.vincent@imm.ox.ac.uk

Antibodies to the *N*-methyl-D-aspartate subtype of glutamate receptor have been associated with a newly-described encephalopathy that has been mainly identified in young females with ovarian tumours. However, the full clinical spectrum and treatment responses are not yet clear. We established a sensitive cell-based assay for detection of *N*-methyl-D-aspartate receptor antibodies in serum or cerebrospinal fluid, and a quantitative fluorescent immunoprecipitation assay for serial studies. Although there was marked intrathecal synthesis of *N*-methyl-D-aspartate receptor antibodies, the absolute levels of *N*-methyl-D-aspartate receptor antibodies were higher in serum than in cerebrospinal fluid. *N*-methyl-D-aspartate receptor antibodies were of the immunoglobulin G1 subclass and were able to activate complement on *N*-methyl D-aspartate receptor-expressing human embryonic kidney cells. From questionnaires returned on 44 *N*-methyl-D-aspartate receptor antibody-positive patients, we identified a high proportion without a detected tumour (35/44, 80%: follow-up 3.6–121 months, median 16 months). Among the latter were 15 adult females (43%), 10 adult males (29%) and 10 children (29%), with four in the first decade of life. Overall, there was a high proportion (29%) of non-Caucasians. Good clinical outcomes, as defined by reductions in modified Rankin scores, correlated with decreased *N*-methyl-D-aspartate receptor antibody levels and were associated with early (<40 days) administration of immunotherapies in non-paraneoplastic patients ($P<0.0001$) and earlier tumour removal in paraneoplastic patients ($P=0.02$). Ten patients (23%) who were first diagnosed during relapses had no evidence of tumours but had received minimal or no immunotherapy during earlier episodes. Temporal analysis of the onset of the neurological features suggested progression through two main stages. The time of onset of the early features, characterized by neuropsychiatric symptoms and seizures

Received August 14, 2009. Revised April 7, 2010. Accepted April 8, 2010
© The Author(s) 2010. Published by Oxford University Press on behalf of Brain.
This is an Open Access article distributed under the terms of the Creative Commons Attribution Non-Commercial License (http://creativecommons.org/licenses/by-nc/2.5), which permits unrestricted non-commercial use, distribution, and reproduction in any medium, provided the original work is properly cited.

preceded by a median of 10–20 days, the onset of movement disorders, reduction in consciousness and dysautonomia. This temporal dichotomy was also seen in the timing of cerebrospinal fluid, electroencephalographic and in the rather infrequent cerebral imaging changes. Overall, our data support a model in which the early features are associated with cerebrospinal fluid lymphocytosis, and the later features with appearance of oligoclonal bands. The immunological events and neuronal mechanisms underlying these observations need to be explored further, but one possibility is that the early stage represents diffusion of serum antibodies into the cortical grey matter, whereas the later stage results from secondary expansion of the immunological repertoire within the intrathecal compartment acting on subcortical neurons. Four patients, who only had temporal lobe epilepsy without oligoclonal bands, may represent restriction to the first stage.

Keywords: *N*-methyl-D-aspartate receptor-antibody encephalitis; autoimmunity; non-paraneoplastic; paraneoplastic; immunotherapy-responsive

Abbreviations: cDNA = complementary DNA; EGFP = enhanced green fluorescent protein; IgG = immunoglobulin G; NMDAR = *N*-methyl-D-aspartate receptor

Introduction

Human auto-antibodies directed against neuronal proteins are of diagnostic importance in defining immunotherapy-responsive neurological diseases. Auto-antibodies with specificity towards intracellular proteins act as diagnostic markers of diseases that are usually associated with an underlying cancer and are rarely immunotherapy-responsive. By contrast, antibodies that target the extracellular domain of surface-expressed neuronal proteins are likely to be pathogenic and their presence usually indicates the possibility of successful immunotherapy. In the peripheral nervous system, it is well established that such antibodies are pathogenic (Vincent *et al.*, 2006).

It is increasingly recognized that some CNS disorders can also be antibody-mediated. Antibodies to voltage-gated potassium channels are often associated with limbic encephalitis, presenting with seizures, amnesia and medial temporal lobe inflammation. These patients do not usually have an underlying neoplasm, and do well following immunotherapies, with a substantial and sometimes complete recovery (Buckley *et al.*, 2001; Thieben *et al.*, 2004; Vincent *et al.*, 2004). Moreover, with the expansion of the voltage-gated potassium channels-antibody-associated phenotype to patients whose diagnosis was drug-resistant epilepsy, new immunotherapy-responsive seizure phenotypes are beginning to be recognized (McKnight *et al.*, 2005; Irani *et al.*, 2008).

More recently, antibodies against the *N*-methyl-D-aspartate subtype of ionotropic glutamate receptors [*N*-methyl-D-aspartate receptor (NMDAR) antibodies] have been reported, predominantly in young women who developed a subacute-onset encephalopathy, commonly associated with a prominent movement disorder and frequently an underlying ovarian teratoma (Dalmau *et al.*, 2007), although two recent reports suggest a much higher incidence of non-paraneoplastic cases in children (Dale *et al.*, 2009; Florance *et al.*, 2009). Removal of the teratoma combined with immunotherapy resulted in substantial recovery, but in the minority of patients without a tumour, recovery appeared to be less impressive (Dalmau *et al.*, 2007, 2008). In those studies, the age range was wide, but only 9% of the patients were males.

The full clinical spectrum associated with NMDAR antibodies is likely to widen with increasing recognition. Here we describe an assay suitable for both serum and CSF detection of the antibodies, modified from that of Dalmau *et al.* (2008), which allowed us to identify 50 patients in the UK and Europe in 2008. Clinical details were gathered on 44 patients and allowed us to correlate serum NMDAR antibodies with clinical outcomes using a novel quantitative fluorescent assay, and to demonstrate the detailed temporal progression of clinical and paraclinical features. Our observations emphasize the importance of early intensive immunotherapies and suggest that the neurological disease occurs in two main stages.

Materials and methods

Clinical data

Ethical approval for this study was from the Oxfordshire Regional Ethical Committee A (07/Q1604/28). Serum and CSF samples were referred for testing by clinicians, mainly from the United Kingdom and Europe. Standardized clinical questionnaires (Supplementary data), patient information sheets and consent forms were distributed to the clinicians referring the first 50 NMDAR-antibody-positive samples from a total of 450 sent for testing. We requested details of clinical features, investigation results and serial modified Rankin scores (Graus *et al.*, 2001). Clinicians were asked to document and detail the timing of specific features such as higher cognitive dysfunction, psychiatric, seizure and movement disorders: we have maintained the categorizations as provided by the clinicians. Eight of the patients have been described in case reports (Schimmel *et al.*, 2009; Zandi *et al.*, 2009; Davies *et al.*, 2010). All data were analysed using GraphPad Prism 5 and the tests used are mentioned in the figures and tables. Thirty-six questionnaires were returned, and eight were completed from clinic letters, emails or telephone conversations.

Cell-based assay for antibodies binding human NMDAR

The NMDAR1 subunit (NR1, Genecopoeia catalogue number EX-XO451-M02) and NMDAR2B subunit (NR2B, IMAGE clone number 8322670) complementary (c)DNAs were modified by *in vitro* mutagenesis to match the respective GenBank ID consensus sequences NM_000832 (GRIN1-1a) and BC113618 (GRIN2B). The NR2B subunit was subcloned from pCRXL-TOPO into the mammalian

expression vector pcDNA3.1hygro(–) using a BamH1/Not1 restriction digest. An enhanced green fluorescent protein (EGFP)-tagged human NR1-1 splice variant was also generated. To create the expression construct for this, the C-terminal stop codon was removed, an NheI restriction site generated and the coding sequence for EGFP inserted with a GT(GS)4 linker between the C-terminus of the NR1-1 and the beginning of the EGFP.

For the cell-based assay, human embryonic kidney (HEK293) cells were grown on glass coverslips in Dulbecco's modified Eagle's medium with 10% foetal calf serum and penicillin, streptomycin and amphotericin. After 24 h, cells were transfected, using polyethylenimine and glucose, with untagged-NR1 and NR2B cDNA at a ratio of 3:1. An EGFP expression vector was co-transfected to visualize cells taking-up cDNAs. To prevent cytotoxicity as a result of glutamate in the medium activating the NMDARs, cells were supplemented with 500 μM ketamine 16 h post-transfection. Live cells were incubated with patient sera (1:20) or undiluted CSF for 1 h before fixation (3% formaldehyde) followed by 35 min incubation with Alexa Fluor 568 anti-human immunoglobulin G (IgG). Cells were subsequently washed three times in phosphate buffered saline and mounted on slides in fluorescent mounting medium (DakoCytomation, Cambridge, UK) containing DAPI (4′,6′-diamidino-2-phenlindoledichloride, 1:1000). They were visualized using a fluorescence microscope with a MacProbe v4.3 digital imaging system and the binding scored on a scale from 0–4 by two independent observers (Supplementary Fig. 1A; as in Leite *et al.*, 2008; Waters *et al.*, 2008). All positive samples were retested on muscle-specific-kinase or glycine α1 receptor transfected cells to exclude non-specific binding to the human embryonic kidney cells. For subclass experiments, cells were incubated with isotype-specific mouse antibodies and subsequently with an Alexa Fluor 568 anti-mouse IgG. For immunoabsorption, the sera (1:20 dilution) were preincubated with 5 million trypsinized EGFP-NR1-expressing human embryonic kidney cells for 30 min at 4°C before testing for binding as above.

For detection of deposited complement on transfected cells, the live cells were incubated with heat-inactivated sera (nine NMDAR-antibody positive and eight healthy individuals) and fresh human plasma, as a source of complement (as in Leite *et al.*, 2008; Waters *et al.*, 2008). After 30 min at 37°C the cells were kept on ice, fixed with 3% formaldehyde, incubated with rabbit antibodies against C3b (DAKO; 1:500), or polyclonal rabbit anti-C5b9 (membrane attack complex; kind gift of Prof BP Morgan; 1:100) and Alexa Fluor 568 anti-rabbit IgG (1:1000). Binding to the cells was scored as positive or negative by a blinded observer (PW).

Fluorescent immunoprecipitation assay for antibodies to NMDAR

Human embryonic kidney 293 cells were transfected as above with NR2B and postsynaptic density 95 (PSD95, Open Biosystems, Image Consortium cDNA clones, USA) cDNA expression constructs and with the NR1-EGFP tagged expression construct in a ratio of 1:1:1. PSD95 was used because it improved NR1-EGFP expression in preliminary studies (data not shown). Cells were solubilized using a buffer containing 1% digitonin. A protease inhibitor cocktail (Sigma-Aldrich, UK) was added to this buffer immediately before use. The supernatant was analysed using antibodies to NR1 (Millipore, USA), NR2B (kind gift from Prof F Anne Stephenson, School of Pharmacy, University of London) and PSD95 (Neuromab, USA), and analysis of EGFP fluorescence in fractions following sedimentation on a continuous sucrose gradient (Waters *et al.*, 2008). For serological studies, 25 μl of serum was incubated with 250 μl of solubilized extract overnight at 4°C, as described previously (Waters *et al.*, 2008). Protein-A beads were rotated with the antigen-antibody mixture for 2 h at room temperature. The beads were washed and the captured fluorescence was measured using a fluorescent plate reader (Gemini XS, Molecular Probes). Results were expressed as relative fluorescent units precipitated by 25 μl serum and are reported as fU.

Results

Detection of NMDAR antibodies

We initially used three assays for the detection of NMDAR antibodies (Fig. 1A–C; 'Materials and methods' section in Supplementary data) based on those reported previously (Dalmau *et al.*, 2007; Niehusmann *et al.*, 2009). Rat brain sections were incubated with undiluted CSF to look for hippocampal 'neuropil' binding (Fig. 1A). To confirm the neuronal cell surface specificity of the antibodies and, thus, their likely clinical relevance, we incubated primary cultures of hippocampal neurons with sera and CSF to observe binding to the surface of live neurons (Fig. 1B). We established an immunofluorescent cell-based assay (Fig. 1C) for detection of NMDAR antibodies, modified from that described previously (Dalmau *et al.*, 2007). Specifically, we employed a 3:1 ratio of NR1:NR2B cDNA (with small amounts of EGFP cDNA) as this gave better results with positive sera (Supplementary Fig. 1B) and the NR1 subunit is thought to contain the main epitope (Dalmau *et al.*, 2008). To observe binding only to the extracellular domain of the NR1/NR2B, we did not permeabilize the cells and applied serum diluted 1:20 and CSF undiluted. Using a semi-quantitative approach similar to that employed for binding of antibodies to other cell surface antigens (Leite *et al.*, 2008; Waters *et al.*, 2008), the binding was scored visually from 0 (no binding) to 4 (very strong binding) by two independent observers. All positive results were retested, and also checked for non-specific binding to the cells using human embryonic kidney cells transfected with other antigens (see 'Materials and methods' section). Examples of different scores are shown in Fig. 1C and Supplementary Fig. 1A. Sera from 32 healthy individuals and from 138 disease controls (with other forms of autoimmune encephalopathy, chronic psychosis, multiple sclerosis, lupus, opsoclonus–myoclonus, herpes encephalitis or seizures) gave values of <1 (range 0–0.5, mean 0.01; median 0) (data not shown).

We found the cell-based assay to be most sensitive and, as it is specific for NMDAR antibodies, it was used for testing the 450 sera and 35 CSF samples sent for NMDAR-antibody testing over the period of study (results shown in Supplementary Fig. 1C). The scores of 14 paired samples from NMDAR-antibody-positive patients are shown in Fig. 1D; one CSF was negative while the paired serum was positive (the remaining 21 paired samples were negative in both CSF and serum). Overall serum at 1:20 was found to be slightly more sensitive than undiluted CSF (Fig. 1D), and many patients were diagnosed on the basis of the serum antibody alone.

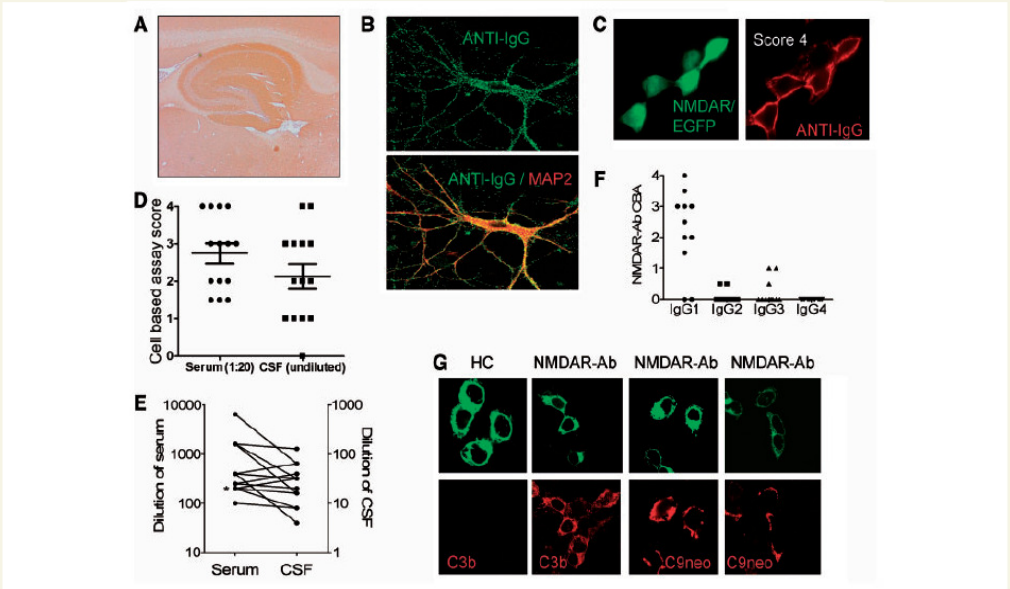


Figure 1 Detection and characterization of NMDAR antibodies. (**A**) NMDAR-antibody-positive CSF shows a hippocampal 'neuropil' binding pattern on rat brain sections. (**B**) NMDAR-antibody-positive serum IgG (green) showing surface binding to primary cultures of live hippocampal neurons identified by the neuronal marker microtubule associated protein 2 (MAP2, in red, within merged lower image; 600× magnification). (**C**) Cell-based assay for NR1/NR2B (NMDAR) antibodies, using transfected human embryonic kidney (HEK293) cells identified by EGFP (enhanced green fluorescent protein) cDNA co-transfection (green), shows surface binding of patient sera (anti-IgG, red). This sample was scored as '4' by visual observation (600× magnification). (**D**) Cell-based assay scores from 14 paired CSF-serum samples; note one CSF was negative. (**E**) Values from end-point titrations of the 14 sera and positive paired CSFs in the cell-based assay; note the different vertical scales and that serum levels of NMDAR antibodies were higher than CSF levels. Two of the data pairs overlapped and their values have been slightly adjusted so that the points are visible. Asterisk indicates one data pair could not be plotted as the CSF was negative (D). (**F**) NMDAR antibodies were found to be predominantly of the IgG1 subclass ($n = 11$). (**G**) NMDAR-antibody-positive sera (NMDAR-Ab) but not control sera (HC) were able to deposit complement C3b and C9neo, the membrane attack complex, on human embryonic kidney cells expressing NMDAR (1000× magnification).

When we serially diluted the 14 available paired samples to find detection endpoints, NMDAR-antibody titres were between 6 and >50 times higher (mean 13.5) in serum than CSF (Fig. 1E). Except in one patient, there was clear evidence of intrathecal synthesis of NMDAR antibodies (median 21.7, range 0–118, $n = 10$ pairs; Supplementary Table 1).

NMDAR antibodies were found to be predominantly of the complement-fixing IgG1 subclass (Fig. 1F) and were able to deposit complement C3b (9/9 NMDAR antibodies; 0/8 control sera) and C9neo, the membrane attack complex (6/9 patients, 0/8 controls), on NMDAR-transfected human embryonic kidney cells (Fig. 1G), as expected for this IgG subclass.

A quantitative assay for antibodies against the NR1 subunit

In order to measure NMDAR-antibody levels more quantitatively, we established a fluorescent immunoprecipitation assay similar to that reported for AQP4 antibodies (Waters *et al.*, 2008). We found the best expression of EGFP-NR1 occurred when it was co-expressed with NR2B and PSD95. The cells were solubilized in a buffer containing 1% digitonin, and the EGFP-NR1 could be immunoprecipitated by anti-NR1 antibodies but not by anti-NR2B or anti-PSD95 antibodies (Fig. 2A). The main EGFP-tagged material sedimented on a sucrose gradient (Supplementary Fig. 2A) with a peak corresponding to 280 kDa. This suggested that the major component is a dimer of NR1-EGFP (predicted size 274 kDa) rather than a tetramer containing both NR1 and NR2B.

Eighty-four percent of the cell-based assay-positive sera immunoprecipitated the EGFP-NR1-dimers at levels greater than the mean + 3SD (970 fU) of the healthy control sera (Fig. 2A), and the values correlated with results of the cell-based assay (Fig. 2B, $P < 0.0001$, $r = 0.86$). However, the fluorescent immunoprecipitation assay was negative in seven of the sera tested and, therefore, was used only for quantitative serial estimations on individual patients (see below). Because eight of the cell-based assay scores were relatively low (1 or 1.5), including five negative by fluorescent immunoprecipitation assay, we re-analysed the binding to NMDAR (Supplementary Table 2). All eight sera were again

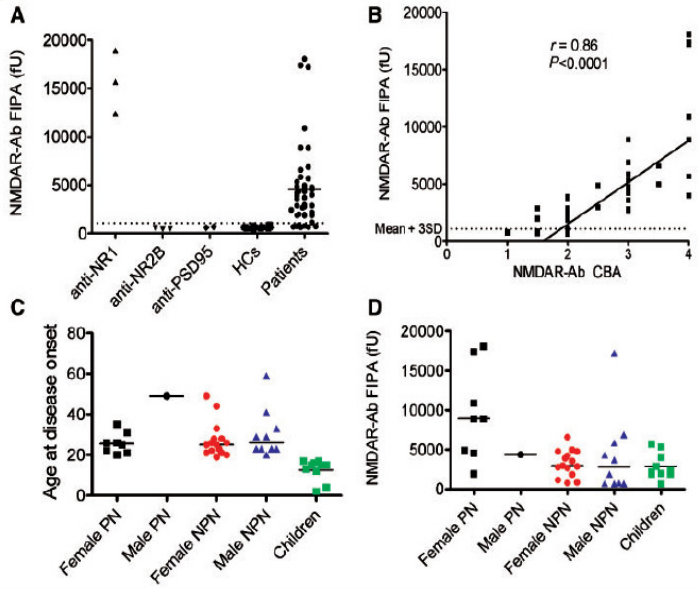


Figure 2 Quantitative analysis of NMDAR antibodies and subgroups of NMDAR-antibody-positive patients. (**A**) The fluorescent immunoprecipitation assay. NR1-specific commercial antibodies (anti-NR1) precipitated large amounts of EGFP-NR1 which was not bound by NR2B-specific (anti-NR2B) or PSD95 (anti-PSD95) antibodies (data from three experiments). Eighty-four percent of 44 NMDAR-antibody-positive patients (as determined by the cell-based assay) precipitated EGFP-NR1 at levels greater than the mean plus three standard deviations (mean + 3SD) of results from 20 healthy controls (HCs). (**B**) There was a strong correlation between the NMDAR-antibody levels determined by the fluorescent immunoprecipitation assay and by the cell-based assay ($r = 0.86$, $P < 0.0001$; Spearman rank correlation). (**C**) The ages at disease onset of the 44 NMDAR-antibody-positive patients shown as male and female paraneoplastic (PN), non-paraneoplastic (NPN), and children (none of whom had tumours detected). (**D**) The results of the fluorescent immunoprecipitation assay showed the NMDAR-antibody levels were higher in paraneoplastic when compared to all non-paraneoplastic cases ($P = 0.0017$, Mann-Whitney U-test). fU = relative fluorescence units precipitated by 25 µl of serum.

positive for binding to NR1/NR2B transfected cells, but they also bound to cells expressing NR1-EGFP alone, and the binding was substantially reduced by prior absorption of the sera with cells expressing NR1 (Supplementary Fig. 2B). These results confirmed the specificity of the antibodies for NMDAR and for the NR1 (Dalmau *et al.*, 2008), but we continue to use the NR1/NR2B combination for diagnostic assays in order not to miss any possible binding to NR2B.

Patients with positive NMDAR antibodies

Overall, 50 of the 450 referred sera were positive for NMDAR antibodies with scores between 1 and 4. Of the 44 patients from whom clinical data were obtained (88%), 10 were identified retrospectively from sera sent over the preceding three years for other antibody tests. The remaining 34 presented over the first 10 months of 2008. Samples were referred from centres in the UK ($n = 28$), Germany ($n = 8$), the rest of Europe ($n = 6$) and elsewhere ($n = 2$). Interestingly, 8 of the 28 patients (29%) seen in the UK were non-Caucasian (two Chinese and one each from Pakistan, Malaysia, Nigeria, India, Iraq and Singapore).

Using assays in routine clinical use, all NMDAR-antibody-positive sera were negative for antibodies against Hu, Yo, Ri, CV2, Ma/Ma2, amphiphysin, glutamic acid decarboxylase and voltage-gated calcium channels. Two patients had low levels of voltage-gated potassium channel antibodies (197 and 241 pM, normal <100 pM) and four had anti-thyroid peroxidase antibodies (137–416, normal <32 IU/ml).

Demographics and tumour association

The ages at onset, stratified for sex and for presence or absence of tumours, are shown in Fig. 2C. Among 44 patients, 31 were females (70%; ages ranging from 2 to 49 years, median 22 years). These had all undergone intensive whole body/pelvic imaging, but strikingly there were only eight female patients with ovarian teratomas (26%; ages between 20 and 35 years), and no other tumours in females. Among the 13 males (age range 4–59, median 23 years) there was only one tumour, a recurrence of a previously-treated Hodgkin's lymphoma at 49 years of age. Of the 23 females and 12 males without detectable tumours, 10 (eight females, two males) were under 18 years at presentation. The youngest were a 2-year-old girl and a 4-year-old boy. It is possible that tumours may still be found, but all have been negative to

date on whole body CT (35 cases), pelvic ultrasound (13 cases), pelvic MRI (eight cases), whole body PET (14 cases) and often more than one imaging modality (26 cases) (follow-up 3.6-121 months, median 16 months).

Clinical features of 44 patients

The full description (summarized in Table 1) relates to the 44 patients, out of the first 50 identified, on whom detailed clinical data were provided by the referring neurologists. Between 1 and 21 days (median 7) before the onset of neurological disease, 11 (25%) patients, including two adults with ovarian teratomas and seven children, developed an infectious episode. Commonly the prodrome consisted of an upper-respiratory tract infection ($n=6$; one mycoplasma IgM, two anti-streptolysin-O antibodies), diarrhoeal illness ($n=2$; one with *Campylobacter jejuni* IgM), one meningitic presentation, and one infected mole. One 13-year-old female received diphtheria/tetanus/pertussis vaccination one day prior to seizure onset. Prodromal headaches or fever were seen in nine of these patients (20%), but more commonly headache and fever occurred after the onset of seizures or neuropsychiatric features (see below for detailed time course).

As described by Dalmau *et al.* (2007, 2008), the most common presenting features included seizures, confusion, amnesia, behavioural changes and psychosis. In our series only 8 of 44 patients presented to a psychiatrist, and all were managed by neurologists. Rarer presenting features included hyperacusis, deafness, ataxia and dystonia. The most distinctive clinical features occurred later and included involuntary choreoathetoid orofacial movements, tachy- or bradycardia and a spontaneous fall in conscious level; central hypoventilation occurred in only seven patients. In Table 1, we describe these clinical features divided into six categories with the percentage of patients exhibiting each feature, divided into early and later categories (see below).

Most patients progressed to a severe clinical syndrome and required admission to intensive care. However, three patients had relatively mild syndromes, and four patients, two males (both aged 23) with 4-year histories of drug-resistant temporal lobe epilepsy, and two females (aged 17 and 33 years) who presented with an acute-onset of complex partial status epilepticus, had had minimal or no cognitive involvement and did not develop any movement disorders or other features consistent with the later stages of the disease. None of these four patients had a malignancy detected and they had some of the lower NMDAR-antibody levels (cell-based assay scores 1–2; for details see Supplementary Table 2).

Comparison of patient subgroups

Quantitative antibody titres on serum samples are shown in Fig. 2D. The fluorescent immunoprecipitation assay values were higher in the paraneoplastic than in the non-paraneoplastic patients ($P=0.0017$, Mann–Whitney U-test; Table 2). There were also a few clinical features that were less evident in the non-paraneoplastic compared with the paraneoplastic patients (Table 2). Of the 44 patients, 10 including eight females, were under age 18 at onset. The most common presenting features in children were seizures and behavioural changes. All children

Table 1 Typical clinical features in 44 NMDAR-antibody positive patients

Early features
Higher cognitive dysfunction 40/44 (91%): confusion 29, behavioural changes 20, amnesia 14, dysphasia 13
Psychiatric 34/44 (77%): hallucinations 22, psychotic 20, agitation 18, depressive 12, anxiety 10, obsessive 1
Seizures 36/44 (82%): generalized 33, complex partial 16, simple partial 12
Later features
Spontaneous reduction in conscious level 20/44 (45%)
Movement disorder 39/44 (89%): choreoathetoid 30 (orofacial 27, upper limbs 22, lower limbs 10), parkinsonian 13, rigidity 10, myoclonus 7, oculogyric crises 3, opisthotonus 3, startle 2
Dysautonomia 32/44 (72%): tachy/brady-cardia 22, hyperhidrosis 12, persistent pyrexia 10, central hypoventilation 7, labile/high blood pressure 6, hypersalivation 4, pseudoobstruction 3, cardiac asystole 2

Total numbers of patients/total number (%). Anxiety was found as an isolated feature, without psychosis or depression, in only two cases. Data were provided by the referring neurologists. Although shown as early and later, there were some individuals in whom this distinction was not evident. Data from individual patients are shown in Fig. 6 and Supplementary Fig. 3.

Table 2 Clinical features that differed in frequency between paraneoplastic and non-paraneoplastic patients

	Paraneoplastic, $n=9$ (%)	Non-paraneoplastic, $n=35$ (%)	P-value[a]
Initial NMDAR-antibody level (mean and range)[b]	7855 (948–17 070)	2255 (0–16 208)	0.001
Confusion	9 (100)	20 (58)	0.02
Agitation	8 (89)	10 (29)	0.001
Amnesia	6 (67)	8 (24)	0.02
Spontaneous reduction in conscious level	8 (89)	12 (35)	0.008

Relapses were found in 10 of the non-paraneoplastic cases compared with none of the paraneoplastic cases, but this difference did not reach significance.
a Fisher's exact test (two-tailed) was used for the comparisons (P-values have not been corrected for multiple comparisons).
b Measured using fluorescent immunoprecipitation assay with solubilised enhanced green fluorescent protein-tagged NR1 subunit.

developed neuropsychiatric features and 80% developed a movement disorder, not obviously different from the adult patients. The incidence of preceding infections was, however, higher in children ($P = 0.0008$) and none had detectable tumours.

Investigations

CSF analysis revealed lymphocytosis in only 30/44 (68%) of patients. CSF lymphocytosis was absent in samples from 35 days after symptom onset (Fig. 3A), except in those who underwent a clinical relapse (data not shown). By contrast, CSF-specific (unmatched) oligoclonal bands were only present in 9% at first CSF sampling but appeared later in the disease course in another 43% (see below).

Brain imaging was normal in 39/44 (89%) at initial MRI and remained normal in 34/44 (77%; Fig. 3B). The few imaging abnormalities were in the hippocampi ($n = 4$) or within white matter regions ($n = 6$) on T_2/fluid attenuated inversion recovery sequences. One non-paraneoplastic male with long-standing drug-resistant epilepsy showed hippocampal sclerosis at 4-year follow-up. Results of brain PET were limited, but it was abnormal in all three patients tested, with frontotemporal, occipital and cerebellar hypermetabolism reported at times when the MRI was normal.

Electroencephalography (EEG) demonstrated epileptiform discharges in 22/44 (50%) patients, usually early during the course of the disease, whereas generalized slowing in the slow theta or delta range was found in 35/44 (80%) patients, generally later during the disorder. Serial EEGs from one additional patient with NMDAR antibodies are shown in Fig. 3C, demonstrating the transition of epileptiform potentials to generalized slowing occurring between 24 and 42 days, followed by normalization at 87 days.

Clinical outcomes and serial estimations of antibodies against the native NR1 subunit

To measure clinical outcomes, the modified Rankin score was reported by the attending clinicians at peak of disease severity and at least two further time points. 37 of 44 (84%) of the patients

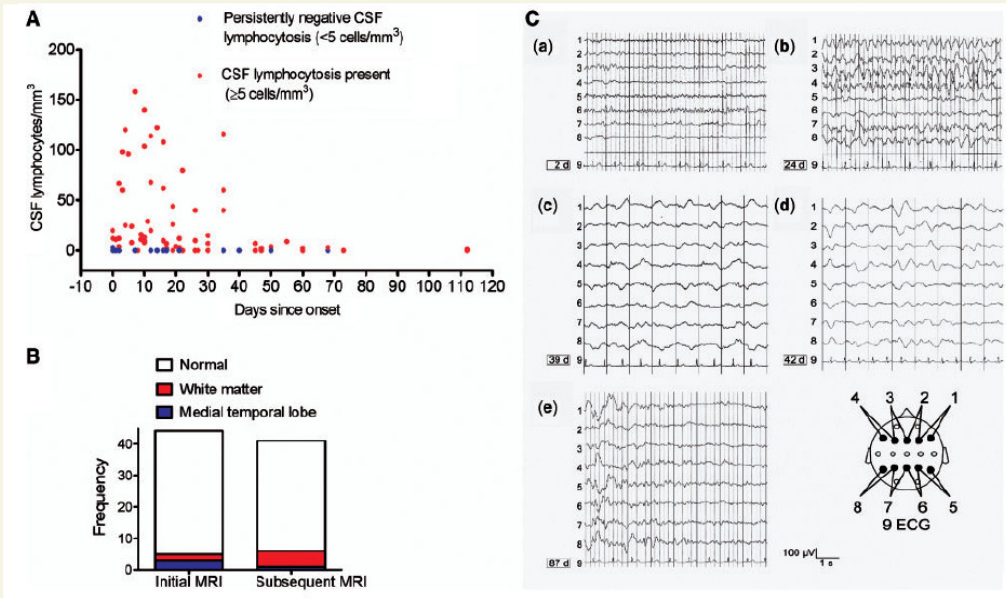


Figure 3 Imaging, cerebrospinal fluid and EEG results. (**A**) The extent of CSF lymphocytosis (>5 cells/mm^3, red dots) observed at different time points across all patients. Thirt-two percent of patients had persistently negative CSF lymphocytosis (<5 cells/mm^3, blue dots). (**B**) MRI was commonly normal (white) and abnormalities were mainly restricted to white matter tracts ($n = 6$, red) and hippocampi ($n = 4$, blue) both at initial (median Day 1) and subsequent (median Day 25) imaging. (**C**) Serial electroencephalograms (EEGs) of a 17-year-old non-paraneoplastic female NMDAR-antibody-positive patient, not within our cohort of 44 cases. Bipolar transverse EEG recordings are shown in the scheme below. (a) EEG was normal after the patient had experienced a generalized convulsion. From Day 21–24, she suffered from frequent complex partial seizures; (b) EEG showed frequent, in part long-lasting frontal epileptiform spike-wave activity; (c–d) subsequently, there was continuous diffuse high-amplitude slowing without epileptiform potentials. From Day 39 on, no further seizures were observed. On Day 42, anti-epileptic therapy consisted of phenytoin (blood level: 25.4 µg/ml), phenobarbital (29.7 µg/ml) and lorazepam (2 mg daily dose). Glucocorticosteroids were instituted on Day 38. From Day 56, the patient recovered; and (e) normal EEG appearances recurred in sections in between abnormally high waves.

had a score of 5 [severe disability with total dependency requiring constant attention (Graus *et al.*, 2001)] at peak of disease, and average duration of hospitalization was 160 days (range 16–850). Thirty-five of the patients were treated with immunotherapy: glucocorticosteroids (33), intravenous immunoglobulins (15), plasma exchange (13), cyclophosphamide (4), rituximab (2), azathioprine (1) and mycophenolate mofetil (1), or a combination of the above (23).

Six examples of serial NMDAR antibodies and modified Rankin scores are shown in Fig. 4 and corresponding clinical vignettes are given in the Supplementary data. Overall there was a good correlation within a patient between the level of serum NMDAR antibody and the modified Rankin scores. Two patients who did well had substantial contemporaneous falls in NMDAR-antibody levels (Fig. 4A and B), whereas two who died had very high absolute antibody levels (>10 000 fU) that persisted despite immunotherapy (Fig. 4C and D). One of these was a patient with an ovarian tumour (Fig. 4C) that was not removed until Day 180. Two patients who were first diagnosed during a relapse (Fig. 4E and F) are discussed below.

The clinical outcomes in all 44 patients are shown in Fig. 5A. Overall, there was no difference in the outcomes between the paraneoplastic, non-paraneoplastic and childhood cases. However, within the paraneoplastic group, there was a correlation between improvement and time to oophorectomy ($r = -0.8$, $P = 0.02$, Spearman rank correlation, data not shown; see Dalmau *et al.*, 2008). Importantly, within the non-paraneoplastic group, those patients administered no immunotherapy or only treated after 40 days, did significantly less well than those treated before 40 days (Kruskal–Wallis, $P < 0.0001$; Dunn's multiple comparisons $P < 0.05$). There was a trend ($P = 0.12$, Mann–Whitney U-test) towards better outcomes when glucocorticosteroids were combined with at least one other immunotherapy rather than given alone (Fig. 5B; additional immunotherapies are listed in the figure legend). Overall, there was a correlation between clinical improvement and reduction in NMDAR antibodies for all 25 patients on whom sequential samples were available (Fig. 5C; $r = 0.54$, $P = 0.005$, Spearman rank correlation).

Relapses

Importantly, 10 of 35 non-paraneoplastic patients experienced relapses (two to four relapses; time between relapses 3 months and 6 years) following some improvement after a previous episode. These were aged between 17 and 44 years (median 25.5 years, two males and eight females) and did not have an occult tumour after at least 14 months of careful follow-up. NMDAR antibodies were detected in all six patients who had samples

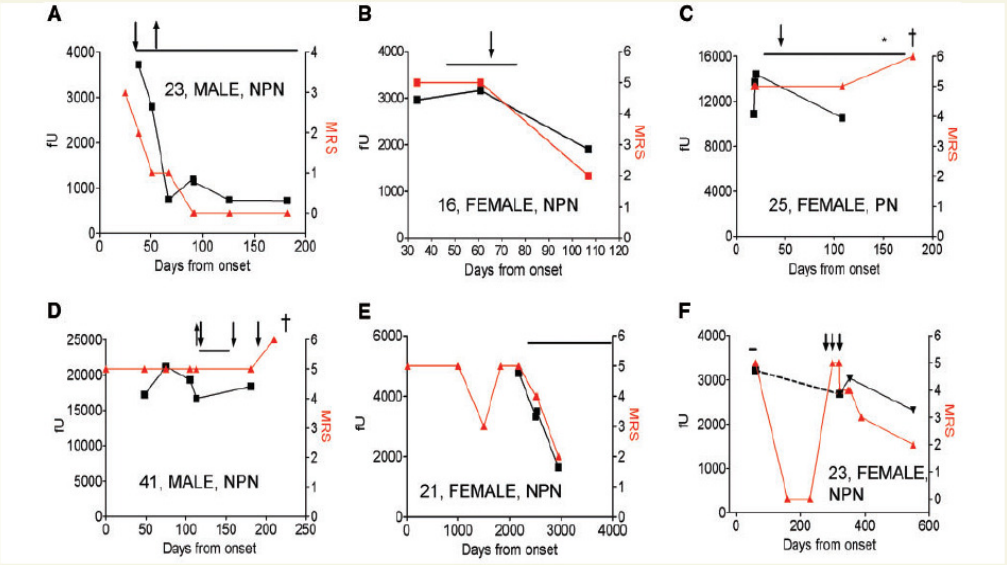


Figure 4 (**A–F**) Effects of immunotherapy [plasma exchange (downward arrow), glucocorticosteroids (solid lines) and intravenous immunoglobulins (upward arrow)] and oophorectomy (asterisk) on NMDAR-antibody titres [fluorescent units precipitated (fU), black] and on clinical outcomes (modified Rankin scores, red). Death is indicated by 'dagger'. Age, sex and neoplasm status (paraneoplastic = PN, non-paraneoplastic = NPN) are shown within each figure. (**A**) and (**B**) show reductions in NMDAR antibodies correlating with clinical outcome after successful immunotherapy, although antibodies persist in (**B**). (**C**) and (**D**) show two patients who died with very high NMDAR-antibody levels persisted throughout the illness despite immunotherapies (**C** and **D**) and late oophorectomy (**C**). (**E**) and (**F**) show patients with clinical relapses after no immunotherapy (**E**) or only 3 days of intravenous glucocortocosteroid therapy (**F**) during their first episode. Both patients showed clinical and serological improvement after immunotherapy administered during their second episode. In (**F**), the dotted line represents unknown titres between episodes. More detailed vignettes of these cases are available in the Supplementary data. MRS = modified Rankin score.

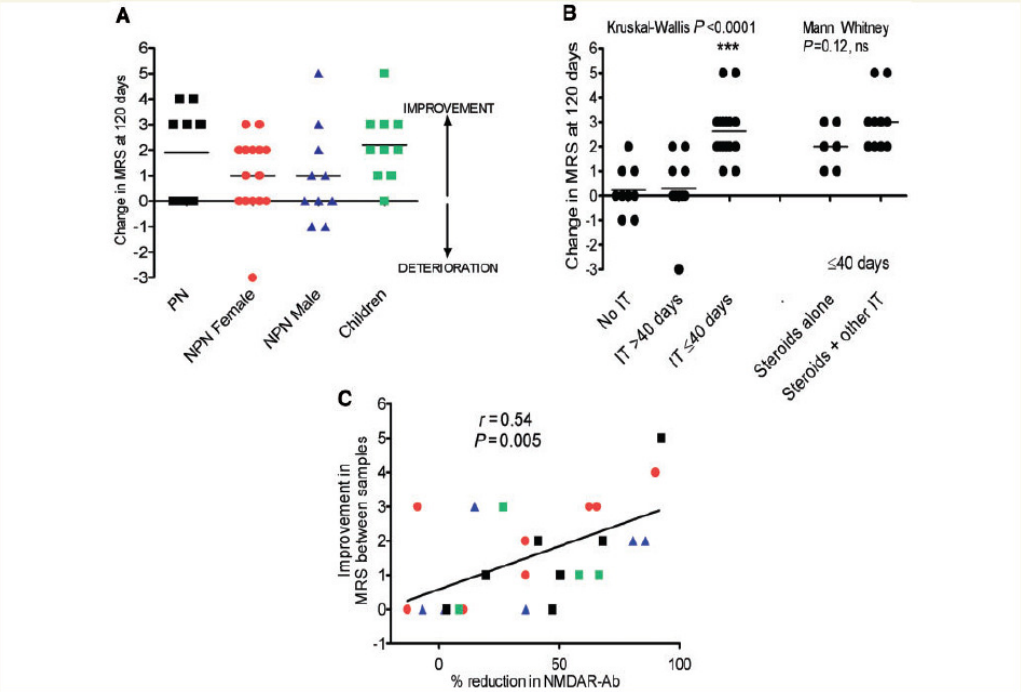


Figure 5 Clinical outcomes and therapeutics. (**A**) The change in modified Rankin score (MRS) at 120 days after onset of symptoms divided into subgroups. (**B**) The improvement in modified Rankin scores at 120 days after onset of symptoms in non-paraneoplastic patients according to administration of no immunotherapy (No IT), any immunotherapy after 40 days (IT > 40 days), or before or at 40 days (IT ≤ 40 days). The other immunotherapies were intravenous Ig ($n = 4$), plasma exchange ($n = 2$), intravenous Ig and plasma exchange ($n = 3$) or cyclophosphamide ($n = 1$). (Kruskal–Wallis, $P < 0.0001$; ***Dunn's multiple comparison test $P < 0.0001$ for no IT or IT > 40 days compared to IT ≤ 40 days. For those administered IT at ≤40 days, there was a trend towards better outcomes when steroids plus other immunotherapies were given (Steroids alone v. Steroids + other IT; Mann Whitney, $P = 0.02$). (**C**) The correlation between percentage change in NMDAR-antibody levels determined by fluorescent immunoprecipitation assay and the corresponding change in modified Rankin scores over the time the two samples were taken ($r = 0.54$, $P = 0.005$; $n = 25$). Symbols as in (**A**).

stored from their previous clinical episode(s). Two examples of relapsing patients, both diagnosed during their second episode after limited immunotherapy had been given in the first episode, are shown in Fig. 4E and F. Overall, during their first episodes, five relapsers received no immunotherapy, three were only administered 3–5 days of intravenous glucocorticosteroids and two relapses occurred immediately after glucocorticosteroid withdrawal. By contrast, most paraneoplastic patients remained severely affected until tumour removal (one improved spontaneously).

Time course of the clinical features

We were struck by the time course of the presenting features and the paraclinical investigations, as shown in Fig. 6A. There was a striking uniformity in the median values of the times at which the seizures, psychiatric and cognitive disorders first appeared, usually within the first few days, whereas the median values for the later features of dysautonomia, movement disorders and fall in consciousness were delayed by ~10–20 days. Data from individual cases are shown in Supplementary Fig. 3. In the majority, there were at least 5 days between the onset of each of the early features and the subsequent development of the later features. In addition, whereas headache or fever associated with a known infection (upper respiratory tract infection or diarrhoeal) preceded the onset of neurological symptoms by around 5 days, headache or fever without evidence of infection showed a similar time course to the later features.

To see whether the paraclinical investigations showed a similar dichotomy, we plotted all the available results for each patient against time after onset over the first 120 days (Fig. 6B) (although these data included a variable number of time points from different individuals, the data compare the presence or absence of a particular finding at each time point). Of most interest, was the early appearance of CSF lymphocytosis compared to the later absence of CSF lymphocytosis ($P = 0.0007$), contrasting with the early absence of CSF-specific oligoclonal bands compared to their later presence ($P = 0.0067$) (data for individual cases shown in Supplementary Fig. 4). There were also clear differences in the

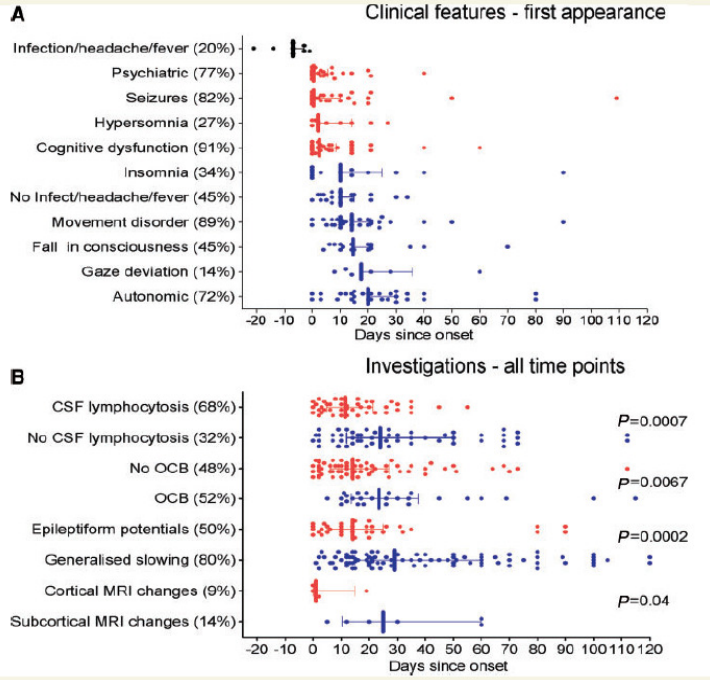


Figure 6 Temporal progression of clinical features and investigations. (**A**) The times of first appearance of the main clinical features for each patient, up to 120 days after onset of neurological symptoms. (**B**) The times of all CSF pleocytosis or oligoclonal bands, and all abnormal EEG or MRI findings. Median and interquartile ranges are shown. *P*-values in B represent Mann–Whitney *U*-tests for each blue-red pairing. OCB = CSF-specific oligoclonal bands. Percentages (bracketed) show the frequency of each feature or investigation within the total NMDAR-antibody patient cohort.

median times at which epileptiform discharges ($P = 0.0002$) occurred compared to generalized slowing, and the few cortical MRI changes were earlier than the equally uncommon subcortical MRI changes ($P = 0.04$).

Discussion

This first predominantly European series of NMDAR-antibody encephalitis broadens the published demographic and clinical features, details the timing of different clinical features and describes treatment responses of paraneoplastic and non-paraneoplastic cases. The condition was first identified in 2007 (Dalmau *et al.*, 2007). In 100 cases described by Dalmau *et al.* (2008) the majority were female (91%) and 59% had ovarian tumours. By contrast, only 9/34 adult patients we studied had tumours, and 11/34 of the adults and 2/10 of the children were male. Here we further characterized the pathogenic potential of the antibodies and show that serial NR1-antibody levels correlate with clinical severity over time within individuals and across the cohort. Moreover, early immunotherapy appeared to be important in improving outcomes, reducing NMDAR-antibody levels and protecting against relapses, which occurred in 23%. By careful analysis of the temporal progression of the clinical features, we found consistent time-lags of 10–20 days between the early/presenting features and the later features that were accompanied by switches in the CSF, MRI and EEG findings, suggesting that the neurological disease occurs in two distinct clinical and neuropathological stages.

For diagnosis, we used a sensitive cell-based assay similar to those we developed for measuring antibodies to other cell surface antigens (Hutchinson *et al.*, 2008; Leite *et al.*, 2008; Waters *et al.*, 2008). The higher proportion of non-paraneoplastic cases in this study compared to the previous report (Dalmau *et al.*, 2008) may reflect the sensitivity of our cell-based assay for serological screening, and the wide referral base of the clinical neuroimmunology service in Oxford, UK. Perhaps partly for this reason, some of the patients had less characteristic syndromes. For instance, relatively low antibody binding scores were found in four adults who presented with seizures and did not progress further (see also one patient in Niehusmann *et al.*, 2009). One of these subsequently developed hippocampal sclerosis, suggesting that NMDAR antibodies may be another cause of limbic encephalitis (Graus *et al.*, 2008) that can progress to hippocampal sclerosis (Bien *et al.*, 2007).

Twenty-three percent of our cases overall were children aged between 2 and 17, confirming the increasing numbers of children, often without tumours, who develop this antibody (Florance *et al.*, 2009), some of whom had been given a previous diagnosis of encephalitis lethargica (Dale *et al.*, 2009). Since some of the features and investigations overlap with those of other disorders, such as Hashimoto's encephalitis (Castillo *et al.*, 2006) and the paediatric autoimmune neuropsychiatric disorder associated with streptococcal infection (PANDAS, Church *et al.*, 2003), the phenotype associated with this antibody may expand in both children and adults.

For serial measurements on sera we used immunoprecipitation of solubilized native NR1-EGFP dimers, but this assay would need further refinement for use in serological diagnosis or on CSF. An enzyme-linked immunosorbent assay (Dalmau *et al.*, 2008) has been used successfully for serum and CSF studies, although at present we feel that the cell-based assay offers the best sensitivity and specificity for diagnosis. Using our NR1-EGFP immunoprecipitation assay, the nine paraneoplastic patients, eight of whom were females aged between 20 and 35 years with ovarian teratomas, had higher serum NR1-antibody levels than the non-paraneoplastic patients and did well after early tumour removal (as in Dalmau *et al.*, 2008). Follow-up in the non-paraneoplastic patients, who accounted for 80% of our cohort, extend previous data (Dalmau *et al.*, 2008; Florance *et al.*, 2009) that reported a less good response to immunotherapy in the non-paraneoplastic patients. Our best outcomes were in those patients treated early ($\leq$40 days), and given glucocorticosteroids and at least one other immunotherapy, whereas 9/10 of the relapsing patients received insubstantial or no immunotherapy during their previous episode(s). In some cases, positive NMDAR antibodies were still present after treatment of the first episode when only partial clinical remission had been obtained (two examples are shown in Fig. 4). This, together with the finding of high and persistent antibody levels in the three patients who died, and reduction of antibody titres in patients who improved, suggests that the condition needs to be treated more intensively and may need long-term maintenance immunosuppression. This contrasts with voltage-gated potassium channel antibodies which, in general, fall rapidly following similar immunotherapy (Thieben *et al.*, 2004; Vincent *et al.*, 2004), although occasionally patients do relapse (Irani and Vincent, unpublished observations). With an average hospital stay of 160 days, long periods of ventilation and multiple infectious complications, this condition is now becoming a recognized and relatively frequent cause of admission to intensive care (Davies *et al.*, 2010).

The idea that this condition could be 'multi-stage' was suggested previously on the basis of four female patients (Iizuka *et al.*, 2008), but the results of our detailed analyses of the timing of clinical features and investigations combine to support a model of the disease occurring in two main stages. The commonest presenting features (seizures, confusion, amnesia and psychosis) seen in 41/44 patients are likely due to cortical temporal lobe dysfunction, as frequently seen in classical limbic encephalitis, and the same applies to the psychotic features (Harrison, 1999; Janssen *et al.*, 2009; Minatogawa-Chang *et al.*, 2009). Clinically, there was a time-lag of 10 to 20 days between the onset of these early features (cognitive, psychiatric, seizure syndromes, CSF lymphocytosis, epileptiform discharges and the few cortical MRI lesions), and the later appearance of basal ganglia and brainstem-localised features (movement disorders, fall in level of consciousness, dysautonomia, CSF oligoclonal bands, generalized slowing or intermittent rhythmic delta activity on EEG, and some subcortical MRI abnormalities). Fever and headache with an obvious infection did precede the neurological features in some cases, but fever and headache without any apparent infection were found later in the disease course, when they might have a subcortical, or perhaps hypothalamic origin. Similarly, whereas hypersomnia was an early feature, insomnia occurred later, possibly reflecting generation by different localisation and mechanisms respectively.

These clinical observations raise many questions regarding the aetiology and the pathogenic mechanisms of this disorder. Firstly, the relatively high proportion of non-Caucasians (but mainly UK resident) individuals in our cohort suggests that there may be human leucocyte antigen or other genetic factors involved in disease susceptibility. Secondly, although numbers of paraneoplastic patients were small, there were no apparent differences in the timing of the CSF, imaging or EEG findings between the paraneoplastic and non-paraneoplastic patients (data not shown) and in all patients, high serum:CSF ratios of NMDAR antibodies suggest that the antigenic stimulus begins initially in the periphery rather than in the CNS. Clearly NMDAR expression by the ovarian tumours provides the antigenic stimulus in young paraneoplastic females (Dalmau *et al.*, 2007; Tuzun *et al.*, 2009), and this strong antigenic stimulus may account for the higher antibody levels. In the more frequent non-paraneoplastic cases, it is possible that occult tumours may have been eliminated by the immune surveillance mechanisms that generated the neurological syndrome, or are still present as has been reported even in some patients who improved spontaneously (Iizuka *et al.*, 2008; Shindo *et al.*, 2009). But in general, for the non-paraneoplastic patients, one needs to invoke some other antigenic stimulus. In our study, preceding infections were common in children, but only two developed their infectious prodrome sufficiently long before the onset of neurological symptoms (i.e. >10 days) to be consistent with the infection generating a novel cross-reacting IgG antibody (one reported in Schimmel *et al.*, 2009) as clearly demonstrated, for instance, in patients with Guillain–Barré syndrome (Willison and Yuki, 2002). Dalmau *et al.* (2008) reported a higher incidence of preceding infections, but they did not perform such a detailed chronological analysis.

It seems likely that the infectious prodrome, when it occurs, represents an inflammatory event. In many cases this may be associated with CSF lymphocytosis, which was detected within the first few days after onset of neurological symptoms, and is seen frequently in paraneoplastic neurological syndromes (e.g. Psimaras *et al.*, 2010). Between them, these could be responsible for a temporary and/or localized disruption of the blood-brain barrier, allowing antibodies to gain entry to the CNS, possibly in the temporal lobe where many of the presenting features may be localised. It is possible that the CSF lymphocytosis might partly represent an influx of antigen-specific T and B cells (data on lymphocyte subsets is unfortunately not available); the intrathecal

synthesis of NMDAR IgG1 antibodies (Tuzun *et al.*, 2009) is likely to require antigen-specific T cell help. Alternatively, our data showing that the antibodies can activate deposition of both C3b and C5b9 (membrane attack complex) on NMDAR expressing cells would be consistent with direct damage and/or complement-dependent chemotaxis being responsible for a subsequent CSF lymphocytosis. Complement deposition was not found at 3 and 4 months, respectively, in two post-mortem studies (Tuzun *et al.*, 2009) but might be important in the early stages. Clearly further studies on serum and CSF taken at different stages of the disease, including looking for specific cellular immune responses, combined with more detailed and investigative imaging, could help unravel the early events but, since the presenting features are not disease-specific, a high suspicion for this condition in young adults and early serological and CSF referral will be important for these studies.

The next questions relate to where and how the antibodies act. It has already been shown that NMDAR-antibody-positive CSF and purified IgG can lead to internalization of NMDARs in hippocampal neurons in culture (Dalmau *et al.*, 2008) and this may play a major role *in vivo*, particularly if complement levels in the parenchymal extracellular fluid are low. From the time-course we describe, it seems likely that the early features, accompanied by epileptiform discharges and sometimes cortical MRI abnormalities, are due to dysfunction of cortical neurons, perhaps by a combination of reduced NMDARs and complement-mediated damage. But why the later features do not occur at this time is not clear. A recent case series proposed that the involuntary movements seen in NMDAR-antibody encephalitis were the result of reduced corticostriatal disinhibition of autonomous central pattern generators in the striatum (Kleinig *et al.*, 2008), but it is difficult to see why this would occur with such a delayed time-course. It may be that the secondary intrathecal synthesis of NMDAR antibodies and development of oligoclonal bands are required before there is more global cerebral involvement with predominant subcortical dysfunction, slow-wave discharges and white matter lesions. An attractive hypothesis is that, concurrent with the later appearance of unmatched CSF oligoclonal bands, intrathecal antigen spreading with production of different antibody specificities occurs; such non-NMDAR antigen immunization might then be responsible for some of the later features. In support of this concept, the four patients restricted to the early, likely cortical, stage, with predominant epilepsy, never developed oligoclonal bands and only one had CSF lymphocytosis. Further clinical investigations and experimental studies in active and passive transfer models should help unravel some of these challenging questions.

Acknowledgements

We are very grateful to Ms P Pettingill for her help and to all of the patients and the clinicians who provided the clinical data and additional samples: Dr M Douglas, Dr R Etti (Birmingham, UK), Dr T Hughes, Dr H Morris (Cardiff, UK), Dr J Miller (Newcastle, UK), Dr M Manford, Prof D Menon, Dr P Molyneux (Cambridge, UK), Dr L Costelloe (Dublin, UK), Dr A Bhattacharya, Dr G Davies, Dr S Slaught, Dr R Walker (London, UK), Dr J Ealing, Dr G Vassallo (Manchester, UK), Dr P Maddison (Nottingham, UK), Prof R Gregory, Dr Y Hart, Dr T McShane (Oxford, UK), Dr Murrigan (Southampton, UK), Dr M Hoppe, Dr J Penzien, Dr B Reuter, Dr M Wolff (Germany), Prof U Aguglia (Italy), Prof E Wilder-Smith (Singapore), Dr A Jiminez Huete (Spain), Dr A Rossetti (Switzerland). We thank Prof F Anne Stephenson (School of Pharmacy, University of London) for the anti-NR2B antibody, and Prof B Paul Morgan for the anti-C5b9 antibody.

Funding

National Institute for Health Research (NIHR), Department of Health, UK (S.R.I.), the Oxford Biomedical Research Centre (P.W. and A.V.), a Wellcome Trust funded OXION studentship (K.B.), the Medical Research Council, UK (D.B. and S.M.), a European Federation of Neurological Society fellowship (L.Z.) and an Eastern Region Neurosciences Training Fellowship (M.S.Z.).

Conflict of Interest: AV and the University Department of Clinical Neurology in Oxford receive royalties and payments for antibody assays. The authors report no other conflict of interests.

Supplementary material

Supplementary material is available at *Brain* online.

References

Ances BM, Vitaliani R, Taylor RA, Liebeskind DS, Voloschin A, Houghton DJ, et al. Treatment-responsive limbic encephalitis identified by neuropil antibodies: MRI and PET correlates. Brain 2005; 128: 1764–77.

Bien CG, Urbach H, Schramm J, Soeder BM, Becker AJ, Voltz R, et al. Limbic encephalitis as a precipitating event in adult-onset temporal lobe epilepsy. Neurology 2007; 69: 1236–44.

Buckley C, Oger J, Clover L, Tuzun E, Carpenter K, Jackson M, et al. Potassium channel antibodies in two patients with reversible limbic encephalitis. Ann Neurol 2001; 50: 73–8.

Castillo P, Woodruff B, Caselli R, Vernino S, Lucchinetti C, Swanson J, et al. Steroid-responsive encephalopathy associated with autoimmune thyroiditis. Arch Neurol 2006; 63: 197–202.

Church AJ, Dale RC, Lees AJ, Giovannoni G, Robertson MM. Tourette's syndrome: a cross sectional study to examine the PANDAS hypothesis. J Neurol Neurosurg Psychiatry 2003; 74: 602–7.

Dale RC, Irani SR, Brilot F, Pillai S, Webster R, Gill D, et al. NMDA receptor antibodies in pediatric dyskinetic encephalitis lethargica. Ann Neurol 2009; 66: 704–9.

Dalmau J, Gleichman AJ, Hughes EG, Rossi JE, Peng X, Lai M, et al. Anti-NMDA-receptor encephalitis: case series and analysis of the effects of antibodies. Lancet Neurol 2008; 7: 1091–8.

Dalmau J, Tuzun E, Wu HY, Masjuan J, Rossi JE, Voloschin A, et al. Paraneoplastic anti-N-methyl-D-aspartate receptor encephalitis associated with ovarian teratoma. Ann Neurol 2007; 61: 25–36.

Davies G, Irani SR, Coltart C, Ingle G, Amin Y, Taylor C, et al. NMDA Receptor Antibodies are a Common Cause of Encephalitis Requiring Intensive Care. Crit Care Med 2010; 89: 679–82.

Florance NR, David RL, Lam C, Szperka C, Zhou L, Ahmad S, et al. Anti-N-methyl-D-aspartate receptor (NMDAR) encephalitis in children and adolescents. Ann Neurol 2009; 66: 11–18.

Graus F, Keime-Guibert F, Rene R, Benyahia B, Ribalta T, Ascaso C, et al. Anti-Hu-associated paraneoplastic encephalomyelitis: analysis of 200 patients. Brain 2001; 124: 1138–48.

Graus F, Saiz A, Lai M, Bruna J, Lopez F, Sabater L, et al. Neuronal surface antigen antibodies in limbic encephalitis: clinical-immunologic associations. Neurology 2008; 71: 930–6.

Harrison PJ. The neuropathology of schizophrenia. A critical review of the data and their interpretation. Brain 1999; 122: 593–624.

Hutchinson M, Waters P, McHugh J, Gorman G, O'Riordan S, Connolly S, et al. Progressive encephalomyelitis, rigidity, and myoclonus: a novel glycine receptor antibody. Neurology 2008; 71: 1291–2.

Iizuka T, Sakai F, Ide T, Monzen T, Yoshii S, Iigaya M, et al. Anti-NMDA receptor encephalitis in Japan: long-term outcome without tumor removal. Neurology 2008; 70: 504–11.

Irani SR, Buckley C, Vincent A, Cockerell OC, Rudge P, Johnson MR, et al. Immunotherapy-responsive seizure-like episodes with potassium channel antibodies. Neurology 2008; 71: 1647–8.

Janssen J, Reig S, Alemán Y, Schnack H, Udias JM, Parellada M, et al. Gyral and sulcal cortical thinning in adolescents with first episode early-onset psychosis. Biol Psychiatry 2009; 66: 1047–54.

Jarius S, Aboul-Enein F, Waters P, Kuenz B, Hauser A, Berger T, et al. Antibody to aquaporin-4 in the long-term course of neuromyelitis optica. Brain 2008; 131: 3072–80.

Kleinig TJ, Thompson PD, Matar W, Duggins A, Kimber TE, Morris JG, et al. The distinctive movement disorder of ovarian teratoma-associated encephalitis. Mov Disord 2008; 23: 1256–61.

Leite MI, Jacob S, Viegas S, Cossins J, Clover L, Morgan BP, et al. IgG1 antibodies to acetylcholine receptors in 'seronegative' myasthenia gravis. Brain 2008; 131: 1940–52.

McKnight K, Jiang Y, Hart Y, Cavey A, Wroe S, Blank M, et al. Serum antibodies in epilepsy and seizure-associated disorders. Neurology 2005; 65: 1730–6.

Minatogawa-Chang TM, Schaufelberger MS, Ayres AM, Duran FL, Gutt EK, Murray RM, et al. Cognitive performance is related to cortical grey matter volumes in early stages of schizophrenia: a population-based study of first-episode psychosis. Schizophr Res 2009; 113: 200–9.

Niehusmann P, Dalmau J, Rudlowski C, Vincent A, Elger CE, Rossi JE, et al. Diagnostic value of N-methyl-D-aspartate receptor antibodies in women with new-onset epilepsy. Arch Neurol 2009; 66: 458–64.

Psimaras D, Carpentier AF, Rossi C. CSF study in paraneoplastic syndromes. J Neurol Neurosurg Psychiatry. 2009 J Neurol Neurosurg Psychiatry 2010; 81: 42–5.

Schimmel M, Bien CG, Vincent A, Schenk W, Penzien J. Successful treatment of anti-N-methyl D-aspartate receptor encephalitis presenting with catatonia. Arch Dis Child 2009; 94: 314–6.

Shindo A, Kagawa K, Ii Y, Sasaki R, Kokubo Y, Kuzuhara S. Anti-N-methyl-D-aspartate receptor-related grave but reversible encephalitis with ovarian teratoma in 2 Japanese women presenting with excellent recovery without tumor resection. Eur Neurol 2009; 61: 50–1.

Thieben MJ, Lennon VA, Boeve BF, Aksamit AJ, Keegan M, Vernino S. Potentially reversible autoimmune limbic encephalitis with neuronal potassium channel antibody. Neurology 2004; 62: 1177–82.

Tuzun E, Zhou L, Baehring JM, Bannykh S, Rosenfeld MR, Dalmau J. Evidence for antibody-mediated pathogenesis in anti-NMDAR encephalitis associated with ovarian teratoma. Acta Neuropathol; Aug 14 2009 [Epub ahead of print].

Vincent A, Lang B, Kleopa KA. Autoimmune channelopathies and related neurological disorders. Neuron 2006; 52: 123–38.

Vincent A, Buckley C, Schott JM, Baker I, Dewar BK, Detert N, et al. Potassium channel antibody-associated encephalopathy: a potentially immunotherapy-responsive form of limbic encephalitis. Brain 2004; 127: 701–12.

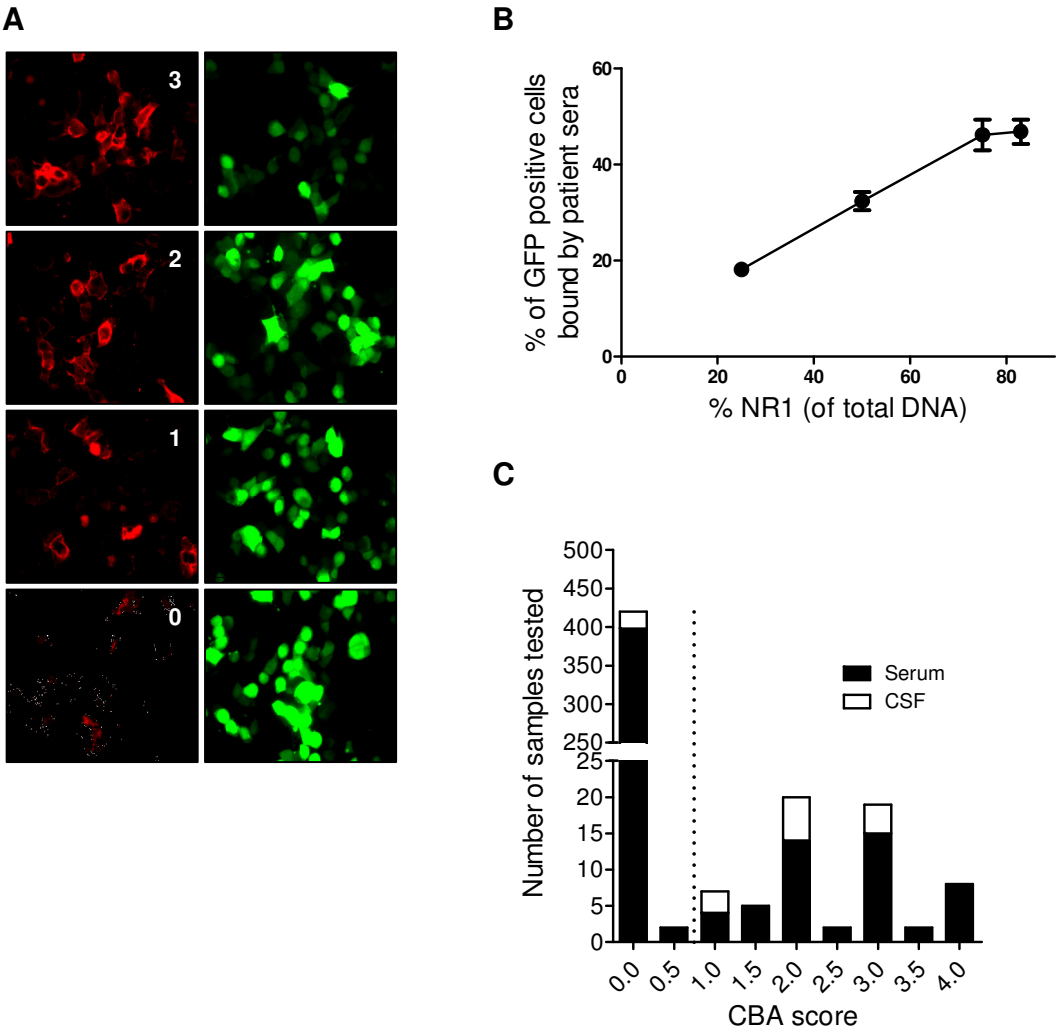
Waters P, Jarius S, Littleton E, Leite MI, Jacob S, Gray B, et al. Aquaporin-4 antibodies in neuromyelitis optica and longitudinally extensive transverse myelitis. Arch Neurol 2008; 65: 913–9.

Willison HJ, Yuki N. Peripheral neuropathies and anti-glycolipid antibodies. Brain 2002; 125: 2591–625.

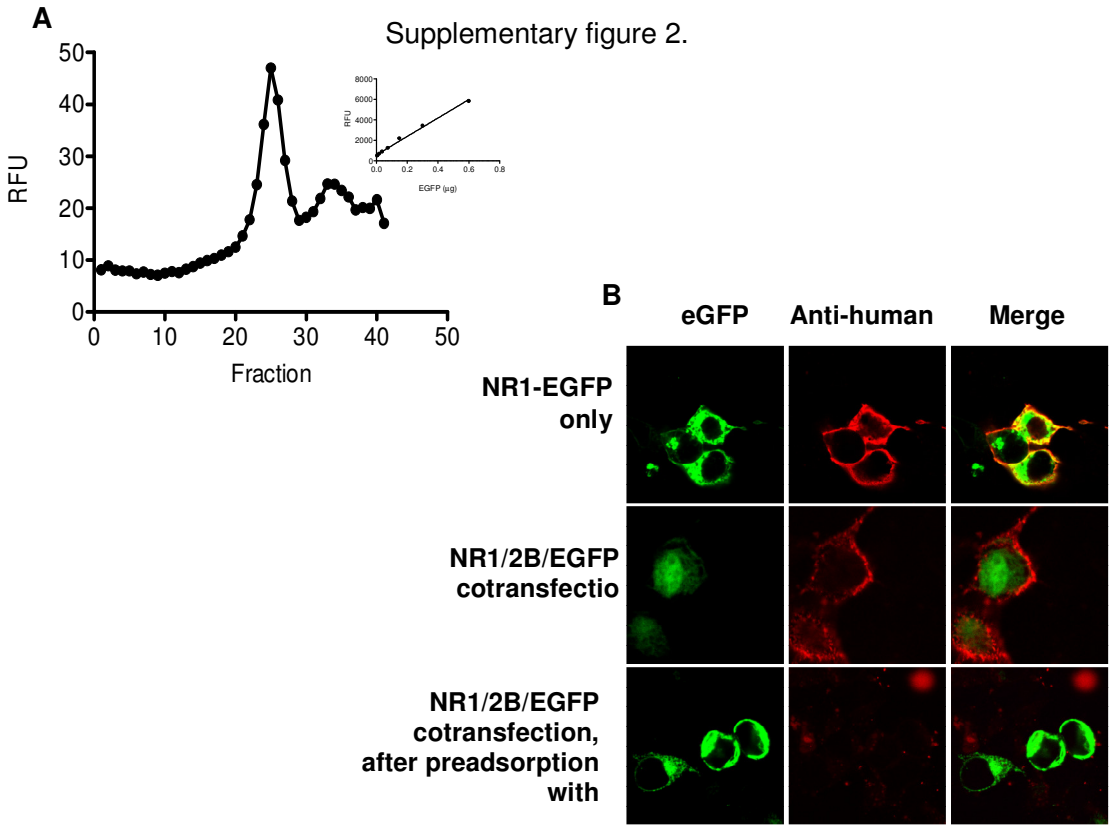
Wingerchuk DM, Lennon VA, Lucchinetti CF, Pittock SJ, Weinshenker BG. The spectrum of neuromyelitis optica. Lancet Neurol 2007; 6: 805–15.

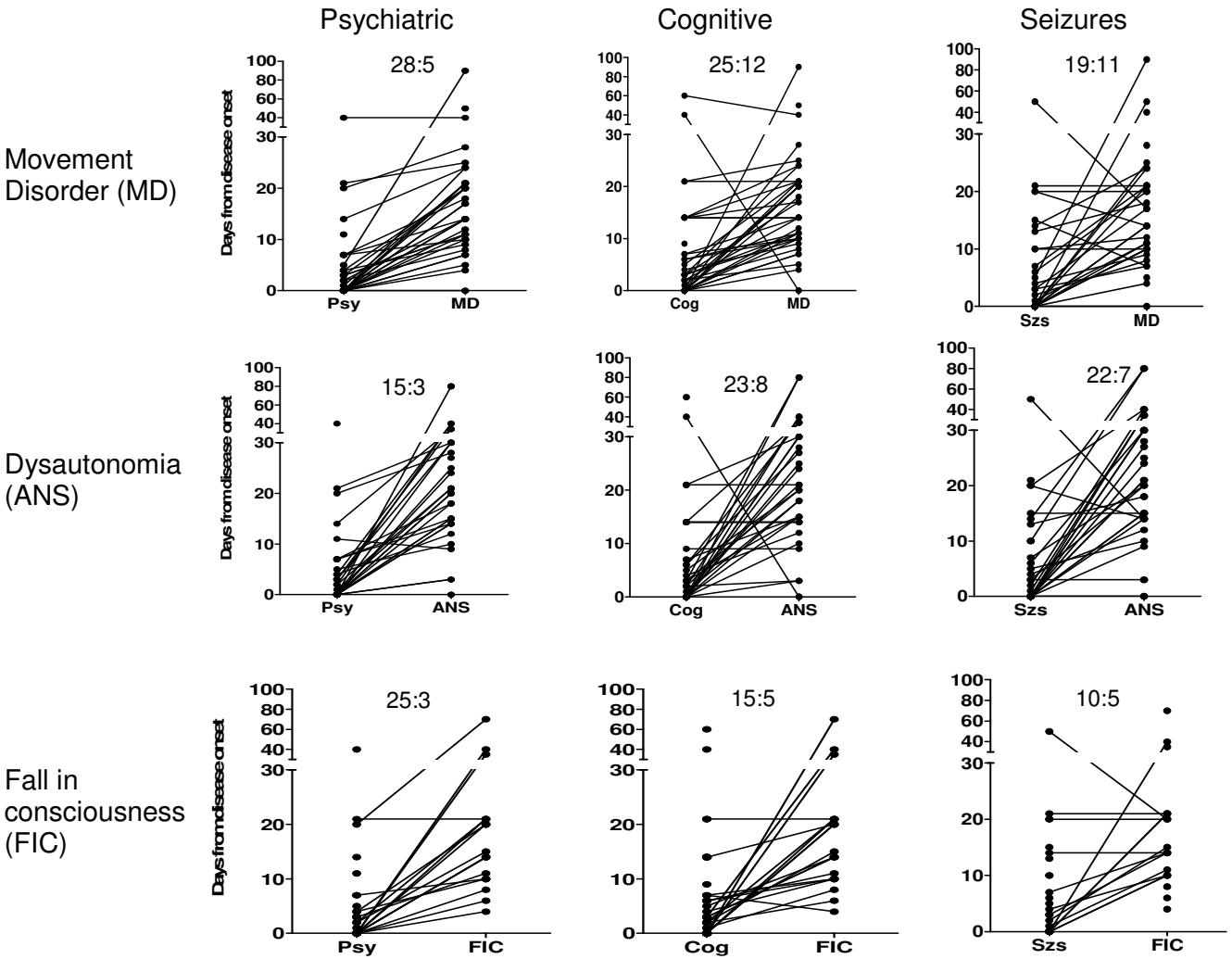
Zandi MS, Irani SR, Follows G, Moody AM, Molyneux P, Vincent A. Limbic encephalitis associated with antibodies to the NMDA receptor in Hodgkin Lymphoma. Neurology 2009; 73: 2039–40.

Supplementary figure 1



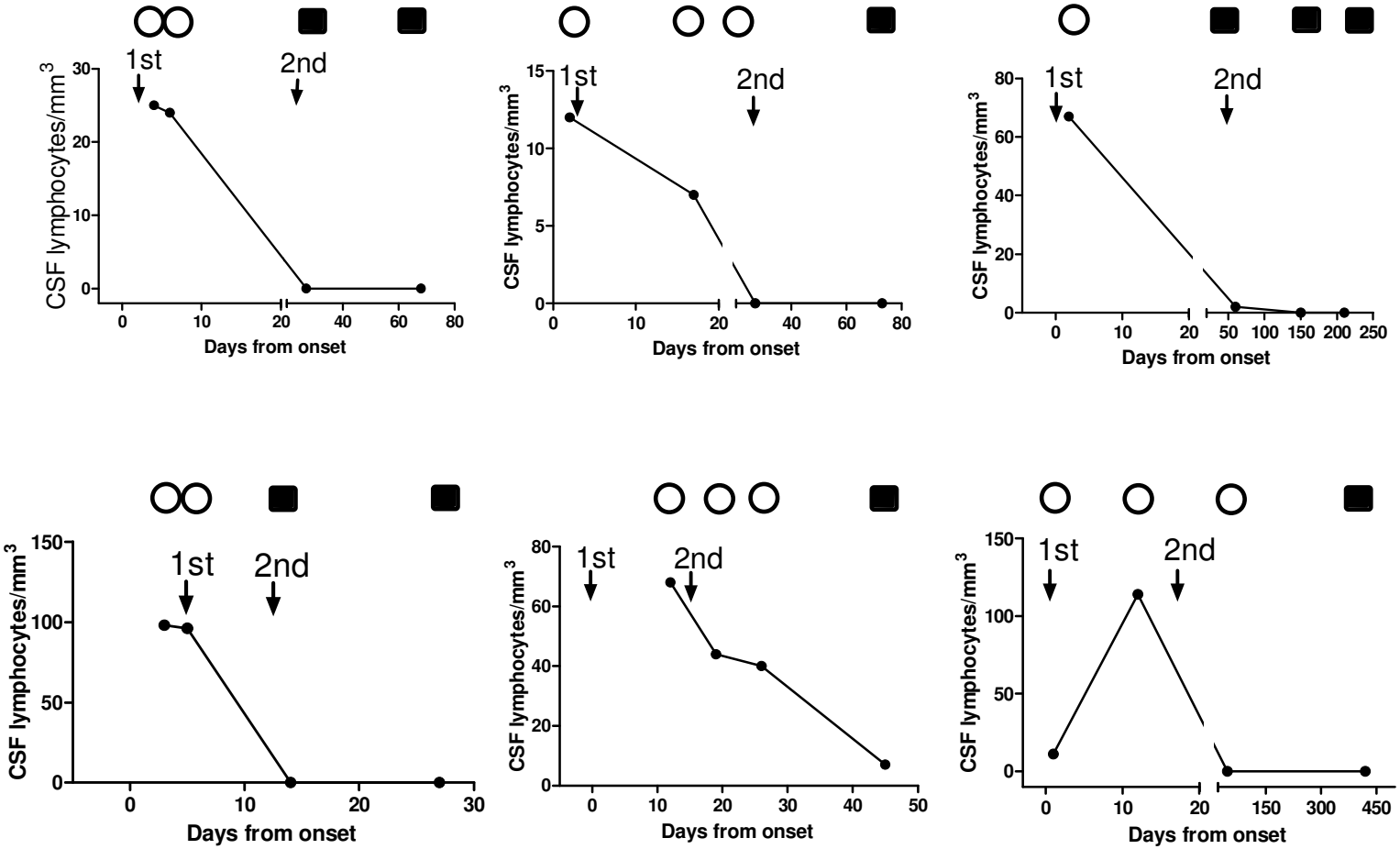
Supplementary figure 2.





Supplementary figure 3

Supplementary figure 4.



APPENDIX 2: N-METHYL-D-ASPARTATE RECEPTOR ANTIBODIES IN PEDIATRIC DYSKINETIC ENCEPHALITIS LETHARGICA

22. Koliatsos VE, Price WL, Pardo CA, et al. Ventral root avulsion: an experimental model of death of adult motor neurons. J Comp Neurol 1994;342:35–44.
23. Martin G, Seguí J, az-Villoslada P, et al. Jun expression is found in neurons located in the vicinity of subacute plaques in patients with multiple sclerosis. Neurosci Lett 1996;212:95–98.
24. Weaver LC, Cassam AK, Krassioukov AV, et al. Changes in immunoreactivity for growth associated protein-43 suggest reorganization of synapses on spinal sympathetic neurons after cord transection. Neuroscience 1997;81:535–551.

N-Methyl-D-Aspartate Receptor Antibodies in Pediatric Dyskinetic Encephalitis Lethargica

Russell C. Dale, PhD,[1*] Sarosh R. Irani, MRCP,[2*] Fabienne Brilot, PhD,[1] Sekhar Pillai, FRACP,[1] Richard Webster, FRACP,[3] Deepak Gill, FRACP,[3] Bethan Lang, PhD,[2] and Angela Vincent, FRCPath[2]

Encephalitis lethargica (EL) describes an encephalitis with psychiatric, sleep, and extrapyramidal movement disorders. Dyskinetic and Parkinsonian forms have been described. EL shares clinical features with the anti–N-methyl-D-aspartate receptor (NMDAR-Ab) encephalitis. We studied 20 sera from pediatric patients with contemporary EL. Ten sera (from 2 males and 8 females, aged 1.3–13 years) and 6/6 cerebrospinal fluid samples were positive for NMDAR-Ab. NMDAR-Ab–positive patients had dyskinesias, agitation, seizures, and insomnia, whereas Parkinsonism and somnolence dominated in the NMDAR-Ab–negative children. We were unable to identify any tumors. The dyskinetic form of EL is an NMDAR-Ab encephalitis and can affect very young children.

Ann Neurol 2009;66:704–709

From the [1]Neuroinflammation Group, Institute for Neuroscience and Muscle Research, the Kids Research Institute at the Children's Hospital at Westmead, University of Sydney, Westmead, Australia; [2]Neurosciences Group, West Wing and Weatherall Institute of Molecular Medicine, John Radcliffe Hospital, Oxford, United Kingdom; and [3]T. Y. Nelson Department of Neurology, the Children's Hospital at Westmead, University of Sydney, Westmead, Australia.

Address correspondence to Dr Vincent, Neuroimmunology Group, West Wing and Weatherall Institute of Molecular Medicine, John Radcliffe Hospital, Oxford OX3 9DS. E-mail: angela.vincent@imm.ox.ac.uk

*R.D. and S.R.I contributed equally to this work.

Potential conflict of interest: A.V. and her department receive payments and royalties for antibody assays.

Pfizer had no role in study design, data collection, data analysis, data interpretation, or the writing of the manuscript.

Received May 19, 2009, and in revised form Jul 1, 2009. Accepted for publication Jul 10, 2009. Published online, in Wiley InterScience (www.interscience.wiley.com). DOI: 10.1002/ana.21807

Epidemics of "lethargic encephalitis" (encephalitis lethargica [EL]) have been described for centuries, classically by Von Economo.[1] Von Economo described 3 classic forms: akinetic mutism, somnolent-ophthalmoplegic, and hyperkinetic.[1] EL describes an encephalitis with dominant psychiatric features (catatonia, agitation, compulsive behaviors), extrapyramidal movement disorders (chorea, oculogyric crises, dystonia, Parkinsonism), and sleep disturbance (insomnia or hypersomnolence).[1,2] Seizures, autonomic dysfunction, encephalopathy, and cognitive features are less common. Some dyskinetic EL cases have been called "immune-mediated chorea encephalopathy syndrome."[3] We previously reported 20 cases, predominantly in children, suggesting this phenotype is not rare.[4] The absence of viral antigens in the central nervous system (CNS), the benefit of immunotherapies, the presence of antineuronal antibodies, and cerebrospinal fluid (CSF) oligoclonal bands suggest that EL is an immune-mediated phenomenon.[2,4–8]

Recently, an encephalitis has been described with dominant psychiatric features, dyskinesias (particularly orofacial), seizures, and autonomic and respiratory features, largely in young females with ovarian teratomas with good responses to tumor surgery,[9–12] and with serum and CSF autoantibodies to the extracellular domain of NR1/NR2 subunits of the N-methyl-D-aspartate receptor (NMDAR-Ab).[12] A recent larger study found NMDAR-Abs in both sexes, and 40% of cases were nonparaneoplastic.[13] We asked whether contemporary EL is associated with NMDAR-Ab.

Materials and Methods

Patients and Controls

Twenty patients (12 female; range, 1.3–15 years; Tables 1 and 2) were studied over 9 years. All patients had encephalitis defined as neurological dysfunction with CNS inflammation on brain magnetic resonance imaging (MRI) or CSF analysis. Their condition was defined as EL because of the dominant movement and psychiatric disorders, and clinical similarity with historical descriptions of EL.[1,4,6] Excluded diagnoses included infectious encephalitis (herpes simplex virus, mycoplasma pneumonia, Epstein-Barr virus), autoimmune disorders (systemic lupus erythematosus, antiphospholipid syndrome), and metabolic disorders. Ten of 20 patients were described previously, and some had antibodies directed against soluble brain proteins using Western blotting,[4,14] as indicated in Tables 1 and 2. The antigens were later identified as ubiquitous intracellular glycolytic enzymes, and we now believe that these antibodies reflect nonspecific autoimmunity. All serum and CSF samples were taken during the first 3 weeks of the encephalitis before any immunotherapies. These were intravenous methyl-prednisolone followed by oral prednisolone (n = 13) or intravenous

 © 2009 American Neurological Association

Table 1. Clinical Details and Outcome of EL Patients With Positive NMDAR-Ab (n = 10)

Age/Sex	1st Symptoms	Psychiatric Symptoms	Early Movement Disorder	Late Movement Disorder	Sleep Disorder	Other	Outcome
1.3/F[a]	Encephalopathy, unresponsive	—	Chorea	Chorea	—	Hypotonia, mutism, regression,	Relapse, chorea, DD
3/F	Chorea, aggression	Agitation, SIB	Chorea	Parkinsonism, stereotypies	Sleep inversion	Seizures, mutism, encephalopathy	Memory loss, relapse
3/F[a]	Seizures	Screaming	Chorea	Chorea and dystonia	—	Encephalopathy, confusion, mutism	Complete recovery
5/F	Agitation, insomnia	Agitation	Chorea and dystonia	Chorea and dystonia	Insomnia	Memory loss, language impairment	Cognitive impairment, memory loss, inattention
7/F	Hemichorea, OGC, seizures	Catatonia, agitation, tricillomania, echolalia	Chorea, dystonia, stereotypies, oralingual dyskinesia	Dystonia, Parkinsonism, waxy flexibility	Insomnia	Seizures, social disinterest, mutism, memory loss, tachycardia[b]	Dystonia, Parkinsonism, cognitive impairment, social disinterest, emotional lability
7/F	Confusion, inappropriate laughter	Agitation, aggression, emotional lability, tricillomania	Dystonia, chorea	Dystonia, chorea	Sleep inversion	Encephalopathy, poor eye contact, mutism, hypoventilation[b]	Emotional lability, OCB
8/F	Dystonia	Agitation, emotional lability, impulsive	Dystonia, hemiballismus	Dystonia	Insomnia	Seizures, urinary incontinence, mutism	Emotional lability
8/M[a]	Irritable, aggression	Agitation, echolalia, palilalia, coprolalia, SIB	Hemiballismus, stereotypies	Dystonia, Parkinsonism, oralingual dyskinesia, OGC	Insomnia	—	Complete recovery
11/F[a,d]	Agitation, panic attacks	Catatonia, panic attacks	Oralingual dyskinesia, stereotypies	Oralingual dyskinesia	Insomnia	Seizures, hyperventilation[b]	Complete recovery
13/M[a]	Agitation, visual hallucinations	Catatonia, aggression, compulsive touching	Stereotypies, hemiballismus, dystonia	Parkinsonism, stereotypies, waxy flexibility	Insomnia	Mutism, hypertension[b]	Complete recovery

[a]Patients with positive antineuronal antibodies defined using Western blotting as described.[4]
[b]Autonomic features.
[c]Previously described EL patients.[2]
[d]Previously described EL patients.[4]
NMDAR-Ab = antibodies to N-methyl-D-aspartate receptor; F = female; M = male; DD = developmental delay; SIB = self-injurious behavior; OGC = oculogyric crises; OCB = obsessive-compulsive behavior.

immunoglobulin (n = 2). Patients were followed-up for a variable period. Nineteen sera from children with opsoclonus myoclonus syndrome (aged 18 months to 10 years) provided controls.

NMDAR, Voltage-Gated Potassium Channel, Glutamic Acid Decarboxylase, and Glycine-Receptor Antibody Assays

The NMDAR-Ab assay was based on the work of Dalmau et al.[12] NR1/NR2B subunits of NMDAR and enhanced green fluorescent protein were cotransfected into human embryonic kidney cells, and human immunoglobulin G binding was detected with secondary antibody (Alexa Fluor red-conjugated). The cells were fixed briefly without permeabilization. Sera were tested initially at 1:20 and CSF samples undiluted or at 1:4, depending on availability. The results were scored visually using immunofluorescence as described for aquaporin-4 assays (for techniques see Waters et al. 2008[15]). Glycine-receptor–transfected cells[16] were run in parallel to assess NMDAR-Ab specificity. Voltage-gated potassium channel (VGKC) and glutamic acid decarboxylase (GAD) antibody assays used techniques in routine clinical use.

Table 2. Clinical Details and Outcome of EL Patients With Negative NMDAR-Ab (n = 10)

Age/Sex	1st Symptoms	Psychiatric Symptoms	Early Movement Disorder	Late Movement Disorder	Sleep Disorder	Other	Outcome
5/F	Confusion, confabulation	Emotional lability, perseveration	Parkinsonism	Parkinsonism	Insomnia	Pyramidal weakness	Insomnia, inattention
5/M[a,b]	Bradykinesia, lethargy	—	Parkinsonism	Parkinsonism	Somnolence	Ophthalmoplegia, ptosis, mutism, nocturnal bradycardia[c]	Complete recovery
6/F	Paralysis	—	Orolingual dyskinesia	Orolingual dyskinesia	—	Axonal neuropathy	Ventilation dependence, profound paralysis
7/F[a,b]	Anxiety	Anxiety, depression	Rigidity	Rigidity	Sleep inversion	Mutism	Anxiety
8/M	Lethargy, Parkinsonism	—	Parkinsonism	Parkinsonism	Somnolence	Encephalopathy	Complete recovery
9/F[a,b]	Dystonia	Disinhibition, compulsive touching	Hemi-Parkinsonism, hemiballismus, OGC	Hemi-Parkinsonism, hemiballismus	Sleep inversion	Ophthalmoplegia, mutism, hiccough[c]	Dystonia, cognitive impairment
10/M[a,b]	Somnolence	Depression	Parkinsonism, motor tics	Parkinsonism, motor tics	Somnolence	Mutism	Depression
14/M[a,b]	Dystonia	Agitation	Dystonia	Dystonia, Parkinsonism	Somnolence	Encephalopathy, mutism, confusion	Dystonia, cognitive impairment
15/M[a,b]	Paranoia, anxiety	Paranoia, anxiety, agitation	Parkinsonism, OGC	Parkinsonism	Somnolence	Hiccough, pupillary abnormalities[c]	Complete recovery
15/M[a,b]	Paranoia, OGC	Catatonia, paranoia, agitation, compulsions	Orolingual dyskinesia, blepharoclonus, OGC	Dystonia, Parkinsonism	Sleep inversion	Poor eye contact, mutism	Mutism, catatonic schizophrenia, cognitive impairment

[a]Previously described EL patients.[4]
[b]Patients with positive antineuronal antibodies defined using Western blotting as described.[4]
[c]Autonomic features.
NMDAR-Ab = antibodies to N-methyl-D-aspartate receptor; F = female; M = male; OGC = oculogyric crises.

Results

The clinical phenotypes of all 20 patients are given in Tables 1 and 2. They presented mainly with psychiatric, behavioral, movement, or sleep disorders. Psychiatric symptoms included agitation and compulsive behaviors. Movements disorders were dyskinetic (hyperkinetic form of EL) or Parkinsonism (akinetic form of EL). Sleep disorders presented as insomnia, sleep inversion, or somnolence. Seizures occurred in 25%, usually associated with an encephalopathy.

Ten of 20 EL patients had serum NMDAR-Ab (see Fig for examples). All 6 available CSF samples from these patients were also positive, but titers in matched serum and CSF samples were highly variable, with ratios of serum/CSF titers ranging between 4 (very high intrathecal synthesis; Fig A, B) and 320 (negligible intrathecal synthesis; Fig C, D) in 1 6-year-old female. Subsequent CSF samples from this patient were negative. Results of all comparisons are shown in Figure E.

No NMDAR-Abs were found in the 19 children with opsoclonus myoclonus. None of the EL patients had GAD antibodies, but 1 NMDAR-Ab–positive patient had a low titer of Voltage-gated potassium channel antibodies (173pM) and 1 NMDAR-Ab–negative patient had weak binding to glycine receptor. EL patients were divided into NMDAR-Ab–positive (Table 1) and –negative (Table 2) groups; the more distinctive clinical features are compared in Table 3.

Clinical Phenotype of NMDAR-Ab–Positive EL

Eight of 10 patients were female, including 4 children ≤5 years of age (Table 1). A preceding infection was only reported in 2 patients. The presentation was often dramatic, with agitation, catatonia, mutism, compulsive, and self-injurious behaviors. Dyskinetic movement disorders with chorea, dystonia, hemiballismus, stereotypies, and oculogyric crises occurred within 4 weeks of presentation. Some of the dyskinetic movements were extraordinary, and included lower limb cycling, stereotypical upper limb flailing, prolonged limb posturing with waxy flexibility, and orolingual dyskinetic "rabbit" movements. The movement disorders were usually generalized, dramatic, and impairing; only 1 patient had orolingual dyskinesia as the main movement disorder. Videos of these movements have been provided previously.[2] Parkinsonism only occurred in 4

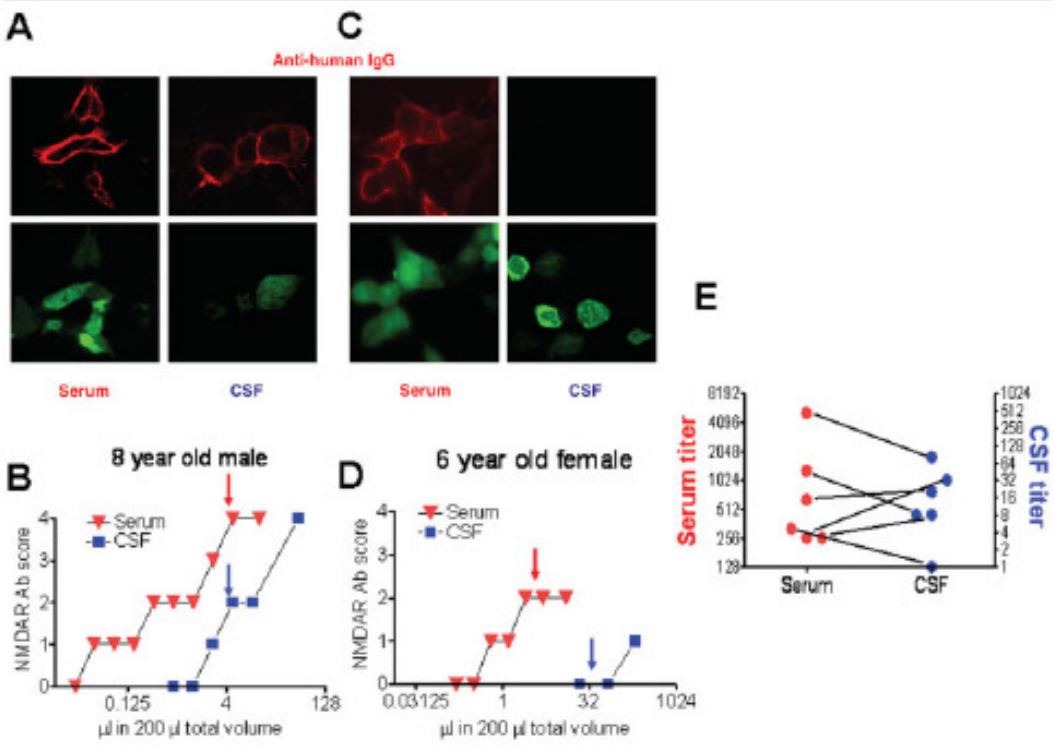


Fig. Titers of antibodies to N-methyl-D-aspartate receptor (NMDAR-Ab) in serum and cerebrospinal fluid (CSF). NR1/NR2B subunits of NMDAR and enhanced green fluorescent protein were transfected into human embryonic kidney cells, and human immunoglobulin G (IgG) binding was detected with secondary antibodies (Alexa Fluor red-conjugated). The results show 1 patient with high serum antibody (score 4 at 1:40) and high CSF antibody (score 2 at 1:40) (A, B), and another patient with moderate serum antibody (score 2 at 1:40 dilution) and very low CSF antibody (score 0 at 1:3 dilution) (C, D). The arrows denote the dilutions used for panels A and C. (E) Relative titers of serum and CSF antibodies in all 6 patients with available CSFs. The titers given are the highest dilution at which binding was scored as 1. Note the different scales of the y axes in E.

NMDAR-Ab patients and always late, 4 weeks after disease onset. Insomnia or sleep inversion was common, but somnolence was not observed (Table 3). Seizures (n = 5) were only found in this group ($p < 0.05$). Four had autonomic dysfunction. Encephalopathy, developmental regression, hypotonia, and social disinterest were common under 10 years of age (Table 1). CSF revealed pleocytosis in 4 of 10 (mean 14 lymphocytes/mm^3; range, 0–58), and oligoclonal bands were abnormal in all 9 patients tested (6 intrathecal synthesis, 3 mirrored pattern). MRI during the first weeks was normal in 7; 3 had subtle cortical grey matter enhancement, which was absent on subsequent imaging. One patient has clear cerebral atrophy on follow-up imaging. The mean time to maximum deficit was 5.5 weeks, and the mean inpatient stay was 13.6 weeks (range, 6–35 weeks). At follow-up (mean, 27 months; range, 6-84), 4 patients had made a complete recovery, 6 patients had significant motor, cognitive, or psychiatric impairments, and 2 of these had a relapsing course. Two NMDAR-Ab–positive female patients with ongoing impairments had ovarian imaging with negative findings.

Clinical Phenotype of NMDAR-Ab–Negative EL

NMDAR-Ab–negative patients were more often male, and none was <5 years of age (Tables 2 and 3). Seven of 10 patients reported a postinfectious onset. Agitation was not common, and the early and dominant movement disorder was typically Parkinsonism. Somnolence was the commonest sleep disturbance, and no patients had seizures (Tables 2 and 3). Autonomic features occurred in 3 patients. MRI was normal in 7 patients, and 3 had basal ganglia and substantia nigra/midbrain lesions. NMDAR-Ab–negative patients had a shorter disease course, with a mean time to maximum

Table 3. Comparisons Between Clinical Phenomenology of NMDAR-Ab–Positive and NMDAR-Ab–Negative Patients

Clinical Features	NMDAR-Ab Positive	NMDAR-Ab Negative	Significance (Fisher Exact 2-Tail Test, Except[a])
Male:female	2:8	6:4	NS
Median age, y (range)	6 (1–13)	8.5 (5–15)	NS[a]
Agitation	9/10	4/10	$P=0.06$
Catatonia	3/10	1/10	NS
Mutism	7/10	6/10	NS
Early dyskinesias	10/10	4/10	$P<0.05$
Early Parkinsonism	0/10	6/10	$P<0.05$
Insomnia	7/10	1/10	$P<0.05$
Somnolence	0/10	5/10	$P<0.05$
Autonomic dysfunction	4/10	3/10	NS
Seizures	5/10	0/10	$P<0.05$
Complete recovery	4/10	3/10	NS

Early dyskinesias include chorea, dystonia, hemiballismus, stereotypies, orolingual dyskinesias, and tics within 1st 4 weeks. Early Parkinsonism describes bradykinesia plus rigidity, rest tremor, or postural instability within the 1st 4 weeks.
[a]Mann-Whitney U test.
NMDAR-Ab = antibodies to N-methyl-D-aspartate receptor; NS = nonsignificant.

deficit of 2.45 weeks and mean in-patient stay of 7.1 weeks (range, 2–26 weeks). Only 3 made a complete recovery; 7 had persistent motor, cognitive, or psychiatric impairments.

Discussion

A clinical presentation characterized by dominant movement, psychiatric, and sleep disorders is not rare in pediatrics, and is often diagnosed as EL or "immune-mediated chorea encephalopathy syndrome."[3] Although EL patients have antineuronal antibodies detected using Western blotting, it is likely that these antibodies, which bind to intracellular glycolytic enzymes, are markers of autoimmunity, rather than pathogenic autoantibodies.[4,14] By contrast, antibodies that bind to cell surface proteins involved in neurotransmission, such as NMDAR-Ab, are widely held to be pathogenic, and in vitro data support a role in reducing NMDAR surface expression.[13] Our results demonstrate that, using an assay similar to that previously reported,[12] a substantial proportion of contemporary EL patients have antibodies that bind to cell-surface–expressed NMDAR.[12,13] Interestingly, the NMDAR-Ab positive patients predominantly fit into the dyskinetic form of EL,[4,6,17] with early, often bizarre, dyskinetic movement disorders and agitation. The patients with the somnolent-Parkinsonian form of EL, considered to be the classic form by most commentators, were negative for NMDAR-Ab.

The different clinical phenotypes of the NMDAR-Ab–positive and –negative patients suggest different pathogenic targets, and the early Parkinsonian features in the NMDAR-Ab–negative patients suggest the involvement of another, as yet unidentified, antibody, perhaps acting directly on striatal regions. The NMDAR-Ab–positive patients tended to be younger, with dyskinetic movements and agitation, and often had seizures, with Parkinsonian features presenting later (if at all). NMDAR-Ab have been shown to reduce the expression of cell surface NMDA receptors in hippocampal cultures,[13] but it is not clear whether it is the serum or CSF antibodies that play the dominant role in vivo. In fact, the relative levels of serum and CSF NMDAR-Ab in our patients were highly variable, although serum levels were consistently higher than CSF levels.

Although reported cases of anti-NMDAR encephalitis now include both sexes and all age groups, it is still more common in young females, many with ovarian pathology.[13] All but 2 of our NMDAR-Ab–positive EL patients were female, as were the majority of EL cases reported over the past 50 years; ovarian tumors were not routinely excluded at the time, but have been in 2 of our patients with persistent symptoms. In our experience of patients with NMDAR-Ab (Irani and Vincent, in preparation), detectable tumors are uncommon under the age of 20 years, although the majority of the children are female. However, it is also possible that tumors have undergone spontaneous regression, or microscopic tumors may exist that are undetectable using conventional imaging.

Anti-NMDAR encephalitis patients have generally been treated with steroids or intravenous immunoglob-

ulin, and recent reports describe success with plasma exchange and rituximab.[18,19] It is difficult to infer benefit of the ad hoc immunotherapies that some of our EL patients received. However, given the poor outcome in many of our EL patients, and this new evidence for a potentially pathogenic antibody, early aggressive immunotherapies appear warranted. Moreover, our findings draw attention to the pressing need to define specific antibodies in other forms of pediatric psychiatric and movement disorders.

RCD and FB have postdoctoral University of Sydney fellowships, and a Pfizer neuroscience award. SRI is supported by the National Institute for Health Research, Department of Health, UK. Work in AV and BL's laboratory is supported by the Oxford Biomedical Research Centre.

R.C.D. and A.V. were involved in study design, data analysis, and writing of the report. R.C.D., R.W., D.G., and S.P. were involved in clinical assessment of the patients. S.R.I., F.B., B.L., and A.V. performed the experimental analyses and contributed to writing the report. We also thank the patients and families involved in this study.

Dedicated to the late Robert Surtees, mentor, role-model, and Professor of Pediatric Neurology, Great Ormond Street Hospital, London, UK. We thank Prof D. Beeson and Ms S. Maxwell for their help in cloning the NMDAR and Dr Tanja Brenner for technical assistance.

References

1. von Economo C. Encephalitis Lethargica, Its Sequelae and Treatment. London, UK: Oxford University Press; 1931.
2. Dale RC, Webster R, Gill D. Contemporary encephalitis lethargica presenting with agitated catatonia, stereotypy, and dystonia-parkinsonism. Mov Disord 2007;22:2281–2284.
3. Hartley LM, Ng SY, Dale RC, Church AJ, Martinez A, de Sousa C. Immune mediated chorea encephalopathy syndrome in childhood. Dev Med Child Neurol 2002;44:273–277.
4. Dale RC, Church AJ, Surtees RA, et al. Encephalitis lethargica syndrome: 20 new cases and evidence of basal ganglia autoimmunity. Brain 2004;127(pt 1):21–33.
5. Kiley M, Esiri MM. A contemporary case of encephalitis lethargica. Clin Neuropathol 2001;20:2–7.
6. Howard RS, Lees AJ. Encephalitis lethargica. A report of four recent cases. Brain 1987;110(pt 1):19–33.
7. Ono Y, Manabe Y, Hamakawa Y, Omori N, Abe K. Steroid-responsive encephalitis lethargica syndrome with malignant catatonia. Intern Med 2007;46:307–310.
8. Blunt SB, Lane RJ, Turjanski N, Perkin GD. Clinical features and management of two cases of encephalitis lethargica. Mov Disord 1997;12:354–359.
9. Nokura K, Yamamoto H, Okawara Y, Koga H, Osawa H, Sakai K. Reversible limbic encephalitis caused by ovarian teratoma. Acta Neurol Scand 1997;95:367–373.
10. Okamura H, Oomori N, Uchitomi Y. An acutely confused 15-year-old girl. Lancet 1997;350:488.
11. Kleinig TJ, Thompson PD, Matar W, et al. The distinctive movement disorder of ovarian teratoma-associated encephalitis. Mov Disord 2008;23:1256–1261.
12. Dalmau J, Tuzün E, Wu HY, et al. Paraneoplastic anti-N-methyl-D-aspartate receptor encephalitis associated with ovarian teratoma. Ann Neurol 2007;61:25–36.
13. Dalmau J, Gleichman AJ, Hughes EG, et al. Anti-NMDA-receptor encephalitis: case series and analysis of the effects of antibodies. Lancet Neurol 2008;7:1091–1098.
14. Dale RC, Candler PM, Church AJ, Wait R, Pocock JM, Giovannoni G. Neuronal surface glycolytic enzymes are autoantigen targets in post-streptococcal autoimmune CNS disease. J Neuroimmunol 2006;172:187–197.
15. Waters P, Larius S, Littleton E, et al. Aquaporin-4 antibodies in neuromyelitis optica and longitudinally–extensive transverse myelitis. Arch Neurol 2008;65:913–919.
16. Hutchinson M, Waters P, McHugh J, et al. Progressive encephalomyelitis, rigidity, and myoclonus: a novel glycine receptor antibody. Neurology 2008;71:1291–1292.
17. Raghav S, Seneviratne J, McKelvie PA, Chapman C, Talman PS, Kempster PA. Sporadic encephalitis lethargica. J Clin Neurosci 2007;14:696–700.
18. Ishiura H, Matsuda S, Higashihara M, et al. Response of anti-NMDA receptor encephalitis without tumor to immunotherapy including rituximab. Neurology 2008;71:1921–1923.
19. Schimmel M, Bien CG, Vincent A, Schenk W, Penzien J. Successful treatment of anti-N-methyl-D-aspartate receptor encephalitis presenting with catatonia. Arch Dis Child 2009;94:314–316.